N-Heterocyclic Carbene Palladium Pincer Complexes: Synthesis, Aggregations and Catalytic Applications

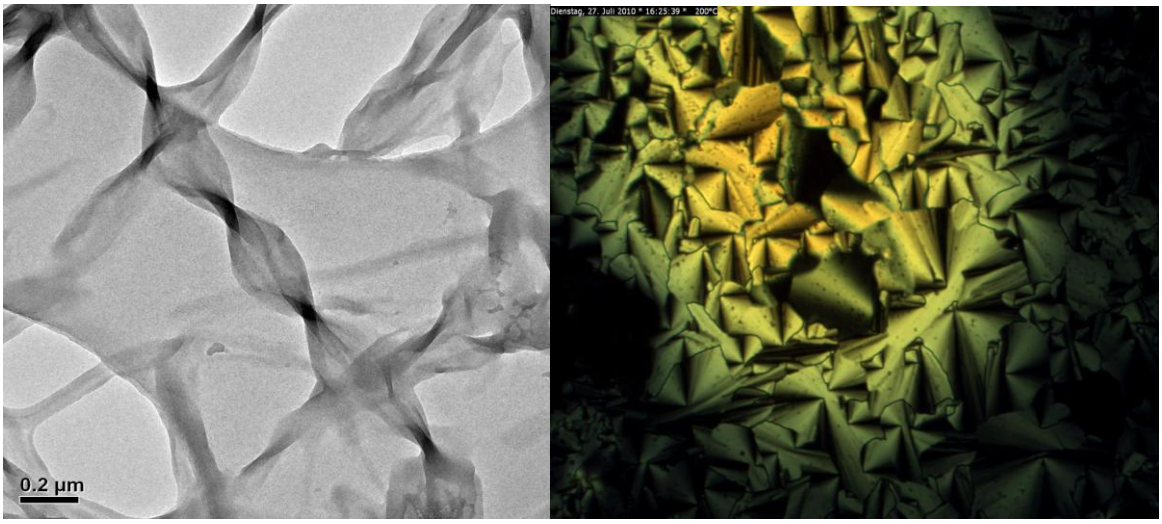

Dissertation
zur
Erlangung des Doktorgrades (Dr. rer. nat.)
der
Mathematisch-Naturwissenschaftlichen Fakultät
der
Rheinischen Friedrich-Wilhelms-Universität Bonn

vorgelegt von
Jagadeesh Malineni
aus
Hyderabad, Indien

Bonn 2011

N-Heterocyclic Carbene Palladium Pincer Complexes: Synthesis, Aggregations and Catalytic Applications

Dissertation
zur
Erlangung des Doktorgrades (Dr. rer. nat.)
der
Mathematisch-Naturwissenschaftlichen Fakultät
der
Rheinischen Friedrich-Wilhelms-Universität Bonn

vorgelegt von
Jagadeesh Malineni
aus
Hyderabad, Indien

Bonn 2011

Die vorliegende Arbeit wurde in der Zeit von January 2008 bis August 2011 unter der Leitung von Prof. Dr. Karl Heinz Dötz am Kekulé-Institut für Organische Chemie und Biochemie der Rheinischen Friedrich-Wilhelms-Universität Bonn

Angefertigt und deren Durchführung von der Mathematisch-Naturwissenschaftlichen Fakultät der Rheinischen Friedrich-Wilhelms-Universität Bonn genehmigt.

Teile dieser Arbeit sind bereits veröffentlicht:

1. "**A Novel Pyridine-Bridged Bis-benzimidazolylidene Pincer Palladium Complex: Synthesis and Catalytic Properties**". Tu Tao, Jagadeesh Malineni, Karl Heinz Dötz, *Adv. Synth. Catal*, **2008**, *350*, 1791-1795.

2. "**A Lutidine-Bridged Bis-Perimidinium Salt: Synthesis and Application as a Precursor in Palladium-Catalyzed Cross-Coupling Reactions**". Tao Tu, Jagadeesh Malineni, Xiaoling Bao and Karl Heinz Dötz, *Adv. Synth. Catal*, **2009**, *351*, 1029-1034.

Members of the examination committee:

1. Prof. Dr. K. H. Dötz
2. Prof. Dr. A. Lützen
3. Prof. Dr. W. Mader
4. Prof. Dr. K. Maier

Tag der Promotion: 20.10.2011
Erscheinungsjahr: 2011

Die vorliegende Arbeit wurde in der Zeit von January 2008 bis August 2011 unter der Leitung von Prof. Dr. Karl Heinz Dötz am Kekulé-Institut für Organische Chemie und Biochemie der Rheinischen Friedrich-Wilhelms-Universität Bonn

Angefertigt und deren Durchführung von der Mathematisch-Naturwissenschaftlichen Fakultät der Rheinischen Friedrich-Wilhelms-Universität Bonn genehmigt.

Teile dieser Arbeit sind bereits veröffentlicht:

1. "**A Novel Pyridine-Bridged Bis-benzimidazolylidene Pincer Palladium Complex: Synthesis and Catalytic Properties**". Tu Tao, Jagadeesh Malineni, Karl Heinz Dötz, *Adv. Synth. Catal*, **2008**, *350*, 1791-1795.

2. "**A Lutidine-Bridged Bis-Perimidinium Salt: Synthesis and Application as a Precursor in Palladium-Catalyzed Cross-Coupling Reactions**". Tao Tu, Jagadeesh Malineni, Xiaoling Bao and Karl Heinz Dötz, *Adv. Synth. Catal*, **2009**, *351*, 1029-1034.

Members of the examination committee:

1. Prof. Dr. K. H. Dötz
2. Prof. Dr. A. Lützen
3. Prof. Dr. W. Mader
4. Prof. Dr. K. Maier

Tag der Promotion: 20.10.2011
Erscheinungsjahr: 2011

It would not have been possible to write this doctoral thesis without the help and support of the kind people around me, to only some of whom it is possible to give particular mention here.

My heart full thanks to my advisor Prof. Dr. Karl Heinz Dötz for giving me the wonderful opportunity to work with him. It has been an honor to be his Ph.D student. I appreciate all his precious and inspiring suggestions for my research. He has been invaluable on both an academic and personal level, for which I am extremely grateful.

I am especially grateful to Prof. Dr. Arne Lützen for his acceptance as a co-referee for my Ph.D viva. In addition I would like to acknowledge Prof. Dr. Werner Mader and Prof. Dr. Karl Maier for their willingness to participate in the examination committee.

I am very much thankful to Dr. Tao Tu for giving his valuable suggestions during my doctoral studies. My special thanks to Prof. Dr. Herwig Peterlik and Dr. Wilfried Assenmacher for their great efforts to measure SAXS and TEM images of my samples.

I appreciate the kindness of Prof. Dr. Sigurd Höger for giving access to use the micro wave, DSC and UV visible spectrophotometer. Especially I am thankful to Joscha Vollmeyer for both his help and advice with the measurements.

I would like to acknowledge the Konrad Adenauer Stiftung for the financial support for my Ph.D program and for giving me the opportunity to join the group meetings and seminar programs. I am thankful to Dr. H.C. Berthold Gees and Prof. Dr. Heinrich Wamhoff for their valuable suggestions and support.

My sincere thanks also goes to the NMR and mass spectrometry employees for their efforts with measuring my samples. For the X-ray structure analysis I would like to thank Dr. Gregor Schnakenburg for his help.

In addition, I would like to thank all my current and former colleagues of the working group for their support and friendship. My special thanks goes to Dr. Jochen Möllmann for his kindness.

And last, but definitely not least, I am forever indebted to my family and friends for their endless patience, encouragement and support throughout my studies.

Contents

I. Introduction

Organometallic chemistry is the study of structures bearing a metal carbon bond. It is one of the most studied parts in chemistry. Organometallics are a very broad field of compounds involving also living organisms; as an example hemoglobin and myoglobin are porphyrins bonded to an iron atom. Organometallic compounds are also involved in the production of fine chemicals and pharmaceuticals.

Recently R. J. Noyori [1] has reported ruthenium-binap organometallic complexes as used for the preparation of anti-inflammatory drugs. Even from last few years organometallic compounds are applying vital roles for the production verity of compounds. Catalysis is one of the themes that were recently rewarded with Nobel prices in 2001, 2005 and 2010.

In 2001 R. J. Noyori [1] and W. S. Knowles [2] shared a half price for catalyzed chiral hydrogenation while K. B. Sharpless [3] got the other half price for his work on catalyzed chiral oxidation reactions. In 2005 Y. Chauvin, [4] R. R. Schrock [5] and R. H. Grubbs [6] received the Nobel prize for their work on the metathesis reaction methodology. This reaction involves a metal carbene and an olefin to form a new unsaturated structure. In 2010 Richard F. Heck, Ei-ichi Negishi and Akira Suzuki received the Nobel prize for their work on palladium-catalyzed cross couplings in organic synthesis.

Metal carbenes are known since 1964 with the first publication of a tungstene carbene complex by E. O. Fischer,[7] but in the early 1990's carbene chemistry entered a new era with the first crystallization of *N*-heterocyclic carbenes (NHC) by Arduengo. *N*-Heterocyclic carbenes have since then become popular ligands in organometallic and inorganic coordination chemistry. Because of their specific coordination chemistry, *N*-heterocyclic carbenes both stabilise and activate metal centers. In 1992/93 Herrmann discovered that NHC and phosphines are similar in terms of ligand properties, metal complex synthesis and coordination.[8]

II. Background

II.1 Types of Carbenes

Transition metal carbene complexes or alkylidene complexes are described as molecules bearing one carbon atom connected to a metal by a formal double bond. These molecules will be then classified according to the metal, its oxidation state, and the substituents at the carbene center as either *Fischer*-Type [7, 9] or *Schrock*-Type[10] carbenes. (Figure 1).

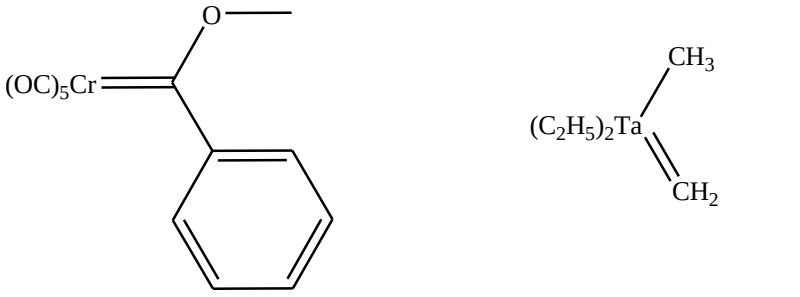

Fischer-carbene complex Schrock-carbene complex

Figure 1: Examples of *Fischer* type and *Schrock* type carbene complexes.

To introduce the carbene complexes theme, and to understand the expectations from *N*-heterocyclic carbenes, a brief description of Fischer and Schrock carbenes is necessary. The molecular orbital diagrams in Figure 2 depict the bonding of Fischer (I), Schrock (II) and *N*-heterocyclic (III) carbenes.

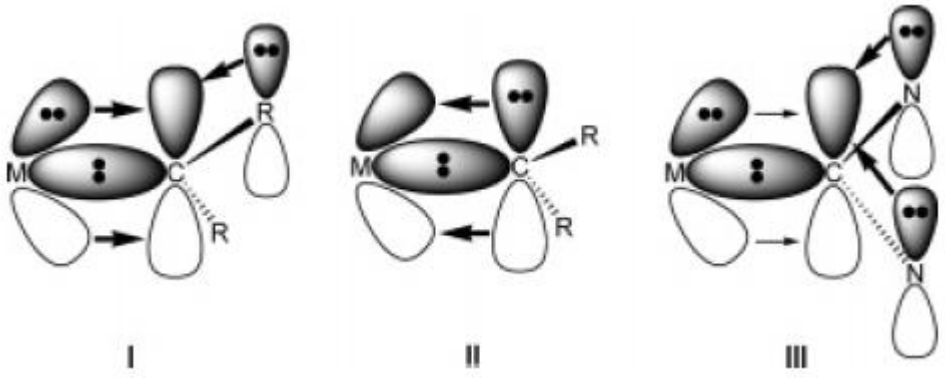

Figure 2: Molecular orbital diagrams of a Fischer (**I**), Schrock (**II**), and *N*-heterocyclic (**III**) carbene complex.

In Fischer type carbenes low oxidation state metals are involved, resulting in high electron density of the metal center. A poor back donation from the metal to the carbene tends to lead to unstable carbenes. Fischer carbene complexes have an electrophilic character that can be seen with its resonance structures. Contrary to this, the Schrock type carbenes are complexed to high oxidation bearing donor ligands, meaning a lack of population on the d orbitals at the metal. The carbene carbon atom involves its π-electron shell in order to fill the d orbitals of the metal and form a bond. The study of its resonance structures leads to the nucleophilic character of this carbene.

II.1.1 Fischer type carbene complexes

The first Fischer carbene complex was published in 1964 by E. O. Fischer und A. Maasböl.[7, 9] Fischer carbenes form a σ bond to the metal and have an empty p orbital to accept electron density. The Fischer carbene carbon p orbital needs significant π-donating contribution from both metal and substituents. This feature is very important for the stability of these carbene complexes which is relayed by the experience that complexes with poor π-donor metals (early transition/high oxidation state) are unstable. On the other hand, complexes of late transition/low oxidation state metals tend to be significantly more stable. This specific structure gives the carbene carbon atom an electrophilic character. This can be rationalised with the mesomeric structures expressed in Figure 3.

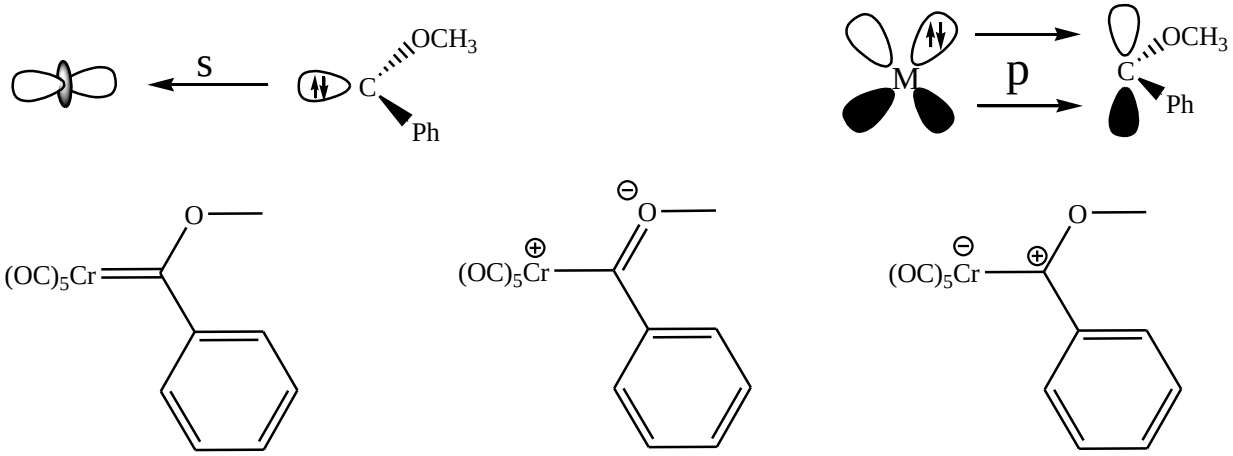

IVa **IVb** **IVc**

Figure 3: Possible Fischer carbene resonance structures.

The structure **IVc** (Figure 3) shows how the carbon center can be attacked by nucleophilic substances. It could be compared to carboxylic systems like esters or amides. This grew out R. Hoffmann's isolobal principle, [11] which compares the frontier molecular orbitals from Fischer carbene complexes and carboxylic systems and states them as similar in terms of energy and symmetry.[12]

II.1.2 Schrock type carbene complexes

Schrock carbenes tend to bind well with early transition metals in high oxidation states. The high oxidation state will limitate the population of the d_π orbital on the metal, which leaves the path free for better π -donation from the filled p orbital of the carbene carbon atom to the d_π orbital of the metal. The repulsive effects inhibit the strength of the π-donation and overall lead to the destabilization of the metal-carbene carbon bond. Good substituents for Schrock carbene ligands are groups that are not π -donors such as alkyl groups. The structure **VIb** (Figure 4) shows the nucleophilicity of the carbon center in the carbene ligand.

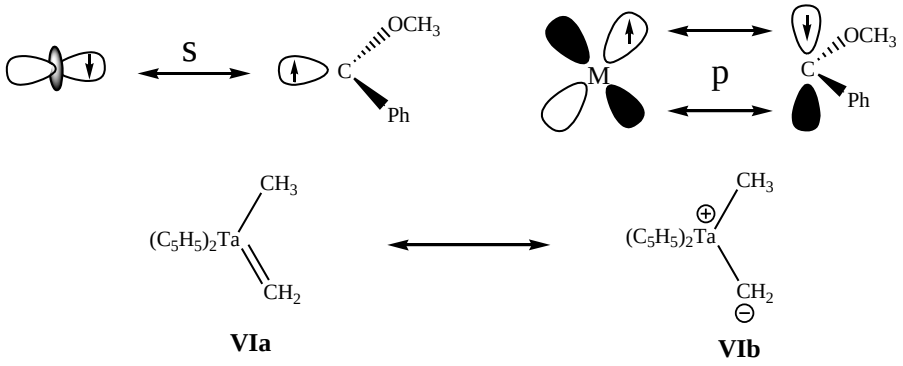

Figure 4: Resonance form for Schrock carbene complexes.

With regard to the isolobal principle these carbene complexes are similar to ylides/ylenes and represent an alternative to Wittig reagents.[13] An example for these structures is the Tebbe reagent [14]; it is used in the methylenation of various carboxylic products like aldehydes, esters or amides. The methyl transfer reagent in this case is the Schrock type carbene $Cp_2Ti{=}CH_2$.

II.1.3 *N*-Heterocyclic carbenes

II.1.3.1 Structure

Carbenes are neutral species, with six electrons in their valence shell [14], and are able to adopt two different geometries: linear or bent. The linear *sp*-hybridized carbene has its two p_x, p_y orbitals degenerated (Figure 5). This degeneracy can be broken when the carbene undergoes any external pressure that forces it to bend. This force will not affect the orbital p_y, which will stay unchanged, but the orbital p_x is stabilised and has its energy lowered, to get a more s-type character (Figure 6). Consequently the p_x will be known as σ and p_y as π orbital. The two lone electrons could form four possible electronic configurations: with one electron in both σ and p_π orbital assigning the carbene a triplet state ($^3B_1$), or with the pair located in either the σ ($^1A_1$) or the p_π ($^1A_1$) orbital, resulting in a singlet state. One last case is also possible with one electron in the σ and one in the p_π, as for $^3B_1$ state, but with antiparallel spins, which makes it a singlet state ($^1B_1$).

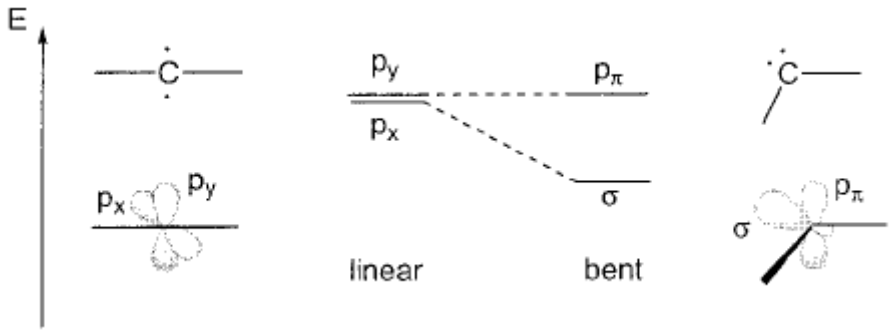

Figure 5: Relationship between the carbene bond angle and the nature of the frontier orbitals.

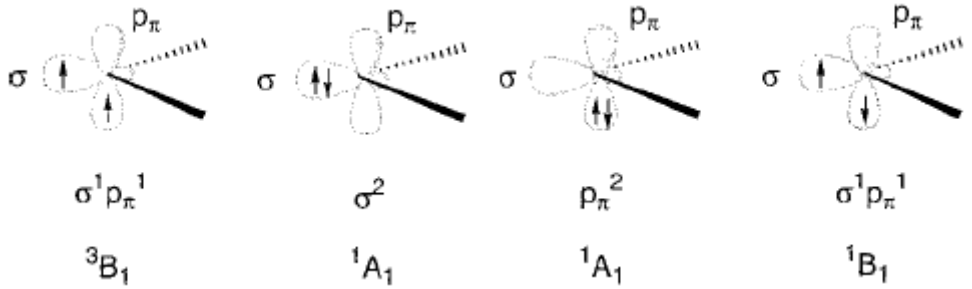

Figure 6: Electronic configurations of carbenes.

The reactivity of carbenes can be understood because of their ground state spin multiplicity, a singlet state carbene with a free orbital and one filled with a pair of electrons can be seen as amphiphilic, potentially able to be attacked by either a nucleophile or an electrophile. [15] With a

single electron in each orbital, triplet state carbenes are regarded as diradicals. The ground state multiplicity is related to the orbital's energy; Hoffmann [16] showed that the bigger the gap between the σ and pπ orbital is, the more the carbene will be in singlet state configuration, while a low energy gap will induce a triplet state carbene. With these informations, electronic and steric effects can now be analysed.

II.1.3.2. Electronic effects

II.1.3.2.1 Inductive effects

The electronic properties of a substituent will affect the energy gap between the σ and p_π orbitals. As understood previously the more the gap is increasing the more the singlet state is favored, and opposite the more the energy difference is diminished the more the carbene will adopt a triplet state. As reported reconfirmed [18], σ electron donating groups will reduce the energy gap thus facilitating the triplet state, while an σ electron withdrawing group will stabilize the σ orbital, enhancing its *s* character, and leave the p_π unchanged. In this case, the energy gap between the two orbitals is then increased favoring a singlet state carbene. (Figure 7)

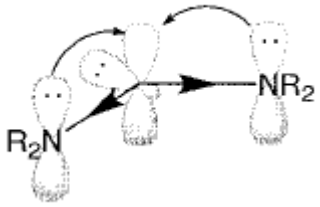

Figure 7: Electronic effects in diaminocarbene.

II.1.3.2.2 Mesomeric effects

As with inductive effects, substituents with mesomeric effects can affect the state of the carbene as well [19] π-Electron donating groups, such as halides, amine derivatives or phosphines are predicted to give bent structures, and π electron withdrawing groups (e.g. boron derivatives, silicon derivatives) are meant to give linear or quasi-linear structure.[20] The π orbitals will then interact and as seen in Figure 8, a π donating group will stabilise the p_π, with its lone pair,

forming two new molecular orbitals, a bonding one and a non-bonding one, increasing the gap between the HOMO and LUMO orbitals, i.e. favoring the singlet state.

In the case of a π withdrawing group, interaction takes place at p_y orbital, perpendicular to the plan, leaving the p_x unchanged and then breaking the $p_{x,y}$ degeneracy, leading to a singlet state.

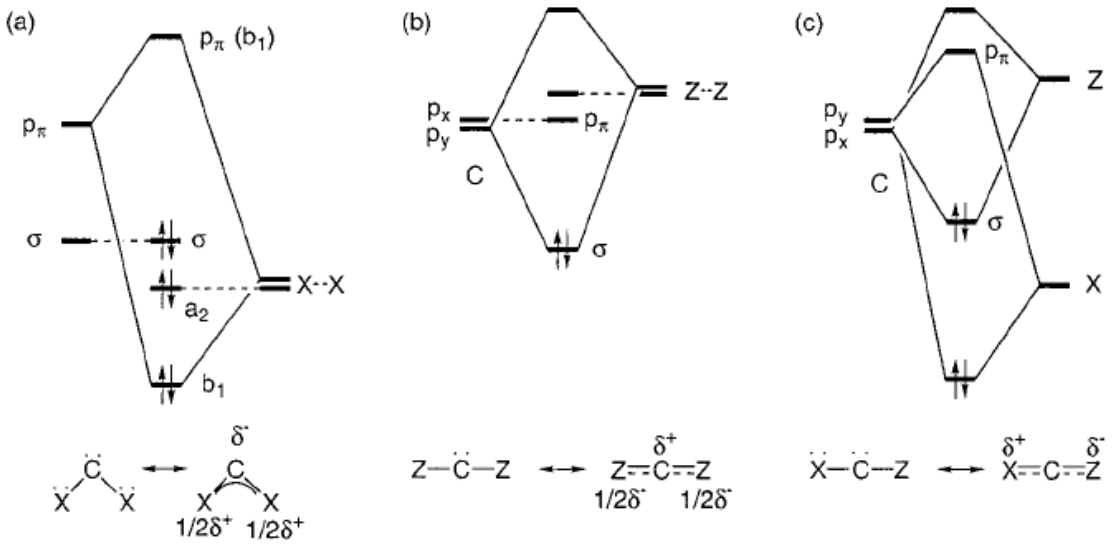

Figure 8: Perturbation orbital diagrams showing the influence of the mesomeric effects.

II.1.3.2.3 Steric effects

Steric congestion around the carbene center is known to stabilise this center, [21] but the more hindered it is, the more it broadens the angle around the carbene carbon, therefore favoring the triplet state (Figure 9).

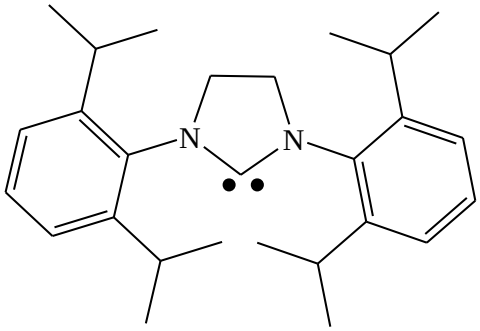

Figure 9: 1, 3-Bis(2, 6-diisopropylphenyl)-imidazol-2-ylidene. (SIPr).

It is understandable that a singlet state carbene is easier to stabilise than a triplet one. The carbon has naturally three out of four possibilities to acquire a singlet state. Then, combining the desired electronic effects previously described lead to the desired carbene. Imidazole provides two σ electron withdrawing groups and at the same time two π electron donating groups, in place of the nitrogens. The closed and rigid five-membered ring provides a good obstacle for preventing the linearisation of the carbene, even for bulky substituents. Finally, the delocalisation in the aromatic system makes the N-heterocyclic carbene a well stabilised conjugated base. As a conclusion NHCs are stable and easy to handle carbenes.

II.1.3.2.4 Reactivity

In 1970, Wanzlick showed that imidazolium salts could be deprotonated by using a highly hindered base (e.g. KOtBu).[22] In 1991, Arduengo managed to obtain the first crystalline free carbene structure, using two adamantyl groups as *N*-substituents [23] (Figure 10). *N*-Heterocyclic carbenes have been of popular interest because of their specific coordination chemistry (they both stabilise and activate metal centers).

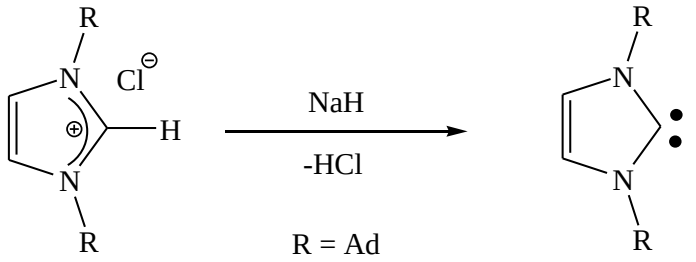

Figure 10: The first stable crystalline structure with adamantyl as *N*-substituent on.

NHCs multiple features, like their lower toxicity than phosphines, make them the ligands of choice for catalysis. They are easily removable from organic reaction mixtures and no excess of ligand is needed. Some ligands are air and room temperature stable, which makes them easy to handle. Electron rich phosphanes and carbenes are similar in terms of metal coordination, ligand properties and metal complex synthesis, but in terms of bonding NHCs are superior to phosphines. [24] The wide range of metals that they can coordinate to, provide great opportunities. The carbon metal bond is longer compared to any of the Fischer or Schrock type carbenes,

because of their low back bonding, giving them the possibility to rotate around the metal carbene-carbon bond. [8] Back donations from the metal to the ligand is believed to be minor; [25] however, recent theoretical and structural evidence [26, 27] has suggested that π back-donation is larger than previously admitted. The degree of back-donation is dependent upon the metal in question. While the degree of π-back donation may come to a question, it is generally accepted that it is smaller than the π back-donation of Fischer carbenes.

II.1.4. Other metal complexes

A large scope of metals can be complexed with NHCs, including iron, iridium, palladium, ruthenium and nickel.[28,29] An iron complex (Figure 11, VIII) can control atom transfer radical polymerisation (ATRP).[30] Ruthenium type catalysts of the latest generation are used for olefin metathesis (Figure 11, IX).[31,32] Carbon-hydrogen bonds can be activated with an iridium complex (Figure 11, XI).[33] Nickel and Palladium complexes are used in cross-coupling chemistry (Figure 11, X, XII).[34]

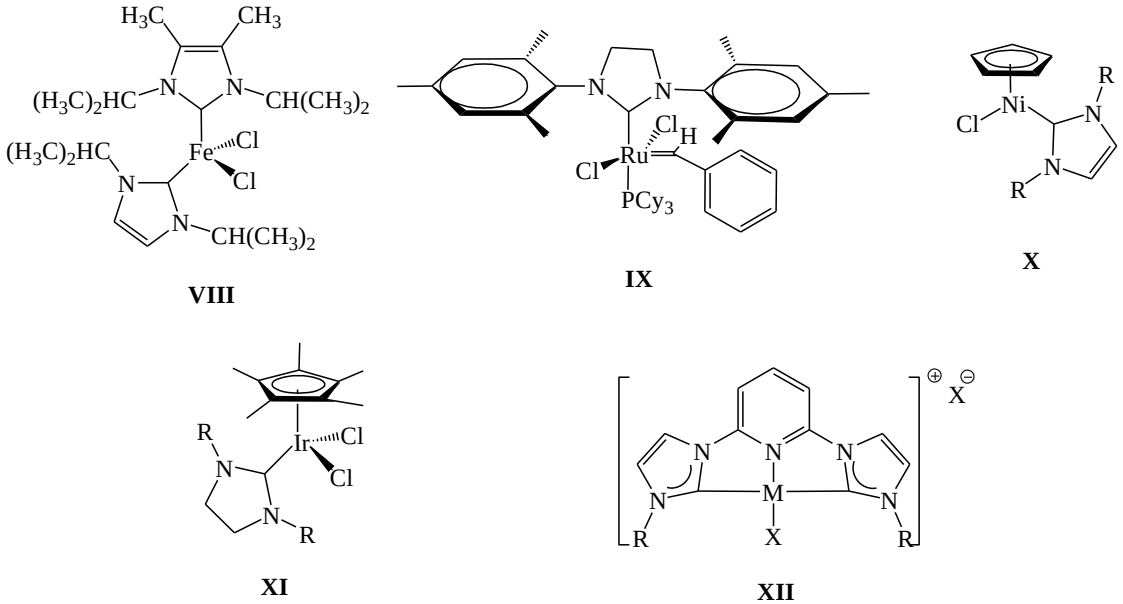

Figure 11: Variety of metal fragments accepted by NHC.

II.2 Gels

II.2.1 Introduction

Gels are everywhere! Starting from protoplasm to shaving cream, they are fascinating solid-like materials containing mostly liquids. A gel is comprised of the two components gelator(s) and solvent(s). The solid-like appearance of the gel is due to the immobilization of the solvent molecules in the three-dimensional (3D) network formed by the gelator molecules. Gels can be classified in different ways depending upon their origin, constitution, the type of cross-linking that creates their 3D network and the medium they encompass. Most of the naturally occurring gelators are macromolecular and they form gels by physical cross-linking (usually H-bonding) such macromolecules include gelatin, collagen, agar, starch and gellan gum. Gels derived from synthetic compounds can be subdivided on the basis of their constitution into macromolecular (polymer) and low-molecular. The formation of gels from macromolecular compounds can either result from chemical cross-linking or physical interactions. When the gels are formed by strong chemical bonds, they cannot be redissolved and are thermally irreversible (e.g., polyester, polyamide, poly (vinyl alcohol), polyethylene) whereas gels formed by weak noncovalent interactions (physical entanglements) are reversible (e.g. polyacrylate, polymethacrylate). Gels derived from low molecular mass compounds are supramolecular in the strictest sense in that they are formed through self-aggregation of the small gelator molecules to form entangled *Self-Assembled Fibrillar Networks* (SAFINs) through a combination of non-covalent interactions like H-bonding, π–π stacking, donor–acceptor interactions, metal coordination, solvophobic forces (hydrophobic forces for gels in water) and van der Waals interactions. Since these networks involve weak interactions, they can be readily transformed to a fluid (sol) by heating and are generally thermally reversible.

Low molecular weight organogelators (LMOG) are small organic compounds having a molecular mass of typically < 3000 and strictly belong to the supramolecular gelator category and are amazingly powerful in immobilizing organic solvents (organogels) and pure water and/or aqueous solvents (hydrogels) at very low concentration of the gelator.[35] In a typical experiment,

when a solution containing a small amount of LMOG in a suitable solvent is heated and cooled below a critical temperature (sol–gel transition), the whole volume of the liquid behaves like a solid. The solid-like visco-elastic material thus obtained is a gel. These physical gels obtained from LMOGs are generally thermo reversible (reversible sol–gel transformation upon heating and cooling) and in some rare occasions[36] display thixotropic (reversible sol–gel transformation under mechanical stress followed by rest) behavior. LMOGs which are able to gel organic liquids, generally do not display hydrogelling[37] capability and vice versa. However, ambidextrous gelators[38] (capable of gelling both organic and aqueous solvents) are also reported. Recent years have witnessed a surge of research work dedicated to LMOGs because of their various potential applications in sensors, [39] electro optics/photonics, [40] structure directing agents, [41] cosmetics, [42] conservation of arts, [43] drug delivery and bio-medical applications [44] etc.

II.2.1.1 Classification of gels

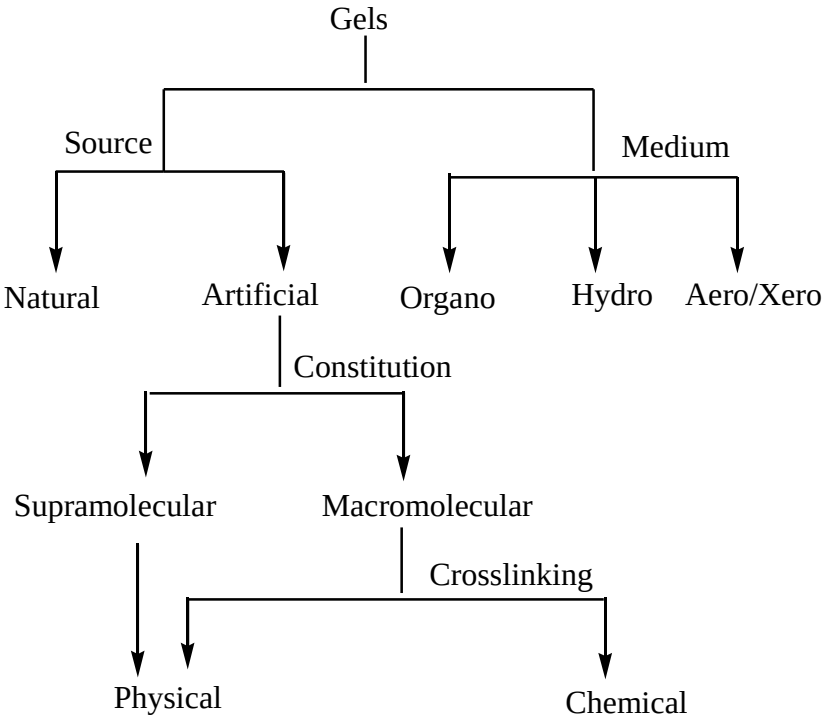

II.2.1.2 Primary structure

The gelation process is thought to arise from nanostructure aggregation and can be assimilated to protein's primary, secondary and tertiary structure. As a reminder, protein primary structure is a

succession of amino acids where the terminal amine functionality is not involved in a peptide bonding. Gelation itself is the delicate art of the balance between hydrophilic and hydrophobic interactions, the will of solvation and at the same time of aggregation. While hydrogen bonding can be the driving force in most gelation cases, they will not help in an aqueous medium where aliphatic interaction can take the duty back, but salt interactions or metal-metal interactions can also help.

II.2.1.3 Secondary structure

The secondary structure is defined as the morphology of the aggregates which can be shaped as micelles, vesicles, fibers, ribbons or sheets. Compared to this, the secondary structure of proteins is caused by saturation of all hydrogen bondings. A peptide will fold itself to obtain the most favored structure by using hydrogen bonding. Micelles are fluid species formed at the critical micelles concentration (CMC) which depends on the structure of the molecule. Above this concentration point, the micelles might form ellipsoidal micelles and further on rods. Rod like monomer functionalised with complementary donor and acceptor groups on opposite sides and chemically different surfaces first assembles into tapes via recognition of the donor and acceptor groups. The chirality is then translated into the twist of the tape, resulting in different affinities for the solvent. This leads to a helical curvature of the tape. Several models have been submitted to explain the formation of the secondary structure.[45, 46, 47] Bagchi and Nandi, [48] as an example, argued that the formation of a helical structure in mono- or bilayers is driven by interactions of chiral centers. Their calculations of the effective pair potential between two molecules showed that the minimum energy conformation in the case of racemic pairs leads to a nearly parallel alignment. For an enantiomeric pair, the repulsion would lead to a twist in the alignment up to 45° provoking a helical structure. Those calculations support and explain the observed results.

II.2.1.4 Tertiary structure

The tertiary structure is based on the interaction between the formed aggregates, and determines if a gel is formed or not. Long flexible fibers are physically more suited to entrap solvents than small ones. The tertiary structure arises from the interaction between the fibers forming entangled

fibers and interconnected networks. It can be again compared to proteins where the tertiary and quaternary structures result from the fitting of the fibers together. According to Pozzo et al. the most important factor in the gelation process is the cooling rate. Depending upon the driving force of the crystallization, a gel or a solid phase in equilibrium with the liquid solvent is obtained. [49] From a very low cooling rate (0.005 °C/min), one would obtain a mixture between solvent, gelified parts and solid parts, while with a faster rate up to 20 °C/min a gelation test can be successful with a complete homogeneous structure. (Figure 12)

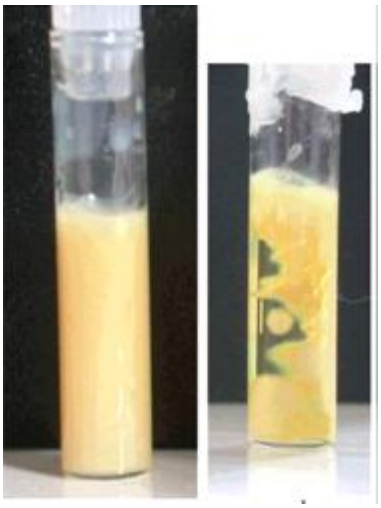

Figure 12: Visible effect of the cooling rate on the degree of gelation (only part of the solvent is trapped, right photo).

II.2.2 Examples

II.2.2.1 Hydrogelators

In order to understand which directions can be taken in the investigation it is good to know what motifs can generally promote gelation. As said earlier, the possibility to have gelation is narrowly linked to the ability of the molecule to balance between precipitation or crystallisation and solvation. In water, structures bearing a hydrophilic group, which provide solubility, and a hydrophobic group, promoting aggregation, are likely to be hydrogelators. So far, it is admitted that not only one but several types of construction motifs can lead to a gelator structure. Amphiphiles, bolaamphiphiles, sugar or steroid based systems are the most common gelators structures.

II.2.2.1.1 Amphiphiles

In the early works from Kutinake which were focused on describing the morphology of amphiphiles that would lead to gels, it is shown that the aggregate morphology could be controlled by appropriated designed structures.[50] According to Kutinake's group, the basic structure contains a hydrophilic head group, a rigid segment and a flexible tail (Figure 13).

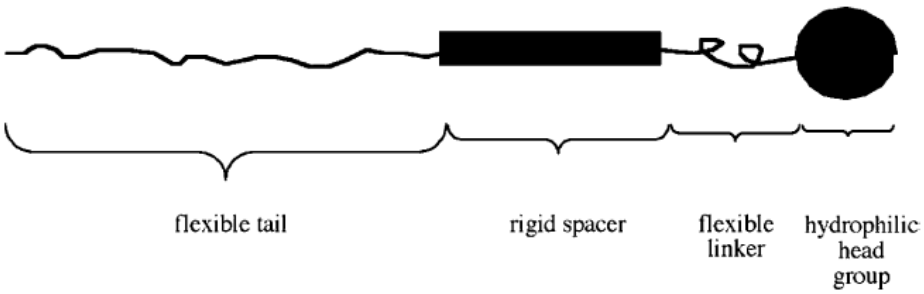

Figure 13: Description of an amphiphilic molecule.

The flexible tail is usually an alkyl chain but functional groups like vinyl groups and esters have also been mentioned. Starting the work with diphenylazomethine as rigid segment, they first investigated the influence of the flexible tail length. They stated that molecules bearing up to C_6 chain length would not form aggregates, while those bearing seven to more methylene groups would form stable layers. They also found out that a branched tail would not provide aggregation. The investigation next focused on the rigid segment, which they showed to be the second most important factor for the morphology. The diphenyl derivatives studies showed that too much bending is not advantageous for molecular ordering. Following their morphology results: "from pre-rods to rods", they claimed that polyoxoethylene or anionic phosphate are better than ammonium salts as hydrophilic head. In conclusion self-assembly is not achieved without flexible tail, rigid segment and hydrophilic group.

II.2.2.1.2 Bolaamphiphiles (two-headed amphiphiles)

Bolaamphiphiles are named after a South American weapon made of two balls connected by a string called "bola". The main difference between bolaamphiphiles and conventional ones is the aggregate morphology. In the case of long linkers these molecules could fold into two parts and adopt another aggregation modus like micelle, vesicle or lamella. (Figure 14) Shimizu and co-workers have thoroughly explored bolaamphiphiles with a variety of head groups including

nucleotides [51,52,53] amino acids [54,55] and sugars,[56,57] that form both gels and fibers. The short linked bolaamphiphiles show concentration dependency to form gels or fibers.

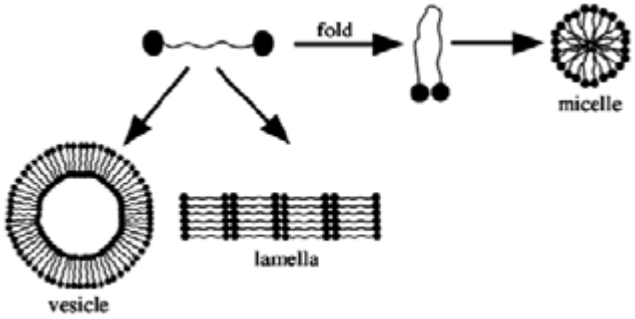

Figure 14: Description of bolaamphiphile aggregation models.

II.2.2.1.3 Carbohydrates

Similarly, Fuhrhop [58] investigated amide properties on gelation, saying that if the head group of amphiphiles are chiral and contain an amide bond, helical fibers and gels may be formed as a kind of vesicular or micellar solutions. He reveals that the hydrogen bonds between the amide groups are responsible for this rearrangement. The work focused on n-alkylgluconamides, using different electron microscopy techniques and differential scanning calorimetry (DSC), they relayed the idea that only chiral substances would produce helical fibers, because the crystallisation range is too slow and would form enantiopolar crystals instead. Shinkai and co [59] have also worked on sugar derivatives, because the carbohydrate family provides a large variety of skeletons. His work focused on pyranose form from glucose, galactose and mannose, with alkyl chains and aminophenyl moiety. They provide three different interactions, hydrogen bonding, hydrophilic interactions and π-π stacking. Gronwald[60] and Shinkai showed the importance of π-π stacking interaction compared to the role of the nitro group in nitrobenzylidene modified monosaccharides. The glucopyranose derivatives were able to gel polar solvents, such as alcohols and water, where the solvent molecules can play a hydrogen bonding donor and acceptor, revealing therefore the importance of the π-π stacking effect. Finally he compared gluco-, manno- and galactopyranose hydrogen bonding lengths [61] to understand why one sugar moiety structure would gelate one solvent and the other one not. He concluded that, as the bonds were not so different from one carbohydrate to another the difference in gelation should be due to a structural preference in the molecular aggregation

II.2.3 Organometallic gelators

II.2.3.1 Chromium carbene gels

In 2003 the Dötz [62] group successfully synthesised a gelator of a new type. (Figure 15) The insertion of a pentacarbonyl chromium Fischer carbene fragment in place of an amide lead to a new molecule with enhanced organic solvent gelation properties.

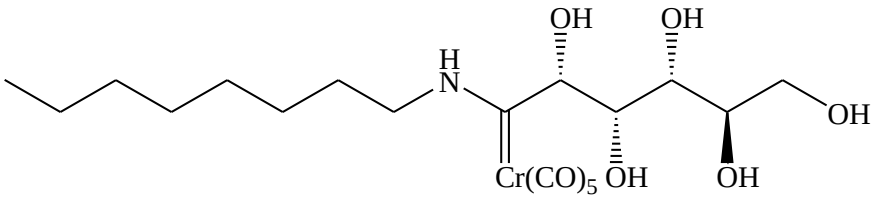

Figure 15: The first organometallic gelator for organic solvents.

Based on a known gelator, [63] *N*-*n*-octyl-D-gluconamide, the metal complex derivative showed to be suited to form gels in dichloromethane, chloroform, benzene and toluene, and also loses at the same time its solubility in water. The interest to synthesise this molecule came from the isolobality of the chromium carbene moiety to the carbonyl group.[64]

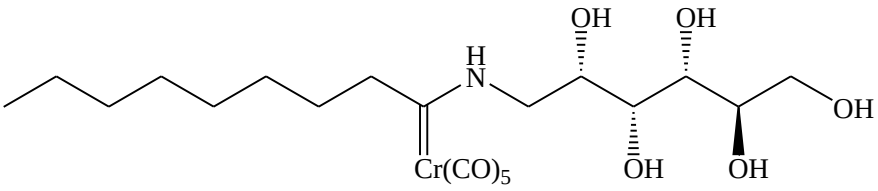

Pentacarbonyl[(2R,3R,4R,5S,6-pentahydroxy)hexylamino-1-nonylidene)]chromium

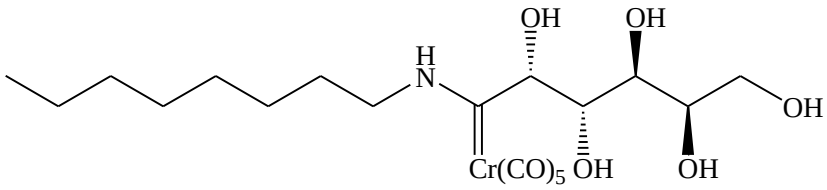

Pentacarbonyl[(2R,3R,4S,5S,6-pentahydroxy(N-n-octylamino)hexylidene)]chromium

Figure 16: Variations of the original gelator.

II.2.3.2 Titanocene gels

In 2007 Gansäuer and Dötz [65, 66] groups are reported a novel type of titanocene amphiphilic organometallic gelators. A promising approach is based on the concept of ALS gelators. These compounds consist of an aromatic unit (A) connected *via* a linker (L) to a steroidal entity (S), typically cholesterol. Based upon the ALS concept a titanocene moiety was connected to a cholesterol molecule by ester linkage.

The metal complex containing the cyclopentadienyl ligand and the geminal methyl groups represents an excellent gelator for a variety of organic solvents, toluene, benzene, ethyl acetate, DMSO, 1,4-dioxane, *n*-Bu_2O, *t*-BuOMe and acetone (Figure 17).

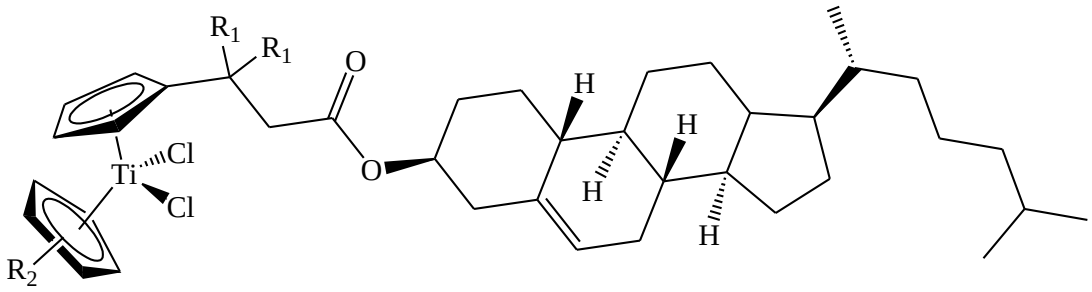

R_1 = H, $(CH_2)_5$ R_2 = H, CH_3

Figure 17: ALS based titanocene gelator.

An aggregation model was shown in Figure 18, represents cholesterol molecules are undergoing inside of the periphery due to hydrophobic interaction and titanocene units were occupied outside of the periphery.

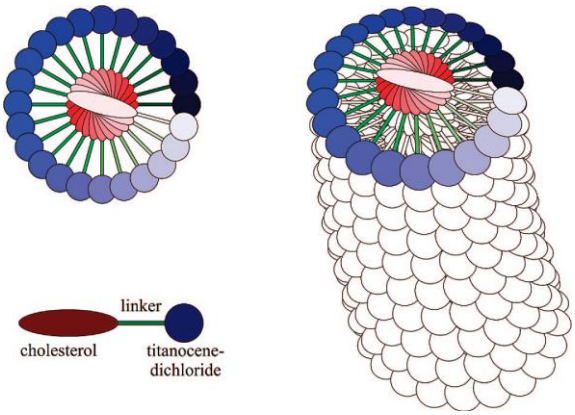

Figure 18: Aggregation model.

II.2.3.3 Palladium pincer carbene gels

In 2007 the Dötz [67] group developed novel palladium pincer carbene complexes as air stable organogels. These complexes are efficient air-stable organometallic low-molecular-mass-gelators, they gelate a broad variety of polar and a polar, protic and aprotic organic solvents even in concentration as low as 0.2 wt % (2.0 x 10^{-3}M) (Figure 19).

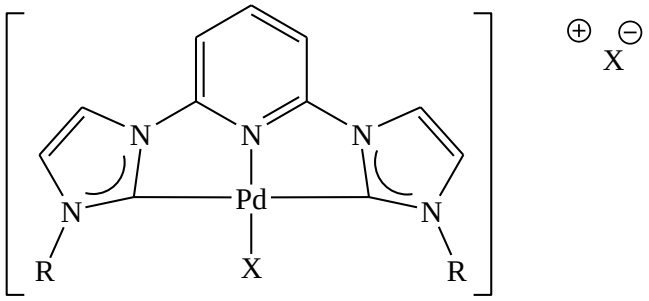

1: R = $C_{16}H_{33}$, X = I
2: R = C_4H_9, X = Br
3: R = CH_3, X = Br

Figure 19: Palladium pincer carbene gelator.

These palladium carbene complexes **2** bearing a short *N*-alkyl chain are efficient catalysts for cross-coupling reactions, for example Suzuki, Heck, and Sonogashira reactions in homogeneous state. Under heterogeneous gel state conditions the Pd-complex **1** shown in Figure 19 also catalyses the Michael addition of α-cyanoacetate to methyl vinyl ketone. This represents the first example of a catalysis reaction in the gel state (Scheme I).

Scheme I

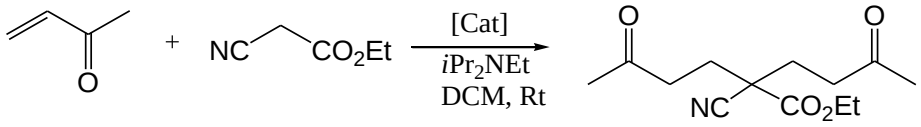

III. Aim of the Work

N-Heterocyclic carbenes and their metal complexes are prevalent in modern organometallic chemistry. One of the main areas of investigation of these systems involves the use of NHCs as ligands in metal-center-mediated catalytic reactions. The aim of this work is to develop novel types of pyridine bridged imidazole, benzimidazole and perimidine based salts and their pincer palladium complexes. Furthermore, their application in material science and catalysis such as in cross coupling reactions shall be investigated. The extension of NHC ligands from imidazole to benzimidazole and perimidine is expected to provide stronger σ-donors and weaker π-acceptors, that increase the electron density at the metal center and improves the catalytic activity towards cross coupling reactions. The extended planar metal hybrid π-system and the σ-donor properties increased by benzannulation may further enhance the gelation ability.

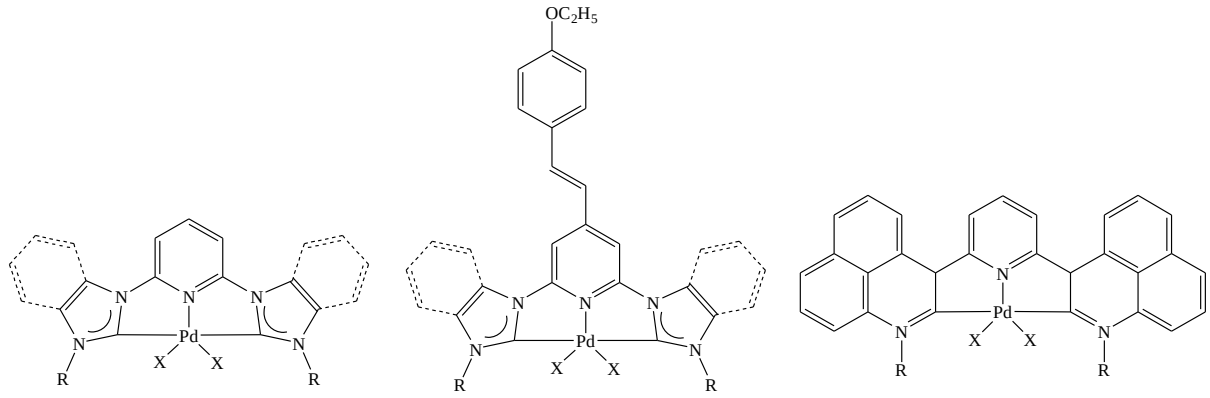

The π-extension of the protocol was also applied in the vertical direction at the γ-position of the pyridine ring. It may increase the electron density on Pd by conjugation thus making cross coupling reactions more efficient. The extended conjugation is expected to lead to more efficient π-π stacking, van der Waals and dipole-dipole interactions through three-dimensional format. Addionally the strong self-assembly of the oligovinylene moiety will have a major influence on the materials and electronic properties.

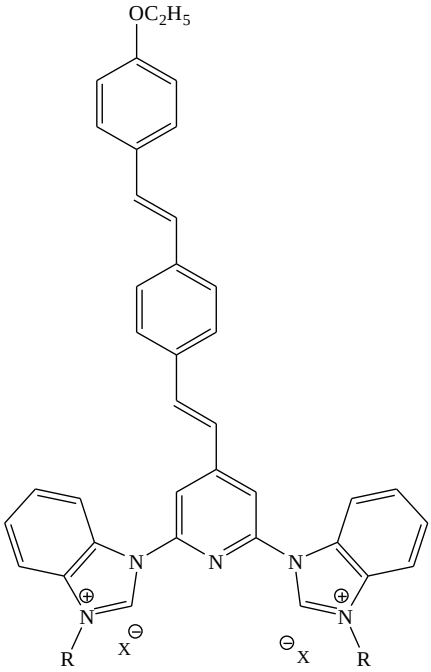
OC2H5
N
N
N
N
N
R
X
X
R

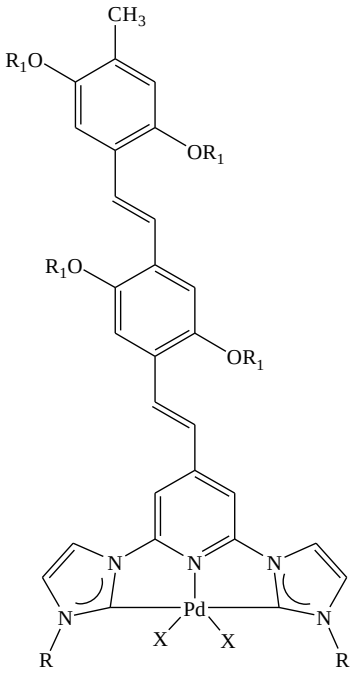
CH3
R1O
OR1
R1O
OR1
N
N
N
N
N
Pd
X
X
R
R

IV Background of the work

In 2008 the Dötz[68, 69] group introduced novel pincer pyridine-bridged bis-benzimidazolium salts and their palladium complexes. These salts gelated efficiently in protic and aprotic solvents, while carbene complexes are gelating in all verity of organic solvents and showing strong catalytical behaviour towards cross coupling reactions.

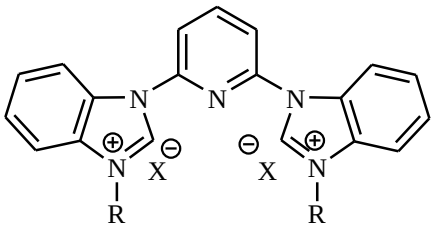

5a: R = $C_{16}H_{33}$, X = Br
5b: R = $C_{16}H_{33}$, X = I
5c: R = $C_{12}H_{25}$, X = I
5d: R = C_8H_{17}, X = I
5e: R = C_4H_9, X = I

The gelation abilities of bisbenzimidazolium halides **5a-e** were studied by heating them to reflux in a variety of protic and aprotic polar organic solvents followed by cooling to room temperature. Generally, bisbenzimidazolium salts **5a-d** form up-taking thermo reversible turbid gels in most polar solvents such as HOAc, ACN or various alcohols within a few minutes. For the shorter alkyl analogue **5e**, however, no gelation was observed under the same conditions. Gelation experiments with 2 wt % (wt/v; equal to 1.97×10^{-2} M for **5b**) of **5a-d** in a selection of solvents are summarized in Table 1. Gelators **5a-d** gelate a wide structural variety of alcohols very efficiently; firm gels are obtained from glycerol, 1, 2-ethanediol, *i*-PrOH, *i*-BuOH as well as from ACN. The gelation ability decreases with the length of the alkyl chains. Whereas iodides **5c** and **5d** bearing C_{12} and C_8 alkyl groups are soluble in MeOH, their C_{16} analogue **5b** induces gelation. This phenomenon which is also observed with other polar solvents such as HOAc, dioxane, THF may suggest that van-der-Waals interactions between the alkyl chains of gelator and solvent molecules are crucial for the self-assembly process required for gelation (Table 1).

Table 1: Gelation behaviour of bis-benzimidazolium salts **5a-d** in selected solvents. [a]

Solvent	**5a**	**5b**	**5c**	**5d**	Solvent	**5a**	**5b**	**5c**	**5d**
Glycerol	G	G	G	G	*t*-BuOH	WG	I[b]	I[b]	I
$(CH_2OH)_2$	G	G	G	G	ACN	G	G	G	G
MeOH	**C**	G	S	S	AcOH	PG	G	G	WG
EtOH	PG	G	G	WG	Dioxane	G	G	PG	I
n-PrOH	S	G	G	G	THF	P	G	PG	I
i-PrOH	G	G	G	G	DCE	P	WG	PG	I
n-BuOH	WG	G	G	G	Acetone	I	WG	WG	I

[a] Gelator concentration 2 wt%, C: crystal; G: gel; I: insoluble; PG: partial gel; P: precipitate; S: soluble;. WG: weak gel. [b] At 1wt% (upper limit of solubility), a weak gel is formed.

In contrast to iodide **5b**, the gelation ability of bromide **5a** in C_1-C_4 alcohols decreases with the alkyl chain length of the solvent used – from MeOH even a needle-shaped crystal could be grown – which indicates a distinct counter-anion effect in the gelation process. Which are also observed in the gels obtained from **5b** with MeOH, EtOH, *n*-PrOH, *i*-PrOH and *n*-BuOH. Film-type morphologies are found in all gels of **5a-d** formed with glycerol and 1, 2-ethanediol. Thinner, denser and straight fibers (ca. 200 - 400 nm wide and several μm long) are observed with gels **5a**/ACN, **5b**/DCE and **4b**/THF. A looser network consisting of thicker fibers (ca. 2 μm wide) is encountered in gels **1a**/EtOH, **5d**/EtOH, **5d**/ACN and gels **5a-d**/ HOAc. Morphologies of gels **5b**/acetone and **5b**/dioxane are similar and form a packed narrow film network. A rod-like gel network consisting of fibers, which are ca. 200 nm wide and 1-2 μm long, is observed in the partial gel **5b**/DMSO. All these morphologies may indicate that the gels are formed by a parallel columnar packing self-assembly.

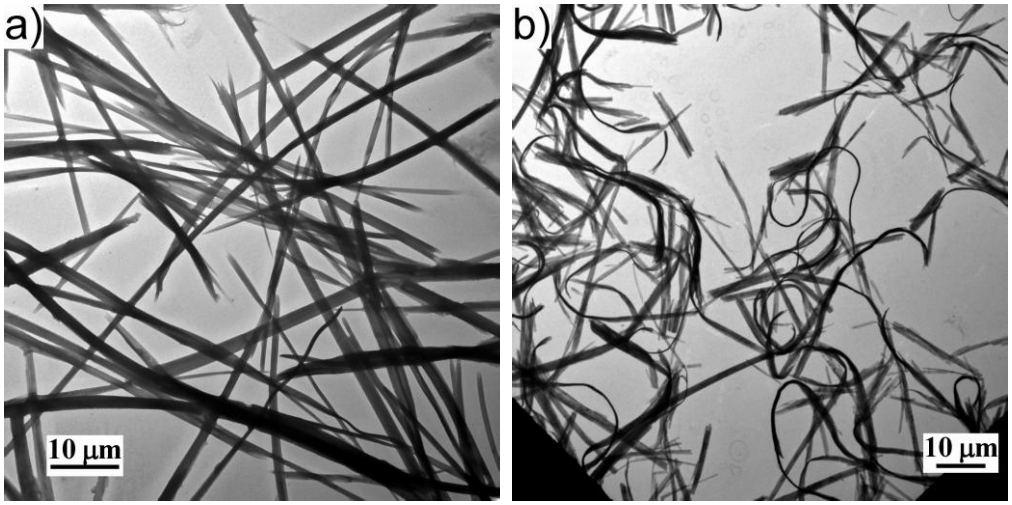

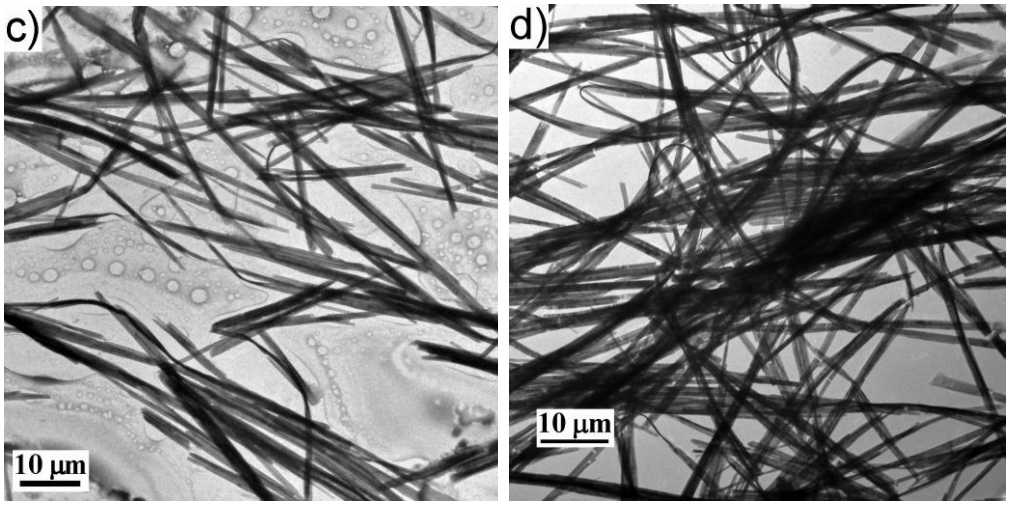

Figure 20: Selected TEM images of gels formed with bis-benzimidazolium salts **5a-d** in *i*-BuOH (3 wt %): Gel from a) **5a**; b) **5b**; c) **5c**; and d) **5d**

The pyridine bridged bis-benzimidazolium salts were applied as phase transfer catalysts in gel state under moderate conditions. Due to the low solubility of the bisbenzimidazolium salts in ACN, saturated solutions of **5a, b** did not accelerate the synthesis of **7a** in comparison with the blank test (50 h/rt; entries 1, 2, Table 2).

When gel **5b**/ACN was applied as PTC, the reaction was completed within 3 hours affording an isolated yield of 89% (entry 3, Table 2). Exchange of I- for Br- slows down the reaction (entry 4, Table 2) indicating a counter-anion effect. Stirring is necessarily required for the phase-transfer catalysis leading to a partial degradation of the gel network to gel fibers which remain visible during the reaction. Due to their insolubility they can be recovered after filtration and reused as a catalyst after re-gelation with ACN. The protocol has been extended to the synthesis of benzotriazole and imidazole analogues **7b, c** (entries 5-7, Table 2) affording slightly lower yields. Dialkylation of *m*-xylene dibromide resulted in a 90% yield of **7d** after 3 hours at room temperature (entry 8, Table 2); better results were observed with *o*- and *p*-xylene dibromides.

Table 2: Phase-transfer catalyzed *N*-alkylation of benzimidazole, benzotriazole and imidazole.

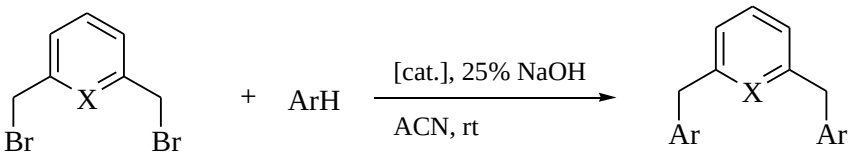

7a. X = N, Ar = Benzimidazole
7b. X = N, Ar = Benzotriazole
7c. X = N, Ar = Imidazole
7d. X = C, Ar = Benzimidazole

Entry	Catalyst	Time (h)[a]	Product	Yield(%)[b]
1	**5a** (**5b**)[c]	50	**7a**	60 (61)
2	Blank	50	**7a**	60
3	gel **5b**/ACN (5 wt%)	3	**7a**	89
4	gel **5a**/ACN (5 wt%)	5	**7a**	92
5	gel **5b**/ACN (5 wt%)	3	**7b**	59
6	gel **5a**/ACN (5 wt%)	6	**7c**	67
7	gel **5b**/ACN (5 wt%)	5	**7c**	63
8	gel **5b**/ACN (5 wt%)	3	**7d**	90

[a] Determined by GC-MS and TLC. [b] Isolated yield. [c] Saturated solution of **5a** (**5b**) in 10 mL ACN.

V Results and Discussion

The recent discovery of imidazole-based carbenes [71] and of their effectiveness as ligands [72] offers an opportunity to develop phosphine-free homogeneous catalysis. These carbenes are not only excellent ligands for late transition metals but are also able to promote a variety of catalytic reactions, including C–C[73] and C–N[74] coupling and olefin metathesis.[75] The thermal stability of carbene complexes is often high and they lack sensitive bonds that might be cleaved in any deactivation process.

In 200 the Crabtree [76] group reported the first tridentate palladium pincer carbene complexes. The palladium atom was strongly bond to two carbene molecules and coordinated with a pyridine molecule leading to the CNC carbene complex. This planar pincer molecule is soluble in high polar solvents. Apart from this, the complex showed high catalytical activity towards the Heck and Suzuki coupling reactions.

With the aim to introduce the unique properties of organopalladium compounds in organic synthesis into organometallic gelators, [67] these studies were extended towards robust functional organometallic compounds as low-molecular-mass gelators. Herein, our group reported the first example of a palladium-based air-stable organometallic LMMG, which is able to gelate a variety of organic solvents and to catalyze C-C bond formation even in the gel state.

Palladium CNC pincer bis (imidazolylidene) complexes **2** and **3** were reported to catalyze cross-coupling reactions. However, their poor solubility hampered a broader application in catalysis. Substitution with longer alkyl chains is a common means to enhance the solubility of compounds in organic solvents and, moreover, is expected to favor aggregation through intermolecular van der Waals interactions, which may assist in gel formation. The CNC pincer palladium carbene complexes of type **1** bearing two C_{16} alkyl substituents showed potential as low-molecular-mass gelators (Scheme 1).

V.1 Synthesis of pyridine-bridged bis-*N*-butyl-benzimidazolylidene pincer palladium complexes

The synthesis of pyridine-bridged bis-benzimidazolylidene pincer palladium complex was started by amination of 2, 6-difluoropyridine with two equivalents of benzimidazole at 185 ^{o} C for 2h and 160 ^{o} C for 30h. After that the reaction mixture was cooled to room temperature and washed with water and ethyl acetate to remove the excess benzimidazole leading to 2,6-bis(imidazol-1-yl)pyridine as a white powder **4** (94 %). The coupling product under went *N*-alkylation with n-alkyl halides in a sealed test tube while heated to 160 ^{o}C for 30 h. The crude product was purified by re-precipitation from $CHCl_3/Et_2O$ to give white solid **5** (98%). Pyridine-bridged bis-benzimidazolium dibromide underwent palladation by treatment of palladium acetate in DMSO and stirring at room temperature under vacuum. The reaction mixture was warmed under stirring in open vessel model at 160 °C for 25 min (at 40 W with a CEM Discover microwave instrument). DMSO was removed *in vacuo* under heating and the crude product was purified by re-precipitation from $CHCl_3$/ cold Et_2O. Another two re-precipitation operations afforded a yellow solid **6**(75%) (Scheme 2).

Scheme 2

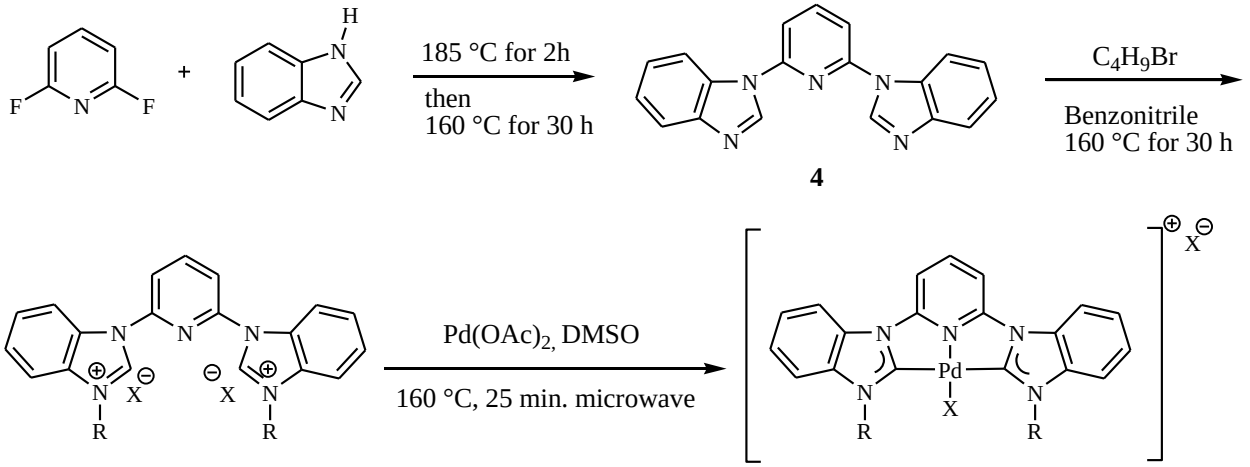

5e: R = C_4H_9, X = Br

6: R = C_4H_9, X = Br

V.1.1 Catalytical behavior towards Heck cross coupling

The catalytic properties of bis-NHC pincer palladium complex **6** was studied in the Heck reaction of aromatic halides and alkyl acrylates.[77] The reactions were performed under aerobic conditions in 1-methyl-2-piperidon (NMP) at 140 °C demonstrating the resistance of carbene complex **6** against air, moisture and heat (Table 3). A 0.2 mol% catalyst loading turned out to be sufficient for the coupling of iodobenzene with butyl acrylate within 8 hours in good to quantitative yields using a selection of organic and inorganic bases (Table 1, entries 1-4). Similarly, the coupling of the less reactive bromobenzene resulted in an almost quantitative yield under these conditions (Table 3, entry 5); chlorobenzene, however, afforded only trace amounts of **7a** even after the reaction time had been extended to 24 hours.

In order to investigate the influences of electronic and steric properties of the substrates, a variety of aryl halides were studied in model reactions using butyl acrylate and K_2CO_3 under our standard conditions in which the catalyst loading was decreased to 10^{-4} mol % Pd. Under these conditions, iodobenzene still afforded a 94 % isolated yield of **7a** after 24 hours (Table 3, entry 6) This, however, decreased to 27 % when bromobenzene was applied (Table 3, entry 7) quantifying the difference in reactivity between aryl iodides and bromides hidden in the proceeding series with a catalyst loading of 0.2 mol %. The yield strongly depends on mesomeric effects in the aryl iodides: The coupling of *ortho*-, *meta*- and *para*-iodotoluenes in the presence of 1 ppm of pincer palladium complex **6e** gave **7b**, **7c** and **7d** in isolated yields of 85, 98 and 65 %, respectively (Table 3, entries 8-10) corresponding to a turnover number (TON) of 9.84×10^5 for the *meta*-isomer. Good TONs were also observed for the coupling of butyl acrylate with *para*-iodoanisole (8.59×10^5) and *para*-iodoacetophenone (7.11×10^5) (Table 3, entries 11-12). Acceptor substituents in the aryl halide reduced the yield dramatically as demonstrated for the CF_3-derivative (Table 3, entry 13, 8 %). No significant steric effect was observed as shown for 1-iodonaphthalene which afforded a 96 % yield (9.63×10^5 TON) (Table 3, entry 14).

The efficiency of the catalyst was demonstrated in the coupling of *meta*-iodotoluene with butyl or methyl acrylates using a steadily reduced catalyst loading. A catalyst loading of 0.1 ppm of palladium pincer carbene complex **6** applied to butyl acrylate under standard conditions (Table 3,

entry 15) gave a 65% yield (TON: 6.53×10^6) while methyl acrylate afforded an 88 % isolated yield (TON: 8.84×10^6, Table 1, entry 16). The more reactive methyl acrylate even tolerated 1 ppb as a minimum loading of **6** to result in a still 1 3% isolated yield of **7i** (TON: 1.32×10^8; TOF: 5.50×10^6 /h or 1.53×10^3/sec).

Table 3

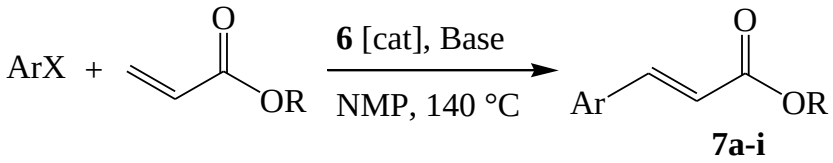

7a-i

Entry	ArX	R	Catalyst (mol %)	Base	Time (h)	Product	Yield (%)	TON
1	Iodobenzene	Bu	0.2	TEA	8	**7a**	98	495
2	Iodobenzene	Bu	0.2	*i*-Pr_2NEt	8	**7a**	99	497
3	Iodobenzene	Bu	0.2	$NaHCO_3$	8	**7a**	80	403
4	Iodobenzene	Bu	0.2	K_2CO_3	8	**7a**	>99	499
5	Bromobenzene	Bu	0.2	K_2CO_3	8	**7a**	99	498
6	Iodobenzene	Bu	0.0001	K_2CO_3	24	**7a**	94	9.38×10^5
7	Bromobenzene	Bu	0.0001	K_2CO_3	24	**7a**	27	2.70×10^5
8	2-Iodotoluene	Bu	0.0001	K_2CO_3	24	**7b**	85	8.49×10^5
9	3-Iodotoluene	Bu	0.0001	K_2CO_3	24	**7c**	98	9.84×10^5
10	4- Iodotoluene	Bu	0.0001	K_2CO_3	24	**7d**	65	6.52×10^5
11	4-Iodoanisole	Bu	0.0001	K_2CO_3	24	**7e**	85	8.59×10^5
12	4-Iodoacetophenone	Bu	0.0001	K_2CO_3	24	**7f**	71	7.11×10^5
13	4-Iodotrifluorobenzene	Bu	0.0001	K_2CO_3	24	**7g**	8	8.1×10^4
14	1-Iodonaphthalene	Bu	0.0001	K_2CO_3	24	**7h**	96	9.63×10^5
15	3-Iodotoluene	Bu	0.00001	K_2CO_3	24	**7c**	65	6.53×10^6
16	3-Iodotoluene	Me	0.00001	K_2CO_3	24	**7i**	88	8.84×10^6
17	3-Iodotoluene	Me	0.0000001	K_2CO_3	24	**7i**	13	1.32×10^8

The Heck reaction of 4-bromoanisole and styrene (K_2CO_3, refluxing DMA, 13 hours) applying a 2 ppm catalyst loading of complex **6** resulted in 67 % yield of arylated styrene (TON 3.36×10^5). A comparison with the highest TON (7.5×10^4) obtained with the pyridine-bridged and lutidine-bridged imidazolylidene [78] palladium analogues applied for the same reaction (even with 20 mol % *n*-Bu_4NBr as an additive) characterizes the pyridine-bridged CNC pincer bis-benzimidazolylidene complex **6** as distinctly more efficient reflecting its better σ-donor properties (electronic effect). In addition, steric factors may also account for the catalytic properties of complex **6** as the planar extended metal-ligand hybrid π-system may enhance the

catalytic activity owing to reduced bond angles in the twisted conformation at the metal center in comparison with its lutidine-bridged benzimidazolylidene analogues.[79]

V.1.2 Catalytical behavior towards Suzuki cross coupling

Under the same conditions palladium pincer complex **6** also efficiently catalyses the Suzuki coupling as demonstrated for aryl halides and phenyl boronic acid; a catalyst loading of 1 ppm resulted in 72 – 97 % isolated yields for the phenylation of iodobenzene and a series of *para*-halobenzenes (Table 4). As observed for the phenylation of 4-bromoacetophenone a comparison of pincer complex **6e** and its imidazolylidene analogue which gave a 88 % yield with 1 mol % catalyst loading and a 70 % yield with 0.2 mol % catalyst loading in dimethylacetamide (DMA) in 30 hours underlined that the catalytic activity is enhanced by the planar extension of the π-system. At 80 °C with 1 ppm catalyst loading, a 62 % yield of **8d** was obtained (Table 4, entry 4), whereas an elevated temperature of 110 °C [80] and a replacement of DMA for NMP as a solvent increased the yield to 78 % (Table 4, entry 5). Even in low loading the pincer complex catalyst **6e** tolerates a variety of substituents differing in their electronic and steric properties and allows for good yields of biphenyl derivatives **8a**-**e** (Table 4, entries 2-9). Nearly identical yields of **8d** were obtained under the same conditions using either 4-bromoacetophenone or 4-iodoacetophenone. However, also 12 % of homo-coupling product after full conversion (Table 4, entries 6, 7) was isolated. The coupling of 1-iodonaphthalene is similarly effective (Table 4, entry 9, 80 %) indicating that steric bulk does not hamper severely the cross-coupling even with a low catalyst loading of 1 ppm. Unlike observed in the Heck reactions, the Suzuki protocol tolerates a strong electron-withdrawing substituent such as in 4-iodo-trifluorobenzene (Table 4, entry 8, 90%). A further decrease of the catalyst loading to 1 ppb still resulted in a 25 % yield (Table 2, entry 10; TON: 2.48×10^8; TOF: 1.03×10^7 / h or 2.87×10^3/sec) for coupling with 4-iodoanisole and a 15 % isolated yield (Table 4, entry11; TON: 1.49×10^8; TOF: 6.21×10^6 /h or 1.72×10^3/sec) for reaction with 4-iodo-trifluorobenzene.

Table 4

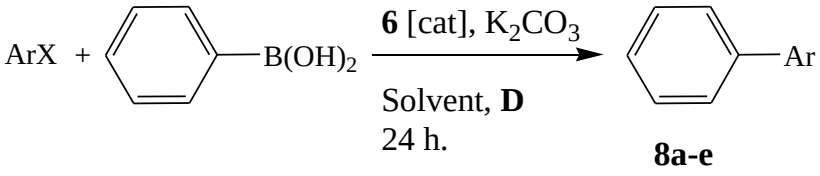

Entry	ArX	Catalyst (mol %)	Solvent	Temperature (°C)	Product	Yield (%)	TON
1	Iodobenzene	0.0001	NMP	140	**8a**	90	9.05×10^5
2	4-Iodotoluene	0.0001	NMP	140	**8b**	72	7.18×10^5
3	4-Iodoanisole	0.0001	NMP	140	**8c**	97	9.69×10^5
4	4-Bromoacetophenone	0.0001	NMP	80	**8d**	62	6.23×10^5
5	4-Bromoacetophenone	0.0001	DMA	110	**8d**	78	7.84×10^5
6	4-Bromoacetophenone	0.0001	NMP	140	**8d**	84	8.43×10^5
7	4-Iodoacetophenone	0.0001	NMP	140	**8d**	83	8.32×10^5
8	4-Iodo-trifluorobenzene	0.0001	NMP	140	**8e**	90	9.03×10^5
9	1-Iodonaphthalene	0.0001	NMP	140	**8f**	80	7.99×10^5
10	4-Iodoanisole	0.0000001	NMP	140	**8c**	25	2.48×10^8
11	4-Iodo-trifluorobenzene	0.0000001	NMP	140	**8e**	15	1.49×10^8

V.1.3 Conclusion

The pyridine-bridged bis-benzimidazolylidene CNC pincer palladium complex **6** which is readily accessible from cheap commercial precursors is an efficient catalyst for Heck and Suzuki cross-coupling reactions even with catalyst loadings as low as 0.1 to 1 ppm. It is stable against air, moisture and heat, and tolerates a variety of functional groups in the arene, varying in their electronic and steric properties, which suggests that the catalytic activity of this type of pincer complex is significantly enhanced by the planar extended metal ligand hybrid π-system.

V.2 Synthesis of conjugated pyridine-bridged bis-(imidazolylidene)-palladium complexes

The synthesis of conjugated pyridine-bridged bis-(imidazolylidene)-palladium complexes were prepared according to modified procedure. 2, 6-dibromo-4-(bromomethyl)-pyridine was prepared by a literature procedure [81] starting from citrazinic acid. Under Arbuzov conditions 2, 6-dibromo-4-(bromomethyl)-pyridine was treated with triethyl phosphite [82] at 140 ^{o}C for 25 mins. After cooling to room temperature, the reaction mixture was dried under vacuum and treated with 4-ethoxy benzaldehyde, potassium *tert*-butoxide in dry THF at room temperature for 24h leading to conjugated 2,6 dibromopyridine **9** as a white powder. The conjugated 2,6-bis-imidazolyl pyridine **10** was prepared through the cross-coupling reaction between imidazole and **9** catalyzed by CuI in dry DMF at 140 ^{o}C for 48 h. The coupling product underwent *N*-alkylation with *n*-alkyl halides in a sealed test tube while heated to 110 ^{o} C for 36h. The crude product was purified by re-precipitation from $CHCl_3$/Et_2O and followed by column chromatography leading to pale yellow solid **11a-b** (98 %). The conjugated pyridine-bridged bis-imidazolium halides underwent to palladation by treatment with palladium acetate in DMSO with stirring at room temperature under vacuum. The reaction mixture was warmed under stirring in an open vessel model at 160 °C for 25 min (at 40 W with a CEM Discover microwave instrument). DMSO was removed *in vacuum* under heating and the crude product was purified by re-precipitation from $CHCl_3$/ cold Et_2O. Another two re-precipitation operations afforded a yellow solid **12a-b** (75 %) (Scheme 3).

Scheme 3

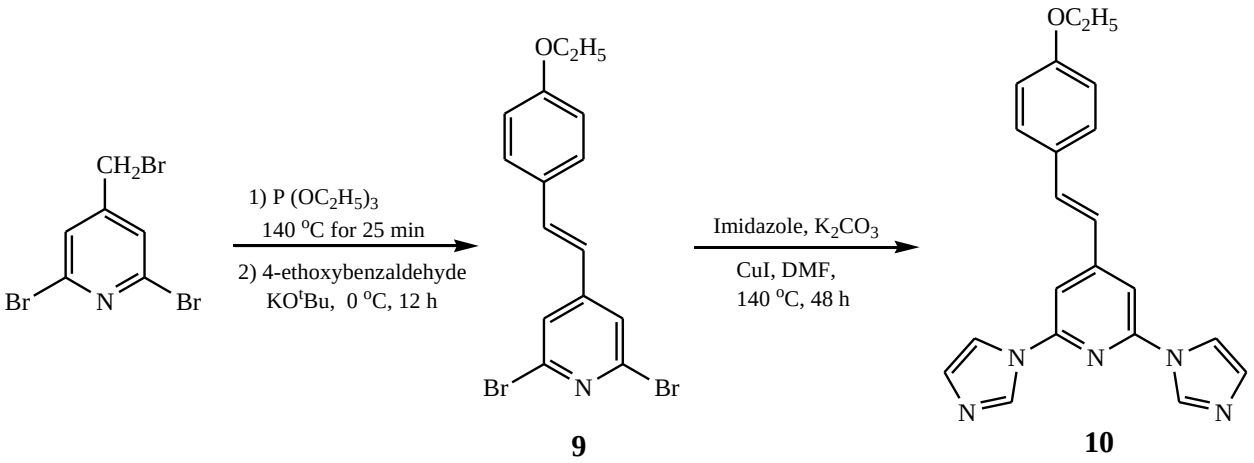

9 **10**

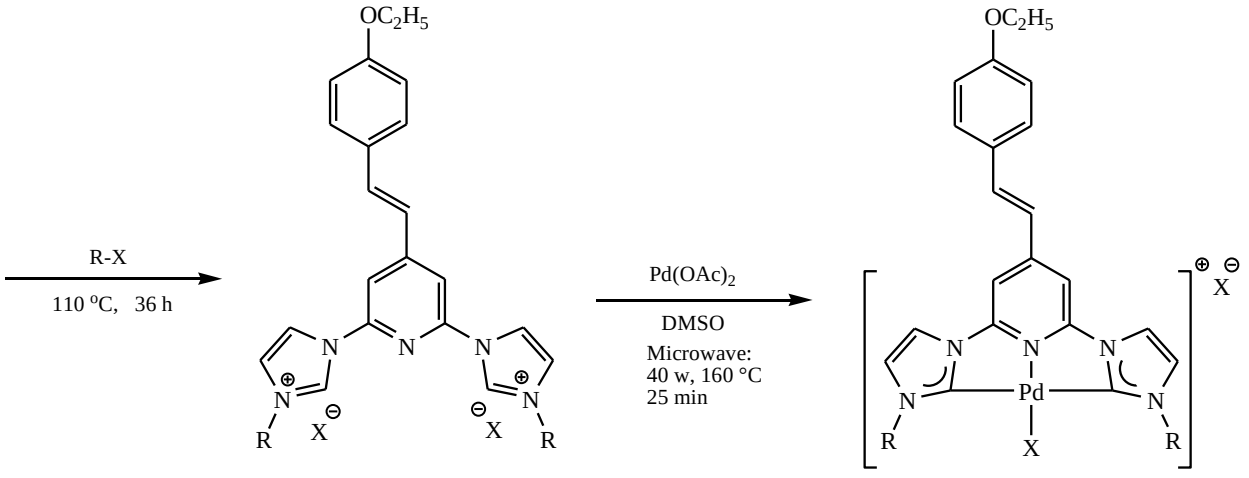

11a: R = C_4H_9, X = Br
11b: R = $C_{16}H_{33}$, X = I

12a: R = C_4H_9, X = Br
12b: R = $C_{16}H_{33}$, X = I

V.2.1 Gelation test with organic solvents

The gelation ability of pincer complex **12b** was studied by heating in a variety of organic solvents and subsequent cooling to room temperature. Complex **12b** forms thermo reversible swellable materials within a few hours. Gelation experiments with 2wt % gelator in a selection of protic and aprotic solvents are summarized in Table 5. A transparent gel was formed in DMSO, while turbid gels were formed in dimethylformamide (DMF), dimethylacetamide (DMA), N-methylpyrrolidone (NMP). Because of the poor solubility of **12b** in organic solvents, turbid gels were formed from pyridine, dioxane and chlorobenzene by adding 20 % DMSO. A partial gel was formed in acetone at room temperature, even after cooling to 5 ^{o}C. The color of the gels darkens with the increasing coordination ability of the solvents as observed for the gels formed by carbene complex **12b**. When the gelator concentration was decreased to 0.5 mg/mL, stable gels still could be formed with carbene complexes **12b** and DMSO, which could be stored at room temperature without any visible collapse.

Table 5. Gelation ability of conjugated CNC pincer complex **12b** in various solvents. [a]

Entry	Solvent	Phase	T_g[°C] [b]
1	DMSO	G	44 [c]
2	DMF	G	72
3	NMP	G	60
4	DMA	G	67
5	Pyridine	G*	61
6	Acetone	PG*	- [d]
7	Chlorobenzene	G*	50
8	Dioxane	G*	73
9	DCM	S	- [d]
10	Benzene	I	- [d]
11	THF	P	- [d]
12	MeOH	I	- [d]

[a] Gelator concentration: 2 wt%; G: gel formed at room temperature; S: Solution; P: Precipitate; I: Insoluble; G* or PG*: Gel or partial gel formed by adding 20% DMSO. [b] Determined by DSC. [c] 2 wt % in DMSO gel. [d] T_g could not be determined accurately by DSC.

However, a gel could not be formed with **12b** at 20 mg/mL in MeOH, reflecting their poor solubility even at reflux condition. Similar results were observed in case of the benzene, and dichloromethane. Because of the poor solubility of the palladium complex in tetrahydrofuran no gel was observed even after adding 20 % of DMSO. Even when the concentration was reduced to 1 wt %, stable gels were also formed from all the solvents.

V.2.2 Transmission electron microscopy

The morphology of xerogels obtained from different solvents (after evaporation of the solvent) was investigated by transmission electron microscopy (TEM). Selected typical 3D networks of xerogels demonstrated that morphologies obtained from different solvents are quite different (Figure 21). Larger fibers are present in xerogels obtained from acetone, chlorobenzene, dioxane, NMP and pyridine, while dense fiber networks result from DMF, DMA and DMSO.

In most cases, gels formed with palladium complex reveal twisted helical ribbon morphology at the microscopic level, which is quite rarely observed in gel networks formed from achiral gelators. Selected TEM images of gels with helical morphologies (*P* and *M*) formed by carbene

complex **12b** are presented in Figure 21. The dimensions of the individual fibers vary with the solvent used. Helical fibers that are about 100 nm wide and 200-1000 nm in pitch were observed in acetone (Figure 20a). More helical fibers with pitch of approximately 200 nm and 1000 nm in width appeared in the TEM image of xerogel **12b**/pyridine (Figure 20b). As shown in Figure 23c, a long and short of with thinner helical fibers about 100 nm was observed with gel **12b**/dioxane; A similar morphology was found with gel **12b**/DMF (Figure 20d). They are composed of tightly intertwined thinner fibers (around 10 nm wide); smaller helical ribbon morphologies, which are approximately 100 nm wide and several micrometers long with a pitch of approximately 500 nm, could be observed in the gel networks obtained from **12b**/DMA. A long, finer, and denser 3D network consisting of fibers, which are ca. 200 nm wide and 2 μm long, was formed in the gels from DMSO and chlorobenzene.

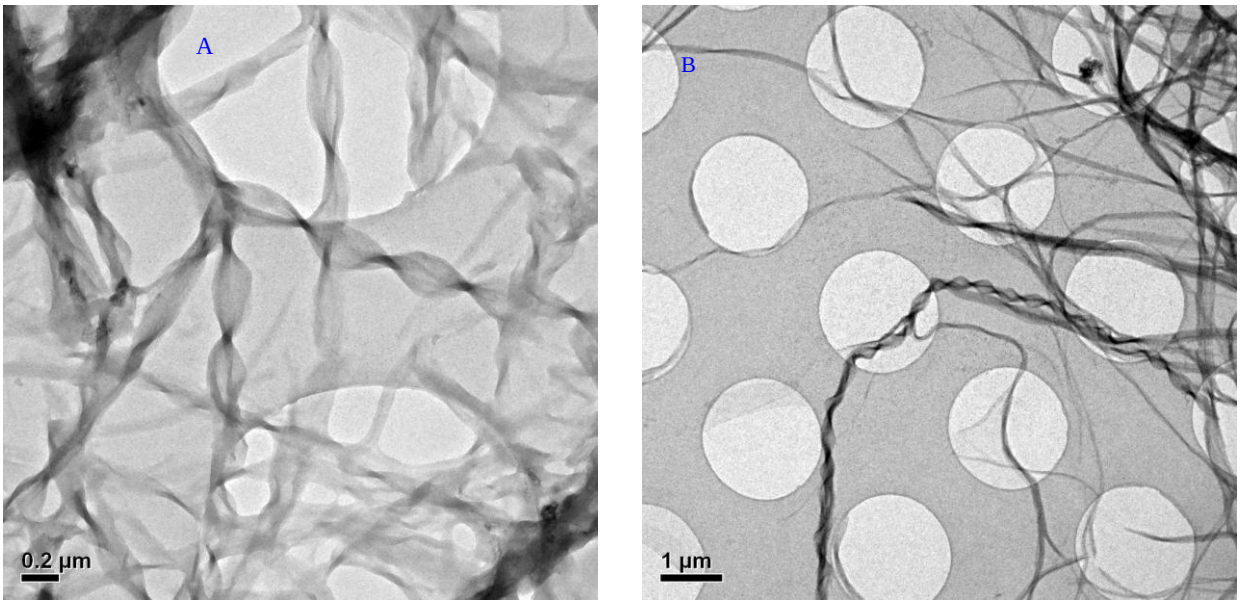

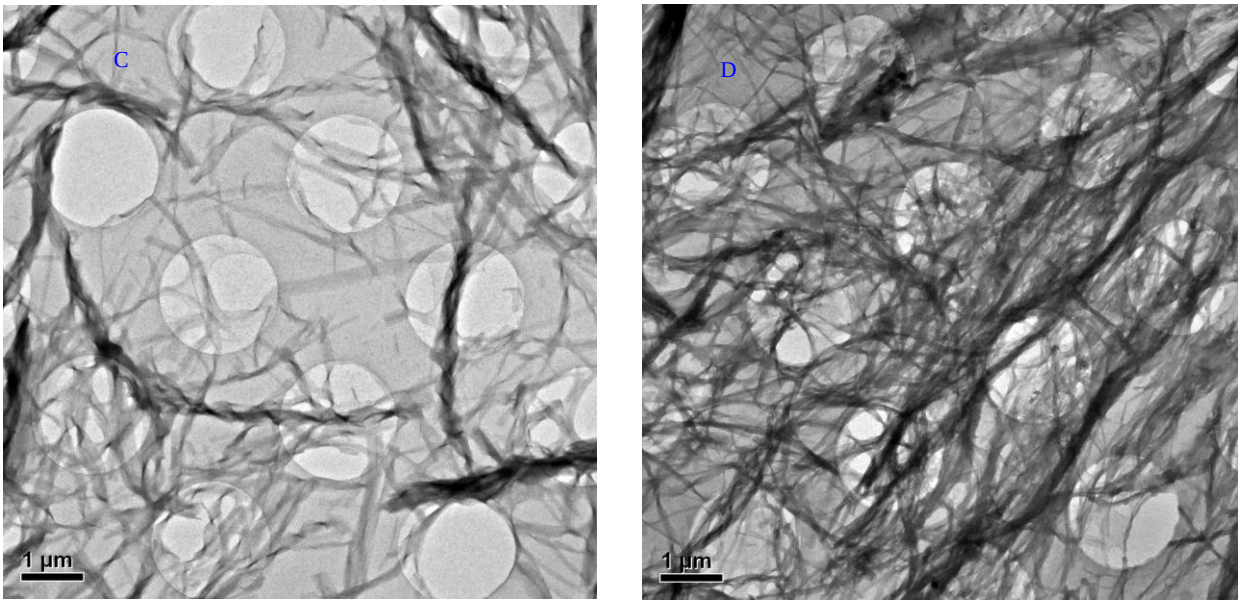

Figure 21. Selected TEM images of gels formed by pincer complex **12b** (concentration 3 wt %). a) Acetone; b) Pyridine; c) Dioxane; d) DMF.

V.2.3 Thermal stability of the gels

The gel–sol phase-transition temperatures (T_g) of gels in selected solvents were determined by differential scanning calorimetry (DSC; Table 5). The DSC thermograms revealed well-defined thermo-reversible gel–sol transitions with accurate T_g and enthalpy parameters, which indicate that the 3D networks responsible for gelation are built up by non-covalent interactions, such as π-stacking, hydrogen bonding and van der Waals interactions. The DSC thermograms recorded for gel **12b**/DMF (3 wt %) revealed well-defined thermo reversible sol-gel transitions with unchanged T_g (72 ^oC) and enthalpy parameters (ΔH = 2 Jg^{-1}). In all tested gels, the gel–sol phase-transition temperatures ($T_{g/H}$) were found to be approximately 15 ^oC higher than those observed for the sol–gel conversion ($T_{g/C}$), a hysteresis behavior which is characteristic of LMMGs. At 3 wt% concentration, the T_g values obtained for Chlorobenzene, pyridine, dioxane and DMSO were corroborated by the "dropping ball method". $T_{g/H}$ and $T_{g/C}$ increase with increasing concentration of gelator **12b** in different solvents, which demonstrates that the stability of the gel increases with gelator concentration. (SAXS measurements will be obtained by collaboration with Prof. Herwig Peterlik)

V.2.4 Conclusion

The conjugate palladium pincer carbene complexes **12a, b** was readily accessible from commercially available starting materials in quantitative yields. The complex **12b** showed a strong gelation effect in polar solvents. A stable and transparent gel was observed in DMSO at 0.5 wt % complex loading, while thermal stability of the gel increased with the gelator concentration.

V.3 Synthesis of conjugated pyridine-bridged bis-(benzimidazolylidene)-palladium complexes

The synthesis of conjugated pyridine-bridged bis-(benzimidazolylidene)-palladium complexes was performed according to our modified procedure. The conjugated 2, 6-bis-benzimidazolyl pyridine **13** was prepared through the cross-coupling reaction between benzimidazole and **9** catalyzed by CuI in dry DMF at 140 ^{o}C for 48 h. The coupling product underwent *N*-alkylation with *n*-alkyl halides (DMF was used in case of *n*-butyl bromide) in a sealed test tube and heated to 110 ^{o}C for 36 h. The crude product was purified by re-precipitation from $CHCl_3$/Et_2O and then by column chromatography leading to a pale yellow solid **14a-b** (98%). The conjugated pyridine-bridged bis-benzimidazolium halides underwent palladation by treatment with palladium acetate in DMSO and stirring at room temperature under vacuum. The reaction mixture was warmed under stirring in an open vessel model at 160 °C for 25 min (at 40 W with a CEM Discover microwave instrument). DMSO was removed *in vacuo* under heating and the crude product was purified by re-precipitation from $CHCl_3$/cold Et_2O. Another two re-precipitation operations afforded a yellow solid of **15a-b** (55%) (Scheme 4).

Scheme 4

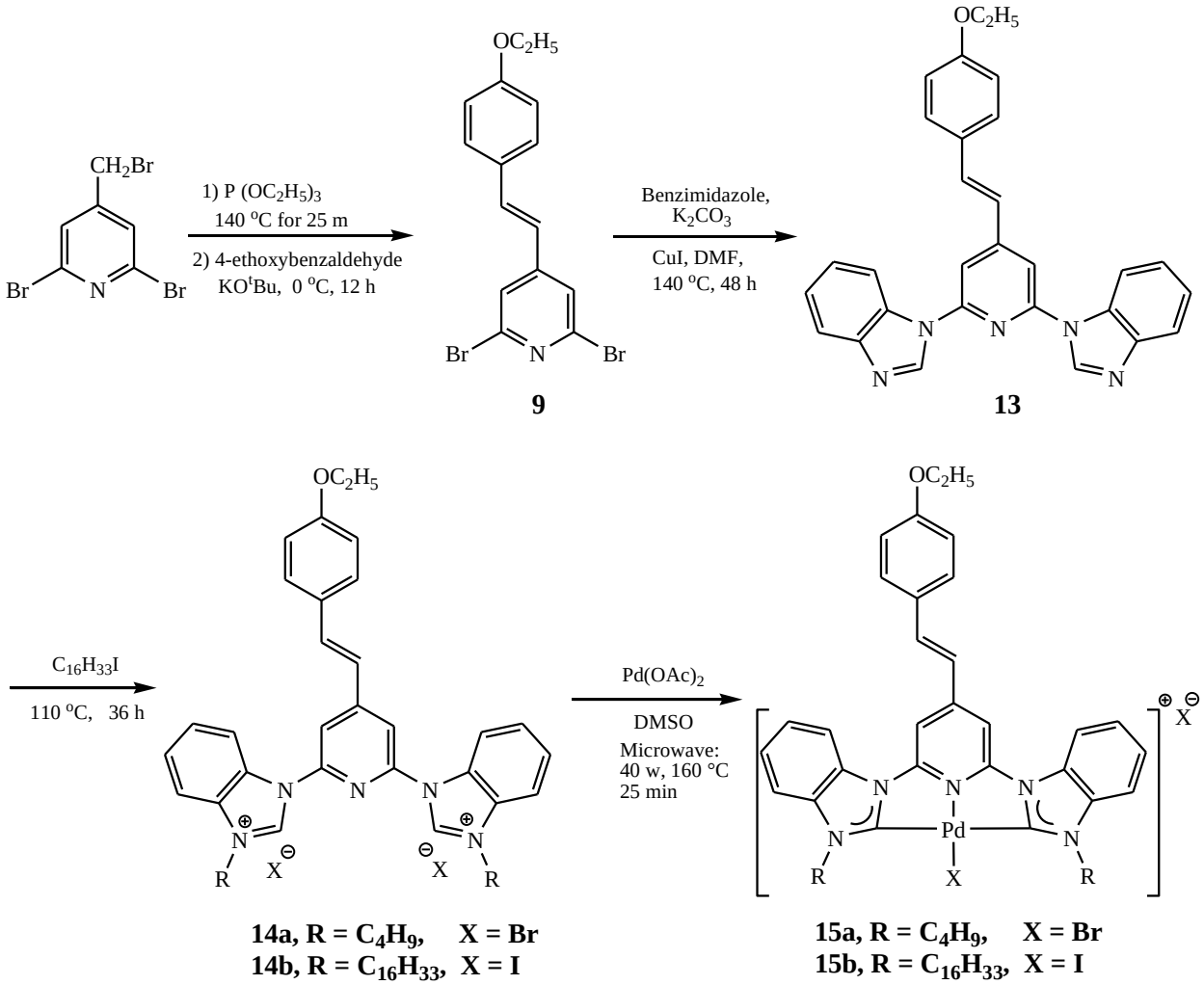

V.3.1 Gelation test with organic solvents

The gelation ability of pincer complex **15b** was studied by heating in a variety of organic solvents and subsequent cooling to room temperature. Complex **15b** forms thermo reversible swellable materials within a few hours. Gelation experiments with 1 wt % gelator in a selection of protic and aprotic solvents are summarized in Table 6. A transparent gel was formed in DMSO with 1 wt % complex loading. Strong and turbid gels were formed from dimethylformamide (DMF), dimethylacetamide (DMA), N-methylpyrrolidone (NMP), and benzonitrile. Because of the lower solubility of **15b** in organic solvents, only partial gels were formed from pyridine and acetone even after the addition of 20% DMSO. A partial gel was formed in dichloromethane (DCM) at

room temperature, while upon cooling to 5 ^{o}C a strong gel was observed. A partial gel was observed in methanol, and cyclohexanol, but a strong gel was formed in EtOH and n-butanol with 2 wt %. The color of the gels darkens with the increasing coordination ability of the solvents as observed for the gels formed with carbene complex **15b**. When the gelator concentration was decreased to 0.3 mg/mL, stable gels still could be formed with carbene complex **15b** in DMSO, these could be stored at room temperature without any visible collapse.

Table 6. Gelation ability of conjugated CNC pincer complex **15b** in various solvents. [a]

Entry	Solvent	Phase	T_g[^{o}C] [b]
1	DMSO	G	76[c]
2	DMF	G	71
3	NMP	G	48
4	DMA	G	53
5	Pyridine	PG*	-- [d]
6	Acetone	PG*	-- [d]
7	EtOH	G	50
8	Dioxane	S	--
9	DCM	G	34[e]
10	Benzene	I	--
11	THF	P	--
12	MeOH	PG	
13	n-BuOH	G	54[e]
14	Cyclohexanol	PG	-- [d]
15	Benzonitrile	G	43

[a] Gelator concentration: 2 wt%; G: gel formed at room temperature; S: Solution; P: Precipitate; I: Insoluble; G* or PG*: Gel or partial gel formed by adding 20% DMSO. [b] Determined by DSC. [c] 1 wt % gel formed in DMSO. [d] T_g could not be determined accurately by DSC. [e] T_g was determined by dropping ball method.

The effect of gelation mainly depends upon π-π stacking, van der Waals and metal-metal interactions. Because of the conjugation at γ-position of the pyridine ring, the electron density at the Pd atom will increase. It also effects the gelation ability of the complex **15b** in different organic solvents.

V.3.2 Transmission electron microscopy

The morphology of xerogels obtained from different solvents (after evaporation of the solvent) was investigated by transmission electron microscopy (TEM). Selected typical 3D networks of

xerogels demonstrated that morphologies obtained are quite different in protic solvents compared to aprotic solvents. (Figure 22).

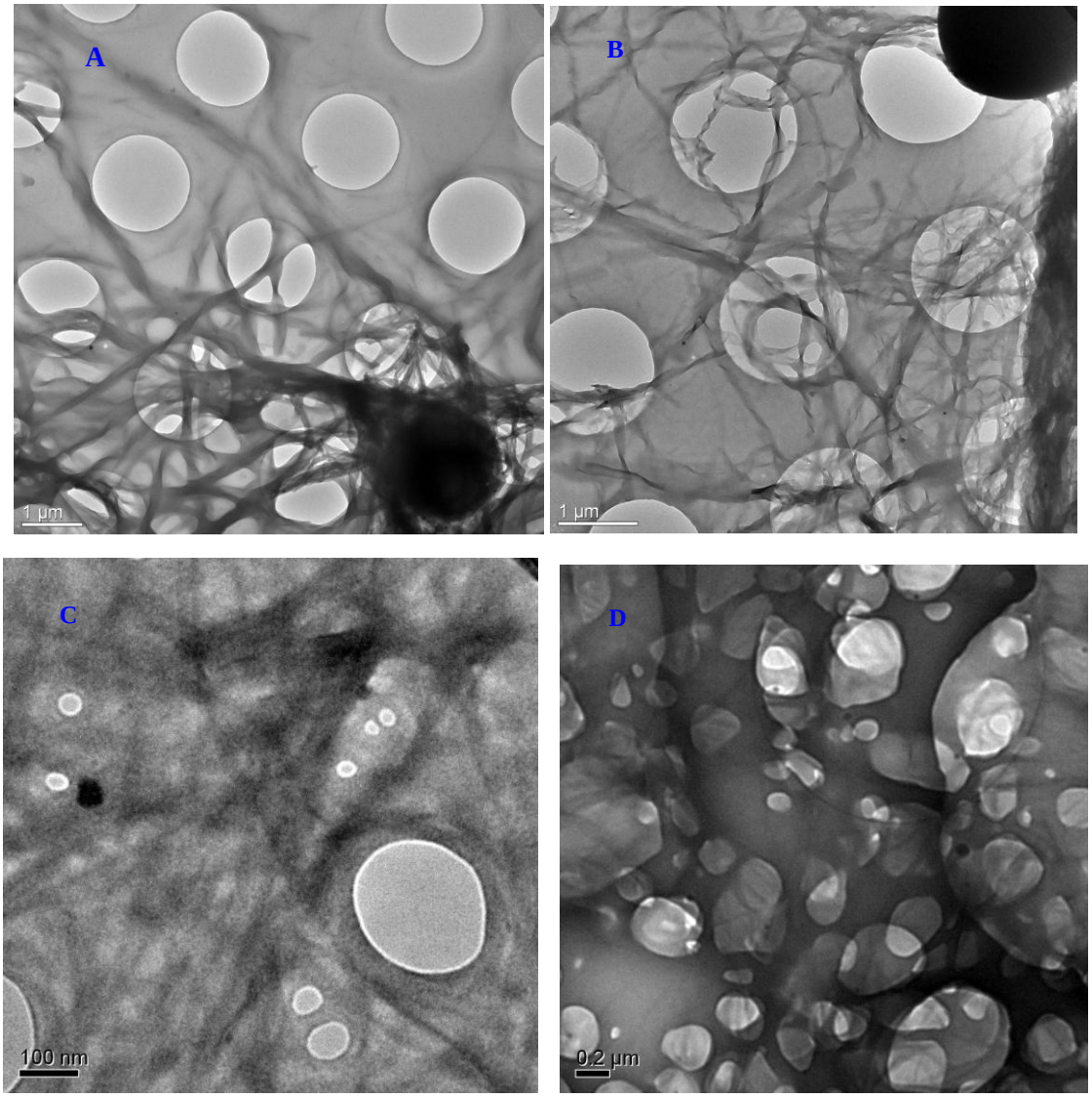

Figure 22. Selected TEM images of gels formed by pincer complex **15b** (concentration 1 wt %). A) EtOH, B) MeOH, C) Pyridine, D) CH_2Cl_2

In most cases, gels were formed with palladium complex **15b** in aprotic solvents showing denser networks consisting of longer and finer fibers. Selected TEM images of gels with helical morphologies (*P* and *M*) formed by carbene complex **15b** are presented in Figure 22. Helical fibers of both *P* and *M* and approximately 1000 nm in width were observed in **15b**/EtOH (Figure 22a), which is quite rarely observed in gel networks formed from achiral gelators. Similar kinds of gel 3D networks are observed in **15b**/MeOH with pitch of 200-1000 nm (Figure 22b). A

mixture of long and short thin fibers of about 100 nm width was observed in MeOH. A strong π-π stacking, van-der-Waals and metal-metal interaction at the orthogonal direction are playing the key role to form a thin film denser fiber gel networks were observed in aprotic solvents in DMSO, DMF, DMA, NMP and benzonitrile. As shown in Figure 22c, a denser fibers network with a pitch of 100 nm in width appeared in the TEM image of xerogel **15b**/pyridine. A width of 200 nm highly denser fiber networks was observed in **15b**/CH_2Cl_2 (Figure 22d).

V.3.3 Thermal stability of the gels

The gel–sol phase-transition temperatures (T_g) of gels in selected solvents were determined by both differential scanning calorimetry (DSC; Table 6) and dropping ball method. The DSC thermograms revealed well-defined thermo-reversible gel–sol transitions with accurate T_g and enthalpy parameters, which indicate that the 3D networks responsible for gelation are built up by non-covalent interactions, such as π- stacking, hydrogen bonding and van der Waals interactions. Compared to conjugated pyridine bridged bis-imadazolylidene complex **12b**, the extended π-stacking bis-benzimadazolylidene complex **15b**, will offer more π-stacking at orthogonal direction which may increase thermo stability of the gelator. The DSC thermograms recorded for gel **15b**/DMF (2 wt %) revealed well-defined thermo reversible sol-gel transitions with unchanged T_g (71 ^oC) and enthalpy parameters (ΔH = 2 Jg^{-1}). In all tested gels, the gel–sol phase-transition temperatures ($T_{g/H}$) were found to be approximately 15 ^oC higher than those observed for the sol–gel conversion ($T_{g/C}$), a hysteresis behavior which is characteristic of LMMGs. At 2 wt % concentration, the T_g values obtained for dichloromethane and n-butanol were corroborated by the "dropping ball method". $T_{g/H}$ and $T_{g/C}$ increase with increasing concentration of gelator **15b** in different solvents, which demonstrates that the stability of the gel increases with gelator concentration. (SAXS measurements will be obtained by collaboration with Prof. Herwig Peterlik)

V.3.4. Conclusion

The extended conjugated pyridine bridged bis-benzimadazolylidene palladium complex **15b** was readily accessible from cheap starting materials with quantitative yields. Compared to conjugated pyridine-bridged bis-imdazolylidene palladium complex **12b**, the extended π- stacking bis-benzimadazolylidene palladium complex **15b** are thermally more stable. A stable and transparent gel was observed in DMSO at 0.3 wt % complex loading, while thermal stability of the gel will increase by gelator concentration.

V.4 Synthesis of highly conjugated pyridine-bridged bis-benzimidazolium salts

In recent years oligo(*p*-phenylene vinylene)s (OPV) have been investigated for use in solar cells and light emitting diodes (LEDs) due to their stability, high luminescent efficiency, and ease of synthesis. One approach to control nanoscale structure of conjugated materials has been to design molecules that could exhibit thermo tropic or lyotropic liquid crystalline (LC) behavior.[83]

The synthesis of highly extended conjugated oligovinylene pyridine bridged bis-benzimidazolium salts was performed according to our modified procedure. Under Arbuzov conditions, 4-ethoxy benzyl bromide was treated with triethyl phosphite at 140 ^{o}C for 4 h, excess triethyl phosphite was distilled off. After cooling to room temperature, the reaction mixture was dried under vacuum and treated with 4-(diethoxymethyl)-benzaldehyde, potassium *tert*-butoxide in dry THF at room temperature for 24h. The reaction mixture was treated with 3N HCl at room temperature for another 12h leading to conjugated benzaldehyde **16** as a white powder. Under similar Arbuzov conditions, 2, 6-dibromo-4-(bromomethyl)-pyridine was treated with triethyl phosphite at 140 ^{o}C for 25 mins. After cooling to room temperature, the reaction mixture was dried under vacuum and treated with **16**, potassium *tert*-butoxide in dry THF at room temperature for 24 h leading to highly conjugated oligovinylene 2,6-dibromopyridine **17** as a yellow powder. The highly conjugated 2, 6-bis-benzimdazolyl pyridine **18** was prepared through the cross-coupling reaction between benzimidazole and **17** catalyzed by CuI in dry DMF 140 ^{o}C for 72 h. The coupling product under went *N*-alkylation with *n*-$C_{16}H_{33}I$ in a sealed test tube, heated to 140 ^{o}C

for 36 h. The crude product was purified by re-precipitation from $CHCl_3/Et_2O$, followed by column chromatography leading to yellow solid **19** (98 %) (Scheme 5).

Scheme 5

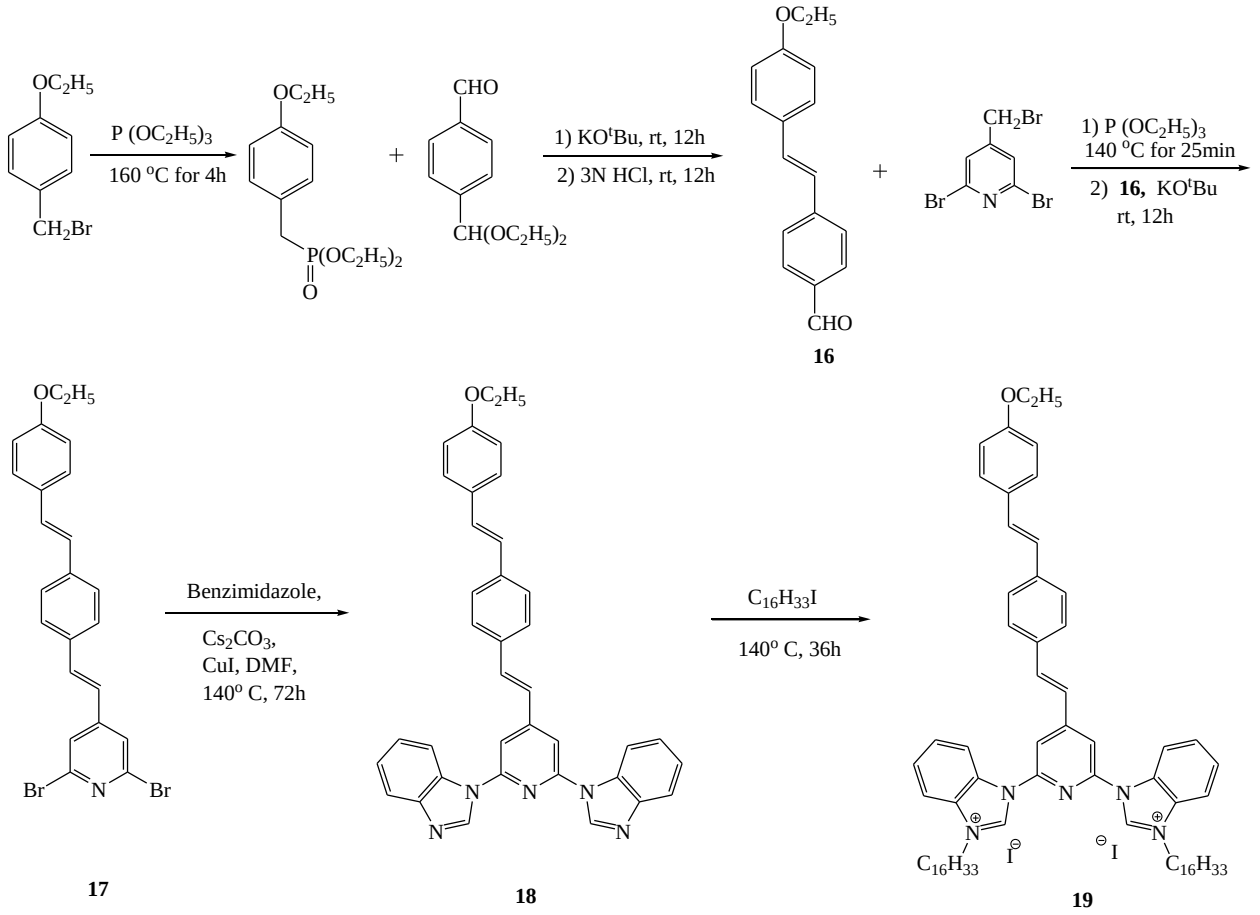

V.4.1 Polarized optical microscopic measurements & DSC studies of 19

The OPV pyridine bridged bis-benzimidazolium salts **19** was found to be a thermotropic liquid crystalline type of material. The self-assembly of the small OPV molecules is supposed to be packing based on π-π stacking, dipole-dipole and van der Waals interactions. The mesomorphic properties of compound **19** was investigated by differential scanning calorimetry (DSC), polarizing optical microscopy (POM) and small angle X-ray scattering (SAXS).

Liquid crystalline behavior of the OPVs was studied using a polarizing optical microscopy attached with a temperature programmable hot stage. The POM image of **19** is shown in Figure 24. A Fan- shaped texture was observed at 200 ^{o}C under crossed polarizers upon heating from room temperature. The sample melted isotropically at 246 ^{o}C, upon cooling from the isotropic phase to 200 ^{o}C no texture was observed due to decomposition. ^{1}H NMR spectra suggest a polymerisation of double bonds leads to amorphous material, excluding any thermoreversibility.

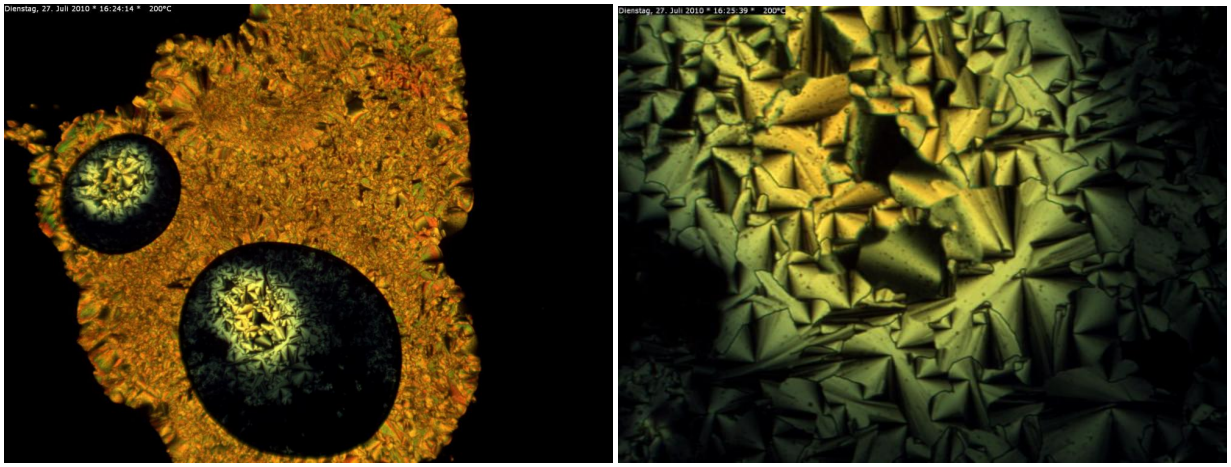

Figure 24: POM images of **19** at 200 ^{o}C.

A typical DSC curve is shown in Figure 23. The compound **19** was heated to melt at 10 °C/min, kept isothermally 20 °C above their isotropic temperature for 2-3 min, and subsequently cooled to room temperature at 10 °C/min. The heating graphs starts from room temperature to the isotropic point and the cooling graph from the isotropic point to room temperature. In the heating phase a crystal to crystal transitions was observed around 54 ^{o}C. The strong endotherm at at 246 ^{o}C indicates decomposition of sample leading to a color change from yellow to dark red. In the subsequent cooling phase the compound did not reveal any crystal to crystal transition due to strong electronic rich and active double bonds under going to polymerization. (SAXS measurements will be obtained by collaboration with Prof. Herwig Peterlik)

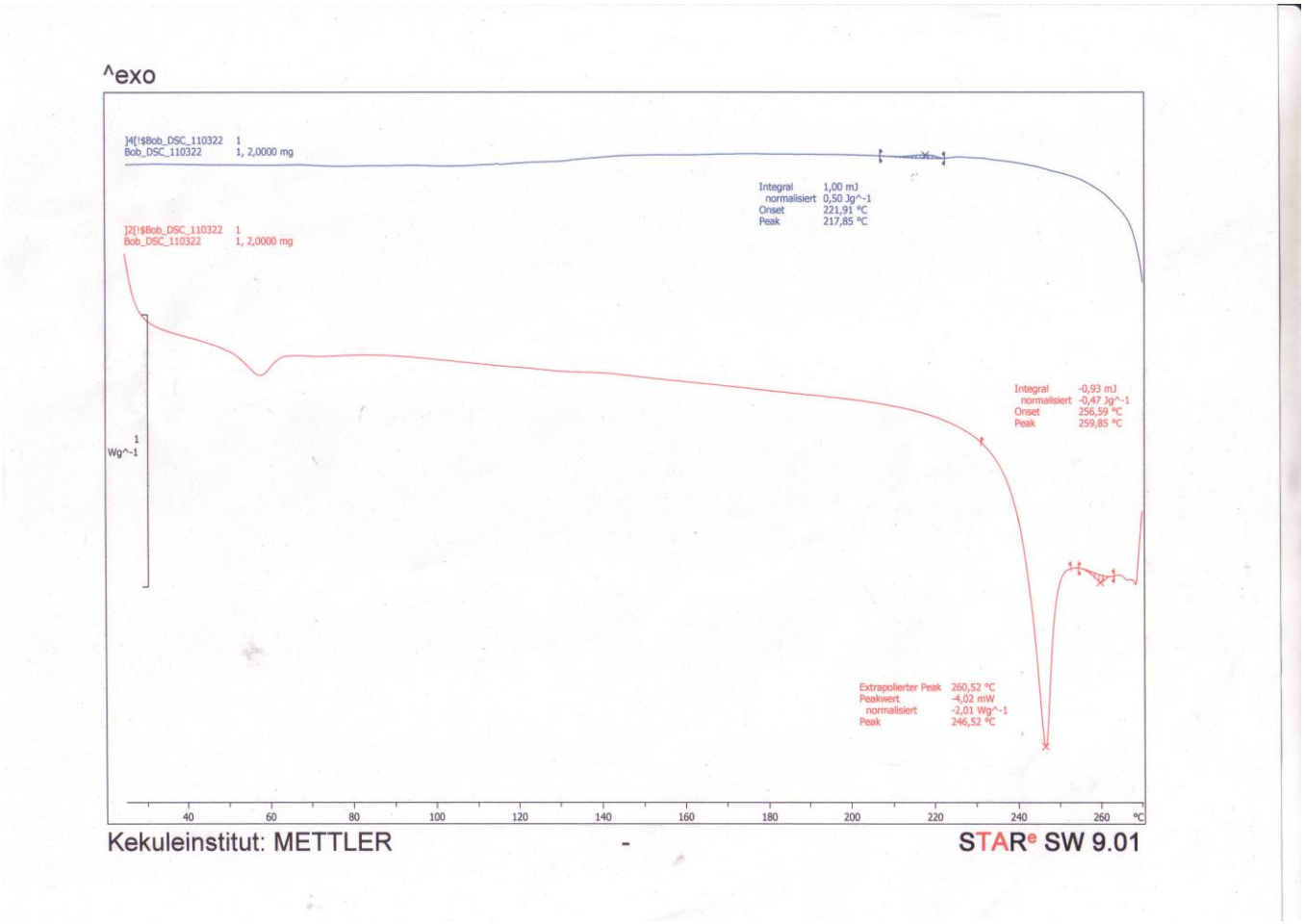

Figure 23: DSC studies of **19**

V.4.3 Conclusion

A novel conjugated oligo vinylene pyridine-bridged bis-benzimidazolium salts was systhesised from commercially available starting materials. The electron rich material shows liquid crystalline type behavior at 200 ^{o}C, when heated to the isotropic phase the compound underwent polymerisation behaving like a plastic crystalline material excluding any thermoreversibility.

V.5 Synthesis of highly conjugated pyridine-bridged bis-imidazolium salts

Conjugated organic materials have attracted considerable attention in recent years due to numerous potential applications in various fields such as light-emitting diodes, [84] photovoltaic cells,[85] optical power limiting,[86] three-dimensional microfabrication,[87] and two-photon laser scanning fluorescence imaging.[88] To date, many types of organic materials have been designed and fabricated for this purpose, most of which have a linear molecular shape, such as oligo(phenylenevinylene) (OPV),[89] oligo(*p*-phenylene) (OPP),[90] oligo- (phenyleneethynylene) (OPE),[91] and oligo(thiophene) (OT).[92] Their particular electronic properties led us to the design of a conjugated organic oligo *p*-phenylene vinylene (OPV) molecule based on *p*-phenylene motifs linked together through double bonds. Such a novel molecular structure may lead to promising applications for light-emitting and nonlinear optical devices.[93]

Due to lack of the hydrophobic interaction of the vinylene moiety the highly conjugated pyridine bridged bis-benzimidazolium salt **19** underwent decomposition at higher temperature, caused by the highly reactive olephenic double bonds. The introduction of additional noncovalent forces at the side chains was expected to assist the van der Waals interactions of the long alkyl chains favoring the self-organization into more complex nanosised structures. Similar intermolecular forces can originate from hydrogen bonds, dipole- or ionic interactions and π-π stacking leading to generate novel functional materials, which highly act as thermo reversible liquid crystalline materials.

The oligo (phenylenevinylene) pyridine bridged bis-imidazolium salt **28** was performed according to modified procedure. Compound **22** was synthesised according to the reported procedure and under Arbuzov conditions. Compound **22** was treated with triethyl phosphite at 140 ^{o}C for 4 h, excess triethyl phosphite was distilled off. After cooling to room temperature, the reaction mixture was dried under vacuum and treated with **20**, potassium *tert*-butoxide in dry THF at room temperature for 24h leading to conjugated derivative **24** as a white solid. The

conjugated bromo compound **24** was converted into aldehyde by treated with *n*-butyl lithium in dry diethyl ether/ THF at room temperature for 12h to afford **25** as a yellow solid (Scheme 6).

Scheme 6

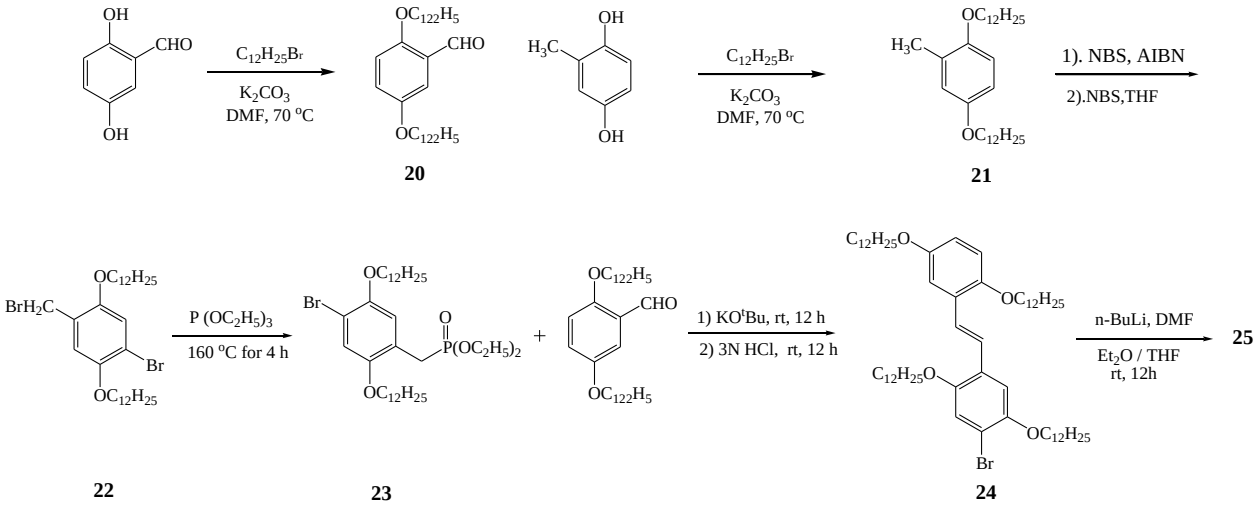

Under Arbuzov conditions, 2, 6- dibromo-4-(bromomethyl) pyridine was treated with triehtyl phosphite at 140 °C for 25 mins. After cooling to room temperature, the reaction mixture was dried under vacuum and treated with conjugated vinyl benzaldehyde **25**, potassium *tert*-butoxide in dry THF at room temperature for 24 h leading to highly conjugated oligo (polyvinylene) 2, 6-dibromopyridine **26** as a yellow powder. The coupling product **27** was prepared through the cross-coupling reaction between imidazole and **26** catalysed by CuI in dry DMF at 140 °C for 72 h; the crude product was purified by column chromatography leading to red solid **27**. The coupling product under went *N*-alkylation with *n*-butyl bromide in a sealed test tube heated to 100 °C for 36 h. The reaction mixture was cooled to room temperature, followed by re-precipitation from $CHCl_3/Et_2O$ leading to dark red solid **28** (98 %) (Scheme 7).

Scheme 7

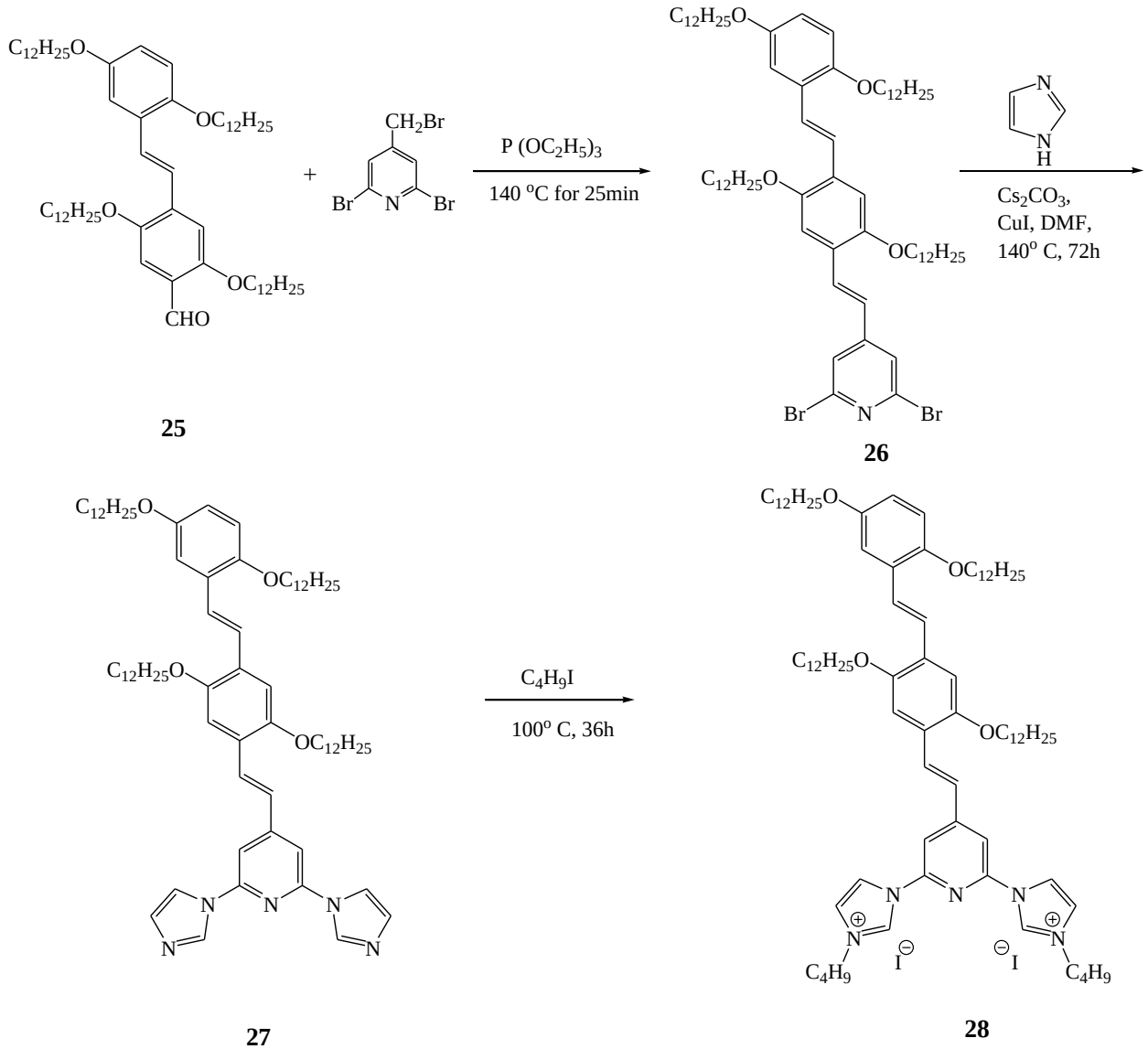

V.5.1 Polarized optical microscopic measurements & DSC studies of 28

The salt **28** was tested for liquid crystalline properties by a differential scanning calorimetry (DSC), polarizing optical microscopy (POM) and small angle X-ray scattering (SAXS).

Liquid crystalline behavior of the OPVs was studied using a polarizing optical microscopy attached with a temperature programmable hot stage. The POM image of **28** was shown in Figure

26; it was obtained during the heating from room temperature to the isotropic point. Within a temperature window between 88 ^{o}C and 134 ^{o}C characteristic textures were observed indicating for liquid crystalline behavior. While cooling from the isotropic phase to 100 ^{o}C again similar kinds of textures were observed. Due to strong π-stacking of oligovinylene salt are stable against air, moisture and high temperatures. More over this liquid crystalline material are shows thermoreversible property.

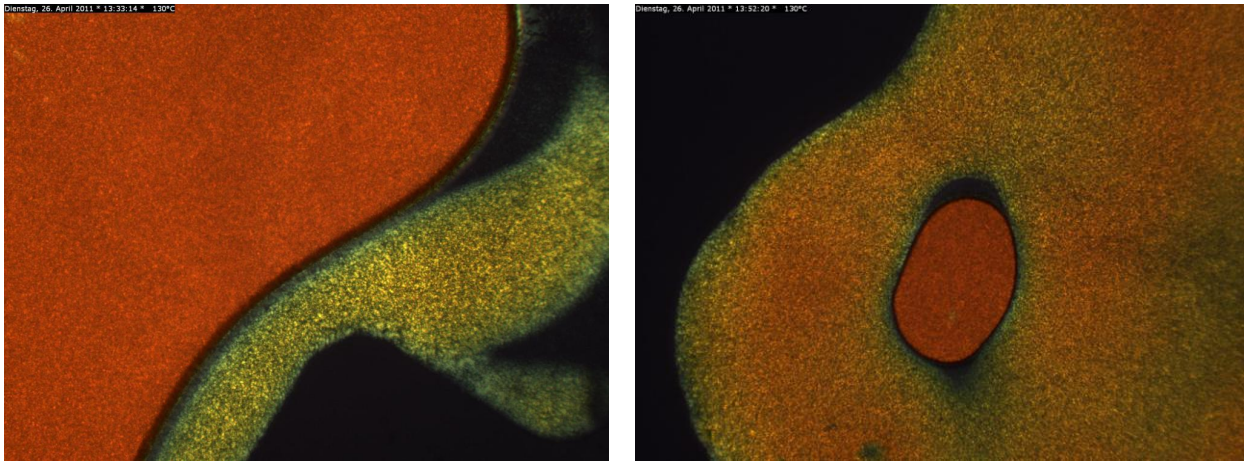

Figure 26: POM images of 28 at 134 ^{o}C.

A typical DSC curve is shown in Figure 23. The compound **28** was heated to melt at 10 °C/min, kept isothermally 20 °C above their isotropic temperature for 2-3 min, and subsequently cooled to room temperature at 10 °C/min. The heating graphs starts from room temperature to the isotropic point and the cooling graph from the isotropic point to room temperature. In the DSC study during the heating phase a crystal to liquid crystal transition was observed around 71 ^{o}C and isotropic melting was found at 144 ^{o}C (Figure 25). Because of the strong π-π stacking, ionic and van der Waals interactions in the conjugated oligo vinylene salt a liquid crystalline behavior was observed around 100 ^{o}C. Subsequently in the cooling phase the material underwent an isotropic phase to liquid crystalline phase transition at 134 ^{o}C. When the material was cooled down to room temperature it appeared as a brown-red film. The highly stable oligovinylene salt displays thermoreversible liquid crystalline property, even after several scannings. The overall DSC analysis revealed that **28** was a very good LC material and possessed large LC temperature window both in cooling and heating cycles. It is very important to note that the LC behavior of OPVs is not easily predictable and is highly dependent on the type of rigid or flexible side chains

attached on the middle and outer aromatic rings. (SAXS measurements will be obtained by collaboration with Prof. Herwig Peterlik)

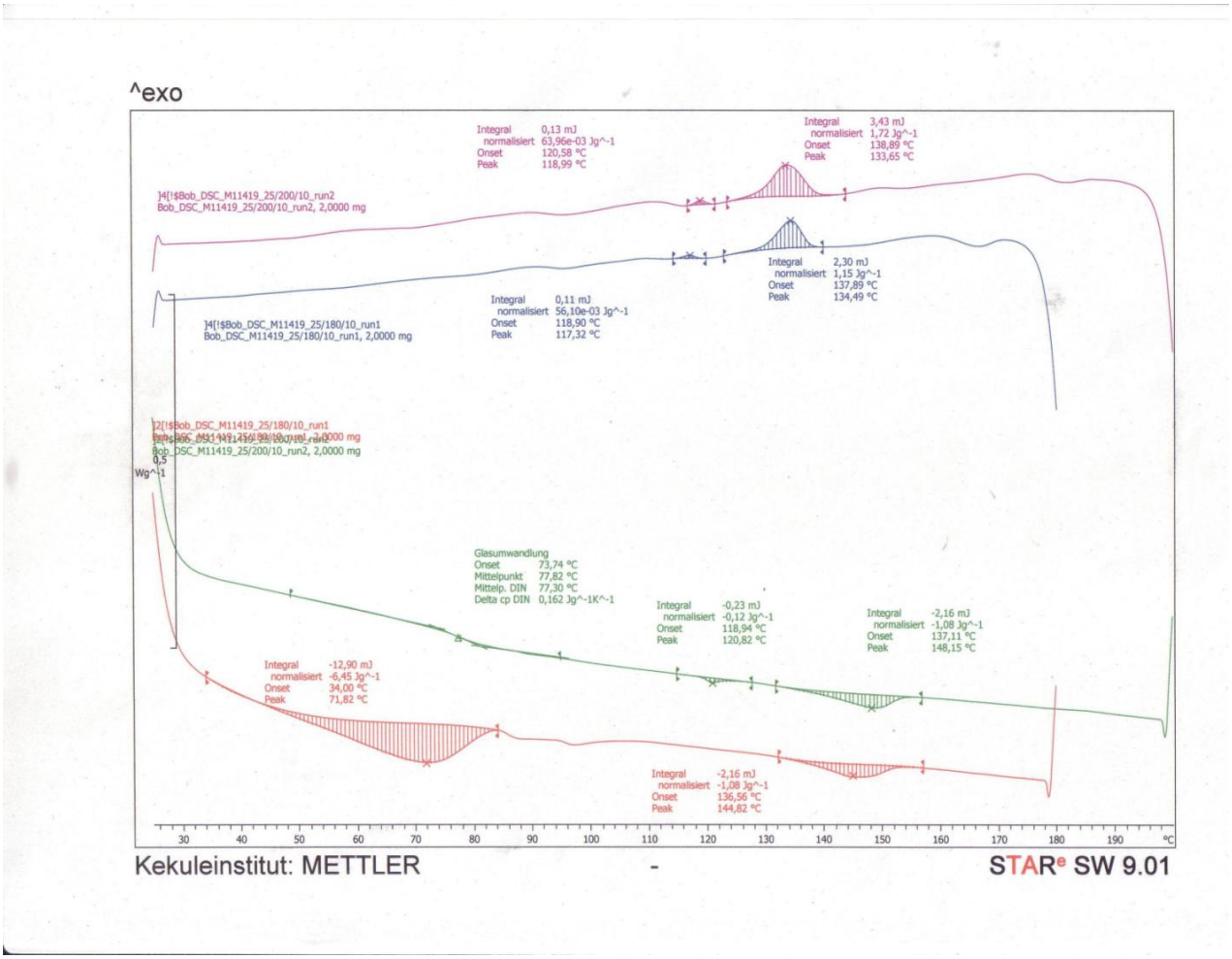

Figure 25: DSC studies of **22**.

V.5.2. Conclusion

A novel highly conjugated pyridine-bridged bis-imidizolium salt **28** was synthesised from materials accessible according to a modified procedure. Due to strong π-stacking favoring towards the self-assembly of the oligo vinylenes salts by three-dimensional format showing to liquid crystalline property. This new class of versatile functional material is stable against air, moisture and heat and shows thermoreversible liquid crystalline properties.

V.6 Synthesis of novel pyridine-bridged bis-perimidinium salts and palladium complexes

N-Heterocyclic carbenes (NHC´s) are known as strong σ-donor and weak π-acceptor ligands, and as such their metal complexes are widely applied in catalysis and material sciences. They increasingly compete successfully with phosphines in terms of compatibility with aerobic conditions, thermo stability and environmental friendliness. In this respect, ylidenes derived from five-membered heterocycles such as imidazolium and benzimidazolium salts, have been developed as typical skeletons of stable NHC´s, and have been successfully applied as ligands in transition-metal catalysed reactions. Ylidenes derived from perimidinium salts provide arene-fused six-membered heterocycles, and thus, represent a novel type of NHC framework which results in stronger σ-donor ability in comparison with *N*-heterocyclic carbenes derived from (benz) imidazolium salts. Therefore, we started to exploit the potential of perimidine-based NHCs in transition-metal catalysed transformations, an approach which has been paid less attention to so far.

Palladium bridged pincer bis-(perimidiniumyidene) carbene complexes **32** are accessible easily from commercially available starting materials. 2,6-Bis-perimidinum pyridine was prepared through cross coupling reaction between 2,6-dibromo pyridine and perimidine by catalyzed by a copper complex (CuI and Ligand **29**) in dry DMF at 140 ^{o}C for 72 h, followed by *N*-alkylation with alkyl iodides in a sealed test tube in DMF affording the bispermidinium salt **31** in almost quantitative yield. With our standard procedure, the Pyridine-bridged bis-permidinium iodide was subjected to palladation by treatment of palladium acetate in DMSO after stirring at room temperature under vacuum. The reaction mixture was warmed under stirring in open vessel model at 160 °C for 25 min (at 40 W with a CEM Discover microwave instrument). The acetate anion is acting as a mild base abstracting the carbene proton atom and generating an *in-situ* carbene. This carbene moiety was stabilised by intramolecular delocalisation and converting as a urea type molecule. However, no cyclometalation product **32** was formed (Scheme 8).

Scheme 8

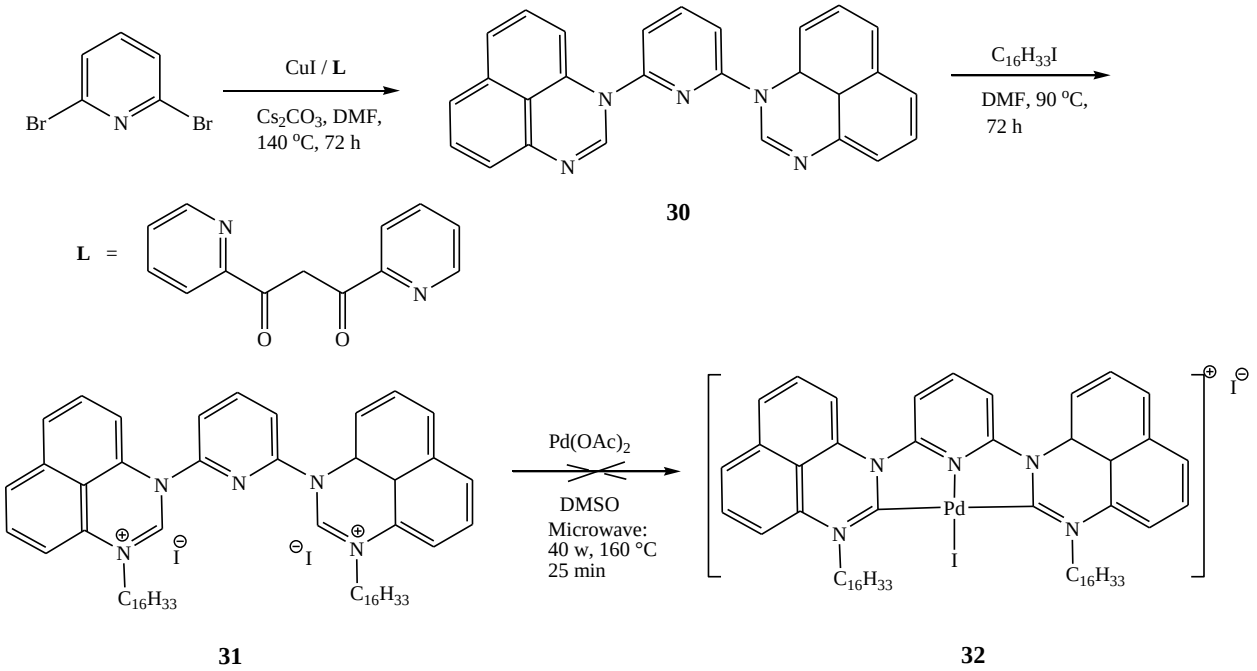

V.6.1 Conclusion

In conclusion the pyridine bridge bis-permidinum was synthesised through copper mediated cross coupling under aerobic conditions, followed by *N*-alkylation leading bispermidinum salts in quantitative yields. The cyclo metalation with palladium was not formed due to stable perimidine carbene.

V.7 Synthesis of lutidine-bridged bis-perimidinium salt

N-Butylimidazole (**33**), *N*-butylbenzimidazole (**34**) and N-butylperimidine **35** were prepared according to the reported procedure [95] by drop-wise addition of *n*-butyl bromide to a solution of perimidine – deprotonated by oil-free NaH in THF at room temperature and subsequent warming of the mixture to reflux. The solvent was removed under reduced pressure and water was added. The crude product was extracted by CH_2Cl_2 and purified by flash column chromatography. The synthesis of Lutidine-bridged bis-perimidinium salt (**38**) was made by treatment of 2, 6-

dibromolutidine with 2 equivalents of *N*-butylperimidine **35** and heating 165 ^{o}C under stirring in a sealed tube for 24 h. The crude product was purified by re-precipitation from $CHCl_3/Et_2O$ to give a yellow solid **38** (98 %) (Scheme 9).

Scheme 9

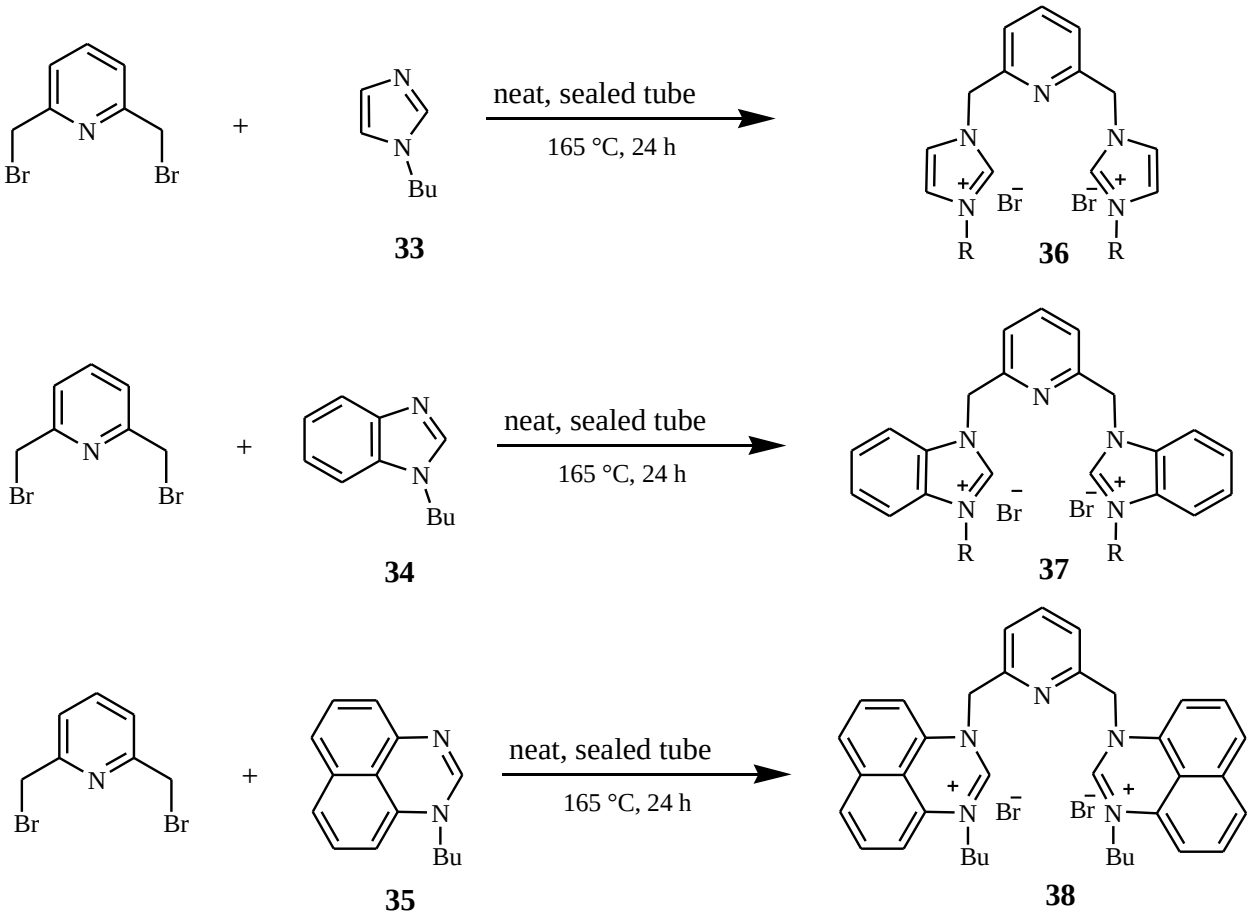

In order to investigate the development of NHC´s and *Fischer* carbenes towards application in catalysis and soft material sciences. To addressed the role of a strong σ-donor in a six-membered heterocycle on the catalytic activity and tested bis-perimidinium salt **38** in palladium-catalysed Heck and Suzuki cross-coupling reactions. The influence of catalyst towards the cross couplings reactions, catalyst was generated an *in-situ* formation in the reaction medium [95, 96] by treatment of equimolar amounts of Pd $(OAc)_2$ and bis-perimidinium dibromide **6**.

V.7.1 Catalytical behaviour towards Heck reaction

The Heck coupling of aromatic halides and *n*-butyl acrylate was chosen as a model reaction. A 2 mol% catalyst loading (equimolar amounts of **38** and $Pd(OAc)_2$) in 1-methyl-2-piperidone (NMP) at 140 °C using K_2CO_3 as a base gave the best results for iodobenzene (98 % after 60 min). A slightly lower yield was observed for bromobenzene (93 % after 90 min). Identical results were obtained under aerobic conditions indicating that the pincer palladium complex intermediate formed *in situ* tolerates higher temperatures and the presence of air and moisture.

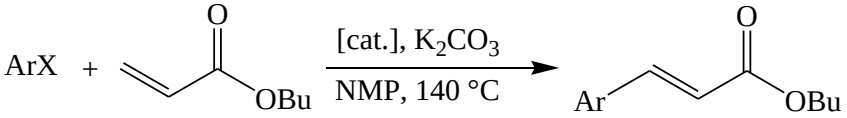

39a-h

If the reaction time is extended to 42 hours under these standard conditions, the catalyst loading can be dramatically reduced to 2 ppm resulting in only moderately decreased yields of *n*-butyl cinnamate **39a** (82 % for iodobenzene and 71 % for bromobenzene; Table 8, entries 1 and 2). In order to investigate the scope of the protocol and, in particular, the electronic and steric implications of the substrates, to test a variety of iodoarenes under our 2 ppm catalyst loading standard conditions (Table 8). For mono-substituted iodoarenes, the catalyst tolerates additional substituents with different electronic and steric properties and allowed for moderate to good isolated yields of biphenyl derivatives **39b-j** (Table 8, entries 3-11). Compared with their *meta*-isomer the coupling of *ortho*- and *para*-iodotoluenes resulted in higher conversions and yields (88 % and 92 % versus 74 %) and in turnover numbers (TON) up to 4.62×10^5 (Table 8, entries 3-5); a lower yield and TON were again observed with *para*-bromotoluene (77 %, 3.85×10^5; Table 1, entry 6). Donor-substitution increases the yield and TON of the *ß*-aryl acrylate as shown for *para*-iodoanisole (4.51×10^5, Table 1, entry 7). Moderate yields and TON´s result from acceptor and sterically more demanding substitution patterns (Table 8, entries 8-12). 1-Iodo-3,5-dimethylbenzene still afforded a 62 % yield (Table 8, entry 12), whereas no coupling product at all, even at extended reaction times, was observed for the strong acceptor analogue 1-iodo-3,5-ditrifluoromethylbenzene indicating a pronounced stereoelectronic effect.

Table 8. Heck cross-coupling reactions of haloarenes with *n*-butyl acrylate catalysed by lutidine-bridged *N*-heterocyclic dibromides **36-38** and $Pd(OAc)_2$.[a]

Entry	ArX	Salt	Product	Yield (%)[b]	TON
1	Iodobenzene	**38**	**39a**	82	4.10×10^5
2	Bromobenzene	**38**	**39a**	71	3.55×10^5
3	2-Iodotoluene	**38**	**39b**	88	4.41×10^5
4	3-Iodotoluene	**38**	**39c**	74	3.71×10^5
5	4-Iodotoluene	**38**	**39d**	92	4.62×10^5
6	4-Bromotoluene	**38**	**39d**	77	3.85×10^5
7	4-Iodoanisole	**38**	**39e**	90	4.51×10^5
8	4-Iodoacetophenone	**38**	**39f**	69	3.45×10^5
9	1-Iodo-2-(trifluoromethyl)benzene	**38**	**39g**	71	3.57×10^5
10	1-Iodo-4-(trifluoromethyl)benzene	**38**	**39h**	73	3.63×10^5
11	1-Iodonaphthalene	**38**	**39i**	73	3.66×10^5
12	1-Iodo-3,5-dimethylbenzene	**38**	**39j**	62	3.08×10^5
13	4-Iodotoluene	**37**	**39d**	69	3.44×10^5
14	4-Iodotoluene	**36**	**39d**	46	2.30×10^5

[a] Reaction conditions: 2 mmol haloarene, 2.4 mmol *n*-butyl acrylate and 3 mmol K_2CO_3 in 3 mL NMP at 140°C for 42 hours with 2 ppm catalyst (prepared *in situ* from equimolar amounts of lutidine-bridged *N*-heterocyclic dibromide and $Pd(OAc)_2$. [b] Isolated yield.

A comparison between the lutidine-bridged bis-perimidinium dibromide **38** and its imidazole and benzimidazole analogues (**36** and **37**, R = *n*-Bu and X = Br) suggests that their catalytic performance increases with the σ-donor ability of the NHC ligand present in the active palladium catalyst. Under the standard conditions of 2 ppm catalyst loading applied to the coupling of *para*-iodotoluenes with *n*-butyl acrylate, the less efficient benzimidazolium (**37**) and imidazolium (**36**) analogues afford reduced yields of 69 and 46 %, respectively (Table 8, entries 13 and 14). Major amounts of starting materials were recovered in the both cases, strictly contrasting the full conversion observed with bis-perimidinium dibromide **38** as precatalyst (Table 8, entry 5). These results underline the role of α-donation of the NHC ligand in palladium catalysis.

In order to characterize the nature of the catalytic species generated from $Pd(OAc)_2$ and salt **38** *in situ* to performed the mercury test which has been reported to allow a discrimination between molecular and nanoparticle/colloidal catalysis.[97,98,99,100] A set of reactions using iodobenzene, butyl acrylate, 1 mol % catalyst in the presence of excess mercury (with respect to the palladium source) added after 0, 15, 30 and 45 minutes was run at 140 °C in NMP and monitored by TLC

and GC-MS. In all four cases a full conversion to butyl cinnamate and an isolated yield of 98% identical with that known for the reaction without mercury was observed suggesting a molecular catalytically active species containing the CNC ligand similar to that previously reported by Crabtree.

V.7.2 Catalytical behaviour towards Suzuki reaction

The influence of bis-perimidinium salt **38** was equally effective in Suzuki coupling reactions and allows for remarkably low catalyst loading (Table 9). Under similar conditions as applied for the Heck cross-coupling, but with a catalyst loading reduced to 0.2 mol %, bromobenzene reacted with phenyl boronic acid to give biphenyl **40a** in a 95 % yield after 6 hours (Table 9, entry 1); reducing the catalyst concentration by another order of magnitude still resulted in a 82 % yield (Table 9, entry 2). A study of the amount of catalyst required for a synthetically useful protocol was carried out for a selection of donor- and acceptor-substituted iodoarenes. The balance of catalyst concentration and reaction time is demonstrated for iodobenzene (Table 9, entries 3-5). With a catalyst loading of 0.02 mol %, 92 % of biphenyl **40a** was isolated after warming a NMP solution at 140 °C for 5 hours (Table 9, entry 3). To secure a similar high yield the amount of catalyst can be even reduced to 5 ppm if the reaction is allowed to proceed for 48 hours. A further reduction of the catalyst loading to 2 ppm resulted in a 63 % yield of **40a** after 36 hours and a TON of 3.15×10^5 while a considerable amount of starting material was recovered (Table 9, entry 4). Since running the reactions in NMP to 140 °C for 48 hours in the presence of 5 ppm catalyst turned out to be the overall optimum conditions they were applied to a comparative study demonstrating the scope of the protocol and influences of electronic and steric properties of the substrates. As observed for the Heck reactions (*vide supra*) *ortho*- and *para*-iodotoluenes are more reactive (yields of 89 and 93% for **40b** and **40d**, respectively) than their *meta*-isomer **40c** (74 %, Table 8, entries 6-8). The examples outlined in Table 9, entries 9-14, are characterized by moderate to good yields (71-89%) and indicate that no obvious electronic or steric effects are operative allowing for a rather broad monosubstitution pattern of the biaryl target molecules. The coupling reactions of 2-iodopyridine (67% of **40k**, Table 9, entry 15) and disubstituted iodoarenes such as 1-iodo-3,5-dimethylbenzene (61% of **40l**, Table 9, entry 16) turned out to be less efficient. As observed for the Heck reaction its electron-poor fluoro analogue, 1-iodo-3, 5-bis

(trifluoromethyl) benzene, was totally unreactive under our standard conditions, and the starting materials were completely recovered.

Table 9. Suzuki-coupling of haloarenes with phenyl boronic acid catalysed by lutidine-bridged dibromides **36-38** and $Pd(OAc)_2$.[a]

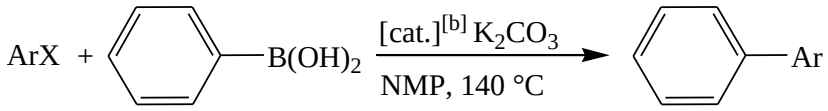

40a-l

Entry	ArX	Salt	Catalyst (mol%)	Time (h)	Product	Yield[c] (%)	TON
1	Bromobenzene	**38**	0.2	6	**40a**	95	475
2	Bromobenzene	**38**	0.02	6	**40a**	82	4120
3	Iodobenzene	**38**	0.02	5	**40a**	92	4600
4	Iodobenzene	**38**	0.0002	36	**40a**	63	3.15×10^5
5	Iodobenzene	**38**	0.0005	48	**40a**	91(81[d])	1.83×10^5
6	2-Iodotoluene	**38**	0.0005	48	**40b**	89	1.79×10^5
7	3-Iodotoluene	**38**	0.0005	48	**40c**	74	1.48×10^5
8	4-Iodotoluene	**38**	0.0005	48	**40d**	93	1.87×10^5
9	4-Iodoanisole	**38**	0.0005	48	**40e**	89	1.77×10^5
10	4-Iodoacetophenone	**38**	0.0005	48	**40f**	71	1.43×10^5
11	1-Iodo-4-(trifluoromethyl)benzene	**38**	0.0005	48	**40g**	82	1.64×10^5
12	1-Iodo-2-(trifluoromethyl)benzene	**38**	0.0005	48	**40h**	83	1.66×10^5
13	1-Fluoro-2-Iodobenzene	**38**	0.0005	48	**40i**	76	1.53×10^5
14	1-Iodonaphthalene	**38**	0.0005	48	**40j**	73	1.45×10^5
15	2-Iodopyridine	**38**	0.0005	48	**40k**	67	1.34×10^5
16	1-Iodo-3,5-dimethylbenzene	**38**	0.0005	48	**40l**	61	1.22×10^5
17	4-Iodotoluene	**37**	0.0005	48	**40d**	70	1.41×10^5
18	4-Iodotoluene	**36**	0.0005	48	**40d**	49	9.72×10^4

[a] Reaction conditions: 2 mmol haloarene, 2.2 mmol phenyl boronic acid and 2.4 mmol K_2CO_3 in 3 mL NMP at 140°C. [b] Catalyst prepared *in situ* from equimolar amounts of **36-38** and $Pd(OAc)_2$. [c] Isolated yield.

The phenylation of iodotoluene was chosen as a model reaction for a comparative study of the lutidine-bridged salts **36-38** as precatalysts for the Suzuki reaction. The yields obtained for the resulting 4-phenyltoluene **40d** increased from 49 % to 70 % and 93 % in the series of bis-imidazolium (**36**), bis-benzimidazolium (**37**) and bis-perimidinium dibromide (**38**), respectively (Table 9, entries 17, 18 and 8) confirming the trend observed for the Heck reaction that the

efficiency of the precatalyst increases with the σ-donor ability of the respective NHC ligand formed in the presence of base and attached to palladium in the active catalyst.

V.7.3 Conclusion

In conclusion the lutidine-bridged bis-perimidinium bromide **38** which is accessible from cheap commercial starting materials in a nearly quantitative reaction is an efficient precatalyst in combination with palladium acetate for Heck and Suzuki cross-coupling reactions under aerobic conditions. This protocol is characterized by good yields even with very low catalyst loadings down to the ppm scale. It is compatible with a broad selection of functional groups in the haloarene varying in their electronic and steric properties. In comparison with bis-imidazolium and bis-benzimidazolium dibromide congeners the deprotonation of bis-perimidinium dibromide generates an NHC ligand with increased σ-donor ability improving the efficiency of the palladium catalyst formed *in situ* in the series of bis-imidazolium, bis-benzimidazolium and bis-perimidinium dibromide precatalysts.

V.8 A Regioselective Pd-catalysed arylation of thiophenes

Metal-catalysed cross-coupling reactions are versatile and efficient processes for academic and industrial applications.[101] In particular, palladium-catalysed reactions are widely used for the synthesis of both bioactive compounds and organic materials bearing a biaryl skeleton.[102,103] Moreover, the regioselective arylation of the thiophene ring receives increasing interest,[104] and poly- and oligoaryl compounds involving thiophene units represent valuable components of electronic devices.[105,106] Five-membered heteroarenes bearing substituents at 2- and 5-positions have been explored as light emitting and liquid crystalline materials[107]. Recently Itami and coworkers described a β- and α-selective arylation of thiophene catalysed by palladium- and iridium phosphine systems.[108]

V.8.1 Homo-coupling of 2-o-tolylthiophene

To a novel phosphine-free palladium catalysed α-selective both inter- and intramolecular arylation of thiophenes with haloarenes giving much attention towards synthesis. The first attempt aimed at the C-H activation of the *ortho*-position in 2-*o*-tolylthiophene. Interestingly, a catalytic C-H-activation at position 5 of the thiophene ring was observed already under mild conditions when one equivalent of palladium acetate was used in methanol at room temperature resulting in a homo-coupling of the thiophene moiety (23%). The molecular structure of 2,2´-bithienyl product was established by X-ray analysis (Scheme 10).

Scheme 10

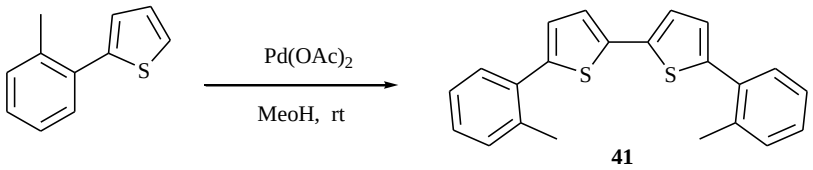

41

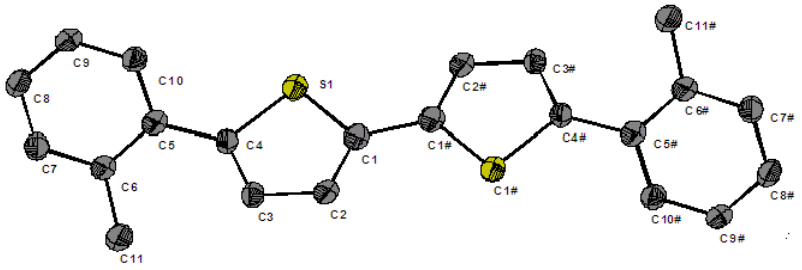

V.8.2 Reaction of 2-phenylthiophene with iodobenzene

By the prominenting results paying much attention towards hetero-coupling of 2-arylthiophenes with iodoarenes probing a variety of palladium catalysts, bases and solvents (Table 10, entries 1-11). In the coupling of 2-phenylthiophene with iodobenzene under aerobic conditions best results were obtained when palladium acetate (5 mol %) and cesium carbonate (1.2 eq.) were used in DMF at 140 ^{o}C for 24 h to afford a 89% yield of 2,5-diphenylthiophene in high regioselectivity (Table 10, entry 11) (Scheme 11). The reaction is also highly chemoselective: Only very low yields of α,β-diarylated products (<5%) and no homo-coupling of iodobenzene were observed.

An attempt to lower the catalyst loading to 2 mol % reduced the yield to 52 % (Table 10, entry 6).

Scheme 11

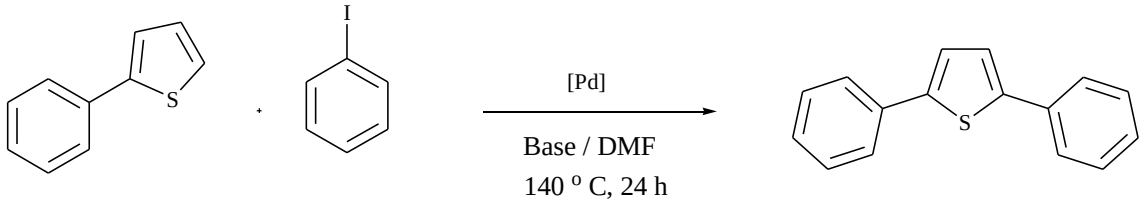

42a

Table 10 : Reaction of 2-phenylthiophene with iodobenzene [a]

Entry	Base	Catalyst [Pd]	mol-% Pd	Yield % [b]
1	K_2CO_3	$Pd(OAc)_2$	2	24
2	Na_2CO_3	$Pd(OAc)_2$	2	34
3	$NaHCO_3$	$Pd(OAc)_2$	2	19
4	DBU	$Pd(OAc)_2$	2	15
5	NEt_3	$Pd(OAc)_2$	2	11
6	Cs_2CO_3	$Pd(OAc)_2$	2	52
7	Cs_2CO_3	Pd(DBA)	5	54
8	Cs_2CO_3	$PdCl_2$	5	45
9	Cs_2CO_3	$Pd(C_3H_5)_2Cl_2$	5	36
10	Cs_2CO_3	$Pd(CH_3CN)_2Cl_2$	5	37
11	Cs_2CO_3	$Pd(OAc)_2$	5	89

(a) Conditions: 2-phenylthiophene (2 mmol), aryliodides (2.2 mmol), base (2.4 mmol) and dry DMF (2 mL) at 140 ^oC for24 h. (b) Isolated yields.

V.8.3 Effect of the substitution pattern haloarene

In order to investigate the influence of electronic and steric properties of the substrates, a variety of iodoarenes was studied in model reactions with 2-phenylthiophene and Cs_2CO_3 with a 5 mol% palladium acetate loading (Table 11) (Scheme 12). Under our conditions the less reactive bromobenzene afforded a 61% yield of **42a** (Table 11, entry 2). The coupling of *ortho*-, *meta*-, and *para*-methyl- and *para*-methoxy-substituted iodoarenes **42b-e** (Table 11, entries 3-6) afforded high to excellent yields of cross-coupling products in perfect α-regioselectivity.

Pronounced acceptor-substitution in the haloarene reduced the yields of **42f-h** to 68-74 % (Table 11, entries 7-9). A weak steric effect was observed for 1-iodonaphthalene which gave a 62 % yield **42i** (Table 11, entry 10).

Scheme 12

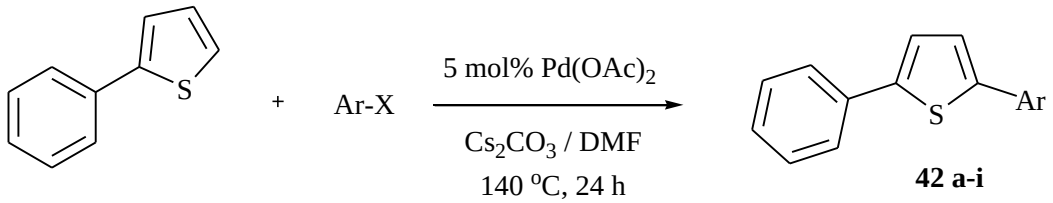

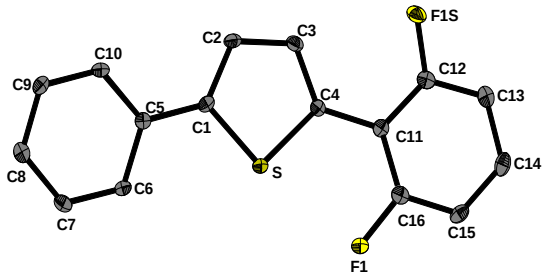

Table 11: Effect of the substitution pattern haloarene [a]

Entry	Ar-X		Yield% [b]
1	Iodobenzene	**42a**	89
2	Bromobenzene	**42a**	61
3	1-Iodo-2-methylbenzene	**42b**	96
4	1-Iodo -3-methylbenzene	**42c**	72
5	1-Iodo-4-methylbenzene	**42d**	97
6	1-Iodo-4-methoxybenzene	**42e**	94
7	1-Iodo-4(trifluoromethyl)benzene	**42f**	68
8	1-Iodo-2(trifluoromethyl)benzene	**42g**	74
9	1-Fluoro-2-iodobenzene	**42h**	71
10	1-Iodonaphthalene	**42i**	62

(a) Conditions: 2-phenylthiophene (2 mmol), ArX (2.2 mmol), Cs_2CO_3 (2.4 mmol) and 5 mol % $Pd(OAc_2)$ in dry DMF (2 mL) under argon at 140 °C for 24 h. (b) Isolated yields.

V.8.4 Tandem biarylation of thienylboronic acid

Based upon these promoting results to extended further studies towards a tandem biarylation strategy involving a Suzuki cross-coupling followed by C-arylation. Under slightly modified

conditions (10 mol % $Pd(OAc)_2$, 48h) 2-thienylboronic acid reacted with 2.2 equivalents of iodoarene to give the 2,5-diarylthiophenes **43a-h** in 36-90 % yield (Table 12) (Scheme 13). The biarylation revealed an only minor impact of donor-acceptor substitution in the iodoarene. *Ortho*-methyl and methoxy substitution resulted in similar yields of **43b** (84%) and **43g** (81%) which exceeded those obtained for the methyl isomers **43c** and **43d** as well as the acceptor analogues**43e-f** (Table 12, entries 2-7). A more bulky substitution pattern as in 1-iodonaphthalene, however, resulted in an significantly decreased yield for **43h** (36%; Table 12, entry 8).

Scheme 13

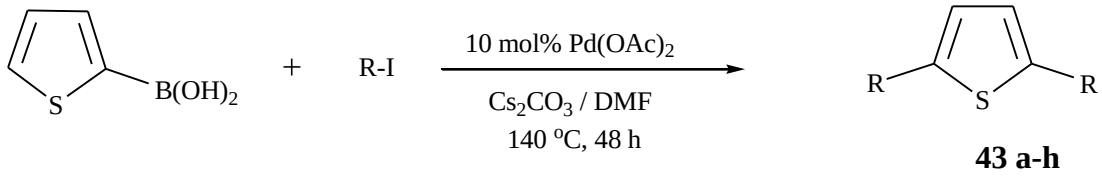

43 a-h

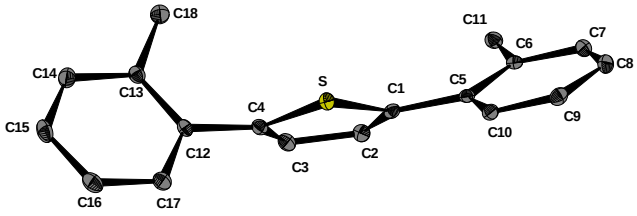

Table 12: Tandem biarylation of thienylboronic acid [a]

Entry	R-I		Yield % [b]
1	Iodobenzene	**43a**	90
2	1-Iodo-2-methylbenzene	**43b**	84
3	1-Iodo-3-methylbenzene	**43c**	59
4	1-Iodo-4-methylbenzene	**43d**	73
5	1-Fluoro-2-iodobenzene	**43e**	70
6	1-Iodo-2(trifluoromethyl)benzene	**43f**	76
7	1-Iodo-2-methoxybenzene	**43g**	81
8	1-Iodonaphthalene	**43h**	36

[a] Conditions: 4 (2 mmol), R-I (4.4 mmol), Cs_2CO_3(5 mmol) and 10 mol% $Pd(OAc)_2$ in dry DMF (2 mL) under argon at 140°C for 48 h. [b] Isolated yields.

V.8.5 Suggested mechanism for the arylation of thiophene

The mechanism operative in the cross-coupling process may be rationalised in terms of a sequence of 1) an oxidative addition of ArI to a Pd(0) species to form intermediate **A**, 2) the coordination of the thiophene to Pd(II) via the sulphur atom to intermediate **B** enhancing the α-CH acidity of the thiophene, 3) a base-assisted α-deprotonation generating a C_α - Pd bond intermediate **C**, and 4) a final reductive elimination to release the cross-coupling product and regenerate the Pd(0) species.

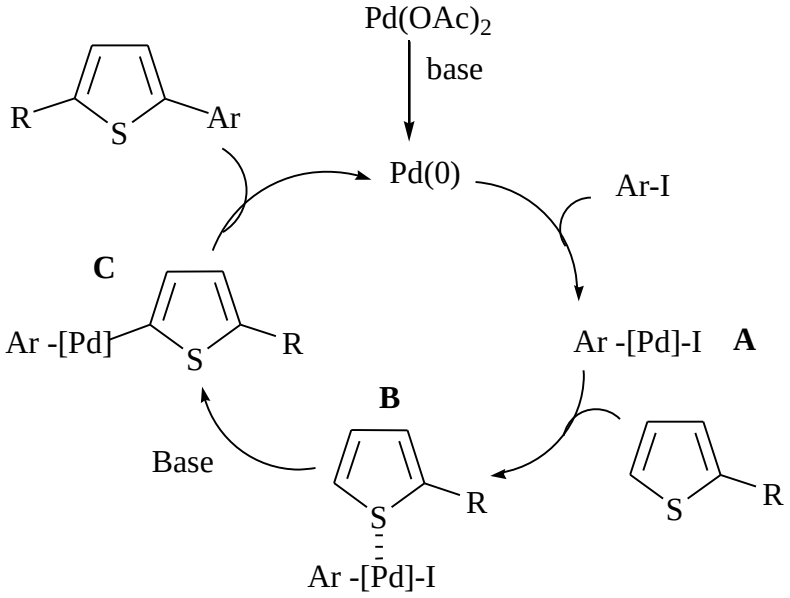

V.8.6 Biarylation of thiophene

This methodology was extended to a one-pot bidirectional arylation of thiophene to give elongated alternate benzene-thiophene skeletons.[109] Under standard arylation conditions (2.2 equivalents of 2-iodotoluene, 10 mol% $Pd(OAc)_2$, 24 h) 1,4-dithienylbenzene **44** was expanded to the pentanuclear 1,4-di(tolylthienyl)benzene **45** in nearly quantitative yield (92%; Scheme 14).

Scheme 14

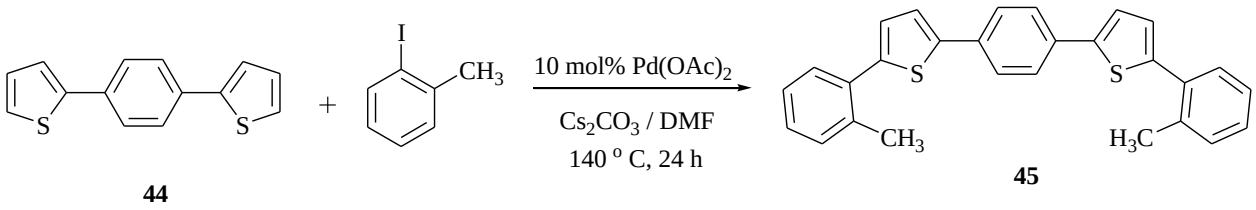

44 **45**

V.8.7 Intramolecular arylation

Finally, this strategy was extended to an intramolecular arylation,[110] to design a *meta*-iodophenoxy-thienyl-benzene precursor **46** which was subjected to standard C-arylation conditions using a 5 mol% Pd catalyst loading. Interestingly, neither an intermolecular nor an intramolecular arylation at the α-position of the thiophene ring was observed. Oxidative addition of the iodoarene functionality is supposed to generate a phenyl-Pd(II) intermediate which is unable to attack either the remote thiophene α-position nor the 2-position of the central benzene ring due to steric congestion. Instead, an intramolecular cross-coupling occurred at the 6-position of the central benzene ring affording the intramolecular arylation product **47** in nearly quantitative yield (98 %; Scheme 3). The molecular structure of **47** was elucidated from ^{1}H-NMR spectroscopy and independently corroborated by X-ray analysis.

Scheme 15

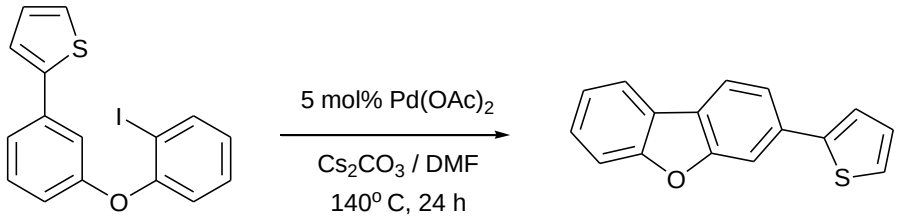

46 **47**

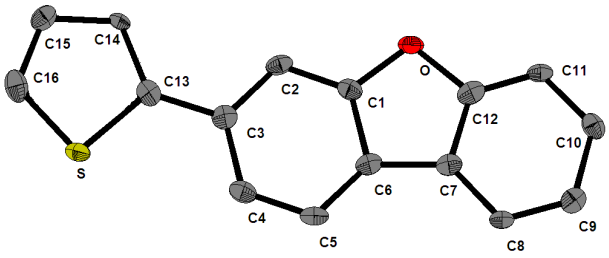

V.8.8 Conclustion

A novel phosphine-free palladium catalysed protocol was applied to regio- and chemoselective α-arylation of the thiophene ring by haloarenes. The cross-coupling is compatible with both electron-donating and electron accepting substituents in the iodoarene and may be conducted in an either inter- or intramolecular fashion. The reaction generally affords high yields and, thus, provides an attractive new protocol for the synthesis of arylthiophenes required for the development of both bioactive compounds and functional materials.

VI. Summary & Outlook

The work presented herein describes an investigation of a new class of pyridine-bridged bis-(benz)imidazolium salts and *N*-heterocyclic pincer carbene complexes derived there from, as well as their implication as homogenious catalysis in Heck and Suzuki cross coupling reactions and their aggregation to liquid crystals and organometallic gels.

The novel pyridine bridged bis-benzimidazolylidene pincer palladium complex **6** is readily accessible by the amination of 2,6-difluoropyridine with benzimidazole, followed by *N*-alkylation with *n*-alkylhalide. The cyclometalation with palladium acetate under microwave conditions leads to palladium carbene complex **6**. The palladium atom was strongly bound to two carbene molecules and coordinated with a pyridine molecule leading to the CNC carbene complex. The palladium carbene complex **6** is an efficient catalyst towards the Heck and Suzuki cross-coupling reactions even with catalyst loadings as low as 0.1 to 1 ppm. The scope of aryl halides as reaction proceeding is not significantly hampered by electronic or steric effects. The carbene complex is stable against air, moisture and high temperature.

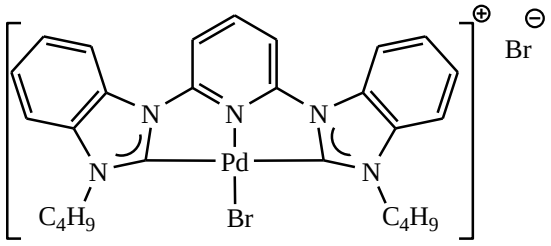

6

A new class of conjugated palladium pincer bis-imidazolylidene complexes **12a,b** were synthesised according to a modified procedure. Conjugated dibromopyridine was prepared through Arbuzov reaction, followed by cross coupling with imidazole under copper catalysis. The cyclometalated palladium complexes were prepared according to a standard procedure. A short C_4 alkyl chain complex **12a** shows strong catalytical activity towards cross coupling reactions. The C_{16} long alkyl chain complex **12b** efficiently gelates polar organic solvents. A co-solvent effect is also playing a key role towards gelation. A stable and transparent gel was observed in DMSO at 0.5 wt%. The thermal stability of the gel increases with the gelator concentration.

According to the similar procedure the π-extended conjugated palladium pincer bis-benzimidazolylidene complexes **15a, b** were prepared. Compared to bis-imidazolylidene complex **12a**, C_4 the short alkyl chain palladium complex **15a** shows a strong catalytical activity towards cross-coupling reactions due to the σ-donor ability of the NHC ligand which increases the electron density on the palladium center. The extended π-system complex **15b** strongly gelates polar, apolar and chlorinated solvents. With the strong coordinating polar solvents thin film TEM images were observed, while long helical fiber (P and M) networks were observed in apolar solvents, which are quite rarely observed in gel networks, formed from achiral gelators. A stable and transparent gel was observed in DMSO at 0.3 wt%. Again the thermal stability of the gel increases with the gelator concentration.

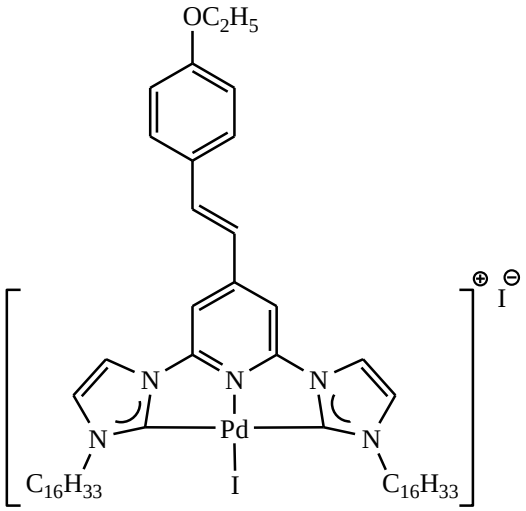

12b

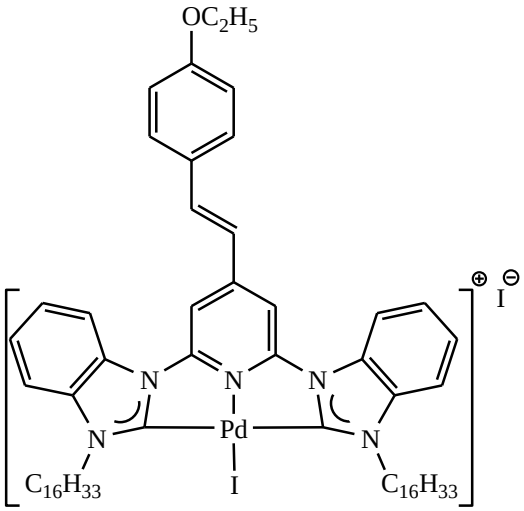

15b

Tuning property of molecules from gels to liquid crystalline behaviour is a challenge towards the design of target oriented synthesis. The highly extended conjugated pyridine-bridged bis-benzimidazolium salt is readily accessible according to modified procedure in quantitative yields. The extended π-system in pyridine-bridged bis-benzimidazolium salts **5a-d** efficiently gelates aprotic solvents; however the conjugated pyridine-bridged bis-(benz)imidazolium salts **11b**, **14b** do not show any significant effect towards gelation. The highly extended pyridine-bridged bis-benzimidazolium salt **19** behaves like liquid crystalline materials at higher temperature. Fan-shaped textures of **19** were observed at 200^{o} C under crossed polarized optical microscopy. Due

to the lack of sufficient van der Waals interactions at orthogonal direction, at the isotropic point electron rich salt **19** was undergoes polymerisation leading to plastic crystalline materials.

The oligovinylene materials have been pain to much attention due to strong π-π stacking, hydrogen bonding ionic and van der Waals interactions towards self-assembly. The self-assembly of the highly conjugated pyridine-bridged bis-imidazolium salt **28** behaves like thermoreversible liquid crystalline materials. Compared to bis-benzimidazolium salt **19**, strong van der Waals interactions in orthogonal direction of **28** allow to pack the molecules in three-dimensional directions to optimize liquid crystalline properties at 100^{o} C. The investigation of mesomorphic properties of **28** by POM and DSC revealed that the thermoreversible liquid crystalline materials are regaining their original property even after cooling from isotropic phase.

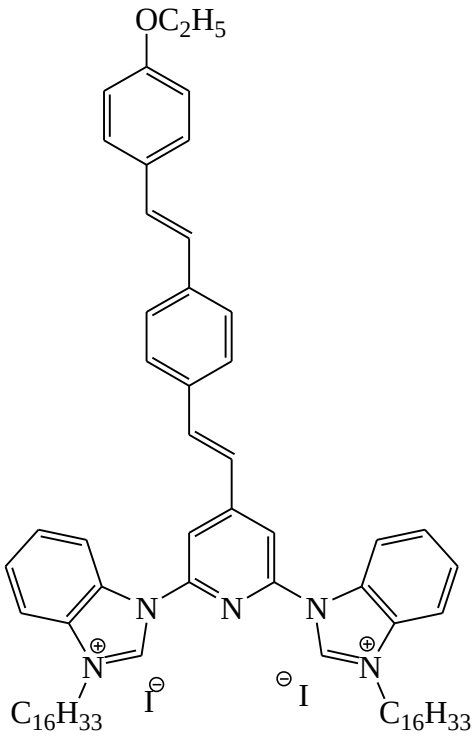

19

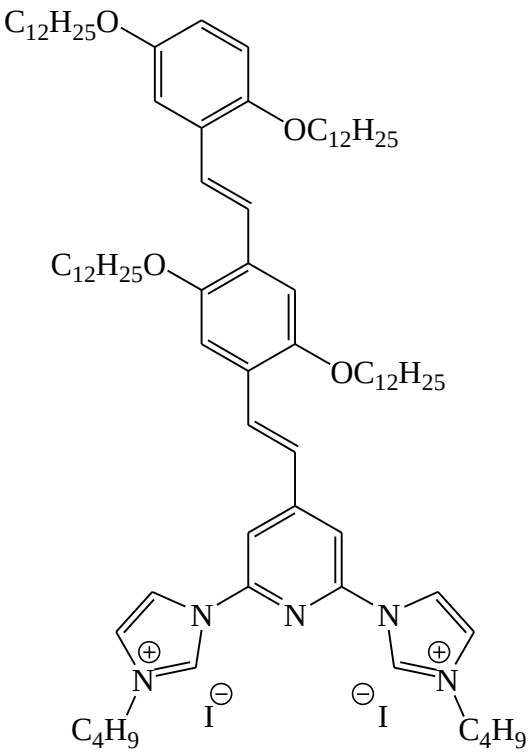

28

The novel *N*-heterocyclic carbenes receive much attention due to their strong σ-donor and π-acceptor ligand ability and their metal complexes are widely applied in catalysis and material

science. A new class of six-membered NHC ligands derived from perimidinium salts show stronger σ-donor ability compared to five-membered NHC ylidenes derived from (benz)imidazolium salts. For the making of novel pyridine bridged bis-perimidiniylidene complex **32** was synthesised according to modified procedure. Under copper catalyzed cross coupling reactions pyridine bridged bis-perimidine was prepared in moderate yields, followed by *N*-alkylation with *n*-alkyl halides. The *in-situ* generation of carbene was stabilized by intramolecular delocalisation leading to urea type molecule; however no cyclometalation product **32** was formed.

The lutidine- bridged bis-(benz)imidazolium and perimidinium salts **33, 34, 38** were prepared according to the reported procedure. The *in-situ* generation of the palladium catalyst by treatment of equimolar amounts of salts and palladium acetate, subjected to the cross coupling reactions. At 5 ppm catalyst loadings the high efficient catalyst shows strong significant effect towards the Heck and Suzuki cross-coupling reactions leading to high turnover numbers. The precatalysts are generated from bis-(benz) imidazolium salts are less effective compared to bis-perimidinum salt due to week σ-donor and π-acceptor ability.

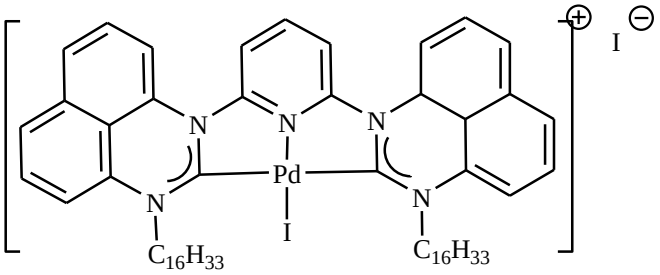

32

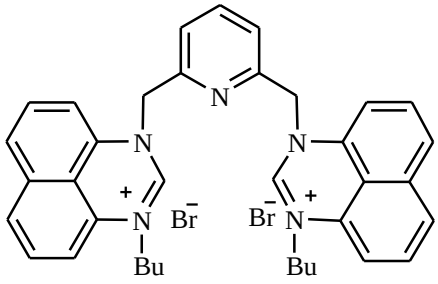

38

Phosphine-free palladium catalysed cross-coupling reactions are very attractive towards regio- and chemoselective C-arylation on thiophene ring with haloarenes. A selective catalytic C-H activation at 5-position of the thiopehene ring with iodoarene with palladium acetate under inert conditions leads to 2, 5-diarylthiophenes with high yields. The cross-coupling is compatible with both electron-donating and electron accepting substituents in the iodoarene and also conducted in

an either inter- or intramolecular fashion. The novel protocol is applied to the synthesis of arylthiophenes as relevant for the development of both bioactive compounds and functional materials, such as in electronic devices or liquid crystals.

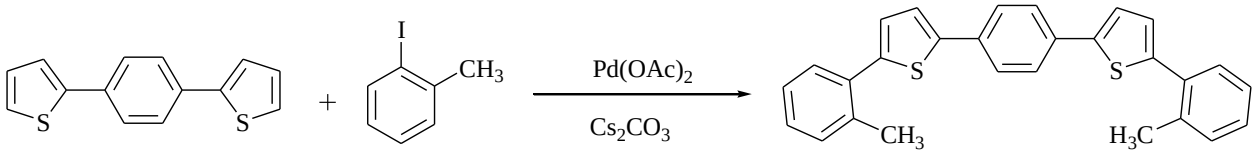

44 **45**

VII. Experimental Part

1. General

All commercial reagents and solvents were used directly without further purification.

Dichloromethane was distilled over calcium hydride, methanol over magnesium and tetrahydrofuran over sodium. Diethyl ether was distilled over calcium chloride. All distillated solvents were kept dried by using 4 Å molecular sieves.
All temperatures mentioned are temperatures measured from oil, water or cooling bath.

All products were purified over silica gel by column chromatography with solvents.

The silica gel is provided by *Merck*, Type 60 (0.063 - 0.200 mm).

The reaction are monitored by TLC, TLC are of Type 60 F254, purchased directly from *Merck.*

2. NMR – Spectroscopy

All ^{1}H- and ^{13}C-NMR spectra were measured on DPX-300, DPX-400 or DRX-500 machines from *Bruker* at room temperature. All deuterated solvents were used as received.
Abbreviations for intensities of ^{1}H-NMR signals
s: singlet
d: doublet dd: doublet of doublets etc.
t: triplet
m: multiplet
br s: broad signal

3. Mass – Spectroscopy

Mass spectra were collected at the *Rheinischen Friedrich-Wilhelms-Universität Bonn* with different machines. Electron Ionisation (EI-MS)) spectra were made with a MS 50 (70eV)

from *Kratos*, the Positiv-Ion Fast Atom Bombardment-experiments spectra (FAB) were obtained from a Concept ^{1}H machine from *Kratos*. MALDI-TOF mass spectra were recorded on a Bruker Daltonics Announces Autoflex TOF/TOF mass spectrometer using DCTB as matrix. GC-MS spectra were recorded on HP 5890 Series II.

4. Gelation

For the preparation of the gel samples, the solvents were used as purchased. For 1 wt % gel: Compounds (10 mg, 9.8 μmol) were filled into a screw-cap tube and the solvent (1 mL) was added by syringe. The exact concentration was determined by differential weighting. Compounds were dissolved by heating with a heat-gun under continuous shaking. Then, the samples were allowed to cool down slowly at room temperature.

5. **Determination of gel-to-solution phase-transition temperatures T_g.**

For the determination of $T_{g/H}$ and $T_{g/C}$, DSC thermograms were carried out on a Netzsch DSC 204 F1 equipped with a cooling device CC 200 F1 which allowed cooling with liquid nitrogen. 2-10 mg of the gelled sample were weighed into aluminum crucibles, sealed and heated from –20°C or r.t. (for DMSO, which melting point is above 0°C) to a temperature 5°C – 10°C below the boiling point of the respective solvent. The heating and cooling rates were 10°C /min. During the measurements, the oven was flushed with 20 mL/min nitrogen as protective gas and 50 mL/min nitrogen as purge gas. The given temperatures correspond to the onset of a thermal effect. Due to the broadness of the thermal effects in the DSC curve in the heating segment, the peak temperature and not the onset of the effect is given exceptionally.

For the determination of T*g* with the dropping ball method. A glass ball (radius 1.5 mm, weight 36 mg) was placed on the gel surface and the samples were heated in an oil bath by 0.2°C per minute. As soon as the ball started dipping into the gel, the corresponding temperature was denoted as T_g.

6. Transmission electron microscopy (TEM).

TEM experiments were carried out on Philips CM300 UT FEG / Philips CM30 / Philips EM400 microscopes; all pictures from Philips CM300 UT FEG / Philips CM30 were taken digitally. Films were used with Philips EM400 microscope. For preparation of the samples carbon-coated copper grids (mesh 200 or 150) were placed on the surface of the gels for a short time. The gel samples were partly destroyed by knocking the test tube on the table to provide a "print" of the inner volume of the gel.

7. Abbreviations

- δ: chemical shift
- ^{1}H: proton NMR
- ^{13}C: carbon NMR
- a.k.a.: also known as
- °C: degree Celsius
- CH_2: methylene group
- DCM: dichloromethane
- DME: dimethoxyethane
- DMF: dimethylformamide
- DMSO: dimethylsulfoxide
-DSC:
- EI: electron ionisation
- ESI: electro spray ionisation
- Et_2O: diethylether
- g: gram
- G: gel
- GCMS: gas chromatography mass spectroscopy
- h: hour
- Hz: Frequency
- I: insoluble
- J: coupling constant

- KO^tBu: potassium *tert*-butoxide
- L: ligand
- M+: molecular ion
- M: molecular mass
- m/z: mass to charge ratio
- ml: milliliter
- min: minute
- MS: mass spectroscopy
- NHC: N-heterocyclic carbene
- NMR: nuclear magnetic resonance
- o.n.: overnight
- P: precipitate
-PG: partial Gel
-PMO: polarized optical microscopy
- ppm: parts per million
- PE: petrol ether
- Rf: retention factor
- rt: room temperature
- S: solution
- TEM: transmission electron microscopy
- THF: tetrahydrofuran
- TLC: thin layer chromatography
-WG: weak Gel

VII.1. Synthesis of 2, 6-bis(imidazol-1-yl)pyridine (4)

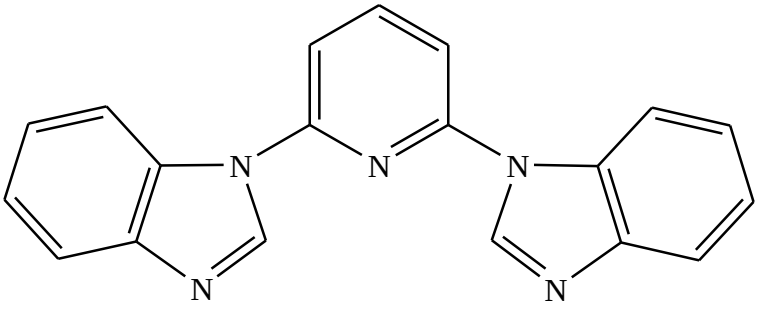

A mixture of 2,6-difluoropyridine (2.99 g, 26 mmol) and benzimidazole (15.34 g, 130 mmol) was heated to 185 ^{o}C under stirring in a sealed tube for 2 h and then at 160 ^{o}C for a further 30 h. The mixture was cooled, and water was added. The precipitate was washed by hot EtOAc. The residue was dissolved in $CHCl_3$ and then reprecipitated upon addition of Et_2O to give 2, 6-bis(imidazol-1-yl)pyridine as a white powder (7.6 g, 94 %).

^{1}H NMR ($CDCl_3$, 300 MHz, 298 K): δ 8.70 (s, 2H), 8.10-8.17 (m, 3H), 7.89-7.95 (m, 2H), 7.60 (d, J = 8 Hz, 2H), 7.38-7.45 (m, 4H); ^{13}C NMR ($CDCl_3$, 75 MHz, 298 K): δ 149.52, 144.64, 142.08, 141.14, 131.93, 124.82, 123.93, 120.94, 112.99, 111.36; HR-MS (MALDI): $C_{19}H_{13}N_5$ *m/z* 310.1171 $[M-1]^+$ (Calcd.); 310.1096 (Found).

VII.2. Synthesis of pyridine-bridged bis-*N*-butylbenzimidazolylium dibromide (5f)

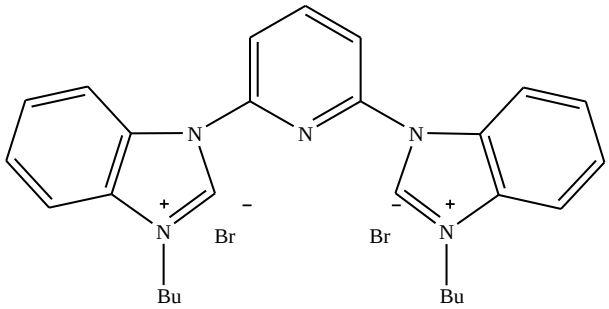

A mixture of 2,6-bis(benzimidazol-1-yl)pyridine (0.622 g, 2 mmol) and *n*-BuBr (0.43 mL, 4 mmol) in benzonitrile (5 mL) was stirred at 160 °C for 30 h in a sealed tube. After cooling, the mixture was dissolved in $CHCl_3$ (50 mL), and then Et_2O (250 mL) was added. The crude product

was purified by reprecipitation from $CHCl_3/Et_2O$ to give a white NMR-pure solid in almost quantitative yield.

^{1}H NMR (DMSO-D_6, 400 MHz, 298 K): δ 9.98 (s, 2H), 7.90 (t, J = 8 Hz, 1H), 7.60 (d, J = 8.1 Hz, 2H), 7.51 (d, J = 8.1 Hz, 2H), 7.43 (d, J = 8 Hz, 2H), 6.92-6.99 (m, 2H), 6.85-6.91 (m, 2H), 3.83 (t, J = 7.3 Hz, 4H), 1.14-1.23 (m, 4 H), 0.61 (tq, J = 7.5 and 7.5 Hz, 4H), 0.12 (t, J = 7.3 Hz, 6H); ^{13}C NMR (DMSO-D_6, 100 MHz): δ 146.8, 144.9, 143.3, 132.1, 130.0, 128.3, 127.8, 118.4, 116.2, 114.7, 47.7, 30.9, 19.6, 13.9; MS (ESI): *m/z* 504.2 $[M\text{-}Br]^+$, 456.3, 424.3 $[M\text{-}2Br]^+$, 368.2 $[M\text{-}2Br\text{-}Bu]^+$, 312.1 $[M\text{-}2Br\text{-}2Bu]^+$, 212.6, 184.6, 156.6; HR-MS(ESI): *m/z* Calad: 504.1757$[M\text{-}Br]^+$; Found: 504.1757; Anal. Calcd for $C_{27}H_{31}Br_2N_5$•0.5 H_2O: C, 54.56; H, 5.34; N, 11.78. Found: C, 54.66; H, 5.35; N, 11.62.

VII.3 Synthesis of pyridine-bridged bis-*N*-butyl(benzimidazol-2-ylidene) palladium complex (6e)

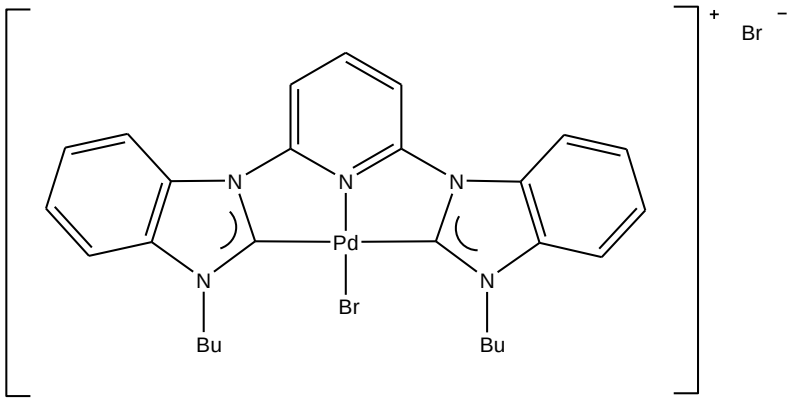

A suspension of pyridine-bridged bis-benzimidazolium dibromide **5** (585 mg, 1 mmol) and $Pd(OAc)_2$ (0.224 g, 1 mmol) was stirred in DMSO (8 mL) for 1 h at room temperature under vacuum. After refilling the argon, the mixture was heated under stirring in the open vessel model at 160 °C for 25 min (at 40 W with a CEM Discover microwave instrument). DMSO was removed *in vacuum* under heating. After cooling to room temperature, the resulting residue was dissolved in 10 mL of $CHCl_3$; then Et_2O was added (100 mL) and the precipitate was collected by filtration and dried *in vacuum*. Another two re-precipitation operations afforded 528 mg (75 %) of a yellowish solid.

^{1}H NMR (DMSO-$D_{6,}$ 500 MHz, 298 K): δ 7.78 (t, J = 8.3 Hz, 1H), 7.68 (d, J = 7 Hz, 2H), 7.64 (d, J = 8.3 Hz, 2H), 7.26 (dd, J = 7 and 2.2 Hz, 2H), 6.85-6.92 (m, 4H), 4.28 (t, J = 7.5 Hz, 4H), 1.04 (q, J = 7.5 Hz, 4 H), 0.68 (tq, J = 7.5 Hz, 4H), 0.13 (t, J = 7.5 Hz, 6H).

^{13}C NMR (DMSO-D_6, 125 MHz, 298 K): δ 175.45, 151.43, 147.46, 134.24, 130.13, 127.78, 127.12, 114.45, 114.05, 110.61, 48.13, 32.79, 20.08, 14.54; MS (ESI): *m/z* 690.0 $[M+2]^+$, 610.1 $[M-Br+2]^+$, 564.1, 484.4, 454.3, 368.2 $[M-2Br-Bu-Pd]^+$, 298.2, 268.1, 212.6; HR-MS(ESI): *m/z* Calcd, 608.0641 $[M–Br]^+$; Found: 608.0640; Anal. Calcd for $C_{27}H_{29}Br_2N_5Pd•H_2O$: C, 45.82; H, 4.41; N, 9.89. Found: C, 45.44; H, 4.32; N, .9.55.

VII.4. General procedure for the Heck Reactions

To a suspension of K_2CO_3 (1.68 g, 12 mmol) in 10 mL NMP aryl halide (10 mmol), alkyl acrylate (11 mmol) and the CNC pincer palladium carbene complex **6e** (solution in NMP) were added. The reaction mixture was heated at 140 °C (monitored by GC-MS) and then allowed to cool to room temperature. Then the reaction mixture was diluted with water, and the product was extracted with ether (3 × 20 mL). The combined extracts were dried over $MgSO_4$, the organic phase was concentrated *in vacuo* and the crude product was purified by flash column chromatography (hexane/EtOAc = 100/1) (see table 3).

VII.5. General procedure for the Suzuki Reactions

A mixture of catalyst **6e**, K_2CO_3 (1.68 g, 12 mmol), aryl halide (10 mmol) and phenyl boronic acid (1.29 g, 11 mmol) in 10 mL NMP was heated at 140 °C for 24 h. The reaction mixture was heated at 140 °C (monitored by GC-MS) and then allowed to cool to room temperature. Then the reaction mixture was diluted with water, and the product was extracted with ether (3 × 20 mL). The combined extracts were dried over $MgSO_4$, the organic phase was concentrated *in vacuo* and the crude product was purified by flash column chromatography (hexane/EtOAc = 100/1) (see table 4).

VII.6 Synthesis of 2, 6-dibromo-4-(4[1]-ethoxystyryl)-pyridine (9)

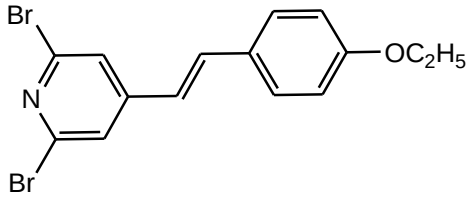

A mixture of 2, 6-dibromo-4-(bromomethyl)-pyridine (329 mg, 1 mmol) and triethyl phosphite (249 mg, 1.5 mmol) was heated to 140^{o} C with stirring for 25 minutes. Access triethyl phosphite was distilled off and the reaction mixture was cooled to room temperature. To this reaction mixture 4-ethoxybenzaldehyde (180 mg, 1.2 mmol) and potassium tert-butoxide (168 mg, 1.5 mmol) were added at 0 ^{o}C in dry THF and the reaction mixture was stirred for 12h at room temperature. 3N HCl (10 mL) was added and the reaction mixture and extracted with CH_2Cl_2; the organic phase was dried ($MgSO_4$) and evaporated under reduced pressure. The residue was purified by column chromatography on silica gel with *n*-hexane/EtOAc 9:1 leading to a white solid (363 mg, 95 %).

^{1}H NMR ($CDCl_3$, 300 MHz, 298 K): δ 7.38 (s, 2H), 7.36 (d, *J* = 8.8, 2H), 7.16 (d, *J* = 15.7, 1H), 7.83 (d, *J* = 8.8, 2H), 6.63 (d, *J* = 15.7, 1H), 3.99 (q, *J* = 6.96, 2H), 1.36 (t, *J* = 7.0, 3H). ^{13} C NMR ($CDCl_3$, 75 MHz, 298 K): δ 159.89, 149.77, 140.73, 135.31, 128.49, 127.46, 123.24, 120.25, 114.58, 63.28, 14.41. HR-MS (ESI-TOF): $C_{15}H_{13}Br_2NO$ *m/z* 381.9462 $[M]^+$ (Calcd.) ; 381.9456 (Found).

VII.7 Synthesis of 4-(4[1]-ethoxystyryl)-2, 6-di(1H-imidazol-1-yl)-pyridine (10)

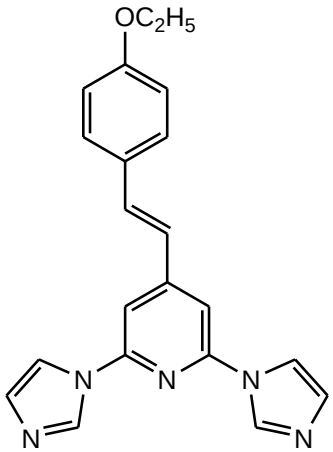

To a dried Schlenk tube charged with 2,6-dibromo-4-(bromomethyl)-pyridine (383 mg, 1 mmol), potassium carbonate (414 mg, 3 mmol), CuI (95 mg 0.5 mmol) and imidazole (170 mg, 2.5 mmol) dry DMF was added under argon atmosphere and the reaction mixture was heated to 140 ^{o}C for 48 h. DMF was distilled off and water was added. The residue was purified by column chromatography on silica gel with CH_2Cl_2/ MeOH 9.5:0.5 leading to a white solid (257 mg, 72%).

^{1}H NMR (CD_2Cl_2, 400 MHz, 298 K): δ 8.28 (s, 2H), 7.61 (bs, 2H), 7.42 (d, *J* =8.7, 2H), 7.29 (d, *J* = 16.2, 1H), 7.2 (s, 2H), 7.09 (bs, 2H), 6.86 (d, *J* = 16.2, 1H), 6.82 (d, *J* = 8.7, 2H), 3.95 (q, *J* = 6.99, 2H), 1.31(t, *J* = 6.98, 3H). ^{13} C NMR (CD_2Cl_2, 100 MHz, 298 K): δ 160.4, 151.77, 148.88, 135.15, 130.75, 128.89, 127.96, 121.94, 116.31, 114.93, 106.51, 63.76, 14.62. HR-MS (ESI-TOF) : $C_{21}H_{19}N_5O$ *m/z* 358.1662 $[M]^+$ (Calcd.) ; 358.1663 (Found).

VII.8 Synthesis of $[CHNCH\text{-}(C_4H_9)_2]Br_2$ (11a)

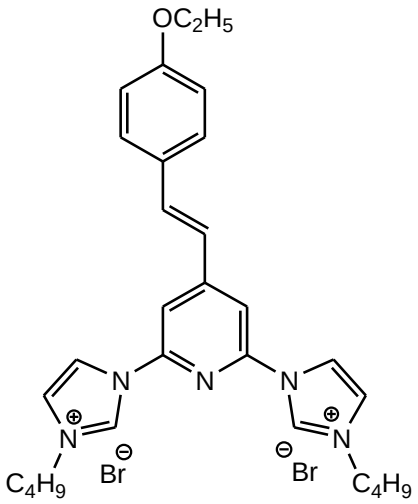

A mixture of 4-(4^{1}-ethoxystyryl)-2, 6-di(1H-imidazol-1-yl)-pyridine (631 mg, 1 mmol) and *n*-butylbromide (5 mmol) was stirred neat at 110 ^{o}C for 36 h. After cooling, the reaction mixture was dissolved in $CHCl_3$ (10 mL) and then cooled Et_2O (100 mL) was added. The crude product was purified by reprecipitation from $CHCl_3$/ Et_2O to give a yellow solid in quantitative yield.

^{1}H NMR (DMSO, 400 MHz, 298 K): δ 10.85 (s, 2H), 8.91 (t, J_1 = 1.6, J_2 = 1.7, 2H), 8.5 (s, 2H), 8.17 (t, J_1 = 1.6, J_2 = 1.7, 2H), 8.12 (d, *J* = 16.3, 1H), 7.62 (d, *J* = 8.7, 2H), 7.16 (d, *J* = 16.3, 1H), 6.99 (d, *J* = 8.7, 2H), 4.37 (t, *J* = 7.2, 4H), 4.07 (q, *J* = 6.9, 2H), 1.93 (quintet, *J* = 7.3, 4H), 1.34 (m, 7H), 0.94 (t, *J* = 7.4, 6H). ^{13} C NMR (DMSO, 100 MHz, 298 K): δ 159.9, 153.5, 145.7,

137.6, 135.7, 129.2, 127.7, 123.7, 120.9, 119.4, 115.03, 110.32, 63.3, 49.4, 31.9, 18.9, 14.6, 13.4. HR-MS (ESI-TOF) : $C_{29}H_{37}Br_2N_5O$ *m/z* $[M\text{-}2Br]^+$. 471.292 (calcd), 471.297 (found).

VII.9 Synthesis of [CHNCH-($C_{16}H_{33}$)2]I_2 (11b)

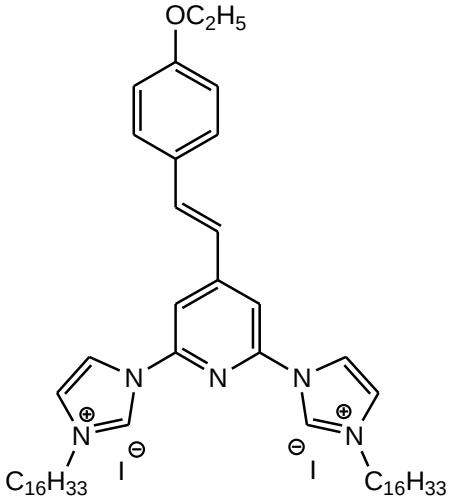

A mixture of 4-(4[1]-ethoxystyryl)-2,6-di(1H-imidazol-1-yl)-pyridine (631 mg, 1 mmol) and $C_{16}H_{33}I$ (5 mmol) was stirred neat at 110 ^oC for 36 h. After cooling, the reaction mixture was dissolved in $CHCl_3$ (10 mL) and then cooled Et_2O (100 mL) was added. The crude product was purified by reprecipitation from $CHCl_3$/ Et_2O to give a yellow solid in quantitative yield.

^{1}H NMR (DMSO, 400 MHz, 298 K): δ 10.42 (s, 1H), 8.8 (t, *J* = 1.84, *J* = 1.81, 2H), 8.38 (s, 2H), 8.18 (t, J_1 = 1.82, J_2 = 1.69, 2H), 7.95 (d, *J* = 16.2, 1H), 7.66 (d, *J* = 8.81, 2H), 7.23 (d, *J* = 16.25, 1H), 7.04 (d, *J* = 8.84, 2H), 4.34 (t, *J* = 7.1, 4H), 4.09 (q, *J* = 6.99, 2H), 1.94 (quintet, *J* = 6.65, 4H), 1.2-1.36 (m, 55H), 0.82 (t, *J* = 7.02, 6H).

^{13} C NMR (DMSO, 100 MHz, 298 K): δ 160.08, 153.47, 145.83, 137.52, 135.47, 129.29, 127.65, 123.85, 121.07, 119.45, 115.14, 110.47, 63.40, 49.88, 31.34, 29.22, 29.11, 29.00, 28.89, 28.76, 28.47, 25.57, 22.14, 14.64, 13.98. HR-MS (ESI-TOF): $C_{53}H_{85}I_2N_5O$ *m/z* $[M\text{-}I]^+$ 934.5793 (calcd), 934.5776 (found).

General procedure for the synthesis of Palladium complexes: A solution of pyridine-bridged bis-imidazolium salt (1.0 mmol) and $Pd(OAc)_2$ (0.224 g, 1.0 mmol) was stirred in DMSO (8 mL) for 1 h at room temperature under vacuum. After refilling the flask with argon, the mixture was

exposed to microwave radiation with stirring in the open vessel model for 25 min at 160 ^{o}C (at 40W with a CEM Discover instrument). Cold Et_2O was added (200 mL) and the precipitate was purified three times by dissolving in hot $CHCl_3$ and precipitating with cold Et_2O, affording a yellowish solid.

VII.10. Synthesis of [PdBr-CNC-(C_4H_9)$_2$][Br] (12a)

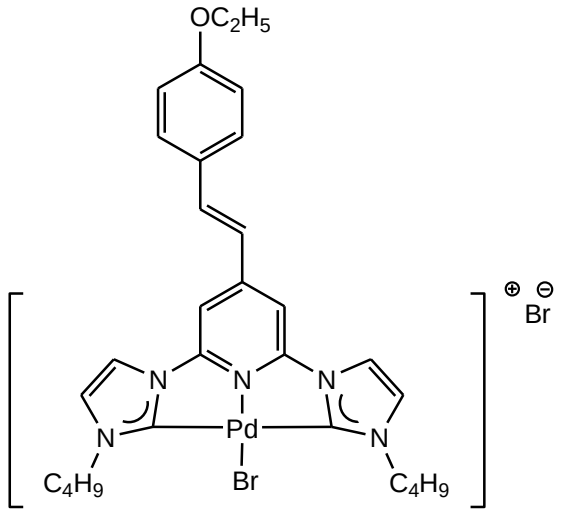

^{1}H NMR (DMSO, 400 MHz, 298 K): δ 8.43 (s, 2H), 8.17 (s, 2H), 7.91 (d, *J* = 16.1, 1H), 7.72 (s, 2H), 7.51 (d, *J* = 8.08, 2H), 6.99 (d, *J* = 16.1, 1H), 6.87 (d, *J* = 8.08, 2H), 4.44 (t, *J* = 6.65, 4H), 4.05 (q, *J* = 6.89, 2H), 1.74 (quintet, *J* = 7.02, 4H), 1.33 (m, 7H), 0.9 (t, *J* = 7.4, 6H). ^{13}C NMR (DMSO, 100 MHz, 298 K): δ 190.44, 165.75, 160.31, 155.07, 149.77, 129.45, 127.5, 123.9, 118.09, 114.84, 109.56, 104.95, 63.36, 49.58, 32.72, 19.09, 14.62, 13.68. HR-MS (ESI-TOF): $C_{29}H_{37}Br_2N_5OPd$; *m/z* $[M\text{-}Br]^+$ 656.1038 (calcd), 656.1040 (found).

VII.11. Synthesis of [PdI-CNC-($C_{16}H_{33}$)$_2$][I] (12b)

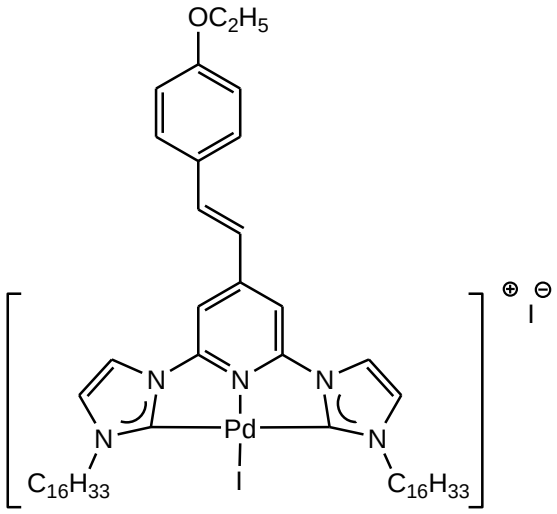

^{1}H NMR (DMSO, 500 MHz, 398 K): δ 8.4 (bs, 2H), 8.16 (bs, 2H), 7.93 (d, *J* = 15.6, 1H), 7.7 (bs, 2H), 7.6 (d, *J* = 7.1, 2H), 7.17 (d, *J* = 15.9, 1H), 7.04 (d, *J* = 7.4, 2H), 4.67 (t, *J* = 7.39, 4H), 4.16 (q, *J* = 6.94, 2H), 1.87 (quintet, *J* = 7.3, 4H), 1.27-1.43 (m, 55H), 0.88 (t, *J* = 5.12, 6H). ^{13} C NMR (DMSO, 100 MHz, 398 K): δ 167.25, 161.45, 156.24, 150.64, 139.95, 130.41, 128.72, 124.94, 124.87, 122.76, 118.94, 116.31, 105.78, 64.51, 52.73, 32.08, 31.75, 29.81, 29.77, 29.67, 29.62, 29.43, 29.37, 26.38, 22.79, 15.35, 14.51. HR-MS (ESI-TOF): $C_{53}H_{85}I_2N_5OPd$; *m/z* $[M\text{-}I]^+$ 1038.4706 (calcd), 1039.4699 (found).

VII.12 TEM images of gel 12b from different solvents

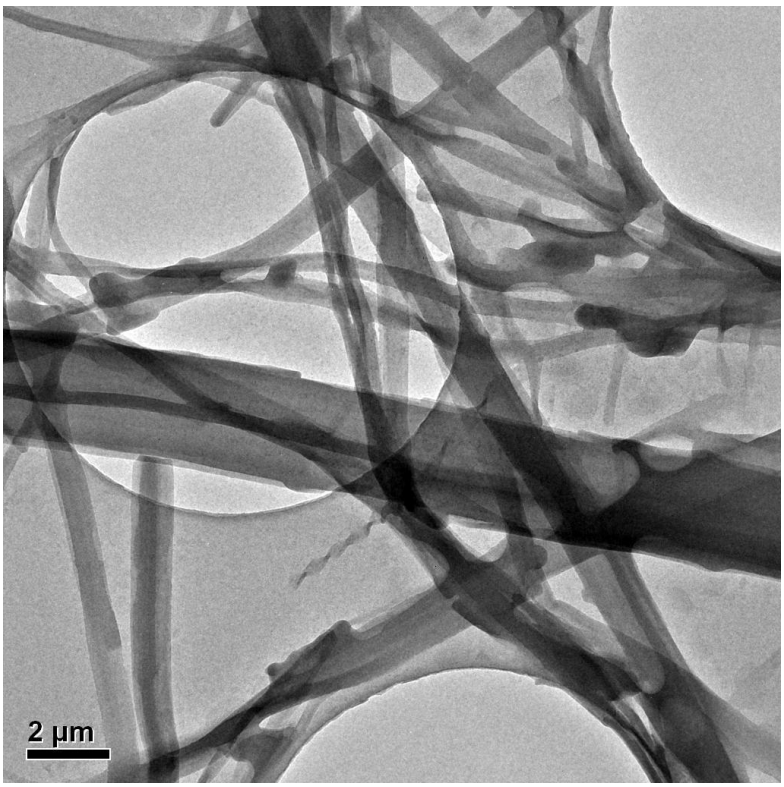

Figure 27. TEM image of gel **12b** in DMSO at 2 wt% concentration.

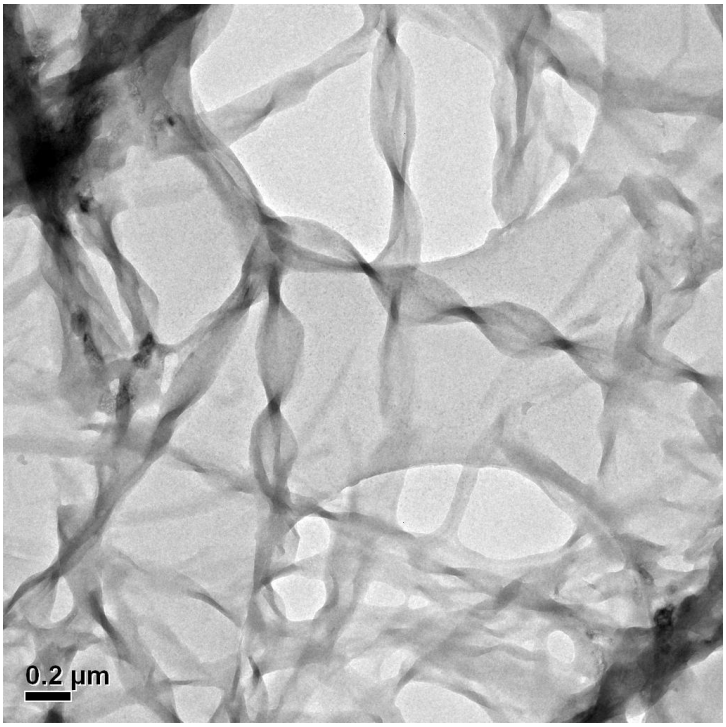

Figure 28. TEM image of gel of **12b** in Acetone at 3 wt% concentration.

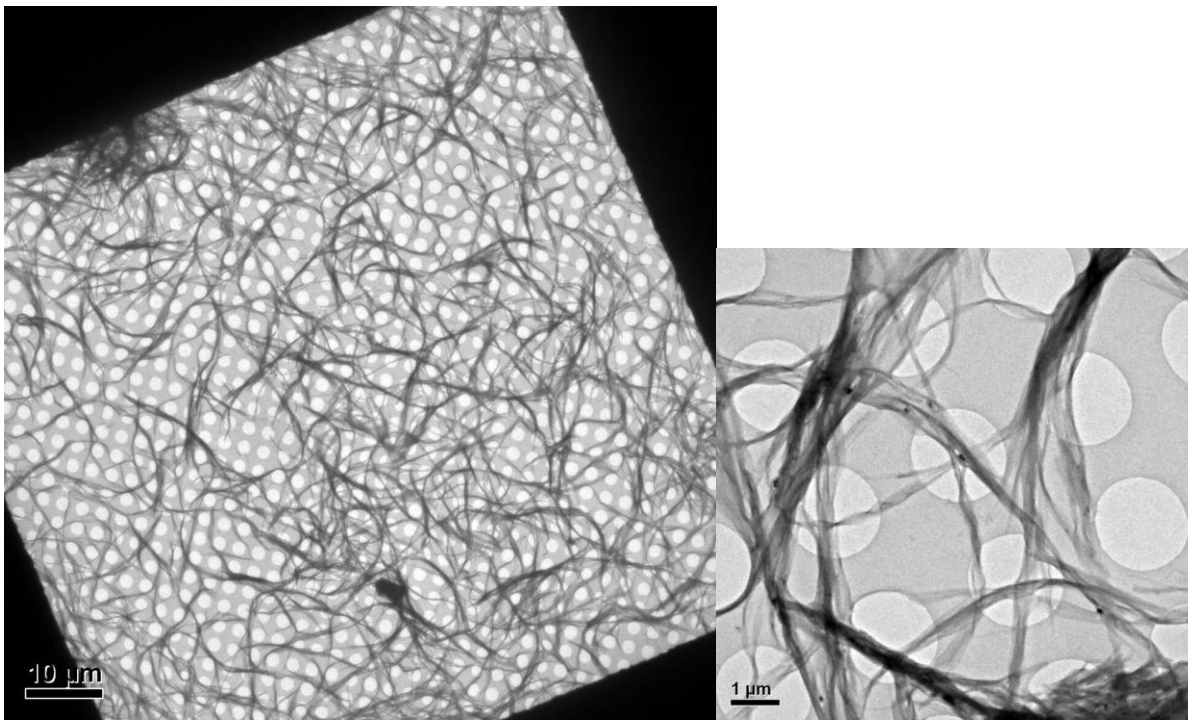

Figure 29. TEM images of gel **12b** in Chlorobenzene at 3 wt% concentration.

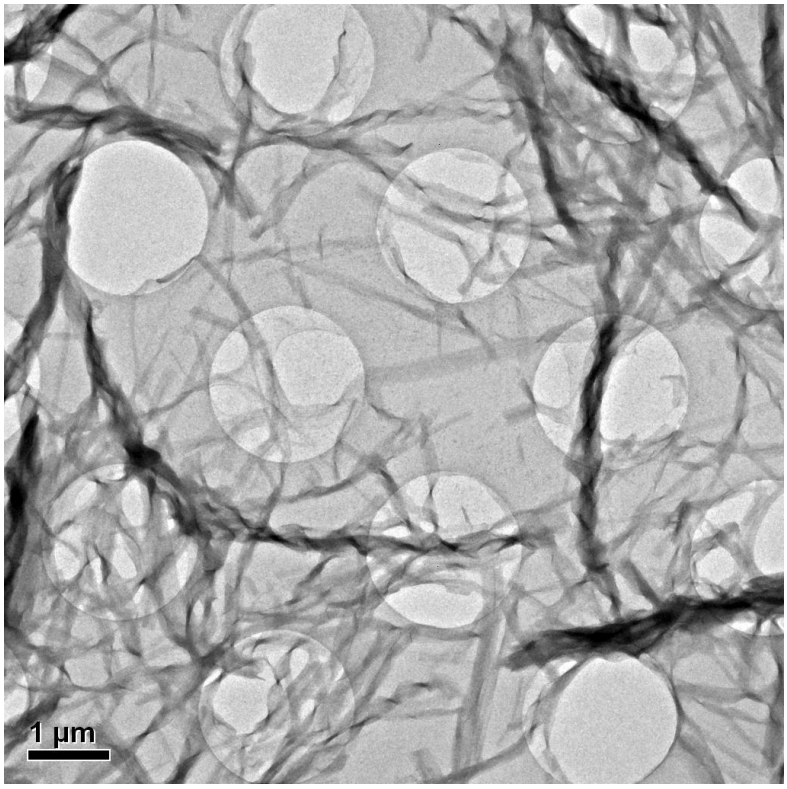

Figure 30. TEM image of gel **12b** in dioxane at 3 wt% concentration.

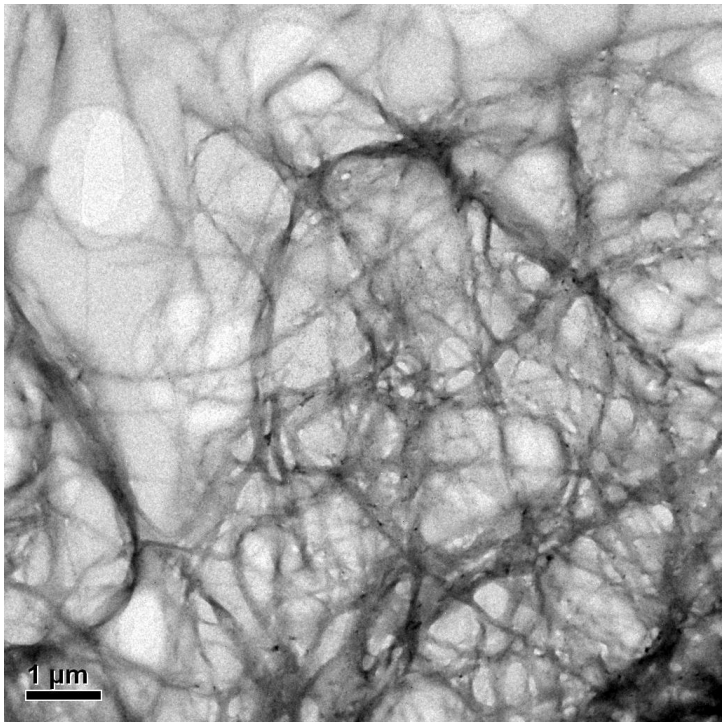

Figure 31. TEM image of gel **12b** in DMA at 3 wt% concentration.

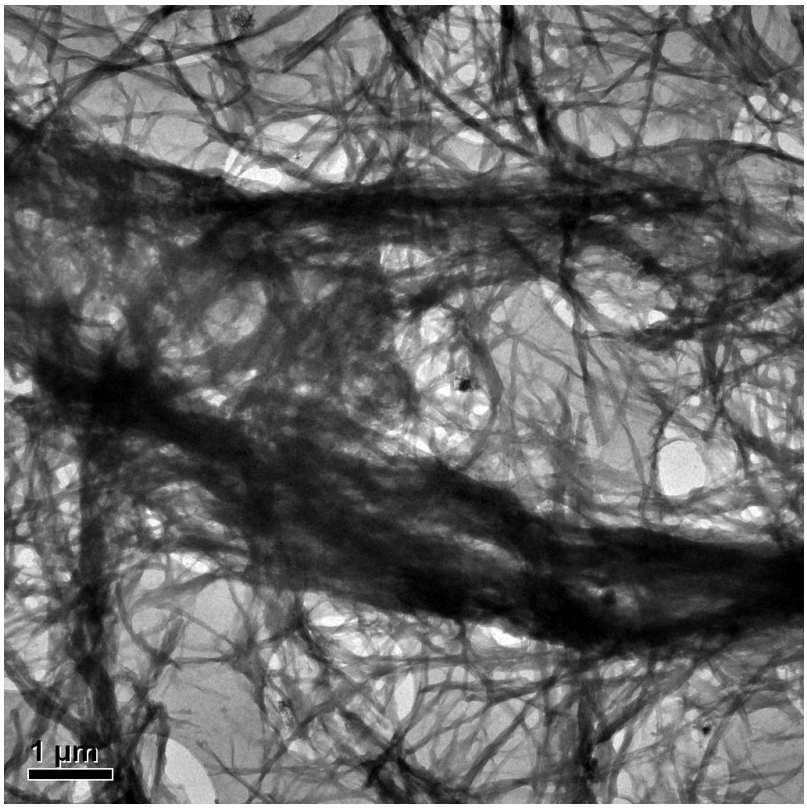

Figure 32. TEM image of gel **12b** in DMF at 3 wt% concentration.

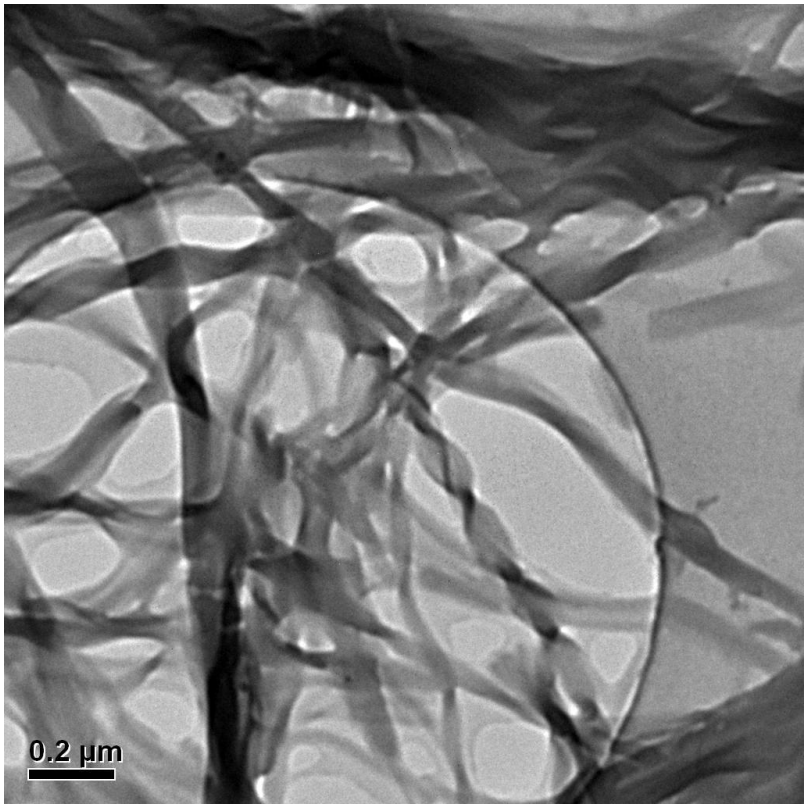

Figure 33. TEM image of gel **12b** in NMP at 3 wt% concentration.

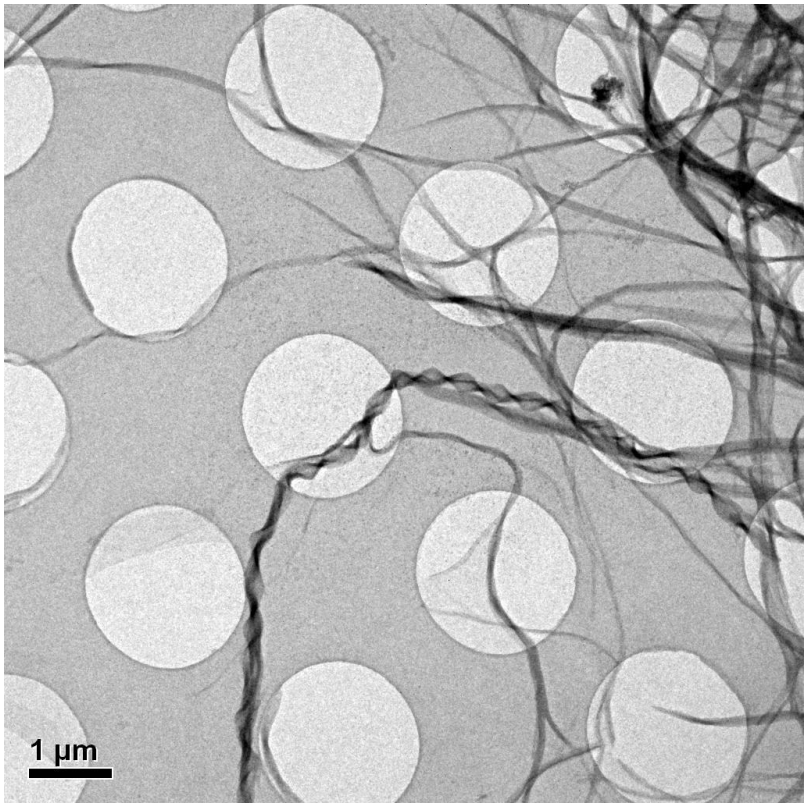

Figure 34. TEM image of gel **12b** in Pyridine at 3 wt% concentration.

VII.13 DSC Studies of 12b

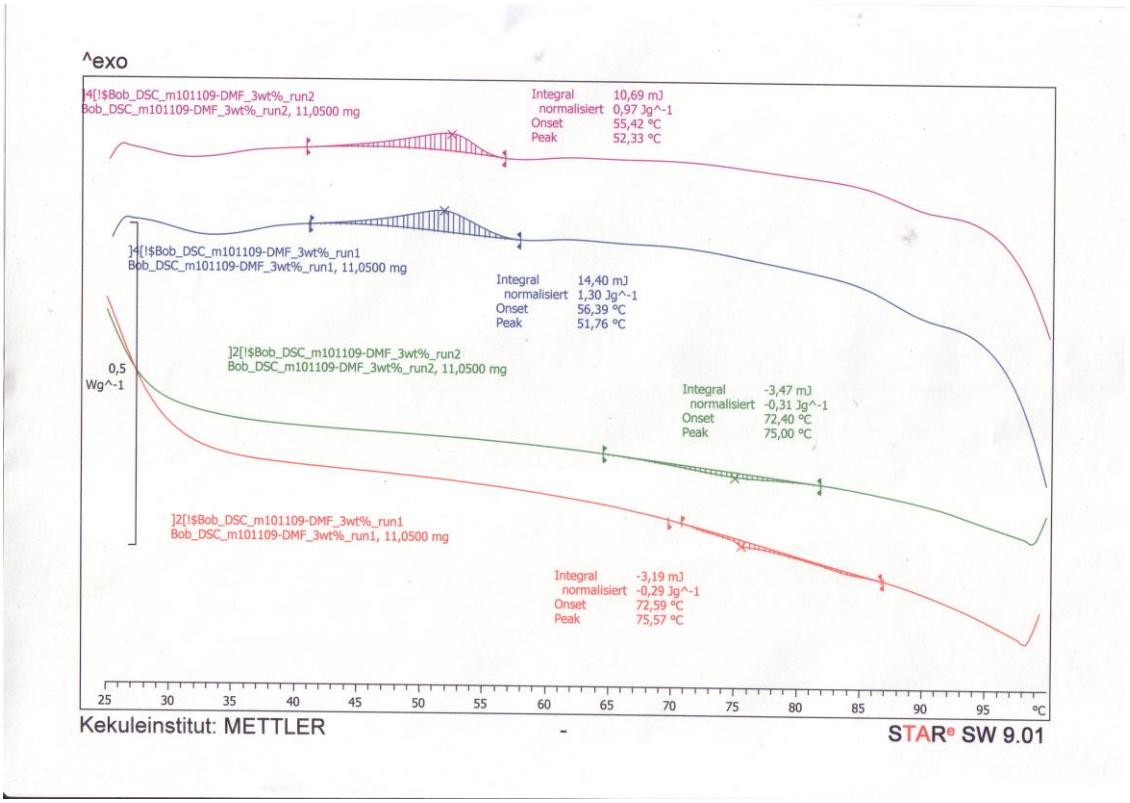

VII.14 Synthesis of (4-(4[1]-ethoxystyryl)-2,6-bis-(benzimidazole)-pyridine (13)

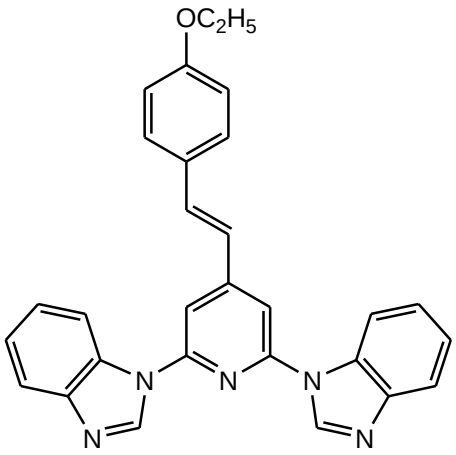

To a oven-dried Schlenk tube charged with 2,6-dibromo-4-(4[1]-ethoxystyry)-pyridine (383 mg, 1 mmol), potassium carbonate (414 mg, 3 mmol), CuI (95 mg 0.5 mmol) and benzimidazole (295 mg, 2.5 mmol) dry DMF (3mL) was added under argon atmosphere. The reaction mixture was warmed to 140 ^{o}C for 48 h. The DMF was distilled off, the he reaction mixture was diluted with

water, and the product was extracted with $CHCl_3$ (3 x 50 ml). The combined extracts were dried over $MgSO_4$, the organic phase was concentrated under vacuum and the crude product was purified by flash column chromatography with CH_2Cl_2/ MeOH 9.5:0.5 leading to a white solid (297 mg, 65%).

^{1}H NMR (DMSO, 400 MHz, 298 K): δ 9.10 (s, 2H), 8.27 (m, 2H), 8.06 (s, 2H), 7.81-7.88 (m, 3H), 7.63 (d, *J* = 8.6, 2H), 7.38 (m, 4H), 7.30 (d, *J* = 16.3, 1H), 7.01 (d, *J* = 8.6, 2H), 4.07 (q, *J* = 6.98, 2H), 1.34 (t, J = 6.97, 3H). ^{13} C NMR (DMSO, 100 MHz, 298 K): δ 159.54, 151.67, 149.37, 144.33, 142.54, 135.41, 131.87, 128.90, 128.33, 124.15, 123.29, 122.55, 120.09, 114.96, 113.82, 108.95, 63.27, 14.66. HR-MS (ESI-TOF): $C_{29}H_{23}N_5O$ *m/z* $[M+H]^+$ 458.1975 (calcd), 458.1975 (found).

VII.15 Synthesis of [CHNCH-$(C_4H_9)_2$]Br_2 (14a)

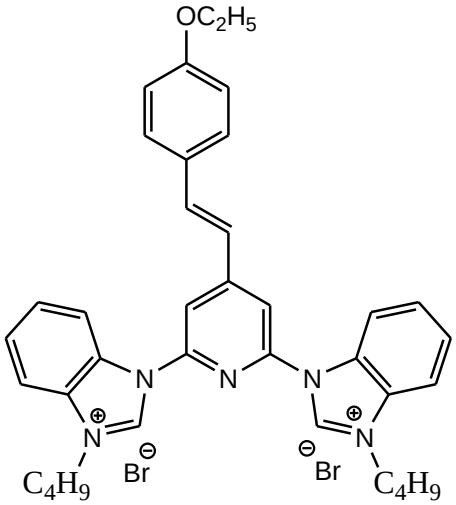

To a mixture of (4-(4^1-ethoxystyryl)-2,6-bis-(benzimidazolyl)-pyridine (457 mg 1 mmol) and 1-bromobutane (1 mL) DMF (1 mL) was added and the reaction mixture was heated to 100 ^{o}C for 20 h. After cooling, the mixture was dissolved in $CHCl_3$ (20 mL) and then Et_2O (50 mL) was added. The precipitate was collected and the product was purified by flash column chromatography on silica gel CH_2Cl_2/ MeOH 9:1 leading to a yellow solid (715 mg, 98%).

^{1}H NMR (DMSO, 400 MHz, 298 K): δ 11.08 (s, 2H), 8.61 (s, 2H), 8.51 (d, *J* = 8.28, 2H), 8.30 (d, *J* = 8.3, 2H), 8.16 (d, *J* = 16.3, 1H), 7.82 (t, *J* = 7.53, 2H), 7.76 (d, *J* = 8.16, 2H), 7.7-7.73

(m, 2H), 7.42 (d, *J* = 16.3, 1H), 7.01 (d, *J* = 8.7, 2H), 4.73 (t, *J* = 7.26, 4H), 4.08 (q, *J* = 6.97, 2H), 2.08 (quintet, *J* = 7.42, 4H), 1.48 (m, 4H), 1.35 (t, *J* = 6.95, 3H), 1.00 (t, *J* = 7.39, 6H).
^{13} C NMR (DMSO, 75 MHz, 298 K): δ 160.01, 153.12, 147.05, 142.76, 137.66, 131.68, 129.55, 129.37, 127.92, 127.85, 127.39, 121.22, 116.03, 115.06, 114.34, 114.00, 63.38, 47.29, 30.59, 19.24, 14.64, 13.33. HR-MS (ESI-TOF): $C_{37}H_{41}Br_2N_5O$; *m/z* $[M\text{-}Br]^+$. 650.2489 (calcd), 650.2489 (found).

VII.16 Synthesis of [PdBr-CNC--$(C_4H_9)_2$][Br] (15a)

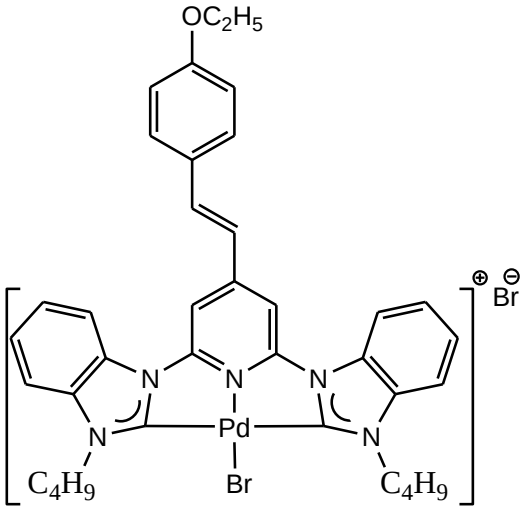

A solution of pyridine-bridged bis-benzimidazolium salt 14a (1.0 mmol) and $Pd(OAc)_2$ (0.224 g, 1.0 mmol) in DMSO (8 mL) was stirred for 1 h at room temperature under vacuum. After refilling the flask with argon, the mixture was exposed to microwave radiation with stirring in the open vessel model for 25 min at 160 ^oC (at 40W with a CEM Discover instrument). Cold Et_2O was added (200 mL) and the precipitate was purified three times by dissolving in hot $CHCl_3$ and precipitating with cold Et_2O, affording a yellowish solid (518 mg, 62%).

^{1}H NMR (DMSO, 400 MHz, 298 K): δ 8.44 (d, *J* = 6.53, 2H), 7.91-7.99 (m, 5H), 7.62 (d, *J* = 8.5, 2H), 7.51-7.55 (m, 4H), 7.37 (d, *J* = 16.3, 1H), 6.98 (d, *J* = 8.52, 2H), 4.73 (t, *J* = 7.39, 4H), 4.09 (q, *J* = 6.96, 2H), 1.76 (quintent, *J* = 6.59, 4H), 1.37-1.42 (m, 7H), 0.90 (t, *J* = 7.36, 6H).

^{13}C NMR (DMSO, 100 MHz, 298 K): δ = 174.47, 160.31, 155.73, 150.07, 139.31, 133.11, 129.88, 128.78, 127.80, 126.82, 126.20, 121.59, 114.71, 113.42, 113.29, 104.66, 63.38, 47.48, 31.77, 19.25, 14.64, 13.58. HR-MS (ESI-TOF): $C_{37}H_{41}Br_2N_5OPd$ *m/z* $[M\text{-}Br]^+$. 754.1375 (calcd), 754.1396 (found).

VII.17 Synthesis of $[CHNCH\text{-}(C_{16}H_{33})_2]I_2$ (14b)

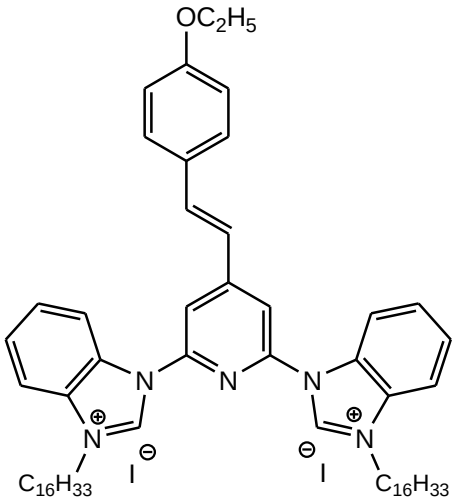

A mixture of (4-(4[1]-ethoxystyryl)-2,6-bis-(benzimidazolyl)-pyridine (457 mg 1 mmol) and 1-iodohexadecane (1.409 g, 4 mmol) was stirred neat at 140 °C for 30 h. After cooling, the mixture was dissolved in $CHCl_3$ (50 mL) and then Et_2O (250 mL) was added. The precipitate was collected and product was purified by flash column chromatography with CH_2Cl_2/ MeOH 9:1 leading to a yellow solid (1.11g, 96%).

^{1}H NMR (DMSO, 400 MHz, 298 K): δ = 10.78 (s, 2H), 8.51 (bd, *J* = 9.59, 4H), 8.31 (d, *J* = 8.26, 2H), 8.03 (d, *J* =16.2, 1H), 7.82 (t, *J* =7.86, 2H), 7.73-7.78 (m , 4H), 7.47 (d, *J* = 16.2, 1H), 7.06 (d, *J* =8.65, 2H), 4.70 (t, *J* = 7.15, 4H), 4.10 (q, *J* = 6.96, 2H), 2.08 (quintet, *J* = 7.1, 4H), 1.45 (m, 4H), 1.21-1.39 (m, 51H), 0.83 (t, *J* = 6.94, 6H).

^{13} C NMR (DMSO, 100 MHz, 298 K): δ = 160.09, 153.07, 147.02, 142.61, 137.45, 131.68, 129.58, 129.40, 127.97, 127.77, 127.43, 121.33, 115.96, 115.15, 114.37, 114.18, 63.41, 47.59,

31.35, 29.12, 29.07,29.05, 28.95, 28.76, 28.62, 28.57, 25.89, 22.14, 14.65, 13.99. HR-MS (ESI-TOF): $C_{61}H_{89}I_2N_5O$ *m/z* $[M\text{-}I]^+$ 1034.6106 (calcd), 1034.6106 (found).

VII.18 Synthesis of [PdI-CNC--$(C_{16}H_{33})_2$][I] (15b)

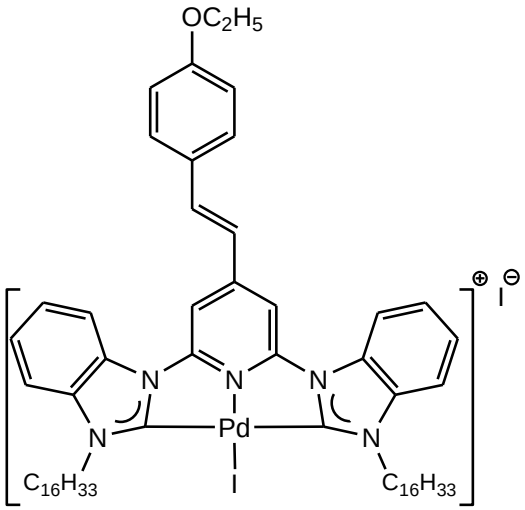

A solution of pyridine-bridged bis-benzimidazolium salt **14b** (1.0 mmol) and $Pd(OAc)_2$ (0.224 g, 1.0 mmol) was stirred in DMSO (8 mL) for 1 h at room temperature under vacuum. After refilling the flask with argon, the mixture was exposed to microwave radiation with stirring in the open vessel model for 25 min at 160^o C (at 40W with a CEM Discover instrument). DMSO was distilled off, the mixture was dissolved in $CHCl_3$ (50 mL) and cold Et_2O (200 mL) was added. The precipitate was purified by flash column chromatography with CH_2Cl_2/ MeOH 9:1 leading to a red solid (569mg, 45%).

^{1}H NMR (DMSO, 400 MHz, 368 K): δ 8.52 (d, J = 8.36, 2H), 8.13 (s, 2H), 8.03 (d, J = 16.2, 1H), 7.92 (bd, J = 7.29, 2H), 7.73 (d, J = 8.67, 2H), 7.6-7.65 (m, 4H), 7.51(d, J = 16.2, 1H), 7.04 (d, J = 8.61, 2H), 4.95 (t, J = 8.04, 4H), 4.16 (q, J = 6.94, 2H), 1.88 (quintet, J = 7.4, 4H), 1.49 (quintet, J = 7.1, 4H), 1.26-1.43 (m, 51H), 0.86 (t, J = 6.7, 6H).

^{13} C NMR (DMSO, 100 MHz, 298 K): δ = 174.47, 160.31, 155.73, 150.07, 139.31, 133.11, 129.88, 128.78, 127.80, 126.82, 126.20, 121.59, 114.71, 113.42, 113.29, 104.66, 63.38, 47.48, 31.77, 19.25, 14.64, 13.58. HR-MS (ESI-TOF): $C_{61}H_{89}I_2N_5OPd$ *m/z* $[M\text{-}I]^+$ 1138.5005 (calcd), 1138.5006 (found).

VII.19 TEM images of gel 15b from different solvents

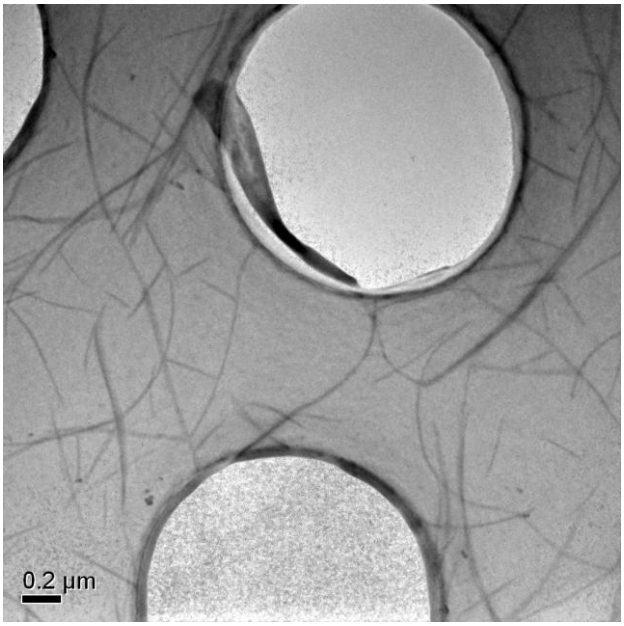

Figure 35. TEM image of gel **15b** in Benzonitrile at 1 wt% concentration

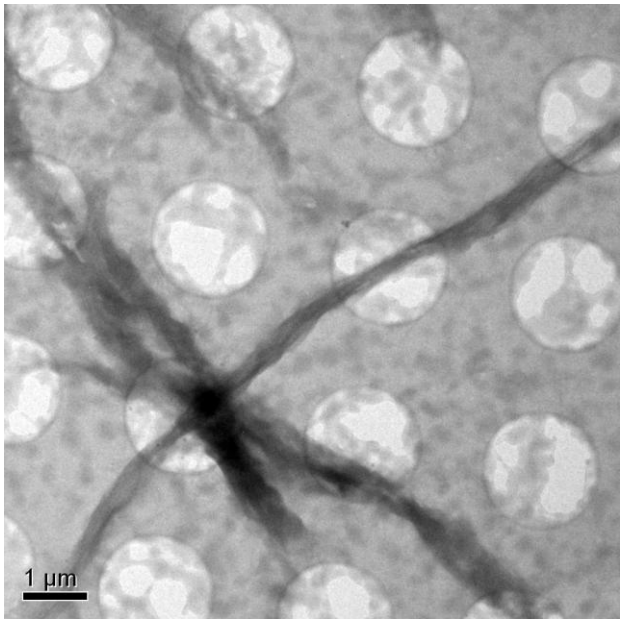

Figure 36. TEM image of gel **15b** in DMSO at 1 wt% concentration

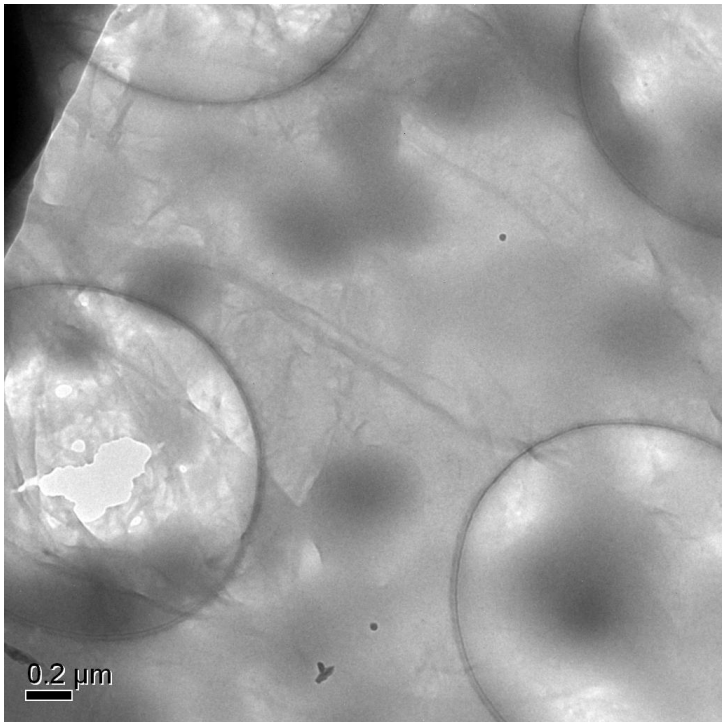

Figure 37. TEM image of gel **15b** in Acetone at 1 wt% concentration

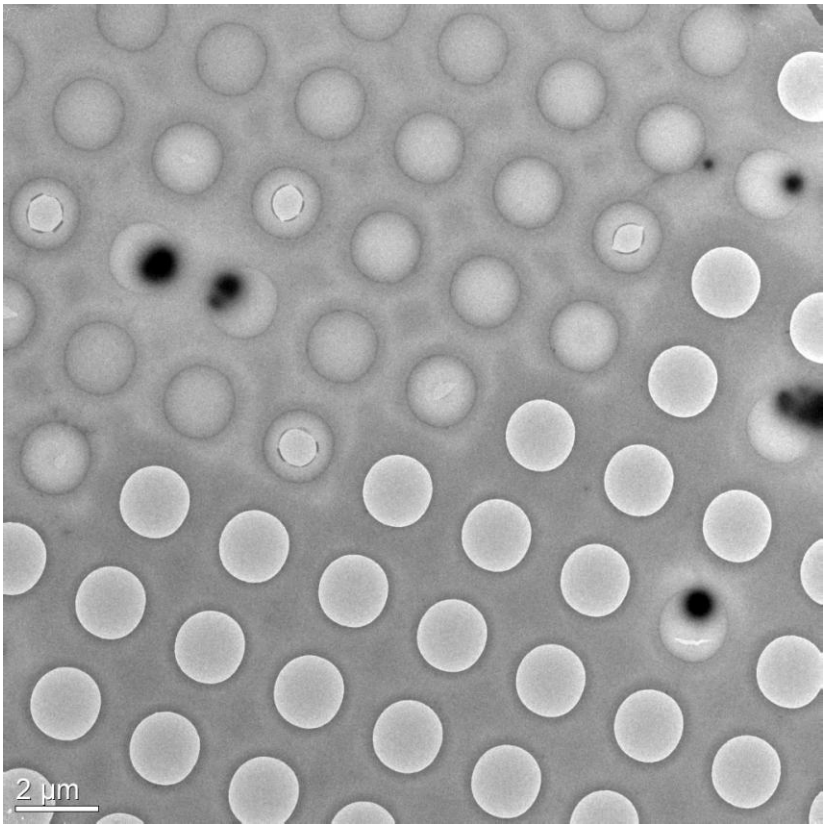

Figure 38. TEM image of gel **15b** in n-Butanol at 1 wt% concentration

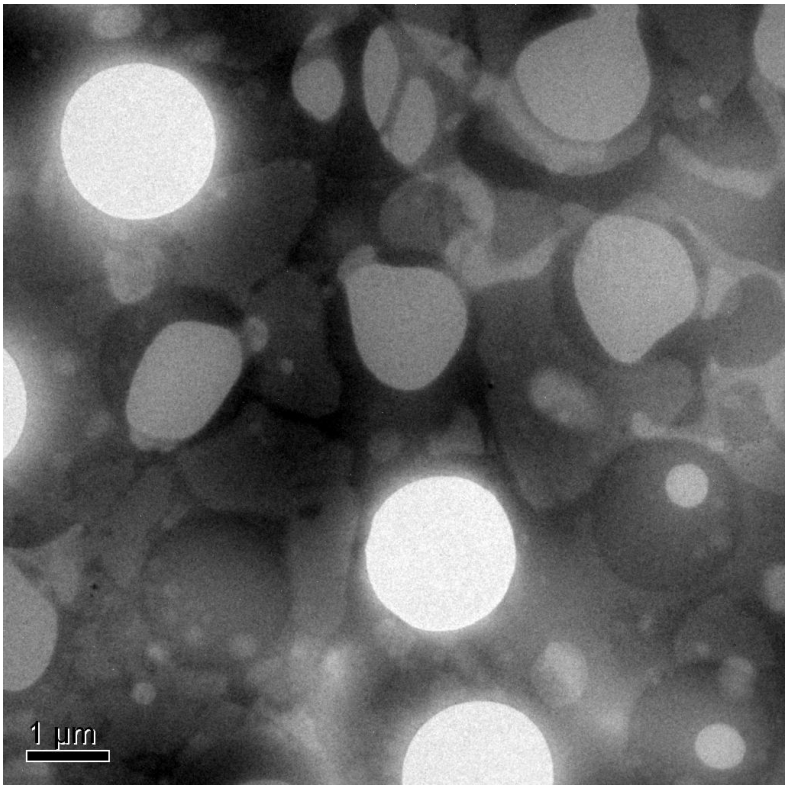

Figure 39. TEM image of gel **15b** in DMA at 1 wt% concentration

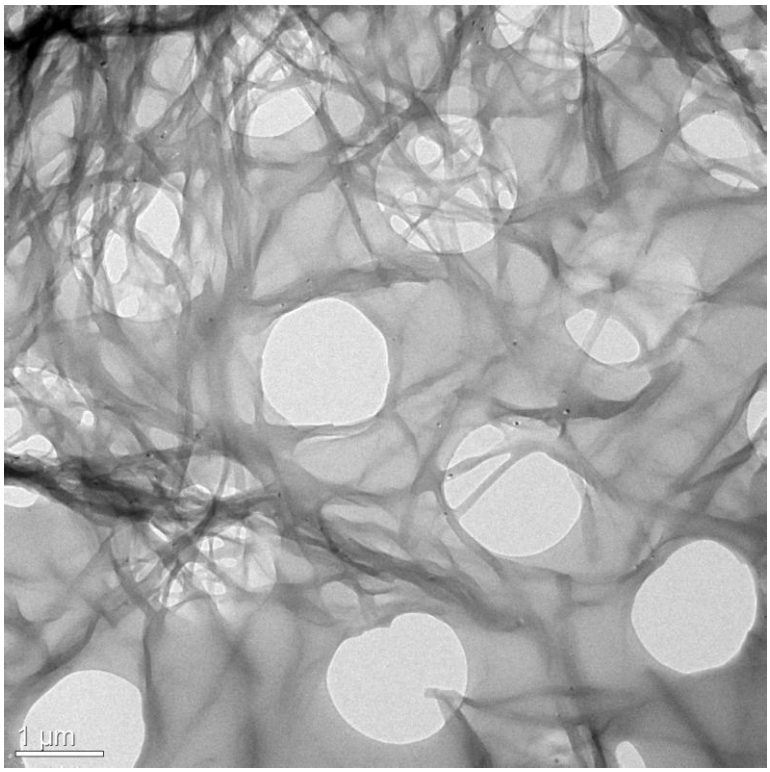

Figure 40. TEM image of gel **15b** in EtOH at 1 wt% concentration

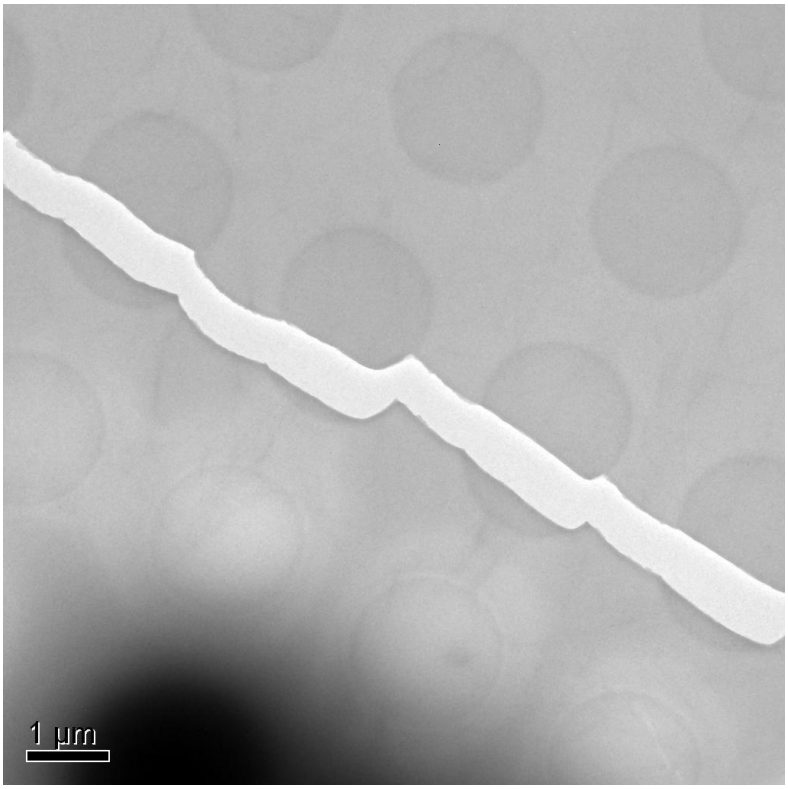

Figure 41. TEM image of gel **15b** in DMF at 1 wt% concentration

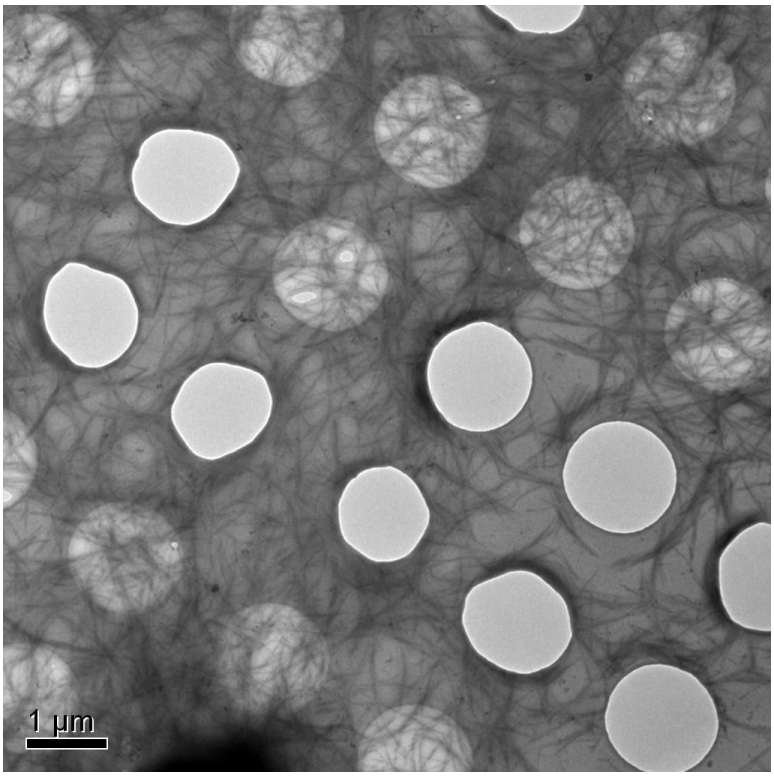

Figure 42.TEM image of gel **15b** in Cyclohexanol at 1wt% concentration

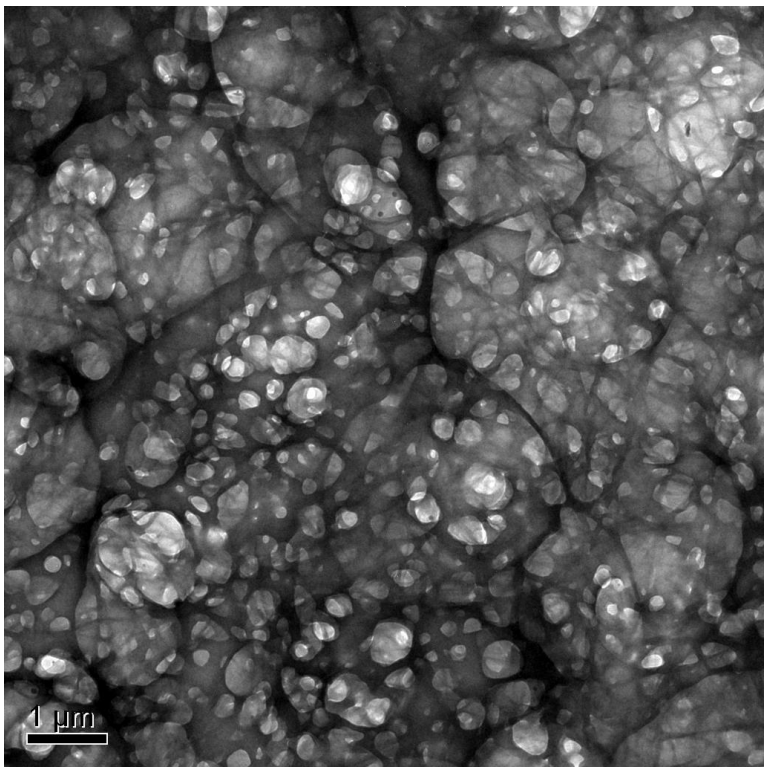

Figure 43.TEM image of gel **15b** in CH_2Cl_2 at 1wt% concentration

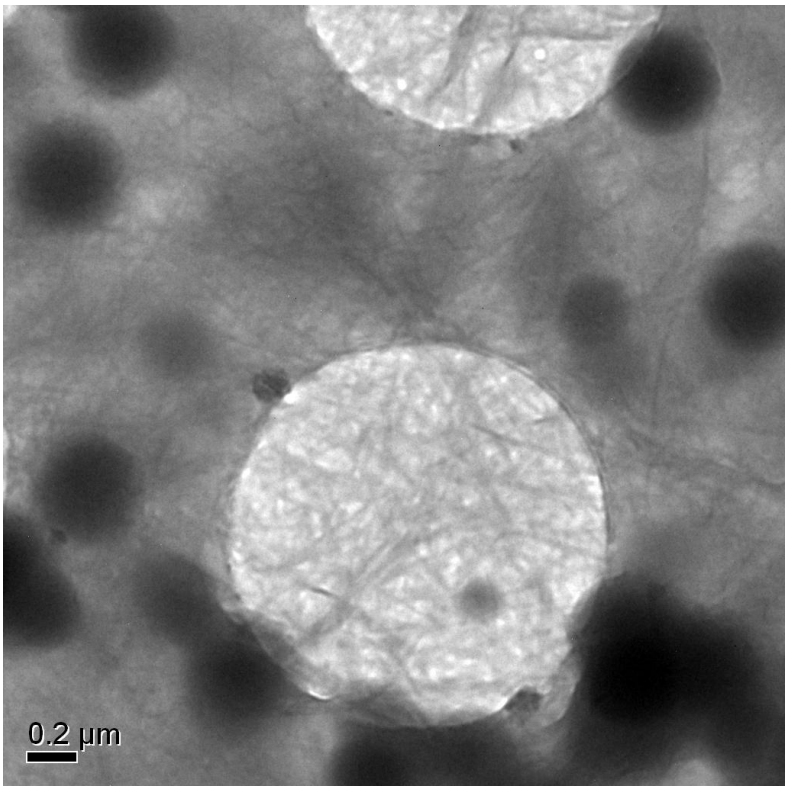

Figure 44.TEM image of gel **15b** in Pyridine at 1wt% concentration

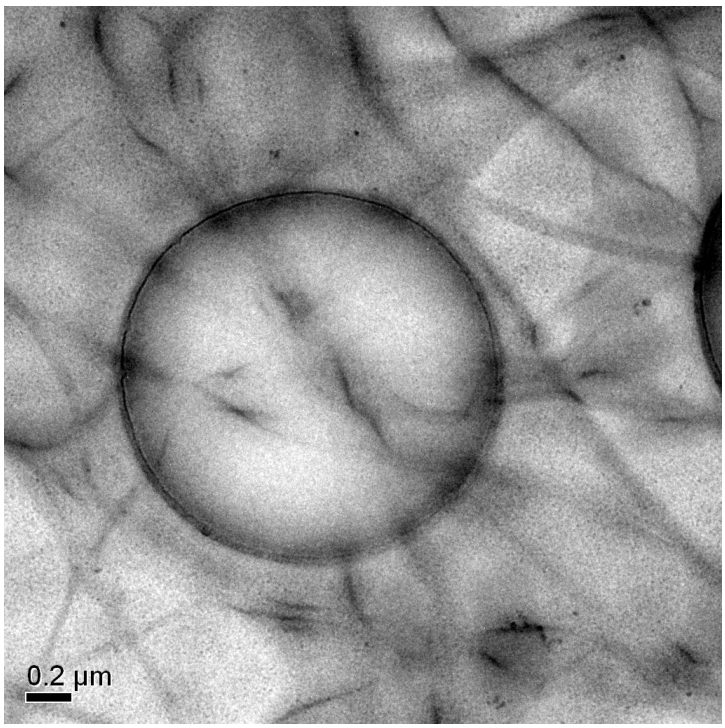

Figure 45.TEM image of gel **15b** in NMP at 1wt% concentration

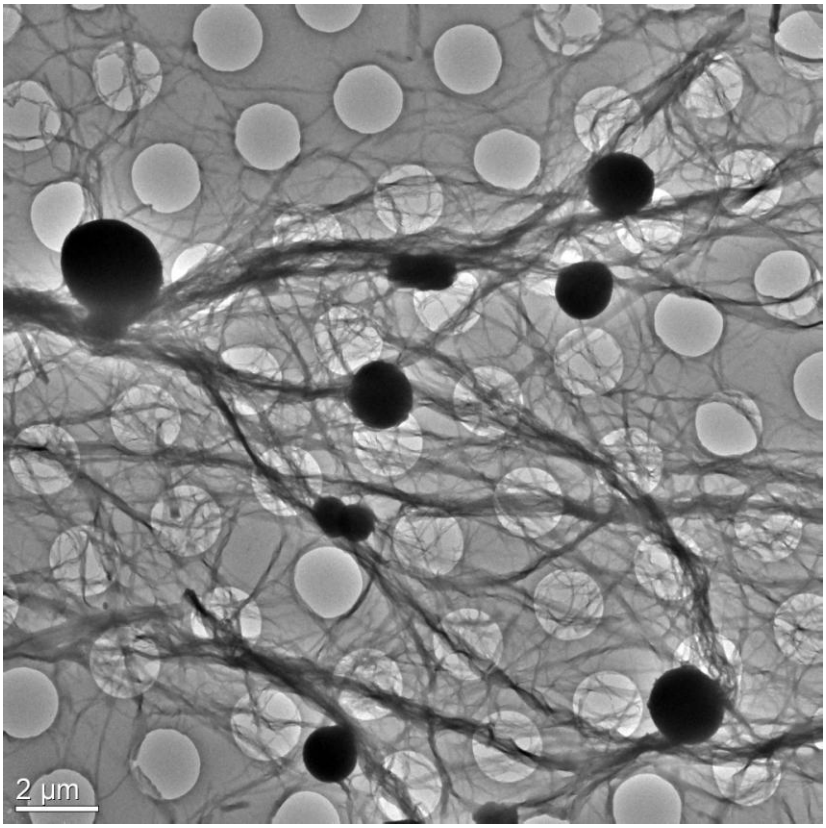

Figure 46.TEM imageof gel **15b** in MeOH at 1wt% concentration

VII.20 DSC of 15b

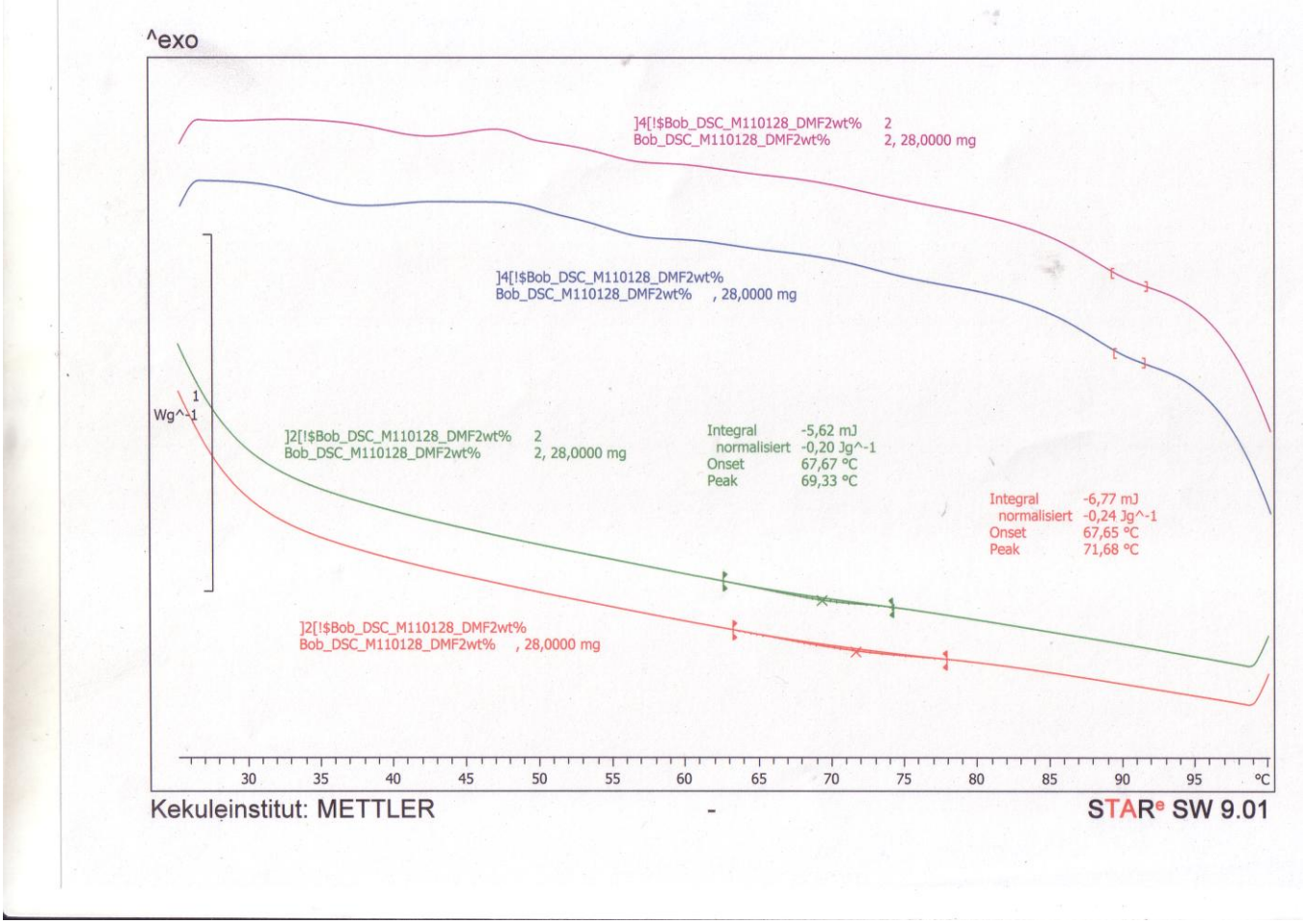

VII.21 Synthesis of 4-(4[1]-ethoxystyryl)benzaldehyde (16)

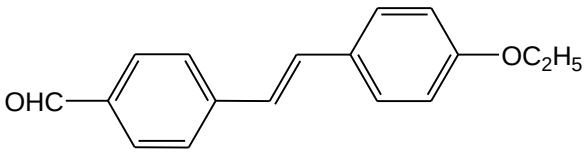

A mixture of 1-(bromomethyl)-4-ethoxybenzene (214 mg, 1 mmol) and triethyl phosphite (249 mg, 1.5 mmol) was heated to 140 ^{o}C with stirring for 4 h. The access triethyl phosphite was distilled off and the mixture was cooled to room temperature. To this reaction mixture 4-(diethoxymethyl)- benzaldehyde (208mg, 1 mmol) and potassium tert-butoxide (168 mg, 1.5 mmol) were added at 0 ^{o}C in dry THF and the mixture was stirred for 12 h at room temperature.

After 12 h at room temperature, 3N HCl (20 mL) was added to the reaction mixture and stirred for another 12 h at room temperature. The reaction mixture was diluted with water and extracted with CH_2Cl_2, the organic phase was dried ($MgSO_4$) and evaporated under reduced pressure. The residue was purified by column chromatography on silica gel with *n*-hexane/ CH_2Cl_2 8:2 leading to a light yellow solid (224 mg, 89%)

^{1}H NMR (DMSO, 300 MHz, 298 K): δ 9.96 (s, 1H), 7.78 (d, *J* = 8.2, 2H), 7.76 (d, *J* = 8.2, 2H), 7.57 (d, *J* = 8.7, 2H), 7.41 (d, *J* = 16.5, 1H), 7.18 (d, *J* = 16.5 1H), 6.94 (d, *J* = 8.7, 2H), 4.04 (q, *J* = 6.9, 2H), 1.32 (t, *J* = 6.9, 3H). ^{13} C NMR (DMSO, 75 MHz, 298 K): δ 192.2, 158.9, 143.6, 134.7, 131.7, 130.04, 129.03, 128.4, 126.6, 124.8, 114.7, 63.1, 14.6. HR-MS (ESI-TOF): $C_{17}H_{16}O_2$ *m/z* $[M+Na]^+$ 275.1043 (calcd), 275.1044 (found).

VII.22 Synthesis of 2, 6-dibromo-4-(4-(4^1-ethoxystyryl)styryl)pyridine (17)

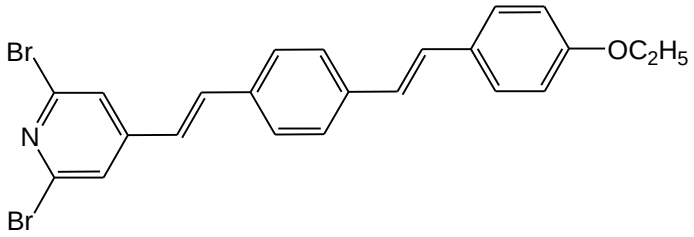

A mixture of 2, 6-dibromo-4-(bromomethyl)-pyridine (329 mg, 1 mmol) and triethyl phosphite (249 mg, 1.5 mmol) was heated to 140 ^{o}C with stirring for 25 minutes. Access triethyl phosphite was distilled off and the mixture was cooled to room temperature. To this reaction mixture **1** (252 mg, 1.2 mmol) and potassium tert-butoxide (168 mg, 1.5 mmol) were added at 0 ^{o}C in dry THF and stirred for 12 h at room temperature. 3N HCl (10 mL) was added to the reaction mixture and extracted with CH_2Cl_2, the organic phase was dried ($MgSO_4$) and evaporated under reduced pressure. The residue was purified by column chromatography on silica gel with *n*-hexane/EtOAc 9:1 leading to a yellow solid (460 mg, 95%).

^{1}H NMR (DMSO, 300 MHz, 298 K): δ 7.86 (d, *J* = 15, 2H), 7.72 (s, 1H), 7.61 (bs, 3H), 7.53 (d, *J* = 8.8, 2H), 7.26 (d, *J* = 16.4, 1H), 7.19 (d, *J* = 16.4, 1H), 7.09 (d, *J* = 16.4, 1H), 6.97 (d, *J* = 8.6, 1H), 6.93 (d, *J* = 8.7, 2H), 4.03 (q, *J* = 6.9, 2H), 1.32 (t, *J* = 6.9, 3H). ^{13} C NMR (DMSO, 75 MHz, 298 K): δ 158.5, 150.7, 140.5, 138.6, 136.1, 134.4, 129.4, 128.02, 127.89, 126.6, 125.4,

124.05, 122.6, 114.7, 63.1, 14.6. HR-MS (ESI-TOF): $C_{23}H_{19}Br_2NO$ *m/z* $[M+Na]^+$ 505.9708 (calcd), 505.9707 (found).

VII.23. Synthesis of (4-(4-(4^1-ethoxystyryl) styryl)))-2, 6-bis-(benzimidazolyl)-pyridine (18)

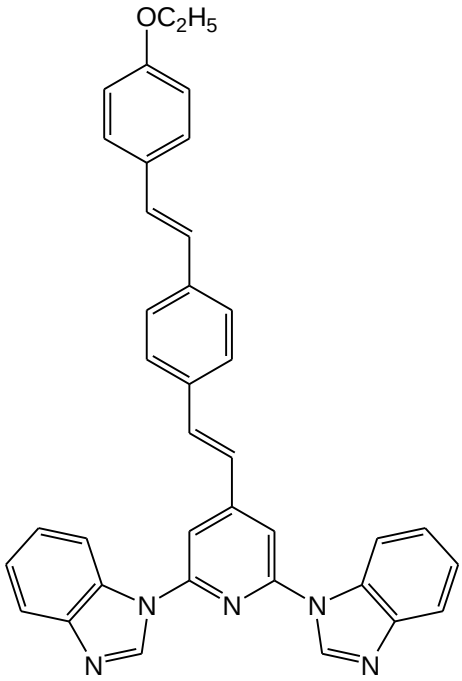

To an oven-dried Schlenk tube charged with 2,6-dibromo-4-(4-(4^1-ethoxystyryl)styryl)pyridine (485 mg, 1mmol), cesium carbonate (975 mg, 3 mmol), CuI (190 mg 1 mmol) and benzimidazole (295 mg, 2.5 mmol) dry DMF 5mL was added under argon atmosphere. The reaction mixture was warmed to 140 ^oC for 72 h. The DMF was distilled off and the reaction mixture was diluted with water, and the product was extracted with $CHCl_3$ (3 x 50 ml). The combined extracts were dried over $MgSO_4$, the organic phase was concentrated under vacuum and the crude product was purified by flash column chromatography with CH_2Cl_2/ MeOH 9.5:0.5 leads to white solid (297mg, 65%).

^{1}H NMR (DMSO, 400 MHz, 298 K): δ 9.1 (s, 2H), 8.27 (d, *J* = 6.5, 2H), 8.08 (d, *J* = 17.2, 2H), 7.91(d, *J* = 16.4, 1H), 7.82 (d, *J* =7.7, 2H), 7.64-7.69 (m, 4H), 7.53 (d, *J* = 8.4, 2H), 7.47 (d, *J* = 16.3, 1H), 7.37 (m, 4H), 7.27 (d, *J* = 16.4, 1H), 7.11 (d, *J* = 16.4, 1H), 6.92 (d, *J* = 8.4, 2H), 4.02

(q, *J* = 6.9, 2H), 1.32 (t, *J* = 6.9, 3H). HR-MS (ESI-TOF): $C_{37}H_{29}N_5O$ *m/z* $[M\text{-}2I]^+$ 559.2456 (calcd), 559.2462 (found).

VII.24. Synthesis of Conjugated Pyridine-Bridged Benzimidazolium Salt (19)

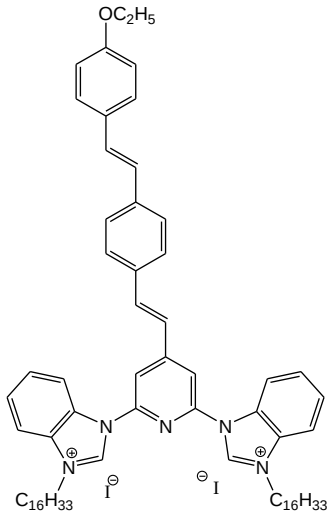

A mixture of 4-(4-(4[1]-ethoxystyryl)styryl)))-2,6-bis-(benzimidazolyl)-pyridine (559 mg 1mmol) and 1-iodohexadecane (1.409 g, 4 mmol) was stirred neat at 140 °C for 36 h. After cooling, the mixture was dissolved in $CHCl_3$ (50 mL) and then Et_2O (250 mL) was added. The precipitate was collected and the product was purified by flash column chromatography with CH_2Cl_2/ MeOH 9:1 leading to a yellow solid (1.213 g, 96%).

^{1}H NMR (DMSO, 500 MHz, 298 K): δ 10.74 (s, 2H), 8.52 (d, *J* = 10.7, 4H), 8.31 (d, *J* = 8.3, 2H), 8.02 (d, *J* = 16.2, 1H), 7.84 (t, *J* =7.3, 2H), 7.77-7.8 (m, 4H), 7.32 (d, *J* = 8.4, 2H), 7.65 (d, *J* = 16.2, 1H), 7.58 (d, *J* = 8.7, 2H), 7.35 (d, *J* = 16.3, 1H), 7.18 (d, *J* = 16.3, 1H), 6.97 (d, *J* = 8.7, 2H), 4.70 (t, *J* =7.3, 4H), 4.05 (q, *J* = 7.0, 2H), 2.08 (quintet, *J* = 7.1, 4H), 1.47 (m, 4H), 1.22-1.39 (m, 51H), 0.84 (t, *J* = 7.1, 6H). ^{13} C NMR (DMSO, 125 MHz, 298 K): δ 159.4, 153.5, 147.9, 143.4, 140.0, 138.06, 134.8, 132.5, 130.4, 130.2, 128.99, 128.97, 128.89, 128.83, 128.31, 127.7, 126.13, 124.2, 116.7, 115.5, 115.28, 115.22, 64.01, 48.43, 32.18, 29.95, 29.91, 29.88, 29.78, 29.6, 29.45, 29.4, 26.7, 22.99, 15.54, 14.85. HR-MS (ESI-TOF): $C_{69}H_{95}I_2N_5O$ *m/z* $[M\text{-}2I]^+$ 1009.7510 (calcd), 1009.7526 (found).

VII.25. POM images of 19

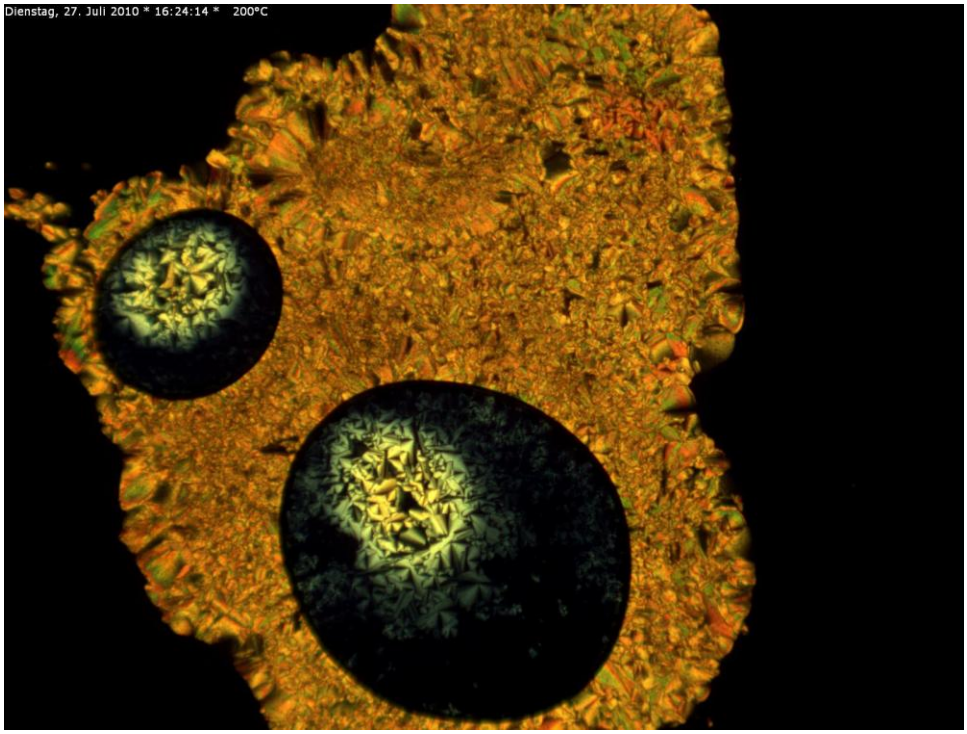

VII.26. DSC of 19

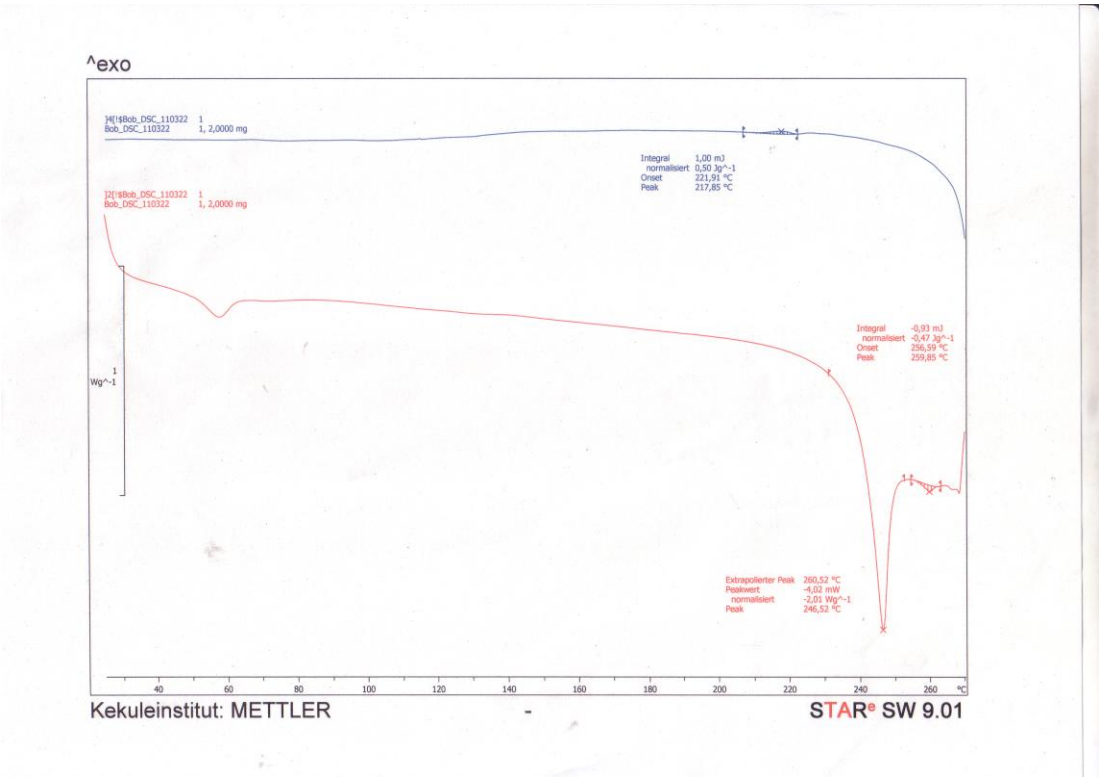

VII.27. 2,5-Bis Dodecyloxy Benzaldehyde (20)

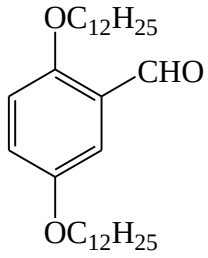

To an oven-dried Schlenk tube charged with 2, 5-dihydroxy benzaldehyde (138 mg, 1 mmol), potassium carbonate (414 mg, 3 mmol), and N-dodecyl bromide (623 mg, 2.5 mmol) dry DMF (5mL) was added under argon atmosphere. The reaction mixture was warmed to 70 ^{o}C for 48 h. The DMF was distilled off and the reaction mixture was diluted with water, and the product was extracted with $CHCl_3$ (3 x 50 ml). The combined extracts were dried over $MgSO_4$, the organic phase was concentrated under vacuum and the crude product was purified by flash column chromatography with petroleum ether/ ethyl acetate 9.5:0.5 leading to a white solid (412mg, 95 %).

1 H NMR ($CDCl_3$, 400 MHz, 298 K): δ = 10.39 (s, 1H), 7.23 (d, *J* = 3.2, 1H), 7.03 (dd, J_1 = 3.2, J_2 = 5.7, 1H), 6.84 (d, *J* = 9.0, 1H), 3.95 (t, *J* = 6.4, 2H), 3.86 (t, *J* = 6.5, 2H), 1.64-1.77 (m, 4H), 1.32-1.43 (m, 4H), 1.19 (m, 32H), 0.80 (t, *J* = 7.0, 6H). ^{13}C NMR ($CDCl_3$, 100 MHz, 298 K): δ = 169.71, 156.3, 153.01, 125.09, 124.08, 114.37, 110.8, 69.22, 68.68, 31.90, 29.64, 29.61, 29.57, 29.36, 29.33, 29.21, 26.05, 25.98, 22.67, 14.10. HR-MS (ESI-TOF): $C_{31}H_{54}O_3$ *m/z* $[M+Na]^+$ 497.3965 (calcd), 497.3960 (found).

VII.28. 2, 5-Bisdodecyloxy-4-methylbenzene (21)

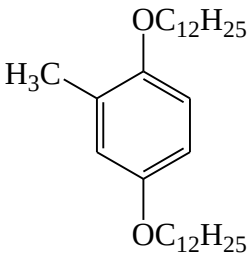

To an oven-dried Schlenk tube charged with 2, 5-dihydroxy-4-methyl benzene (124 mg, 1 mmol), potassium carbonate (414 mg, 3 mmol), and N-dodecyl bromide (623 mg, 2.5 mmol) dry

DMF (5mL) was added under argon atmosphere. The reaction mixture was warmed to 70 ^{o}C for 48 h. The DMF was distilled off and the reaction mixture was diluted with water, and the product was extracted with $CHCl_3$ (3 x 50 ml). The combined extracts were dried over $MgSO_4$, the organic phase was concentrated under vacuum and the crude product was purified by flash column chromatography with petroleum ether/ ethyl acetate 9.5:0.5 leading to a white solid (450 mg, 98 %).

^{1}H NMR ($CDCl_3$, 400 MHz, 298 K): δ = 6.65 (d, J = 3.2, 1H), 6.63 (s, 1H), 6.56 (dd, J_1 = 2.9, J_2 = 5.9, 1H), 3.81 (dd, J_1 = 2.4, J_2 = 4.2, 4H), 2.12 (s, 3H), 1.63-1.72 (m, 4H), 1.32-1.42 (m, 4H), 1.19 (m, 32H), 0.81 (t, J = 6.9, 6H). HR-MS (ESI-TOF): $C_{31}H_{56}O_2$; *m/z* $[M+Na]^+$ 483.4256 (calcd), 497.4268 (found).

VII.29. 1-Bromo-2, 5-bisdodecyloxy-4-bromomethylbenzene (22)

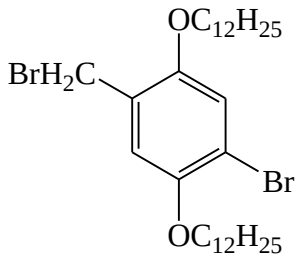

NBS (8.6 g, 4.8 mmol) and AIBN (229mg g, 1.4 mmol) were added to a solution of **21** (1.84 g, 4 mmol) in dry CCl_4 (10 mL) under an atmosphere of dry argon. After the reaction mixture was stirred for 2 h under reflux, it was subsequently allowed to cool to room temperature and filtered. After evaporation of the solvent, hexane (10 mL) was added to the residue and the resulting suspension was filtered and evaporated to dryness. The remaining residue was dissolved in dry THF (10 mL); NBS (930 mg, 5.2 mmol) was added, and the reaction mixture was stirred at reflux temperature for 1 h. After evaporation of the solvent, hexane (10 mL) was added. The solution was filtered and the solvent was removed in *vacuo*, the crude product was purified by column chromatography (silica gel, hexane/CH_2Cl_2 7:3). Recrystallization from ethanol yielded 1.23g (50 %) of **22** as a white crystalline solid:

^{1}H NMR ($CDCl_3$, 400 MHz, 298 K): δ = 6.98 (s, 1H), 6.81 (s, 1H), 4.42 (s, 2H), 3.88 (td, J_1 = 1.6, J_2 = 4.8, 4H), 1.69-1.76 (m, 4H), 1.37-1.42 (m, 4H), 1.94 (m, 32H), 0.81 (t, J = 7, 6H). ^{13}C NMR ($CDCl_3$, 100 MHz, 298 K): δ = 151.19, 149.46, 126.06, 117.39, 116.03, 113.20, 70.96,

70.22, 69.18, 31.91, 29.66, 29.61, 29.58, 29.56, 29.35, 26.20, 26.02, 25.97, 22.68, 14.11. HR-MS (ESI-TOF): $C_{31}H_{54}Br_2O_2$ *m/z* $[M]^+$ 616.2483 (calcd), 994.2489 (found).

VII.30. 4-(4[1]-Methyl-2,5-bisdodecyloxystyryl)-2,5-bisdodecylbromobenzene (24)

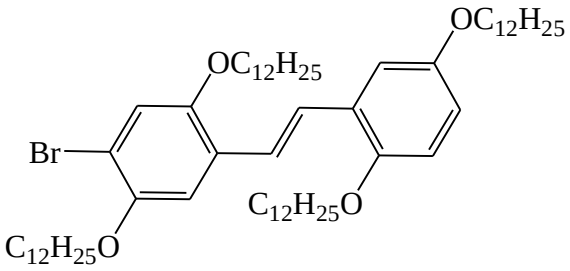

Triethyl phosphite (498 mg, 3 mmol) and **22** (1.23 g, 2 mmol) were stirred at 160 °C for 2 h while the liberated ethyl bromide was distilled off. The excess triethyl phosphite was removed by distillation under reduced pressure to leave **23** as light yellow oil. A solution of aldehyde **20** (949 mg, 2 mmol) in dry THF (10 mL) was added dropwise to a solution of **23** and *t*- BuOK (336 mg, 3 mmol) in dry THF (10 mL) under an atmosphere of dry argon. The resulting viscous reaction mixture was stirred overnight at room temperature and subsequently poured on crushed ice (100 g). Aqueous HCl (3 M, 10 mL) was added, and the aqueous phase was extracted with CH_2Cl_2. After the organic phase was dried over Na_2SO_4 and the solvent was evaporated in *vacuo*, the crude product was purified by column chromatography (silica gel, petroleum ether/CH_2Cl_2 3:2) leading to a white solid (974 mg, 98 %).

1 H NMR ($CDCl_3$, 400 MHz, 298 K): δ = 7.36 (d, *J* = 16.6, 1H), 7.28 (d, *J* = 16.6, 1H), 7.06-7.07 (m, 2H), 6.99 (s, 1H), 6.74 (d, *J* = 8.9, 1H), 6.68 (dd, J_1 = 2.5, J_2 = 6.1, 1H), 3.94 (t, *J* = 6.5, 2H), 3.85-3.90 (m, 6H), 1.72-1.74 (m, 8H), 1.38-1.41 (m, 8H), 1.19 (m, 64H), 0.80 (t, *J* = 7.0, 12H). HR-MS (ESI-TOF): $C_{62}H_{107}BrO_4$ *m/z* $[M]^+$ 994.7354 (calcd), 994.7358 (found).

VII.31. (4-(4-Methyl-2,5-bisdodecyloxystyryl)-2,5-bisdodecylbenzaldehyde (25)

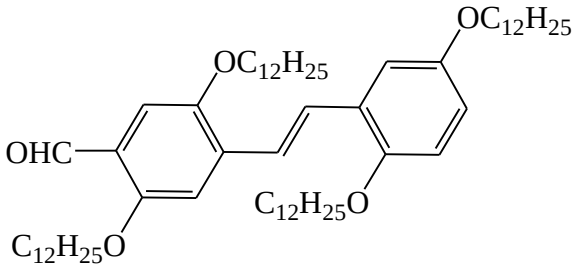

Bromo derivative **24** (945 mg, 1 mmol) was dissolved in a mixture of dry diethyl ether (10 mL) and dry THF (10 mL) under argon atmosphere. The solution was cooled to 0 °C, and 1.6 M *n*-butyllithium in hexane (2 mL) was added slowly. After the mixture was stirred for 30 min, the cooling bath was removed and dry DMF (1.5 mL) was added dropwise. The mixture was stirred for another 12 h at room temperature. After addition of 3 M HCl (10 mL) the product was extracted with CH_2Cl_2. The organic layer was further washed with water and saturated NaCl solution. The organic layer was dried over Na_2SO_4, and the solvent was evaporated. The crude product was purified by column chromatography (silica gel, heptane/CH_2Cl_2 4:6) leading to a yellow solid **25** (709 mg, 75 %).

^{1}H NMR ($CDCl_3$, 400 MHz, 298 K): δ = 10.43 (s, 1H), 7.56 (d, *J* = 16.5, 1H), 7.45 (d, *J* = 16.5, 1H), 7.30 (s, 1H), 7.24 (s, 1H), 7.17 (s, 1H), 7.14 (d, *J* = 2.6, 1H), 6.77-6.83 (m, 2H), 4.08 (t, *J* = 6.3, 2H), 3.92-4.02 (m, 6H), 1.74-1.84 (m, 8H), 1.25 (m, 72H), 0.84-0.88 (m, 12H).

^{13}C NMR ($CDCl_3$, 100 MHz, 298 K): δ = 189.13, 156.21, 153.24, 151.20, 150.69, 135.11, 127.33, 124.01, 123.21, 115.67, 115.22, 113.79, 112.66, 110.55, 110.02, 108.03, 69.41, 69.11, 69.08, 68.63, 31.91, 29.68, 29.64, 29.45, 29.41, 29.35, 29.30, 29.25, 26.23, 26.15, 26.13, 26.10, 22.68, 14.10. HR-MS (ESI-TOF): $C_{63}H_{108}O_5$; *m/z* $[M]^+$ 945.9105 (calcd), 945.9112 (found).

VII.32. 4-(4[1]-(2, 5-bis (dodecyloxy)styryl)-2, 5-bis(dodecyloxy)styryl)-2, 6 dibromopyridine (26)

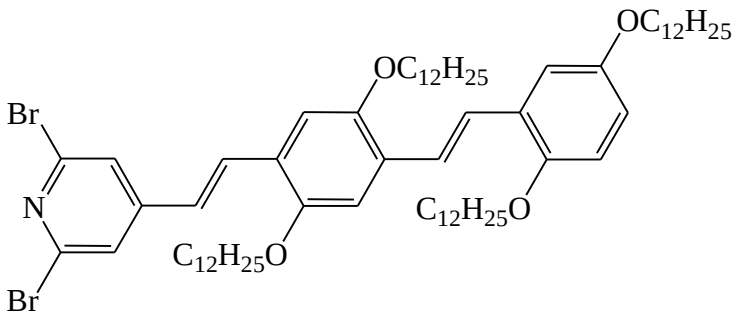

A mixture of 2,6-dibromo-4-(bromomethyl)-pyridine (329 mg, 1 mmol) and triethyl phosphite (249 mg, 1.5 mmol) was heated to 140 ^{o}C with stirring for 25 minutes. Access triethyl phosphite was distilled off and cooled to room temperature. To this reaction mixture **25** (945 mg, 1 mmol) and potassium tert-butoxide (168 mg, 1.5 mmol) was added at 0 ^{o}C in dry THF and stirred for 12 h at room temperature. 3N HCl (10 mL) was added to the reaction mixture and extracted with CH_2Cl_2, the organic phase was dried ($MgSO_4$) and evaporated under reduced pressure. The residue was purified by column chromatography on silica gel with *n*-hexane/EtOAc 9:1 leads to yellow solid (1.12g, 95 %).

^{1}H NMR ($CDCl_3$, 400 MHz, 298 K): δ = 7.55 (d, *J* = 16.3, 1H), 7.41 (bd, *J* = 6.1, 3H), 7.36 (d, *J* = 16.5, 1H), 7.09 (d, *J* = 2.8, 1H), 7.08 (s, 1H), 6.95 (s, 1H), 6.86 (d, *J* = 16.5, 1H), 6.75 (d, *J* = 8.9, 1H), 6.70 (dd, J_1 = 2.8, J_2 = 6.9, 1H), 4.0 (t, *J* = 6.4, 2H), 3.94 (t, *J* = 6.62, 2H), 3.86-3.91 (m, 4H), 1.67-1.84 (m, 8H), 1.35-1.49 (m, 8H), 1.18 (m, 72H), 0.78-0.82 (m, 12H). ^{13}C NMR ($CDCl_3$, 100 MHz, 298 K): δ = HR-MS (ESI-TOF): $C_{69}H_{111}Br_2NO_4$; *m/z* $[M]^+$ 1175.6913 (calcd), 1175.6920 (found).

VII.33. 4-(-4[1]-(2, 5-bis(dodecyloxy)styryl)-2, 5-bis(dodecyloxy)styryl)-2, 6-di(imidazole)pyridine (27)

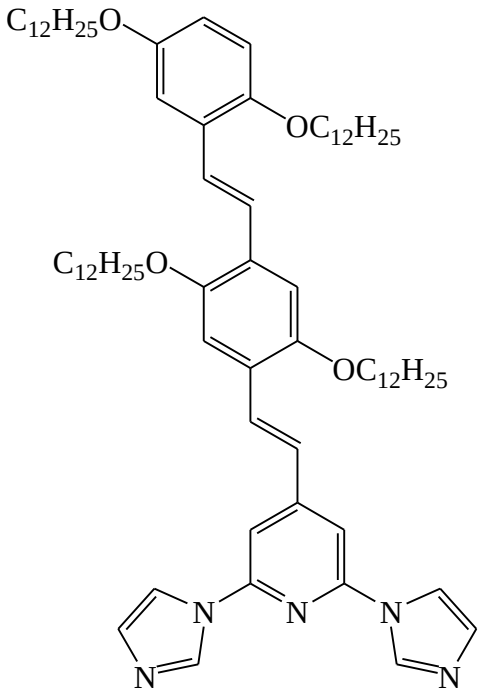

To a dry schlenk tube charged with **26** (1.17g, 1mmol), cesium carbonate (977 mg, 3 mmol), CuI (190 mg, 1 mmol) and imidazole (170 mg, 2.5 mmol) dry DMF were added under argon atmosphere and the mixture was heated to 140 ^{o}C for 48 h. DMF was distilled off and water was added. The residue was purified by column chromatography on silica gel with CH_2Cl_2/ MeOH 9.5:0.5 leading to a yellow solid (714 mg, 62 %).

1 H NMR ($CDCl_3$, 400 MHz, 298 K): δ = ^{13}C NMR ($CDCl_3$, 100 MHz, 298 K): δ = 8.4 (bs, 2H), 7.63-7.70 (m, 3H), 7.44 (d, *J* = 16.5, 1H), 7.37 (d, *J* = 16.6, 1H), 7.23 (m, 2H), 7.18 (s, 1H), 7.06-7.08 (m, 2H), 6.93-7.01 (m, 2H), 6.64-6.67 (m, 2H), 6.40-6.48 (m, 1H), 4.08 (t, *J* = 6.4, 2H), 3.93 (t, *J* = 6.4, 2H), 3.83-3.90 (m, 4H), 1.68-1.78 (m, 8H) 1.16-1.42 (m, 72H), 0.78 (m, 12H). HR-MS (ESI-TOF): $C_{75}H_{117}N_5O_4$; *m/z* $[M+H]^+$ 1115.9113 (calcd), 1115.9117 (found).

VII.34. 4-(-4[1]-(2, 5-bis (dodecyloxy)styryl)-2, 5-bis(dodecyloxy)styryl)-2, 6-bis-*N*-butl-(imidazolium)pyridine diiodide (28)

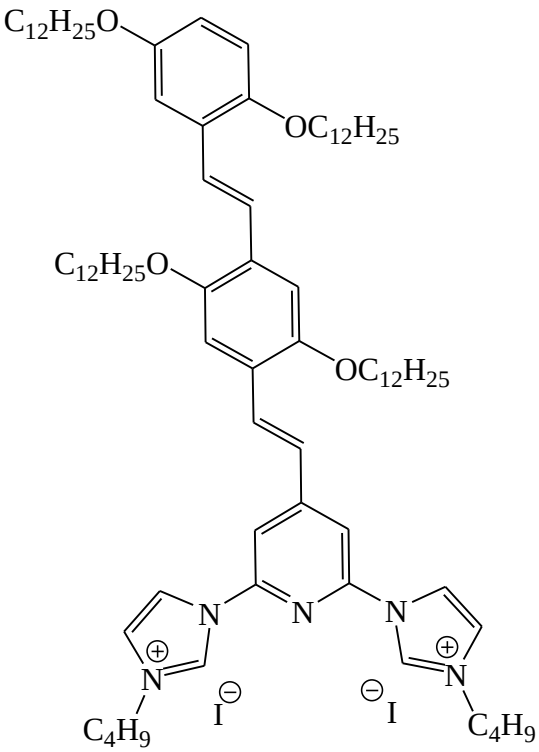

A mixture of **27** (1.158 g 1mmol) and 1-iodobutane (2mL) was stirred neat at 110 °C for 30 h. After cooling, the reaction mixture was dissolved in $CHCl_3$ (20 mL) and purified by flash column chromatography with CH_2Cl_2/ MeOH 9:1 leading to a red solid (1.45g, 96 %).

1 H NMR ($CDCl_3$, 400 MHz, 298 K): δ = 11.31 (s, 2H), 9.09 (s, 2H), 8.37 (bs, 2H), 7.92 (d, *J* = 16.4, 1H), 7.62 (d, *J* = 16.5, 1H), 7.48 (d, *J* = 16.3, 1H), 7.37 (s, 2H), 7.28 (d, *J* = 2.5, 1H), 7.23 (bs, 2H), 6.93 (s, 1H), 6.76 (d, *J* = 8.9, 1H), 6.72 (dd, J_1 = 2.65, J_2 = 6.2, 1H), 4.44 (t, *J* = 7.4, 4H), 4.09 (t, *J* = 6.5, 2H), 4.0 (t, *J* = 6.4, 2H), 3.92 (t, *J* = 6.9, 2H), 3.87 (t, *J* = 6.9, 2H), 1.70-1.89 (m ,12H), 1.4-1.51(m, 8H), 1.12-1.35 (m, 68H), 0.89 (t, *J* = 7.4, 6H), 0.76-0.83 (m, 12H). HR-MS (ESI-TOF): $C_{83}H_{135}I_2N_5O_4$ *m/z* $[M\text{-}2I]^+$ 1266.0504 (calcd), 1266.0482 (found).

VII.36. DSC of 28

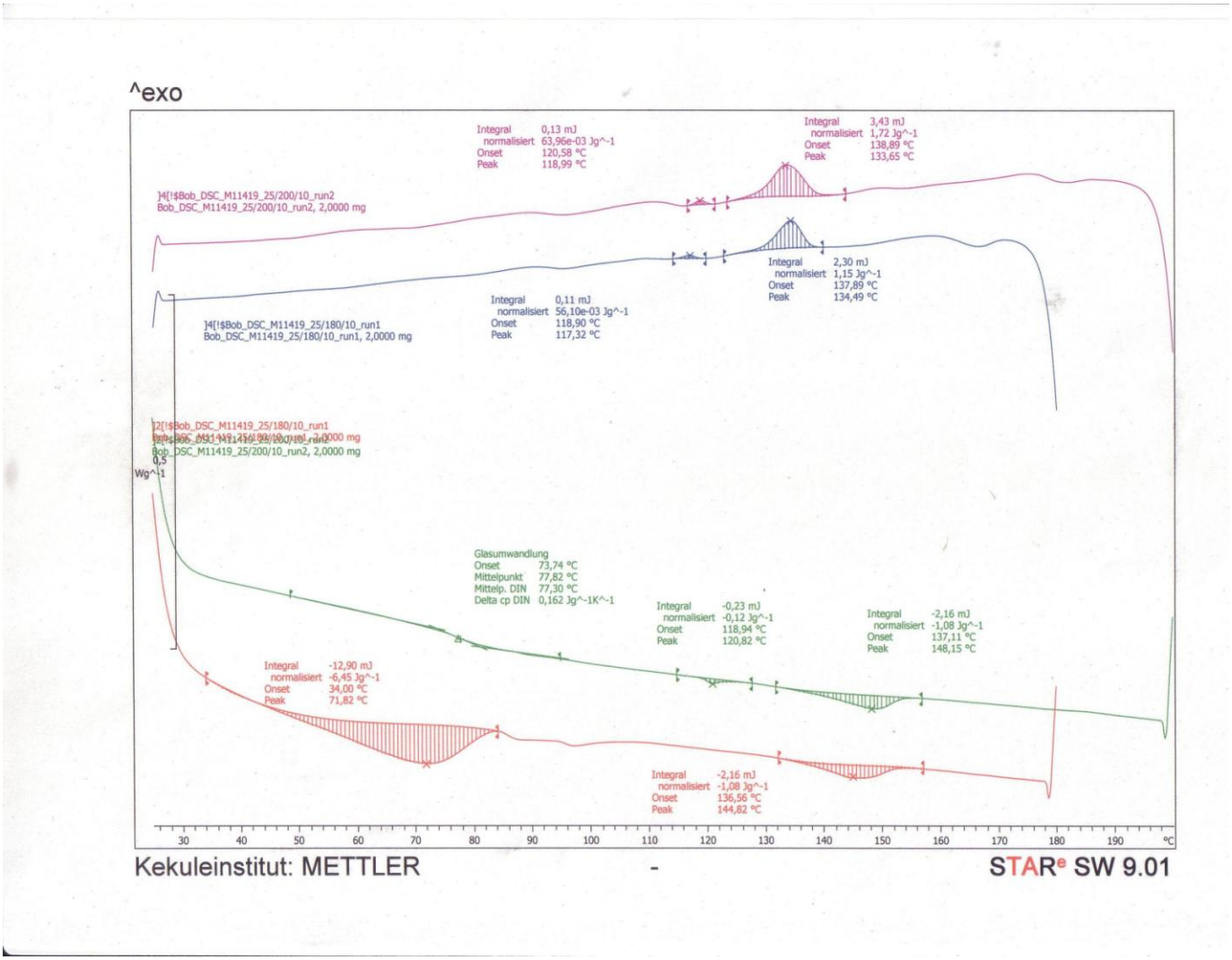

VII.35. POM images of 28

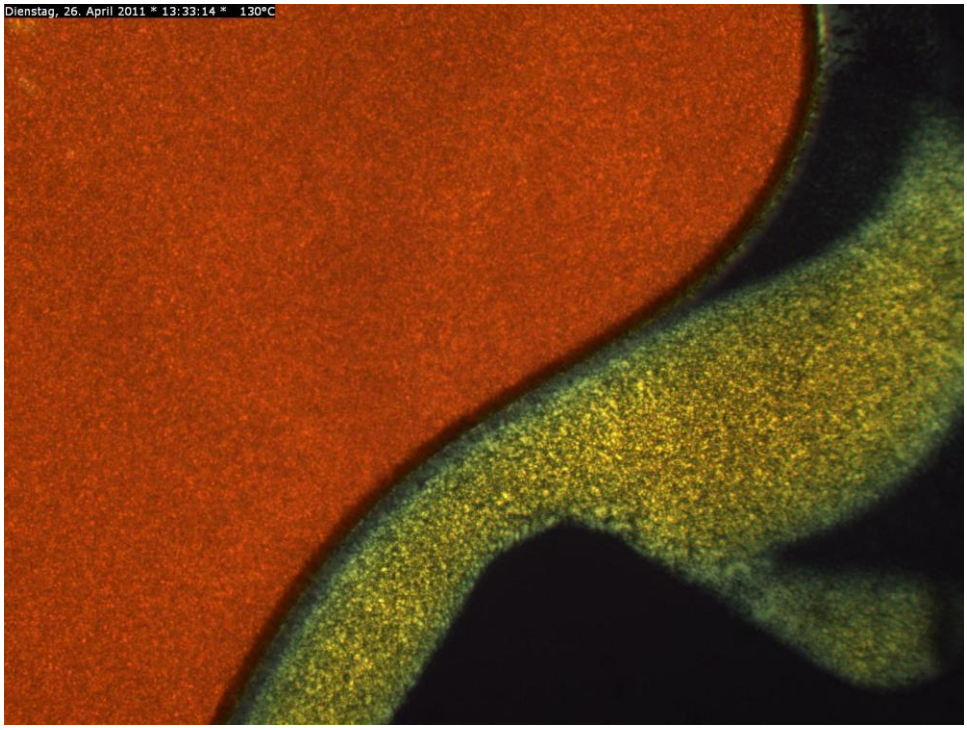

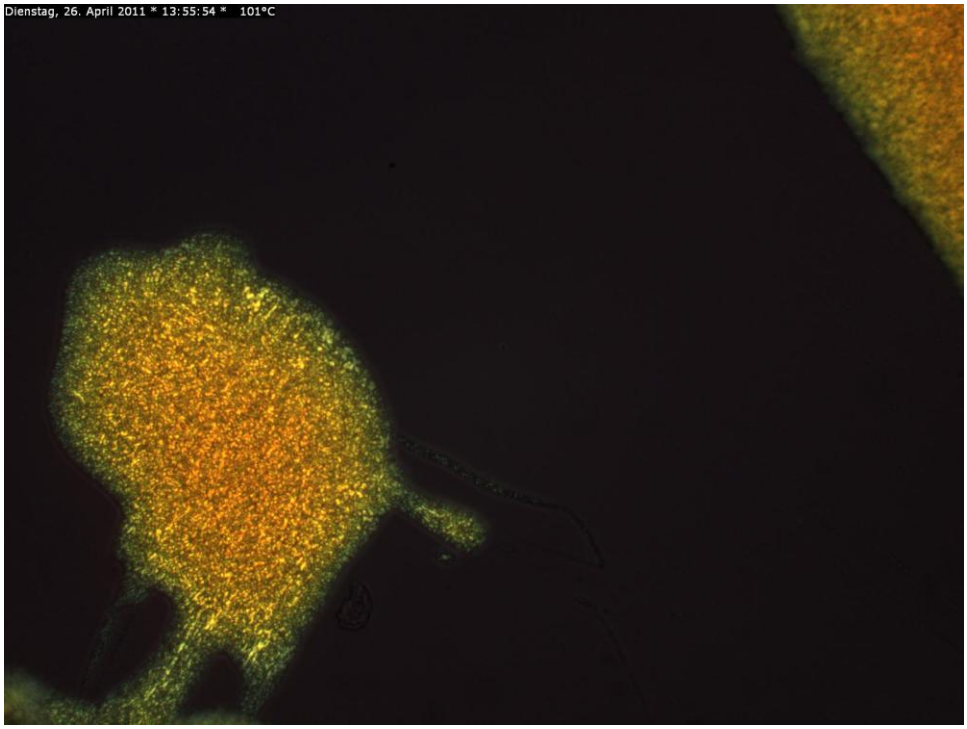

VII.37. Synthesis of 2, 6-di (perimidin-1-yl)pyridine (30)

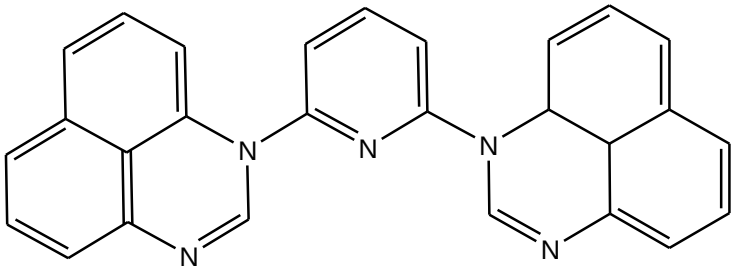

To an oven dried Schlenk flask with a magnetic stirring bar was charged CuI (201 mg, 1.06 mmol), Cs_2CO_3 (6.9 g, 21.2 mmol), pyrimidine (1.9g, 11.2 mmol), dibromopyridine (1.27g, 5.3 mmol), 1, 3-di (pyridin-2-yl) propane-1, 3-dione (242 mg, 1.06 mmol), and dry DMF (10 mL) under argon. The reaction mixture was stirred for 30 min at room temperature, and then heated to 140 ^oC for 48 h. The reaction mixture was then cooled to ambient temperature, water was added and the residue was filtered, dried. The residue was purified by column chromatography on silica gel to provide the desired product (930mg, 45%).

^{1}HNMR (500MHz, DMSO-(D6), 298K): δ= 8.37 (t, *J* = 7.8, 1H), 7.8 (d, *J* = 7.8, 2H), 7.72 (s, 2H), 7.26-7.29 (m, 4H), 7.22 (d, *J* = 8.3, 2H), 7.13 (t, *J* = 7.8, 2H), 6.8 (dd, *J* = 2, *J* = 4, 2H), 6.47 (d, *J* = 7.63, 2H). ^{13} C NMR (125 MHz, DMSO-(D6), 298K): δ= 152.4, 147.6, 144.9, 142.7, 137.6, 135.8, 129.6, 128.4, 122.4, 122.1, 121.6, 120.9, 116.4, 103.8. HR-MS (ESI-TOF): $C_{27}H_{19}N_5$; *m/z* $[M+H]^+$ 414.1652 (calcd), 414.1671 (found).

VII.38. Synthesis of Pyridine bridged 2, 6-bis-*N*-hexadecyl (perimidinium) diiodide (31)

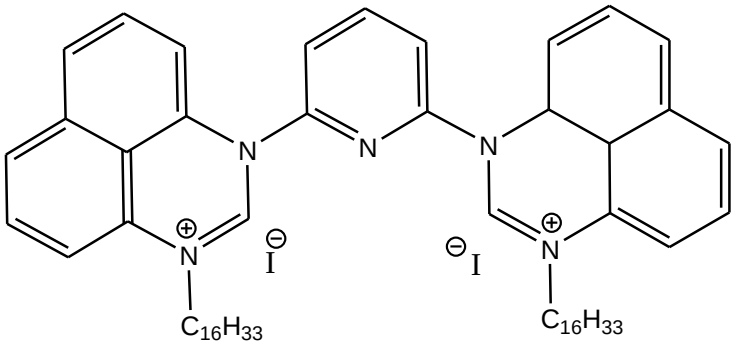

A mixture of 2, 6-di (1H-perimidin-1-yl) pyridine (411 mg, 1 mmol) and 1-iodohexadecane (775 mg, 2.2 mmol) in 10 mL DMF was heated to 90 °C for 72 h. After cooling to room temperature, DMF was distilled off under *vacuum*. The crude product was dissolved in $CHCl_3$ (10 mL) and then Et_2O (100 mL) was added. The crude product was purified by re-precipitation from $CHCl_3/Et_2O$ to give the yellow solid in quantitative yield. ^{1}HNMR (500MHz, DMSO-(D6), 298K): δ= 9.33 (s, 2H), 8.76 (t, *J* = 7.8 1H), 8.27 (d, *J* = 7.8, 2H), 7.69 (q, *J* = 5, *J* = 8.5, 4H), 7.56 (t, *J* = 8.3, 2H), 7.41 (t, *J* = 8,2H), 7.29 (d, *J* = 7.5, 2H), 6.89 (d, *J* = 7.3 2H), 4.11 (t, *J* = 7.05, 4H), 1.85 (quintet, *J* = 6.7, 4H), 1.43 (quintet, *J* = 7.5, 4H), 1.21 (m, 48H), 0.83 (t, *J* = 7.05, 6H). ^{13} C NMR (125 MHz, DMSO-(D6), 298K): δ= 163.17, 153.69, 149.37, 135.39, 133.08, 131.97, 129.35, 128.95, 125.68, 125.51, 125.15, 121.81, 110.26, 109.93, 52.82, 36.65, 35.33, 32.10, 31.69, 29.82, 29.74, 29.48, 29.43, 26.78, 26.47, 22.88, 14.72. HR-MS (ESI-TOF): $C_{59}H_{85}I_2N_5$ *m/z* $[M-2I]^+$ 863.6814 (calcd), 863.6826 (found).

VII.39. Synthesis of lutidine-bridged bis-*N*-butylperimidinium dibromide (38)

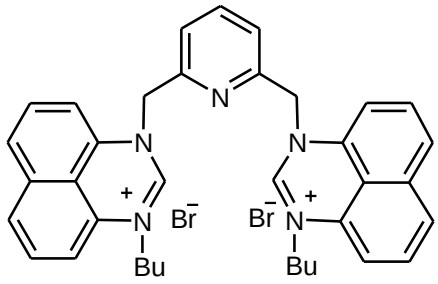

A mixture of 2, 6-dibromolutidine (265 mg, 1 mmol) and *N*-butylperimidine **35** (500 mg, 2.2 mmol) was heated to 165 ^{o}C under stirring in a sealed tube for 24 h. Then the mixture was cooled to room temperature, the residue was dissolved in $CHCl_3$ and reprecipitated upon addition of cold Et_2O to give NMR-pure bis-perimidinium dibromide **38** as a bright yellow powder in almost quantitative yield. ^{1}H NMR (DMSO-D_6, 400 MHz, 298 K): δ 8.44 (s, 2H), 7.21 (t, *J* = 7.8 Hz, 1H), 6.91 (d, *J* = 7.8 Hz, 2H), 6.62-6.69 (m, 4H), 6.47 (d, *J* = 8.3 Hz, 2H), 6.13-6.18 (m, 4H), 5.72 (d, *J* = 7.5 Hz, 2H), 4.52 (s, 4H), 2.97(t, *J* = 7.5 Hz, 4H), 0.83-0.92(m, 4 H), 0.61 (sextet, *J* = 7.5 Hz, 4H), 0.12 (t, *J* = 7.3 Hz, 6H); ^{13}C NMR (DMSO-D_6, 75 MHz): δ 153.63, 152.18, 138.73, 134.05, 133.40, 132.23, 131.87, 130.87, 129.54, 128.31, 127.52, 124.03, 123.36, 122.49, 120.58, 108.15, 108.06, 54.70, 50.95, 27.91, 19.00, 13.55; MS (ESI): *m/z* 634.3 $[M-Br]^+$, 588.3, 329.2,

276.7[M-2Br]$^{2+}$, 224.1; HR-MS(ESI): *m/z* Calad, 632.2383 [M–Br]$^{+}$; Found: 632.2383; Anal. Calcd for $C_{37}H_{39}Br_2N_5$•$2H_2O$: C, 59.29; H, 5.78; N, 9.34. Found: C, 59.04; H, 5.71; N, 9.25.

VII.40. General procedure for the Heck reactions

To a suspension of K_2CO_3 (414 mg, 3 mmol.) in 10 mL NMP, haloarene (2 mmol), *n*-butyl acrylate (307 mg, 2.4 mmol) and the catalyst (prepared from equimolar amounts of $Pd(OAc)_2$ and bis-perimidinium bromide **38** in NMP) was added. The reaction mixture was heated at 140 °C (monitored by GC-MS) and then allowed to cool to room temperature after the reaction was finished. Then the reaction mixture was diluted with water, and the product was extracted with ether (3 X 20 mL). The combined extracts were dried over $MgSO_4$, the organic phase was concentrated *in vacuum* and the crude product was purified by flash column chromatography (hexane/EtOAc = 100/1). (See Table 8)

VII.41. General procedure for the Suzuki reactions

To a suspension of K_2CO_3 (331 mg, 2.4 mmol.) in 3 mL NMP, haloarene (2 mmol), phenyl boronic acid (258 mg, 2.2 mmol) and catalyst (prepared from equimolar amounts of $Pd(OAc)_2$ and bis-perimidinium bromide **38** in NMP) were added. The reaction mixture was heated at 140 °C (monitored by GC-MS and TLC) and then allowed to cool to room temperature. Then the reaction mixture was diluted with water, and the product was extracted with ether (3 X 20 mL). The combined extracts were dried over $MgSO_4$, the organic phase was concentrated *in vacuum* and the crude product was purified by flash column chromatography (hexane/EtOAc = 100/1). (See Table 9)

VII.42. Homo coupling of 2-phenyl thiophene (41)

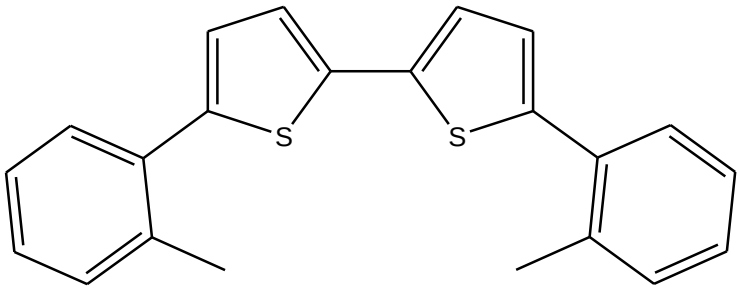

2-*o*-Tolylthiophene (174 mg, 1 mmol) and $Pd(OAc)_2$ (224 mg, 1 mmol) were dissolved in 30 mL of dry methanol and stirred at room temperature for 24 h. The solvent was removed under reduced pressure and the crude product was purified by flash column chromatography (hexane). ^{1}H NMR (300 MHz, $CDCl_3$, 298 K): δ = 7.35-7.37 (2H, m), 7.14-7.19 (6H, m), 7.1 (2H, d, *J* = 3.7 Hz), 6.91 (2H, d, *J* = 3.7 Hz), 2.4 (6H, s). ^{13}C NMR (75 MHz, $CDCl_3$, 298 K): δ = 141.7, 136.7, 135.6, 133.4, 130.5, 129.8, 127.5, 126.8, 125.6, 123.2, 20.9. GC-MS: $C_{22}H_{18}S_2$ m/z 346.1 $[M]^+$.

VII.43. General procedure for the C-arylation reactions 42a-i

An oven-dried Schlenk tube was charged with 2-phenylthiophene (352 mg, 2 mmol), iodobenzene (436 mg, 2.2 mmol), cesium carbonate (781 mg, 2.4 mmol), $Pd(OAc)_2$ (21 mg, 5 mmol). Dry DMF (2ml) was added under argon atmosphere. The reaction mixture was warmed to 140 ^{o}C for 24 h and then cooled to the room temperature. The reaction mixture was diluted with water, and the product was extracted with diethyl ether (3 x 20 ml). The combined extracts were dried over $MgSO_4$, the organic phase was concentrated under vacuum and the crude product was purified by flash column chromatography on silica gel (hexane). (See Table 11)

VII.44. 2,5-Diphenylthiophene (42a)

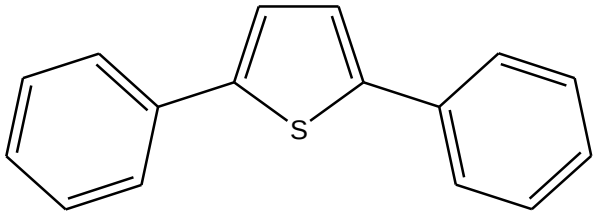

^{1}H NMR (300 MHz, $CDCl_3$, 298 K): δ = 7.63 (4H, d, *J* = 7.7 Hz), 7.39 (4H, t, *J* = 7.7 Hz), 7.27-7.32 (4H, m). ^{13}C NMR (75 MHz, $CDCl_3$, 298 K): δ = 143.2, 133.9, 128.5, 127.1, 125.3123.6. GC-MS: $C_{16}H_{12}S$ m/z 236.1 $[M]^+$.

VII.45. 2-(2-Methylphenyl)-5-phenylthiophene (42b)

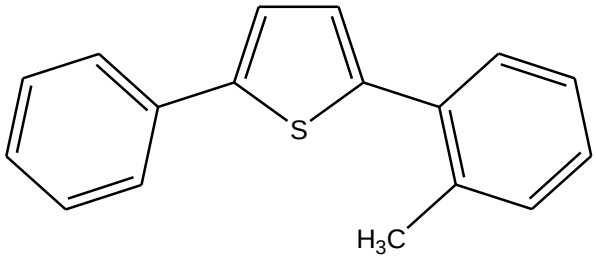

^{1}H NMR (300 MHz, $CDCl_3$, 298 K): δ = 7.50 (1H, t, *J* =1.3 Hz), 7.47 (1H, t, *J* =1.1 Hz), 7.31 (1H, m), 7.18-7.25 (2H, m), 7.07-7.14 (5H, m), 6.88 (1H, d, *J*=3.8 Hz), 2.33 (1H, s, CH_3). ^{13}C NMR (75 MHz, $CDCl_3$, 298 K): δ = 143.7, 142.3, 135.7, 134.1, 133.8, 130.6, 129.9, 128.6, 127.6, 127.1, 125.7, 125.4, 122.9, 21.05. GC-MS: $C_{17}H_{14}S$ m/z 251. $[M]^+$

VII.46. 2-(3-Methylphenyl)-5-phenylthiophene (43c)

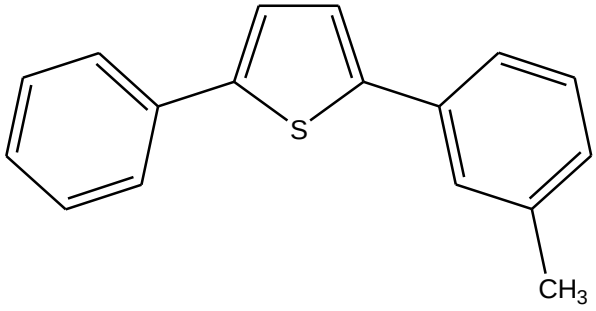

1H NMR (300 MHz, $CDCl_3$, 298 K): δ = 7.56 (1H, t, *J* = 1.3 Hz), 7.53 (1H, bs), 7.27-7.36 (4H, m), 7.15-7.21 (4H, m), 7.0 (1H, d, *J*=7.2 Hz). ^{13}C NMR (75 MHz, $CDCl_3$, 298 K): δ =143.4, 143.0, 138.2, 134.0, 133.8, 128.5, 128.4, 127.9, 127.1, 126.0, 125.2, 123.6, 123.5, 122.4, 21.1. GC-MS: $C_{17}H_{14}S$ m/z 251. $[M]^+$

VII.47. 2-(4-Methylphenyl)-5-phenylthiophene (42d)

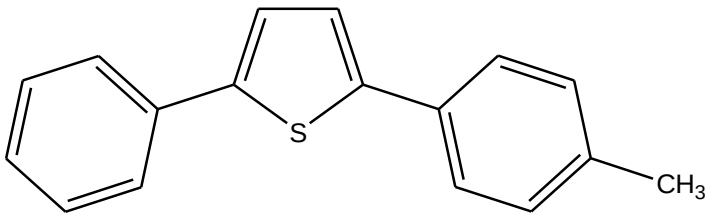

^{1}H NMR (300 MHz, $CDCl_3$, 298 K): δ = 7.54 (1H, t, *J* = 1.4 Hz), 7.52 (1H, bs), 7.45 (1H, bs), 7.42 (1H, bs), 7.29 (2H, m), 7.14-7.20 (3H, m), 7.11 (1H bs), 7.09 (1H, bs), 2.28 (3H, m). ^{13}C NMR (75 MHz, $CDCl_3$, 298 K): δ = 143.4, 142.7, 137.0, 134.0, 131.2, 129.2, 128.5, 127.0, 125.2, 125.2, 123.5, 123.1, 20.8. GC-MS: $C_{17}H_{14}S$ m/z 251. $[M]^+$

VII.48. 2-(4-Methoxyphenyl)-5-phenylthiophene (42e)

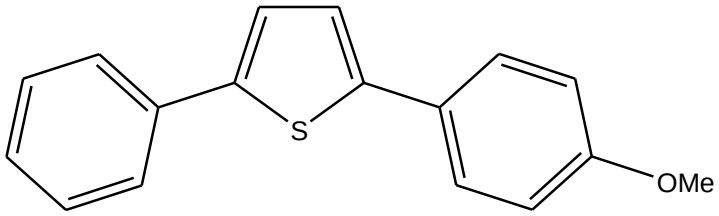

^{1}H NMR (300 MHz, $CDCl_3$, 298 K): δ = 7.56 (1H, d, *J* = 1.4 Hz), 7.53 (1H, m), 7.50 (1H, d, *J* = 2.2 Hz), 7.47 (1H, d, *J* = 2.2 Hz), 7.28-7.33 (2H, m), 7.18-7.20 (2H, m), 7.10 (1H, d, *J* =3.7 Hz), 6.87 (1H, d, *J* = 2.2 Hz), 6.84 (1H, d, *J* = 2.1 Hz), 3.77 (3H, s). ^{13}C NMR (75 MHz, $CDCl_3$, 298 K): δ = 158.9, 143.2, 142.2, 134.0, 128.5, 126.9, 126.5, 125.1, 123.5, 122.5, 113.9, 55.0. GC-MS: $C_{17}H_{14}SO$ m/z 266.3 $[M]^+$.

VII.49. 2-(4-(Trifluoromethyl) phenyl)-5-phenylthiophene (42f)

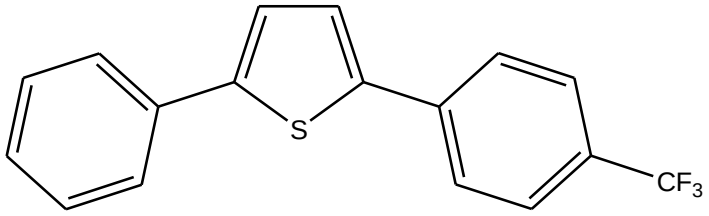

^{1}H NMR (500 MHz, CD_2Cl_2, 298 K): δ = 7.81 (1H, bs), 7.79 (1H, bs), 7.69-7.71 (3H, m), 7.44-7.47 (4H, m), 7.40 (1H, d, *J* =3.8 Hz), 7.35-7.38 (1H, m). ^{13}C NMR (125 MHz, CD_2Cl_2, 298 K): δ = 145.5, 144.8, 138.1, 134.2, 129.4, 128.3, 126.34, 126.31, 126.28, 126.25, 126.03, 125.9, 124.7 GC-MS: $C_{17}H_{11}F_3S$ m/z 305.1 $[M]^+$.

VII.50. 2-(2-(Trifluoromethyl) phenyl)-5-phenylthiophene (42g)

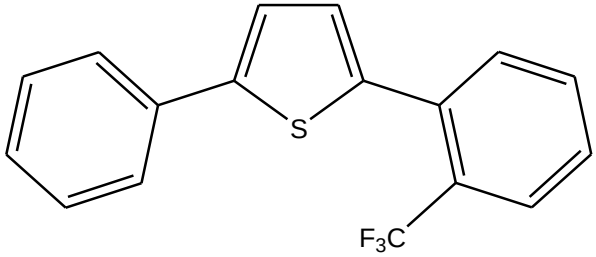

^{1}H NMR (300 MHz, $CDCl_3$, 298 K): δ = 7.68-7.71 (1H, m), 7.54-7.57 (2H, m), 7.49 (1H, t, *J* =1.3 Hz), 7.47 (1H, d, *J* =0.7 Hz), 7.38-7.42 (1H, m), 7.31-7.34 (1H, m), 7.28 (1H, t, *J* =1.5 Hz), 7.21-7.23 (1H, m), 7.1-7.2(1H, m), 7.01-7.03 (1H, m, *J* =0.7 Hz). ^{13}C NMR (75 MHz, $CDCl_3$, 298 K): δ = 144.8, 138.5, 133.7, 132.7, 131.06, 131.04, 128.5, 128.45, 128.41, 127.6, 127.3, 126.18, 126.11, 125.4, 122.7. GC-MS: $C_{17}H_{11}F_3S$ m/z 305.1 $[M]^+$.

VII.51. 2-(2-Fluorophenyl)-5-phenylthiophene (42h)

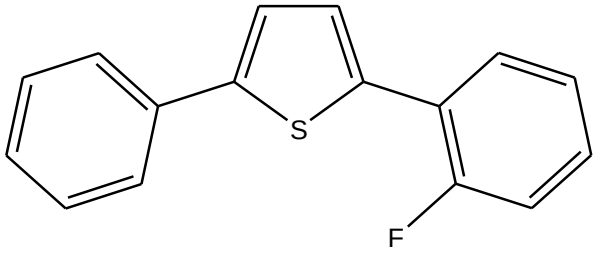

^{1}H NMR (300 MHz, $CDCl_3$, 298 K): δ = 7.45-7.50 (3H, m), 7.30 (1H, dd, *J* =2.5 Hz), 7.22 (2H, m) 7.10-7.15 (2H, m), 6.95-7.08 (3H, m). ^{13}C NMR (75 MHz, $CDCl_3$, 298 K): δ = 160.4, 157.1, 137.0, 128.5, 128.4, 128.2, 128.1, 126.7, 126.6, 124.2, 124.1, 121.8, 116.2, 115.9. GC-MS: $C_{16}H_{11}FS$ m/z 254.1 $[M]^+$.

VII.52. 2-(1-Naphthyl)-5-phenylthiophene (42i)

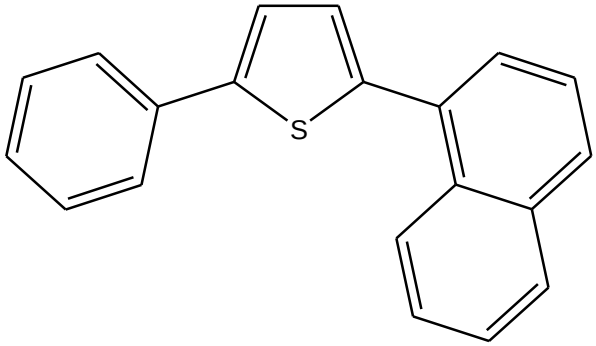

^{1}H NMR (300 MHz, $CDCl_3$, 298 K): δ = 8.48-8.51 (1H, m), 7.94-8.09 (2H, m), 7.81 (1H, t, *J* = 1.2 Hz), 7.78 (1H, bs), 7.35 (1H, d, *J* = 6.5 Hz), 7.65-7.56 (3H, m), 7.53-7.47 (3H, m), 7.41 (1H, d , *J* = 7.0 Hz), 7.33 (1H, d, *J* = 3.6 Hz). ^{13}C NMR (75 MHz, $CDCl_3$, 298 K): δ = 144.3, 141.0, 134.1, 133.7, 132.1, 131.5, 128.7, 128.3, 128.2, 127.8, 127.3, 126.3, 125.8, 125.57, 125.54, 125.1 123.1. GC-MS: $C_{20}H_{14}S$ m/z 286 $[M]^+$.

VII.53. General Procedure for Tandem Biarylation of Thienylboronic Acid 43a-h

To an oven-dried schlenk tube was charged with thiophene boronic acid (255 mg, 2 mmol), iodobenzene (897 mg, 4.4 mmol), cesium carbonate (1.629 g, 5mmol), $Pd(OAc)_2$ (44 mg, 10 mmol) and dry DMF 2ml was added under argon atmosphere. The reaction mixture was warmed to 140 ^{o}C for 48 h and then cooled to the room temperature. The reaction mixture was diluted with water, and the product was extracted with diethyl ether (3 x 20ml). The combined extracts were dried over $MgSO_4$, the organic phase was concentrated under vacuum and the crude product was purified by flash column chromatography on silica gel (hexane). (See Table 12)

VII.54. 2, 5-Diphenylthiophene (43a)

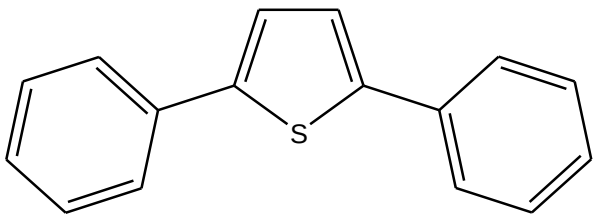

^{1}H NMR (300 MHz, $CDCl_3$, 298 K): δ = 7.63 (4H, d, *J* = 7.7 Hz), 7.39 (4H, t, *J* = 7.7 Hz), 7.27-7.32 (4H, m). ^{13}C NMR (75 MHz, $CDCl_3$, 298 K): δ = 143.2, 133.9, 128.5, 127.1, 125.3123.6. GC-MS: $C_{16}H_{12}S$ m/z 236.1 $[M]^+$.

VII.55. 2, 5-Di-2-methylphenyl thiophene (43b)

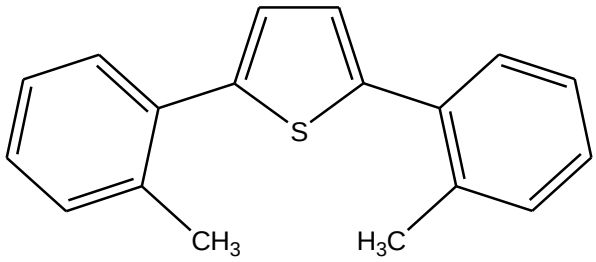

^{1}H NMR (300 MHz, $CDCl_3$, 298 K): δ =7.32-7.35 (2H, m), 7.08-7.12 (6H, m), 6.91 (2H, bs), 2.36 (6H, s). ^{13}C NMR (75 MHz, $CDCl_3$, 298K) δ = 142.6, 135.6, 133.8, 130.6, 130.0, 127.5, 126.2, 125.7, 21.0. GC-MS: $C_{18}H_{16}S$ m/z 264.1 $[M]^+$.

VII.56. 2,5-Di-3-methylphenyl thiophene (43c)

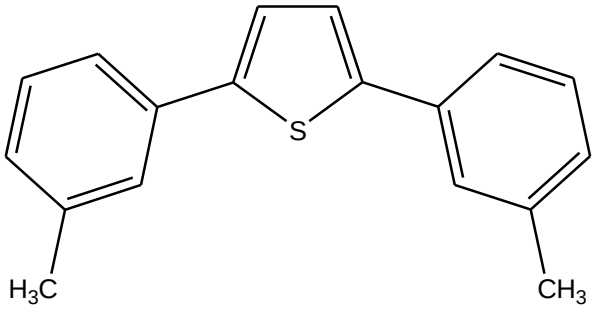

^{1}H NMR (300 MHz, $CDCl_3$, 298 K): δ = 7.33 (3H, bs), 7.31 (1H, bs), 7.12-7.17 (4H, m) 6.98 (1H, bs), 6.96 (1H, bs), 2.27 (6H, s). ^{13}C NMR (75 MHz, $CDCl_3$, 298 K): δ = 143.2, 138.2, 133.9, 128.5, 127.9, 126.0, 123.5, 122.4, 21.1. GC-MS: $C_{18}H_{16}S$ m/z 265.1 $[M+1]^+$.

VII.57. 2,5-Di-4-methylphenyl thiophene (43d)

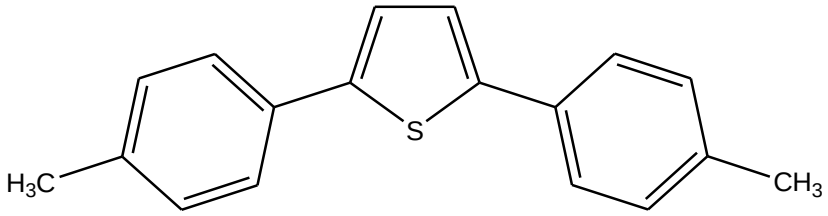

^{1} H NMR (300 MHz, $CDCl_3$, 298 K): δ = 7.44 (2H, t, *J* = 2.0 Hz), 7.41 (2H, t, *J* = 2.0 Hz), 7.13 (2H, bs), 7.10 (2H, bs, *J* = 1.0 Hz), 7.01 (2H, bs, *J* = 1.0 Hz), 2.27 (6H, 5). ^{13}C NMR (75 MHz, $CDCl_3$, 298 K): δ = 142.9, 136.9, 131.3, 129.2, 125.1, 123.0, 20.8. GC-MS: $C_{18}H_{16}S$ m/z 265.1 $[M+1]^+$.

VII.58. 2,5-Bis(2-fluorophenyl)thiophene (43e)

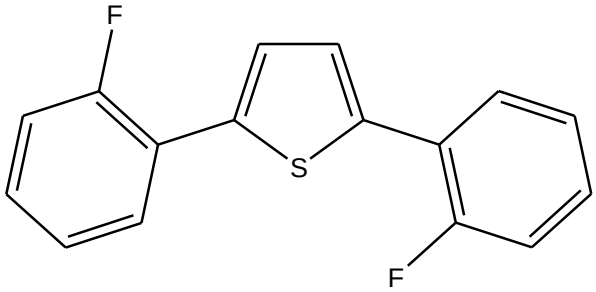

1 H NMR(300 MHz, $CDCl_3$, 298 K): δ = 7.55-7.60 (2H, m), 7.4 (2H, t, J = 1 Hz), 7.13-7.20(2H, m), 7.03-7.10(4H, m). ^{13}C NMR (75 MHz, $CDCl_3$, 298 K): δ = 160.42, 157.15, 137.0, 136.97, 136.91, 128.4, 128.3, 128.2, 128.15, 126.7, 126.66, 124.15, 124.11, 121.7, 126.63, 116.20, 115.8. GC-MS 272, GC-MS: $C_{16}H_{10}F_2S$ m/z 272.1 $[M]^+$.

VII.59. 2,5-Bis(2-(trifluoromethyl)phenyl)thiophene (43f)

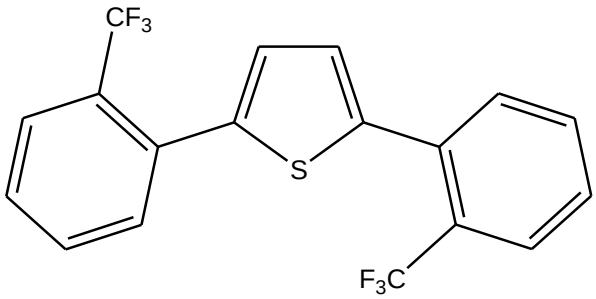

^{1}H NMR(300 MHz, $CDCl_3$, 298 K): δ = 7.70 (1H, bs), 7.67 (1H, bs), 7.46-7.49 (3H, m),7.37-7.44 (3H, m), 6.99 (2H, s). ^{13}C NMR (75 MHz, $CDCl_3$, 298 K): δ = 140.15, 132.903, 132.80, 131.01, 130.28, 129.04, 128.98, 128.58, 127.77, 127.72, 127.45, 127.42, 127.37, 127.35, 126.21, 126.14, 126.06, 125.99, 125.41, 121.78.GC-MS 372, GC-MS: $C_{18}H_{10}F_6S$ m/z 372.1$[M]^+$.

VII.60. 2,5-Bis(2-methoxyphenyl)thiophene (43g)

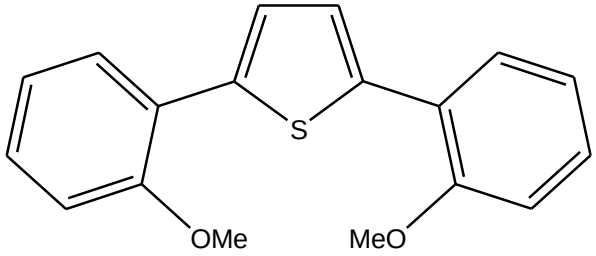

^{1}H NMR (300 MHz, $CDCl_3$, 298 K): δ = 7.60 (1H, d, *J* = 1.7 Hz), 7.58 (1H, d, *J* = 1.5 Hz), 7.4 (2H, s), 7.13-7.16 (2H, m), 6.93-6.94 (1H, m), 6.91-6.92 (2H, m), 6.88-6.89 (1H, m), 3.84 (6H, s). ^{13}C NMR (75 MHz, $CDCl_3$, 298 K): δ = 155.4, 138.9, 131.1, 128.1, 127.8, 125.3, 120.5, 111.3, 55.2. GC-MS: $C_{18}H_{16}O_2S$; m/z 296 $[M]^+$.

VII.61. 2, 5-Di (naphthalen-1-yl) thiophene (43h)

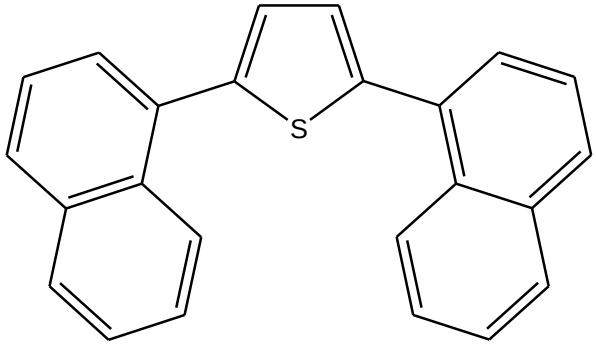

^{1}H NMR (300 MHz, $CDCl_3$, 298 K): δ = 7.82 (3H, m), 7.79 (3H, m), 7.46 (1H, s), 7.44 (1H, d, *J* =0.9 Hz), 7.41 (1H, bs), 7.38-7.4 (1H, m), 7.37 (2H, d, *J* =1.3 Hz), 7.34 (1H, bs), 7.32 (1H, t, *J* =1.5 Hz), 7.29-7.3 (1H, m), 7.26 (1H, bs), 7.16 (1H, d, *J* =1.3 Hz), 7.13 (1H, t, *J* =1.7 Hz). ^{13}C NMR (75 MHz, $CDCl_3$, 298 K): δ = 138.1, 133.2, 132.5, 127.8, 127.8, 127.6, 127.5, 126.9, 126.3, 125.8, 125.7, 125.5, 125.1. GC-MS: $C_{24}H_{16}S$; m/z 336 $[M]^+$.

VII.62. Bi-arylation of 1, 4-bis (5-o-tolylthiophen-2-yl) benzene (45)

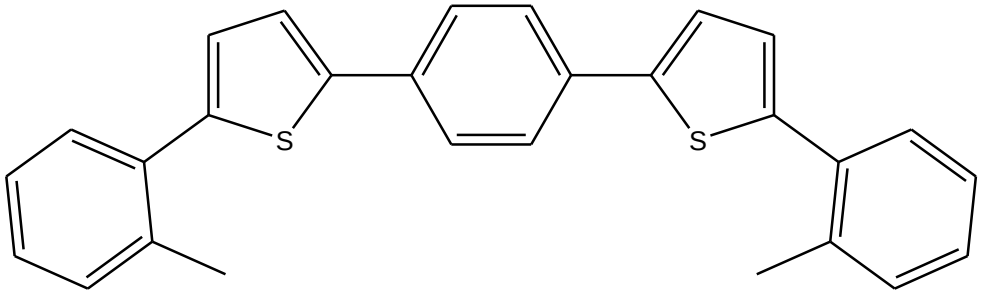

An oven-dried Schlenk tube was charged with **44** (242 mg, 1 mmol), 2-iodotoluene (954 mg, 4.4 mmol), cesium carbonate (1.629 g, 5 mmol), Pd $(OAc)_2$ (44 mg, 10 mmol). Dry DMF (2 ml) was added under argon atmosphere. The reaction mixture was warmed to 140 ^oC for 24 h and then cooled to room temperature. The reaction mixture was diluted with water, and the product was extracted with diethyl ether (3 x 20ml). The combined extracts were dried over $MgSO_4$, the organic phase was concentrated under vacuum and the crude product was purified by flash column chromatography (hexane).

^{1}H NMR (400 MHz, $CDCl_3$, 298 K): δ = 7.57 (4H, s), 7.38-7.40 (2H, m), 7.26 (2H, bd, *J* = 3.69 Hz), 7.16-7.23 (6H, m), 6.99 (2H, bd, *J* = 3.69 Hz), 2.42 (6H, s). ^{13}C NMR (100 MHz, $CDCl_3$, 298 K): δ = 143.45, 142.72, 135.98, 133.98, 133.36, 130.86, 130.21, 127.87, 127.52, 125.99, 123.14, 21.27. GC-MS: $C_{28}H_{22}S_2$; m/z 423 $[M]^+$.

VII.63. Intramolecular arylation (47)

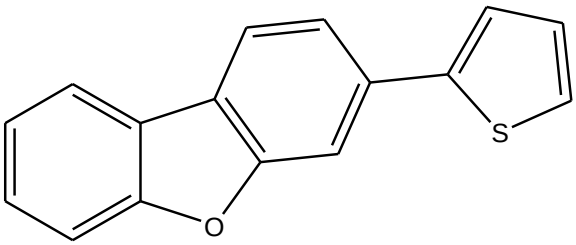

An oven-dried Schlenk tube was charged with **46** (378 mg, 1 mmol), cesium carbonate (390 mg, 1.2 mmol), $Pd(OAc)_2$ (11 mg, 5 mmol). Dry DMF (1ml) was added under argon atmosphere. The reaction mixture was warmed to 140 ^oC for 24 h and then cooled to the room temperature. The reaction mixture was diluted with water, and the product was extracted with diethyl ether (3 x

20ml). The combined extracts were dried over $MgSO_4$, the organic phase was concentrated under vacuum and the crude product was purified by flash column chromatography (hexane).

^{1}H NMR (400 MHz, $CDCl_3$, 298 K): δ = 7.95(1H, bd, *J* = 4.7 Hz), 7.93 (1H, bd, *J* = 5.0 Hz), 7.81 (1H, d, *J* = 1.5 Hz), 7.62 (1H, dd, *J* =6.5 Hz), 7.57 (1H, bd, *J* = 8.2 Hz), 7.46 (1H, dt, J_1 = 6.0 Hz, J_2 = 6.9 Hz), 7.41 (1H, dd, *J* = 2.5 Hz), 7.36 (1H, dd, *J* = 6.7 Hz), 7.32 (1H, dd, *J* = 4.0 Hz), 7.12(1H, dd, *J* = 3.6 Hz). ^{13}C NMR (100 MHz, $CDCl_3$, 298 K): δ = 156.6, 156.6, 144.33, 133.76, 128.1, 127.2, 127.1, 125.1, 123.9, 123.5, 122.8, 121.1, 120.8, 120.5, 111.6, 108.1. GC-MS: $C_{16}H_{10}OS$; m/z 250.1 $[M]^+$.

VIII. References

1. Noyori, R. Asymmetric catalysis: science and opportunities (Nobel Lecture) *Angew. Chem. Int. Ed.* **2002**, *41*(12), 2008-2022
2. Knowles, W. S. Asymmetric hydrogenations (Nobel Lecture) *Angew. Chem. Int. Ed.* **2002**, *41*(12), 1998-2007
3. Sharpless, K. B. Searching for new reactivity (Nobel Lecture) *Angew. Chem. Int. Ed.* **2002**, *41*(12), 2024-2032
4. Chauvin, Y. Olefin metathesis: the early days (Nobel Lecture) *Angew. Chem. Int. Ed.* **2002**, *45*(23), 3741-3747
5. Schrock, R. R.. Multiple metal-carbon bonds for catalytic metathesis reactions (Nobel Lecture) *Angew. Chem. Int. Ed.* **2002**, *45*(23), 3748-3759
6. Grubbs, R. H. Olefin-metathesis catalysts for the preparation of molecules and materials (Nobel Lecture) *Angew. Chem. Int. Ed.* **2002**, *45*(23), 3760-3765
7. Fischer, E. O.; Maasböl, O.; *Angew. Chem.* **1964**, *76*, 645.
8. Herrmann, W. A.; *Angew. Chem. Int. Ed.*, **2002**, *41*, 1290-1309
9. Fischer, E. O.; Maasböl, A.; *Angew. Chem.* **1973**, *85*, 618.
10. Schrock, R. R.; *Acc. Chem. Res.* **1979**, *12*, 98.
12. a) R. Hoffmann, *Science* **1981**, *211*, 995; b) R. Hoffmann, *Angew. Chem.* **1982**, *94*, 725; F. G. A. Stone, *Angew. Chem. Int. Ed.* **1984**, *96*, 85-96.
13. Wittig, G.; Geißler, G.; *Liebigs Ann. Chem.* **1953**, *44*, 580.
14. Tebbe, F. N.; Parsall, G. W.; Reddy, G. S.; *J. Am. Chem. Soc.* **1978**, *100*, 3611.
15. Bourrissou, D.; Guerret, O.; Gabbaï F, P.; Bertrand, G.; *Chem. Rev.*, **2000**, *100*, 39.
16. Schuster, G. B.; *Adv. Phys. Org. Chem.* **1986**, *22*, 311.
17. Gleiter, R.; Hoffmann, R.; *J. Am. Chem. Soc.*, **1968**, *90*, 1475.
18. Irikura, K. I.; Goddard, W. A. III; Beauchamp, J. L.; *J. Am.Chem. Soc.* **1992**, *114*, 48.
19. a) Hoffmann, R.; Zeiss, G. D.; Van Dine, G. W.; *J. Am. Chem.Soc.* **1968**, *90*, 1485; b) Baird, N. C.; Taylor, K. F.; *J. Am. Chem. Soc.* **1978**, *100*, 1333.
20. a) Schoeller, W. W.; *J. Chem. Soc., Chem. Commun.* **1980**, 124; b) Pauling, L.; *J. Chem. Soc., Chem. Commun.* **1980**, 688.
21. Gilbert, B. C.; Griller, D.; Nazran; A. S. *J. Org. Chem.*, **1985**, *50*, 4738.
22. Wanzlick, H. W.; Schönherr, H. J.; *Liebigs Ann. Chem.*, **1970**, *731*, 176.
23. Arduengo, A. J. III; Harlow R. L.; Kline M.; *J. Am. Chem. Soc.* **1991**, *113*, 361.
24. Huang, I.; Schanz, H.-J.; Stevens, E. D.; Nolan, S. P.; *Organometallics* **1999**, *18*, 2370.
25. Herrmann, W. A.; *Angew. Chem. Int. Ed.* **2002**, *41*, 1290.
26. Green, J. C.; Scurr, R. G.; Arnold, P. L.; Cloke, F. G. N.; *Chem. Comm.* **1997**, *20*, 1963.
27. Nemcsok, D.; Wichmann, K.; Frenking, G.; *Organometallics* **2004**, *23*, 3640.
28. a) Frison, G.; Sevin, A.; *J. Phys. Chem. A* **1999**, *103*, 10998; b) Frison, G.; Sevin, A.; *J. Organomet. Chem.* **2002**, *643-644*, 105; c) Frison, G.; Sevin, A.; *J. Chem. Soc., Perkin Trans. 2* **2002**, 1692.
29. a) Voges, M. H.; Romming, C.; Tilset, M.; *Organometallics* **1999**, *18*, 529; b) Abernathy, C. D.; Cowley, A. H.;

Jones, R. A.; *J.Organomet. Chem.*, **2000**, *596*, 3.

30. Pugh, D.; Danopoulos, A. A. *Coord. Chem. Rev.* **2007**, *251*, 610
31. Louie, J.; Grubbs, R. H.; *Chem. Commun.*, **2000**, 1479.
32. a) Chatterjee, A. K.; Grubbs, R. H.; *Org. Lett.*, **1999**, *1*, 1751; b) Chatterjee, A. K.; Morgan, J. P.; Scholl, M.; Grubbs, R. H.; *J. Am. Chem. Soc.*, **2000**, *122*, 3783; c) Trnka, T.; Grubbs, R. H.; *Acc. Chem. Res.*, **2001**, *34*,18.
33. a) Prinz, M.; Grosche, M.; Herdtweck, E.; Herrmann, W. A.; *Organometallics*, **2000**, *19*,1692; b) Prinz, M. *Dissertation*,Technische Universität Müchen, **2001**.
34. a) Nielsen, D. J, Magill, A. M.; Yates, B. F.; Cavell, K. J.; Skelton, B. W.; White, A. H. Chem. Commun. 2002, 2500.
35. a) Peris, E.; Loch, J. A.; Mata, J.; Crabtree, R. H.; *Chem. Commun.* **2001**, 210; b) Loch, J. A.; Crabtree, R. H.; *Pure Appl. Chem.* **2001**, *73*,119.
36. Reviews on LMOGs, (a) in Molecular Gels. Materials with Self-Assembled Fibrillar Networks, ed. R. G. Weiss and P. Terech, Springer, Dordrecht, The Netherlands, 2005; (b) M. George and R. G. Weiss, *Acc. Chem. Res*., **2006**, *39*, 489; (c) N. M. Sangeetha and U. Maitra, *Chem. Soc. Rev*., **2005**, *34*, 821; (d) O. Gronwald, E. Snip and S. Shinkai, *Curr. Opin. Colloid Interface Sci*., **2002**, *7*, 148; (e) P. Terech and R. G. Weiss, *Chem. Rev*., **1997**, *97*, 3133; (f) D. J. Abdallah and R. G. Weiss, *Adv. Mater*., **2000**, *12*, 1237.
37. J. Brinksma, B. L. Feringa, R. M. Kellogg, R. Vreeker and J. H. van Esch, *Langmuir*, **2000**, *16*, 9249.
38. L. A. Estroff and A. D. Hamilton, *Chem. Rev*., **2004**, *104*, 1201.
39. P. K. Vemula, U. Aslam, V. Ajay Mallia and G. John, *Chem. Mater*., **2007**, *19*, 138.
40. (a) K. Murata, M. Aoki, T. Nishi, A. Ikeda and S. Shinkai, J. Chem. Soc., *Chem. Commun*., **1991**, 1715; (b) J. J. D. de Jong, L. N. Lucas, R. M. Kellogg, J. H. van Esch and B. L. Feringa, *Science*, **2004**, *304*, 278.
41. (a) T. Kato, *Science*, **2002**, *295*, 2414; (b) A. Ajayaghosh, V. K. Praveen, C. Vijayakumar and S. J. George, *Angew. Chem., Int. Ed*., **2007**, *46*, 6260.
42. (a) K. J. C. van Bommel, A. Friggeri and S. Shinkai, *Angew. Chem., Int. Ed*., **2003**, *42*, 980; (b) H. Basit, A. Pal, S. Sen and S. Bhattacharya, *Chem.–Eur. J*., **2008**, *14*, 6534; (c) S. Ray, A. K. Das and A. Banerjee, *Chem. Commun*., **2006**, 2816; (d) G. Gundiah, S. Mukhopadhyay, U. G. Tumkurkar, A. Govindaraj, U. Maitra and C. N. R. Rao, J. *Mater. Chem*., 2003, 13, 2118.
43. A. Wynne, M. Whitefield, A. J. Dixon and S. Anderson, *J. Dermatol. Treat*., **2002**, *13*, 61.
44. E. Carretti and L. Dei, *in Molecular Gels. Materials with Self-Assembled Fibrillar* Networks, ed. G. Weiss and P. Terech, Springer, Dordrecht, The Netherlands, **2005**, *27*, 929.
45. (a) K. Y. Lee and D. J. Mooney, *Chem. Rev*., **2001**, *101*, 1869; (b) Z. Yang, G. Liang, L. Wang and B. Xu, *J. Am. Chem. Soc*., **2006**, *128*, 3038.
46. Aggeli, A.; Nyrkova, I. A.; Bell, M.; Harding, R.; Carrick, L.; McLeish, T. C. B.; Semenov, A. N.; Boden, N.; *Proc. Natl. Acad. Sci.* **2001**, *98*, 11857.
47. Israelachvili, J. N.; *Intermolecular and Surface Forces*, 2nd ed.; Academic Press: New York, **1991**.
48. Schnur, J. M.; *Science* **1993**, *262*, 1669.
49. Nandi, N.; Bagchi, B.; *J. Am. Chem. Soc.* **1996**, *118*, 11208.

50. Lescanne, M.; Colin, A.; Mondain-Monval, O.; Fages, F.; Pozzo, J. L.; *Langmuir* **2003**, *19*, 2013.

51. Kunitake, T.; Okahata, Y.; Shimomura, M.; Yasunami, S.;Takarabe, K. *J. Am. Chem. Soc.* **1981**, *103*, 5401.

52. Iwaura, R.; Yoshida, K.; Masuda, M.; Ohnishi-Kameyama, M.;Yoshida, M.; Shimizu, T.; *Angew. Chem., Int. Ed.* **2003**,*42*, 1009.

53. Iwaura, R.; Yoshida, K.; Masuda, M.; Yase, K.; Shimizu, T.; *Chem. Mater.* **2002**, *14*, 3047.

54. Shimizu, T.; Iwaura, R.; Masuda, M.; Hanada, T.; Yase, K.; *J.Am. Chem. Soc.* **2001**, *123*, 5947.

55. Kogiso, M.; Hanada, T.; Yase, K.; Shimizu, T.; *Chem. Commun.***1998**, 1791.

56. Kogiso, M.; Ohnishi, S.; Yase, K.; Masuda, M.; Shimizu, T.; *Langmuir* **1998**, *14*, 4978.

57. Nakazawa, I.; Masuda, M.; Okada, Y.; Hanada, T.; Yase, K.; Asai,M.; Shimizu, T.; *Langmuir* **1999**, *15*, 4757.

58. Shimizu, T.; Masuda, M.; *J. Am. Chem. Soc.* **1997**, *119*, 2812.

59. Fuhrhop, J. H.; Schnieder, P.; Rosenberg, J.; Boekema, E.; *J. Am.*Chem. Soc. **1987**, 109, 3387.

60. Jung, J. H.; Shinkai, S.; Shimizu, T.; *Chem. Eur. J.* **2002**, *8*, 2684.

61. Gronwald, O.; Shinkai, S.; *J. Chem. Soc., Perkin Trans. 2*, **2001**, 1933.

62. Yoza, K.; Ono, Y.; Yoshihara, K.; Akao, T.; Shinmori, H.; Takeuchi, M.; Shinkai, S.; Reinhoudt, D. N.; *Chem. Commun.***1998**, 907.

63. Bühler, G., Feiters, M. C., Nolte, R. J. M., Dötz, K. H. *Angew. Chem. Int. Ed.* **2003**, *42*, 2494-2497

64. Hafkamp, R. J. H., Feiters, M. C., Nolte, R. J. M.; *J. Org. Chem.***1999**, *64*, 412.

65. T. Klawonn, A. Gansäuer, I. Winkler,T. Lauterbach, D. Franke, R. J. M. Nolte, M. C. Feiters, H. Börner, J. Hentschel, K. H. Dötz: *Chem. Commun*. **2007**, 1894.

66. A. Gansäuer, I. Winkler, T. Klawonn, R. J. M. Nolte, M. C. Feiters, H. Börner, J. Hentschel, K. H. Dötz. *Organometallics*, **2009**, *28*, 1377.

67. T. Tu, W. Assenmacher, H. Peterlik, R. Weisbarth, M. Nieger, K. H. Dötz, *Angew. Chem.* **2007**, *119*, 6486; *Angew. Chem. Int. Ed.* **2007**, *46*, 6368;

68. T. Tu, W. Assenmacher, H. Peterlik, G. Schnakenburg, K. H. Dötz, *Angew. Chem*. **2008**, *120*, 7236; *Angew. Chem. Int. Ed*. **2008**, *47*, 7127.

69. T. Tu, X. Bao, W. Assenmacher, H. Peterlik, J. Daniels, K. H. Dötz, *Chem. Eur. J*. **2009**, *15*, 1853.

70. a) P. Rajakumar, M. Dhanasekaran, *Synthesis* **2006**, 654; b) M. V. Baker, M. J. Bosnich, D. H. Brown, L. T. Byrne, V. J. Hesler, B. W. Skelton, A. H. White, C. C. Williams, *J. Org. Chem*. **2004**, ***69***, 7640; c) P. Rajakumar, M. Dhanasekaran, *Tetrahedron*, **2002**, 1355.

71. a) A. J. Arduengo, III, R. L. Harlow, M. Kline, *J. Am. Chem. Soc*, **1991**, *113*, 361; b) A. J. Arduengo, III, *Acc. Chem. Res.*, **1999**, *32*, 913.

72. K. Öfele, W. A. Herrmann, D. Mihalios, M. Elison, E. Herdtweck, W. Scherer and J. Mink, *J. Organomet. Che.*, **1993**, *459*, 177.

73. (*a*) V. P. W. Böhm, C. W. K. Gstottmayr, T. Weskamp, W. A. Herrmann, *J. Organomet. Chem*, **2000**, *595*, 186; (b) J. Schwarz, V. P. W. Böhm, M. G. Gardiner, M. Grosche, W. A. Herrmann, W. Hieringer, G. Raudaschl-Sieber, *Chem. Eur. J.*, **2000**, *6*, 1773; (c) T. Weskamp, V. P. W. Böhm, W. A. Herrmann, *J. Organomet. Chem.*, **1999**, *585*, 348; (d) W. A. Herrmann, C.-P. Reisinger, M. Spiegler, *J. Organomet. Chem.*,

1998, ***557***, 93; (e) W. A. Herrmann, M. Elison, J. Fischer, C. Köcher, G. R. J. Artus, *Angew. Chem., Int. Ed. Engl.*, **1995**, *34*, 2371; (f) C. Zhang, M. L. Trudell, *Tetrahedron Lett.*, **2000**, *41*, 595; (g) C. Zhang, J. Huang, M. L. Trudell, S. P. Nolan, *J. Org. Chem*, ***1999***, *64*, 3804; (h) J. Huang and S. P. Nolan, *J. Am. Chem. Soc.*, **1999**, *121*, 9889; (i) D. S. McGuiness, K. J. Cavell, *Organometallics*, **2000**, *19*, 741; (j) D. S. McGuiness, K. J. Cavell, B. W. Skelton, A. H. White, *Organometallics*, **1999**, *18*, 1596.

74. (a)S. R. Stauffer, S. Lee, J. P. Stambuli, S. I. Hauck and J. F. Hartwig, *Org. Lett.*, **2000**, *2*, 1423; (b) J. Huang, G. Grasa, S. P. Nolan, *Org. Lett.*, 1999, **1**, 1307.
75. (a) C. W. Bielawski, R. H. Grubbs, *Angew. Chem., Int. Ed.*, **2000**, *39*, 2903; (b) M. Scholl, S. Ding, C. W. Lee, R. H. Grubbs, *Org. Lett.*, **1999**, *1*, 953; (c) T. Weskamp, F. J. Kohl, W. Hieringer, D. Gleigh, W. A. Herrmann, *Angew. Chem., Int. Ed.*, **1999**, *38*, 2416; (d) U. Frenzel, T. Weskamp, F. J. Kohl, W. C. Schattenman, O. Nuyken, W. A. Herrmann, *J. Organomet. Chem.*, **1999**, *586*, 263; (e) J. Huang, E. D. tevens, S. P. Nolan, J. L. Petersen, *J. Am. Chem. Soc.*, **1999**, *121*, 2674; (f) J. K. Huang, H. J. Schanz, E. D. Stevens, S. P. Nolan, *Organometallics*, **1999**, *18*, 5375; (h) S. B. Garber, J. S. Kingsbury, B. L. Gray, A. H. Hoveyda, *J. Am. Chem. Soc.*, **2000**, *122*, 8168.
76. a) J. A. Loch, M. Albrecht, E. Peris, J. Mata, J. W. Faller, R. H. Crabtree, Organometallics **2002**, *21*, 700; b) E. Peris, J. A. Loch, J. Mata, R. H. Crabtree, Chem. Commun. **2001**, 201.
77. T. Tu, J. Malineni, K. H. Dötz, *Adv. Synth. Catal.* **2008**, *350*, 1791.
78. a) V. Lillo, E. Mas-Marzá, A. M. Segarra, J. J. Carbó, C. Bo, E. Peris, E. Fernandez, *Chem. Commun.* **2007**, 3380; b) F. Churruca, R. SanMartin, B. Inés, I. Tellitu, E. Domínguez, *Adv. Synth. Catal.* **2006**, *348*, 1836; c) J. A. Loch, M. Albrecht, E. Peris, J. Mata, J. W. Faller, R. H. Crabtree, *Organometallics* **2002**, *21*, 700; d) E. Peris, J. Mata, J. A. Loch, R. H. Crabtree, *Chem. Commun.* **2001**, 201; e) J. C. C. Chen, I. J. B. Lin, *Dalton Trans.* **2000**, 839; for lutidine-bridged palladium carbene complexes, see: f) A. A. D. Tulloch, A. A. Danopoulos, G. J. Tizzard, S. J. Coles, M. B. Hursthouse, R. S. Hay-Motherwell, W. B. Motherwell, *Chem. Commun.* **2001**, 1270; g) S. Gründemann, M. Albrecht, J. A. Loch, J. W. Faller, R. H. Crabtree, *Organometallics* **2001**, *20*, 5485.
79. a) F. E. Hahn, M. C. Jahnke, T. Pape, *Organometallics* **2007**, *26*, 150; b) F. E. Hahn, M. C. Jahnke, T. Pape, *Organometallics* **2006**, *25*, 5927; c) F. E. Hahn, M. C. Jahnke, V. Gomez-Benitez, D. Morales-Morales, T. Pape, *Organometallics* **2005**, *24*, 6458.
80. J. A. Loch, M. Albrecht, E. Peris, J. Mata, J. W. Faller, R. H. Crabtree, *Organometallics*, **2002**, *21*, 700.
81. H. Abe, S. Takashima, T. Yamamoto, M. Inouye., *Chem. Commun*, **2009**, 2121.
82. U. Horn, F. Mutterer, C. D. Weis, *HelV. Chim. Acta*, **1976**, *59*, 190–211.
83. J. F. Hulvat, M. Sofos, K.Tajima, S. I. Stupp, *J. Am. Chem. Soc.* **2005**, *127*, 366.
84. (a) S. A. Jenekhe, *AdV. Mater.* **1995**, *7*, 309. (b) F.Hide, M. A.Diaz- Garcia, B. J. Schwartz, A. J. Heeger, *Acc. Chem. Res.* **1997**, *30*, 430. (c) A. Kraft, A. C. Grimsdale, A. B. Holmes, *Angew. Chem., Int. Ed*. **1998**, *37*, 402. (d) R. L. Carroll, C. B. Gorman, *Angew. Chem., Int. Ed.* **2002**, *41*, 4378.
85. (a) G. Yu, J. Gao, J. C. Hummelen, F. Wudl, A. J. Heeger, *Science* **1995**, *270*, 1789. (b) M. Grandström, K. Petrisch, A.C. Arias, A. Lux, M. R. Anderson, R. H. Friend, *Nature* **1998**, *395*, 257.
86. J. D. Bhawalkar, G. S. He, P. N. Prasad, *Rep. Prog. Phys.* **1996**, *59*, 1041.

87. D. A. Parthenopoulos, P. M. Rentzepis, *Science* **1989**, *245*, 843.

88. W. Denk, Strickler, J. H.; Webb, W. W. *Science* **1990**, *248*, 73.

89. (a) K. Müllen, G. Wegner, *Electronic Materials: The Oligomer Approach*; Wiley-VCH: Weinheim, **1998**. (b) R. E. Martin, F. Diederich, *Angew. Chem., Int. Ed.* **1999**, *38*, 1350. (c) F. S. Precup-Blaga, J. C. A.Garcia-Martinezand, P. H. J. Schenning, E. W. Meijer, *J. Am. Chem. Soc.* **2003**, *125*, 12953.

90. Yang, Y.; Pei, Q.; Heeger, A. J. *Synth. Met.* **1996**, *78*, 263.

91. Weder, C.; Wrighton, M. S. *Macromolecules* **1996**, *29*, 5157.

92. Granstro¨m, M. *Polym. Adv. Technol.* **1997**, *8*, 424.

93. S. J. George, Z. Tomovic, M. M. J. Smulders, T. F. A. de Greef, P. Leclere, E. W. Meijer, A. Schenning, *Angew. Chem., Int. Ed*. **2007**, *46*, 8206– 8211.

94. a) B. Alıcı, I. Özdemir, K. Karaaslan, E. Çetinkaya, B. Çetinkaya, *J. Mol. Catal. A - Chem.* **2005**, *231*, 261; b) B. Alıcı, T. Hökelek, E. Çetinkaya, B. Çetinkaya, *Heteroatom Chem.* **2003**, 82.

95. a) N. Marion, S. P. Nolan, *Acc. Chem. Res.* **2008**, *41*, 1440. b) N. Marion, S. P. Nolan, *Chem. Soc. Rev.* **2008**, *37*, 1776; c) S. Wuertz, F. Glorius, *Acc. Chem. Res.* **2008**, *41*, 1523; d) N. Marion, S. Diez-Gonzalez, S. P. Nolan, *Angew. Chem. Int. Ed.* **2007**, *46*, 2988.

96. a) P. Bazinet, T.-G. Ong, J. S. O'Brien, N. Lavoie, E. Bell, G. P. A. Yap, I. Korobkov, D. S. Richeson, *Organometallics* **2007**, *26*, 2885; b) Ö. Alýcý, N. Gürbüz, B. Çetinkaya, *Russ. J. Coord. Chem.* **2005**. *31*, 142; c) İ. Özdemir, B. Alıcı, N. Gürbüz, E. Çetinkaya, B. Çetinkaya, *J. Mol. Catal. A - Chem.* **2004**, *217*, 37; d) P. Bazinet, G. P. A. Yap, D. S. Richeson, *J. Am. Chem. Soc.* **2003**, *125*, 13314.

97. a) N. T. S. Phan, M. V. Der Sluys, C. W. Jones, *Adv. Synth. Catal.* **2006**, *348*, 609; b). K. Q. Yu, W. Sommer, J. M. Richardson, M. Weck, C. W. Jones, *Adv. Synth. Catal.* **2005**, *347*, 161; c) K. Q. Yu, W. Sommer, M. Weck, C. W. Jones, *J. Catal.* **2004**, *226*, 101; d) W. J. Sommer, K. Q. Yu, J. S. Sears, Y. Y. Ji, X. L. Zheng, R. J. Davis, C. D. Sherrill, C. W. Jones, M. Weck, *Organometallics* **2005**, *24*, 4351.

98. D. E. Bergbreiter, P. L. Osbum, J. D. Frels, *Adv. Synth. Catal.* **2005**, *347*, 172.

99. a) D. Olsson, P. Nilsson, M. El Masnaouy, O. F. Wendt, *Dalton Trans*. **2005**, 1924; b) P. Nilsson, O. F. Wendt, *J. Organomet. Chem.* **2005**, *690*, 4197; c) M. R. Eberhard, *Org. Lett.* **2004**, *6*, 2125.

100. a) E. Peris, R. H. Crabtree, *Coord. Chem. Rev.* **2004**, *248*, 2239; b) E. Peris, J. A. Loch, J. Mata, R. H. Crabtree, *Chem. Commun*. **2001**, 201.

101. (a) *Metal-catalyzed Cross-coupling Reactions*, eds. F. Diederich, P. Stang, Wiley-VCH: Weinheim,Germany, **1998**; (*b) Cross-Coupling Reactions*, ed. N. Miyaura, Springer: Berlin, Germany, **2002**.

102 (a) G. Bringmann, R. Wlater, R. Weirich, *Angew. Chem. Int. Ed*, **1990**, *29*, 977; *(b)* G. Bringmann, M. Breuning, S. Tasler, *Synthesis*, **1999**, 525.

103. (a) L. Ackermann, R. Vincente, A. Kapdi, *Angew. Chem. Int. Ed*. **2009**, *48*, 9792; *(b)* B. Li, S. Yang, Z. Shi, *Synlett*, **2008**, 949; (c) D. Stuart, K. Fagnou, *Science* **2007**, *316*, 1172; (d) R. Phipps, M, Gaunt. *Science*, **2009**, *323*, 1593; (e) J, Lewis. R, Bergman. J. Ellman, *Acc. Chem. Res*, **2008**, *41*, 1013; (f) J. Norinder, A. Matsumoto,

N. Yoshikai, E. Nakamura, *J. Am. Chem. Soc*, **2008**, *130*, 5858;(g) H.-Q. Do, R. Khan, O. Daugulis, *J. Am. Chem. Soc*, **2008**, *130*, 15185; (h) L. Ackermann, A. Althammer, S. Fenner, *Angew. Chem. Int. Ed*, **2009**, *48*, 201; (i) L.-C. Campeau, D. R. Stuart, J. P. Leclerc, M. Bertrand-Laperle, E. Villemure, H.-Y. Sun, S. Lasserre, N. Guimond, M. Lecavallier, K. Fagnou, *J. Am. Chem. Soc*, **2009**,*131*, 3291; (j) C. Wang, I.Piel, F. Glorius, *J. Am. Chem. Soc*, **2009**, *131*, 9651; (k) C. Huang, V. Gevorgyan, *J. Am. Chem. Soc*, **2009**, *131*, 10844; (l) M. Tobisu, I. Hyodo, N. Chatani, *J. Am. Chem. Soc*, 2009, **131**, 12070; (m) M. Kim, J. Kwak, S. Chang, *Angew. Chem. Int. Ed*, **2009**, *48*, 8935; (n) C.-L. Sun, B.-J. Li, Z.-J. Shi, *Chem. Commun*, **2010**, *46*,77; (0) B. Xiao, Y. Fu, J. Xu, T.-J. Gong, J.-J. Dai, J. Yi, L. Liu, *J. Am. Chem. Soc*, **2010**,*132*, 468; (p) T. Nishikata, R. Abela, B. H. Lipshutz, *Angew. Chem. Int. Ed*, **2010**, *49*,781; (q) M. Wasa, B. T. Worrell, J.-Q. Yu, *Angew. Chem Int. Ed*, **2010**, *49*, 1275; (r) F. Valle, J. J. Mousseau, A. B. Charette, *J. Am. Chem. Soc*, **2010**, *132*, 1514; (s) W. Liu, H. Cao, A. Lei, *Angew. Chem. Int. Ed*, **2010**, *49*, 2004; (t) P. Xi, F. Yang, S. Qin, D. Zhao, J. Lan, G. Gao, C. Hu, J. You, *J. Am. Chem. Soc*, **2010**, *132*, 1822; (u) H. Hachiya, K. Hirano, T. Satoh, M. Miura, *Angew. Chem. Int. Ed*, **2010**, *49*, 2202; (v) C. Wang, I. Piel, F. Glorius, *J. Am. Chem. Soc*, **2009**, *131*, 4194.

104. (a) T. Okazawa, T. Satoh, M. Miura, M. Nomura, *J. Am. Chem. Soc*, **2002**, *124*, 5286;(b) K. Ueda, S.Yanagisawa, J. Yamaguchi,K. Itami, *Angew. Chem. Int. Ed*, **2010**, *49*, 8946.

105. (a) D. J. Schipper., K. Fagnou, *Chem. Mater*, **2011**, *23*, 1594; (b) C. W. Tang, S. A. VanSlyke, C. H. Chen, *J. Appl. Phys*, **1989**, *65*, 3610; (c) A. C. Grimsdale, K. L. Chan, R. E. Martin, P. G. Jokisz, A. B. Holmes, *Chem. Rev*, **2009**, *109*, 897; (d) *Organic Light-Emitting Devices: Synthesis, Properties and Applications*; K. Müllen, U. Scherf, Wiley-VCH: Weinheim, Germany, **2006**; (e) G. Bringmann, R. Wlater, R. Weirich, *Angew. Chem. Int. Ed*, **1990**, *29*, 977 ;(e) G. Bringmann, M. Breuning, S. Tasler, *Synthesis*, **1999**, 525.

106. (a) W. Li, C. Du, F. Li, Y. Zhou, M. Fahlman, Z. Bo, F. Zhang, *Chem. Mater*, **2009**, *21*, 5327; (b) A. Facchetti, M.-H. Yoon, C. L. Stern, H. E. Katz, T. J. Marks, *Angew. Chem. Int. Ed*, **2003**, *42*, 3900; (c) M. Yang, Q. Zhang, P. Wu, H. Ye, X. Liu, *Polymer*, **2005**, *46*, 6266.

107. (a) A. Mori, A. Sekiguchi, K. Masui, T. Shimada, M. Horie, K. Osakada, M. Kawamoto, T. Ikeda, *J. Am.Chem. Soc*, 2003, **25**, 1700 ; (b) H. Mochizuki, T. Hasui, M. Kawamoto, T. Shiono, I. Ikeda, C. Adachi, Y.Taniguchi, T. Shiroto, *Chem. Commun*, **2000**,1923.

108. (a) K. Ueda, S.Yanagisawa, J. Yamaguchi, and K. Itami, *Angew. Chem. Int. Ed*, **2010**, *122*, 9130. (b) S. Kirchberg, S. Tani, K. Ueda, J. Yamaguchi, A. Studer, K. Itami, *Angew.Chem Int. Ed*, **2011**, *50*, 1; (c) B. Join, T. Yamamoto, K. Itami, *Angew. Chem. Int. Ed*, **2009**, *48*, 3644. (d) S. Yanagisawa, K. Ueda, H. Sekizawa, K. Itami, *J. Am.Chem. Soc*, **2009**, *131*, 14622 ;(e) S. I. Gorelsky, D. Lapointe, K. Fagnou, *J. Am. Chem. Soc*,

2008, *130*, 10848; (f) C. Gozzi, L. Lavenot, K. Ilg, V. Penalva, M. Lemaire, *Tetrahedron Lett*, **1997**, *38*, 8867; (g) T. Okazawa, T. Satoh, M. Miura, M. Nomura, *J. Am. Chem.Soc*, **2002**, *124*, 5286; (h) L. Chen, J. Roger, C. Bruneau, P. H. Dixneuf, H. Doucet, *Chem. Commun*, **2011**, *47*, 1872.

109. K. Stefan, F. J. Wolter, J. D. Theo, J. P. Stephen, *Liquid Crystals*, **2009**, *36*, 389.

110. D. E. Ames, A. Opalko, *Synthesis*, **1983**, *3*, 234.

IX. ^{1}H and ^{13}C NMR spectras

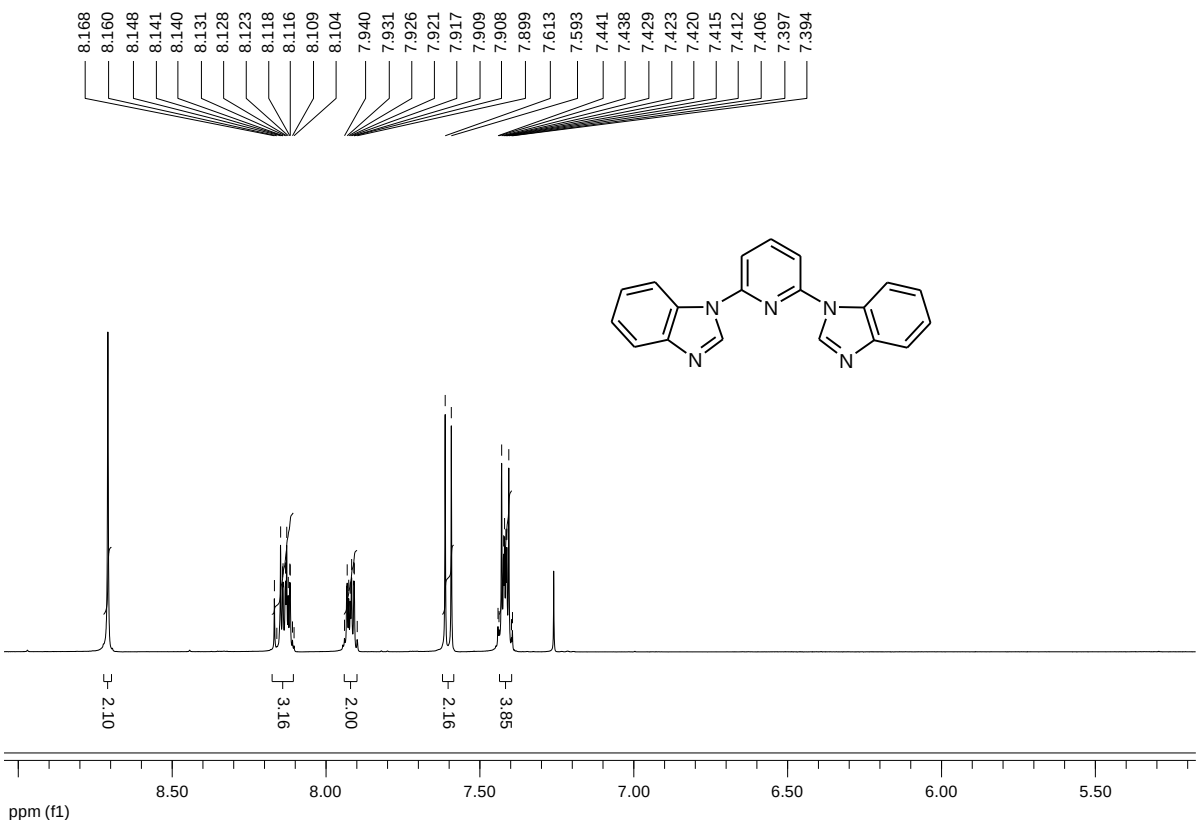
8.168
8.160
8.148
8.141
8.140
8.131
8.128
8.123
8.118
8.116
8.109
8.104
7.940
7.931
7.926
7.921
7.917
7.909
7.908
7.899
7.613
7.593
7.441
7.438
7.429
7.423
7.420
7.415
7.412
7.406
7.397
7.394
N
N
N
N
2.10
3.16
2.00
2.16
3.85
8.50
8.00
7.50
7.00
6.50
6.00
5.50
ppm (f1)

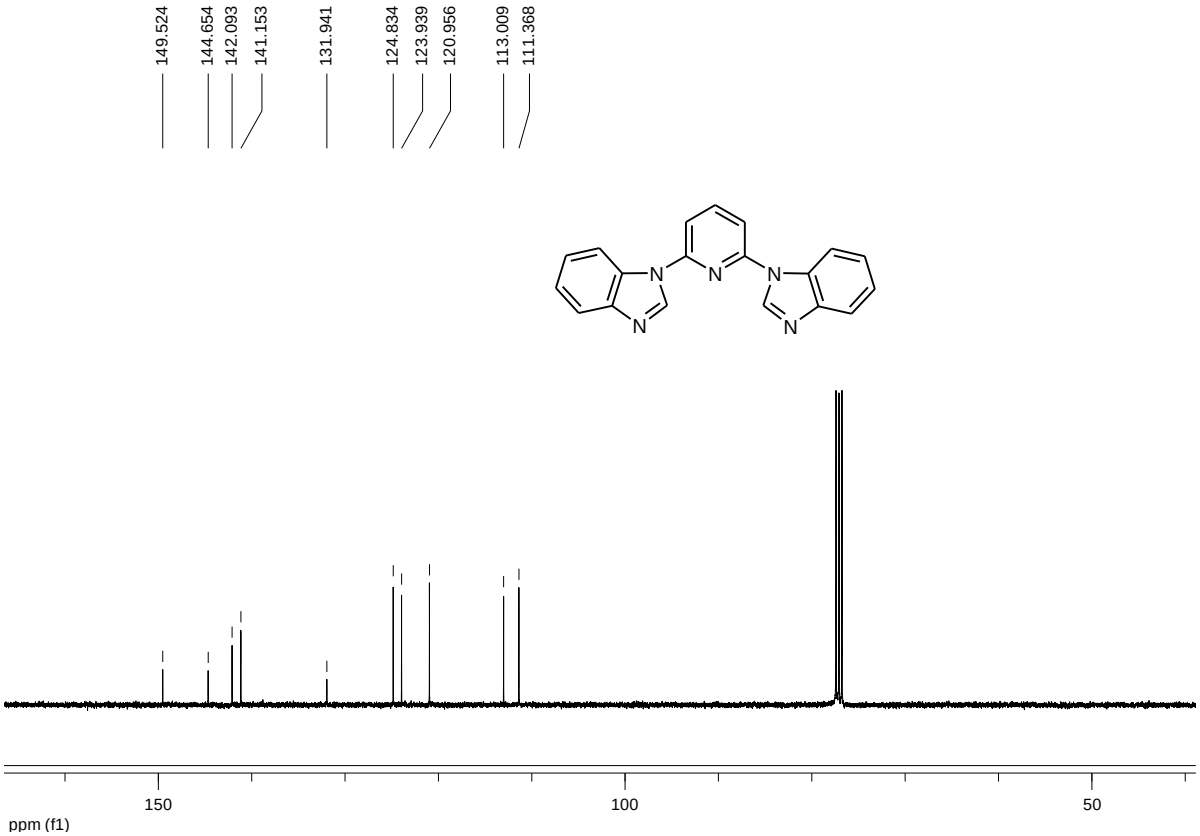
149.524
144.654
142.093
141.153
131.941
124.834
123.939
120.956
113.009
111.368
N
N
N
N
150
100
50
ppm (f1)

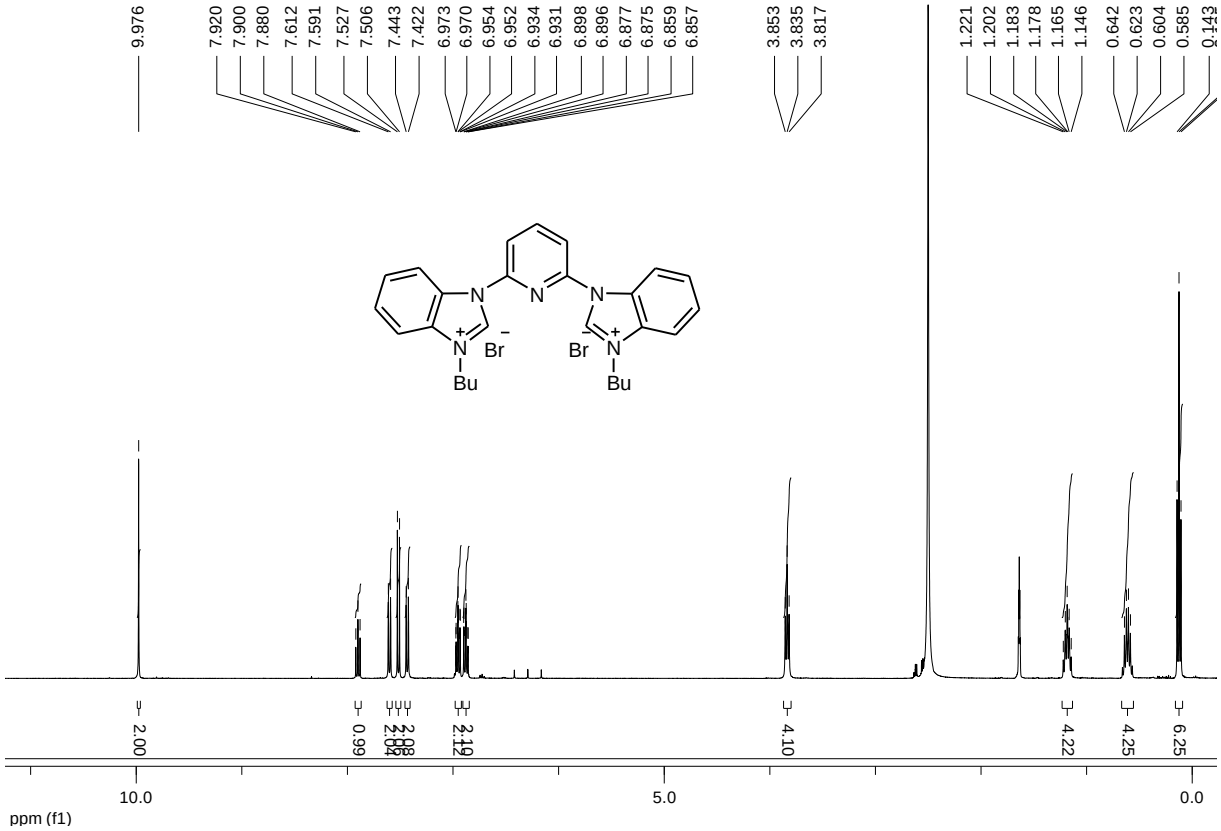
9.976
7.920
7.900
7.880
7.612
7.591
7.527
7.506
7.443
7.422
6.973
6.970
6.954
6.952
6.934
6.931
6.898
6.896
6.877
6.875
6.859
6.857
3.853
3.835
3.817
1.221
1.202
1.183
1.178
1.165
1.146
0.642
0.623
0.604
0.585
0.143
2.00
0.99
2.08
2.04
2.19
4.10
4.22
4.25
6.25
10.0
5.0
0.0
ppm (f1)

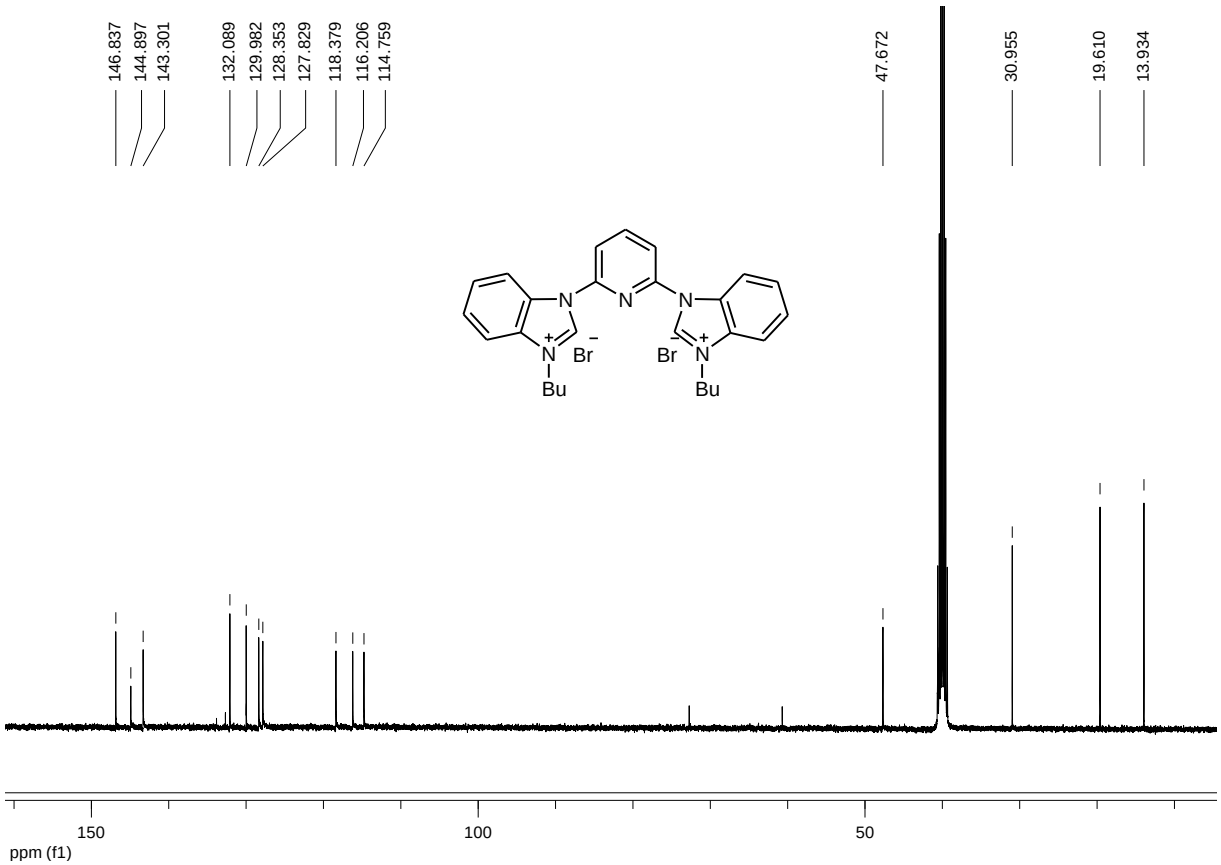
146.837
144.897
143.301
132.089
129.982
128.353
127.829
118.379
116.206
114.759
47.672
30.955
19.610
13.934
150
100
50
ppm (f1)

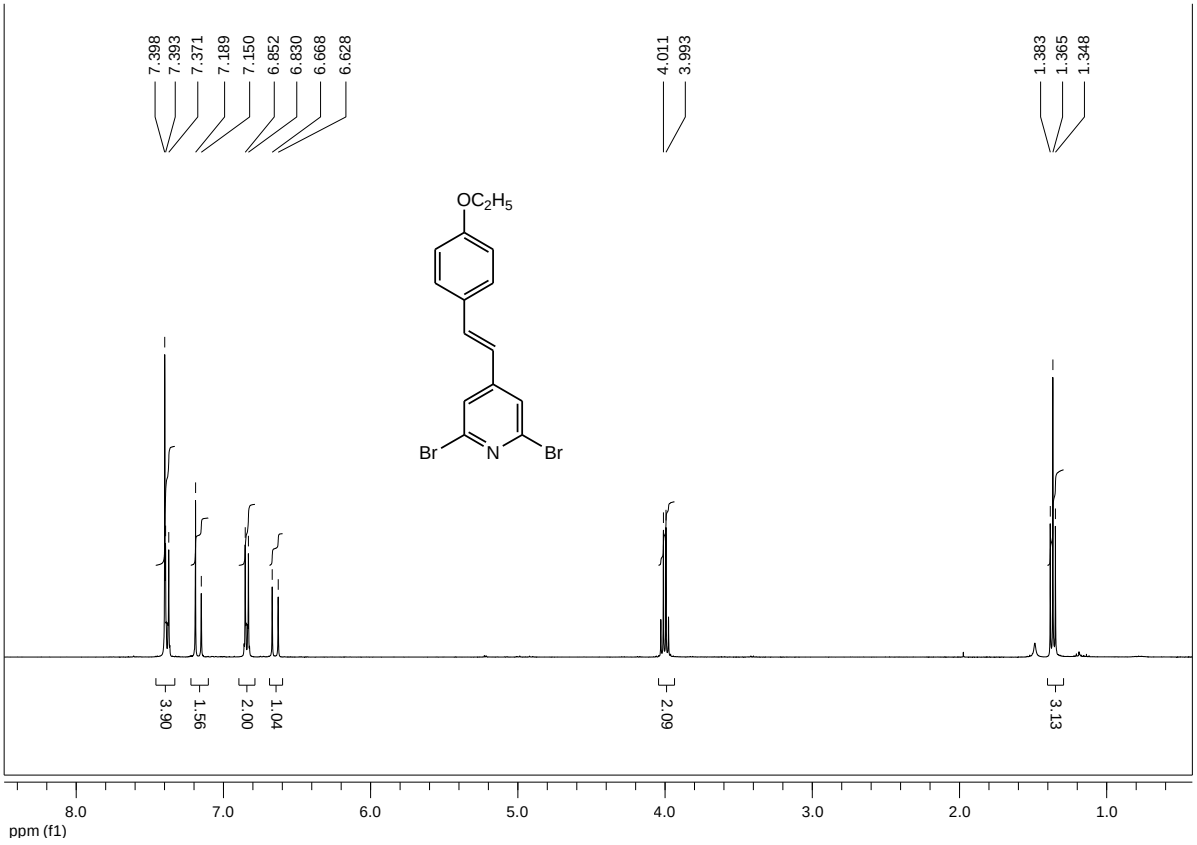
7.398
7.393
7.371
7.189
7.150
6.852
6.830
6.668
6.628
4.011
3.993
1.383
1.365
1.348
OC2H5
Br
N
Br
3.90
1.56
2.00
1.04
2.09
3.13
8.0
7.0
6.0
5.0
4.0
3.0
2.0
1.0
ppm (f1)

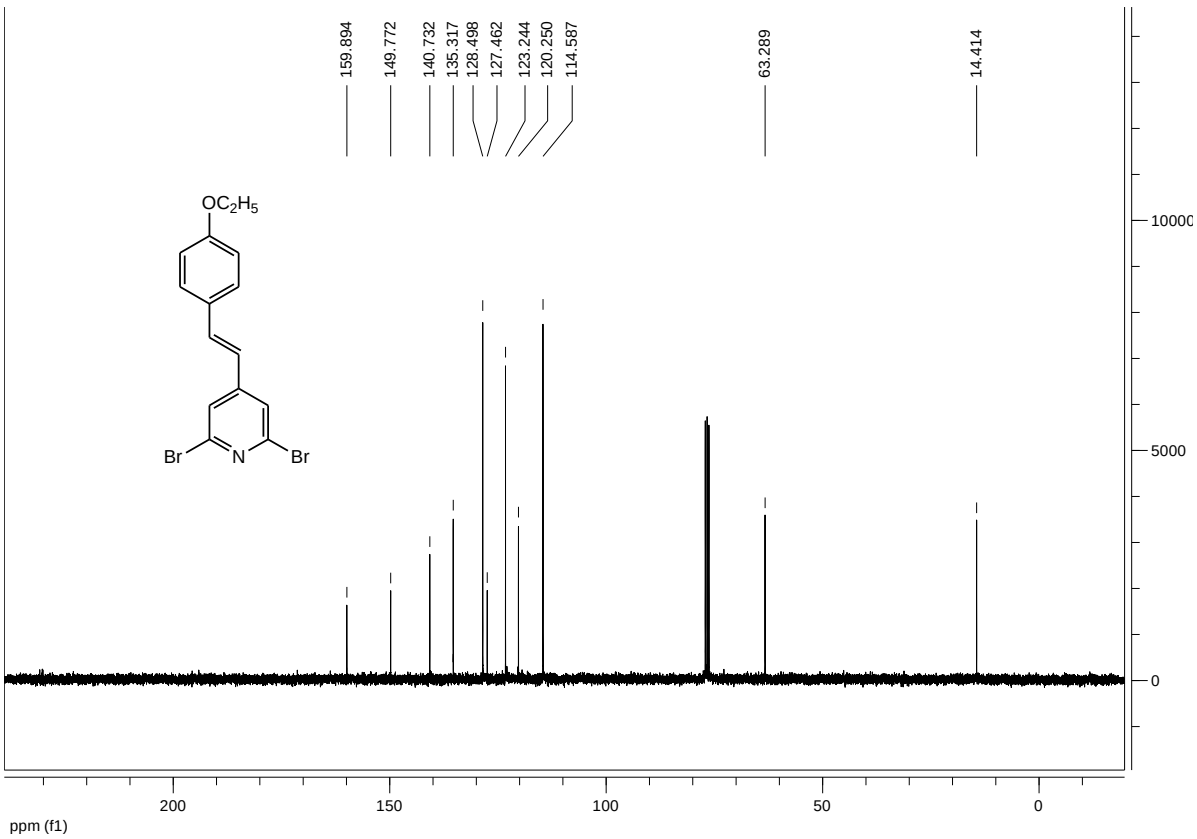
159.894
149.772
140.732
135.317
128.498
127.462
123.244
120.250
114.587
63.289
14.414
OC2H5
Br
N
Br
10000
5000
0
200
150
100
50
0
ppm (f1)

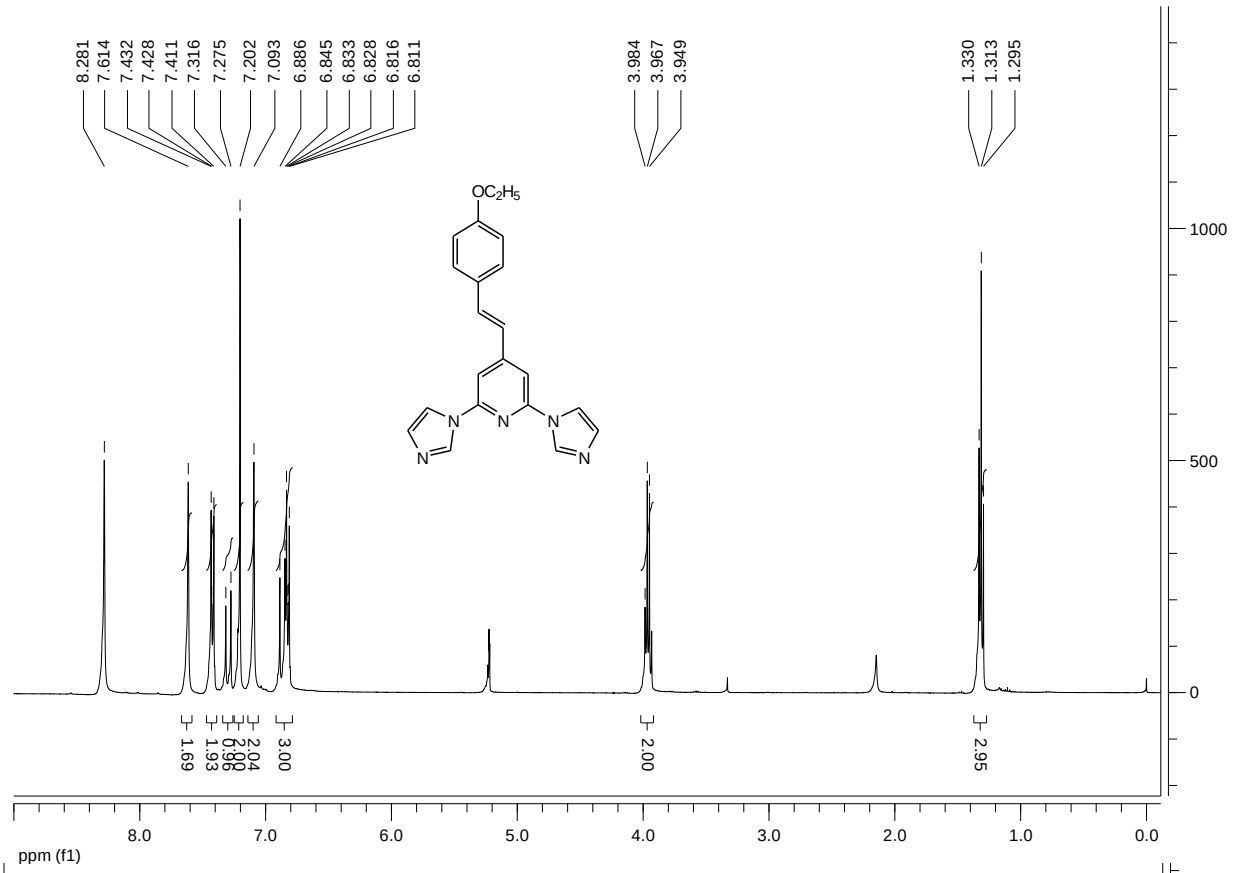
8.281
7.614
7.432
7.428
7.411
7.316
7.275
7.202
7.093
6.886
6.845
6.833
6.828
6.816
6.811
3.984
3.967
3.949
1.330
1.313
1.295
OC2H5
N
N
N
N
1000
500
0
1.69
1.93
2.00
3.00
2.00
2.95
8.0
7.0
6.0
5.0
4.0
3.0
2.0
1.0
0.0
ppm (f1)

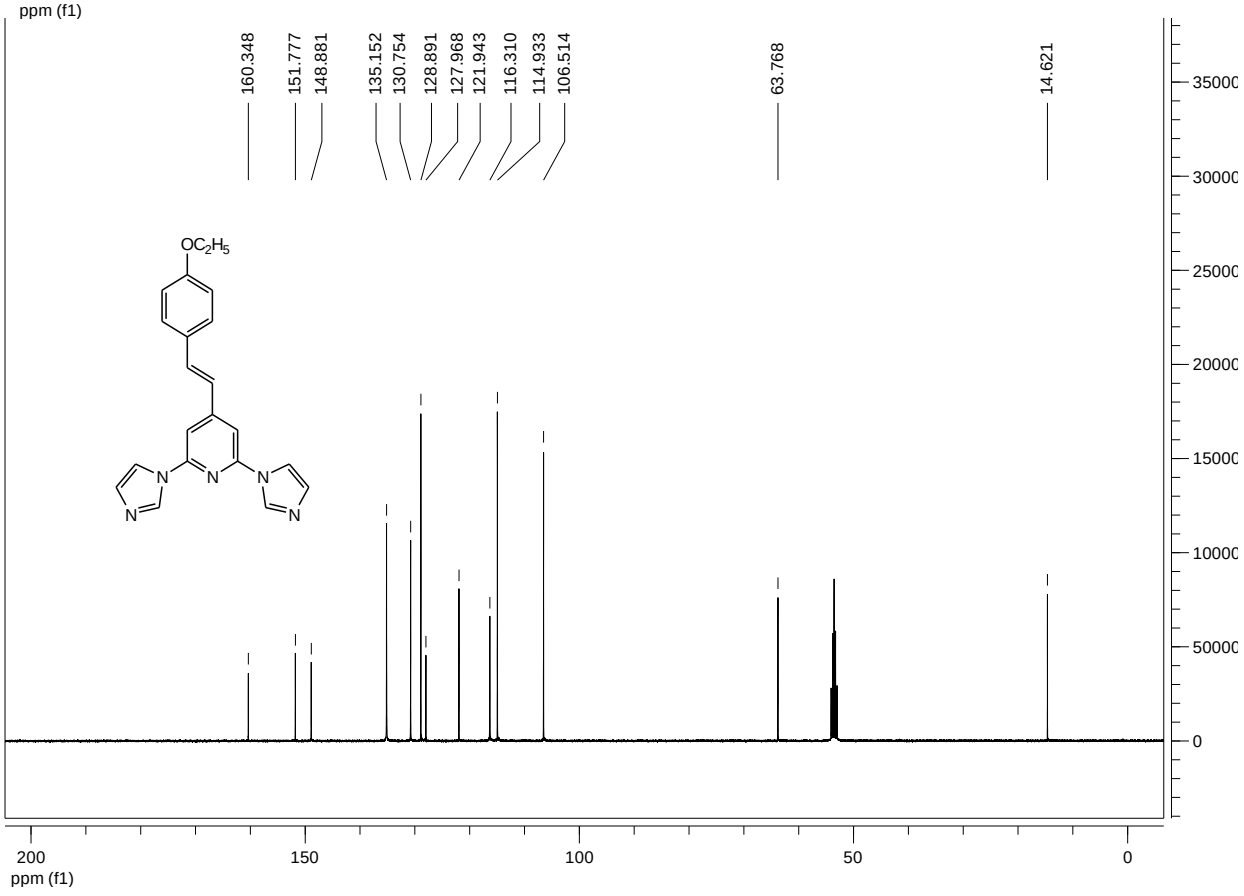
160.348
151.777
148.881
135.152
130.754
128.891
127.968
121.943
116.310
114.933
106.514
63.768
14.621
OC2H5
N
N
N
N
35000
30000
25000
20000
15000
10000
50000
0
200
150
100
50
0
ppm (f1)

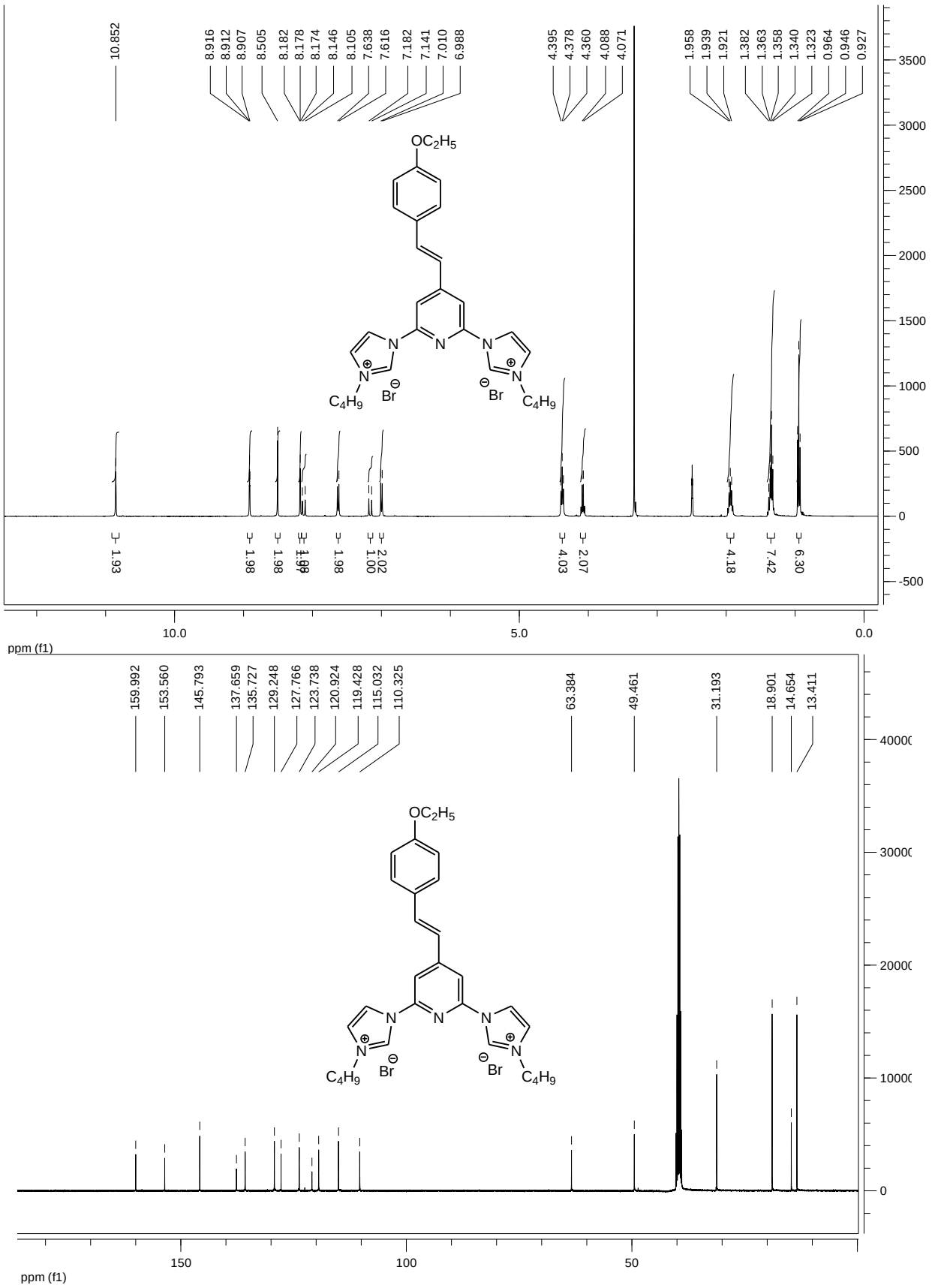
10.852
8.916
8.912
8.907
8.505
8.182
8.178
8.174
8.146
8.105
7.638
7.616
7.182
7.141
7.010
6.988
4.395
4.378
4.360
4.088
4.071
1.958
1.939
1.921
1.382
1.363
1.358
1.340
1.323
0.964
0.946
0.927
OC2H5
C4H9
Br
1.93
1.98
1.98
1.98
1.98
2.02
1.00
4.03
2.07
4.18
7.42
6.30
10.0
5.0
0.0
ppm (f1)
159.992
153.560
145.793
137.659
135.727
129.248
127.766
123.738
120.924
119.428
115.032
110.325
63.384
49.461
31.193
18.901
14.654
13.411
150
100
50
ppm (f1)

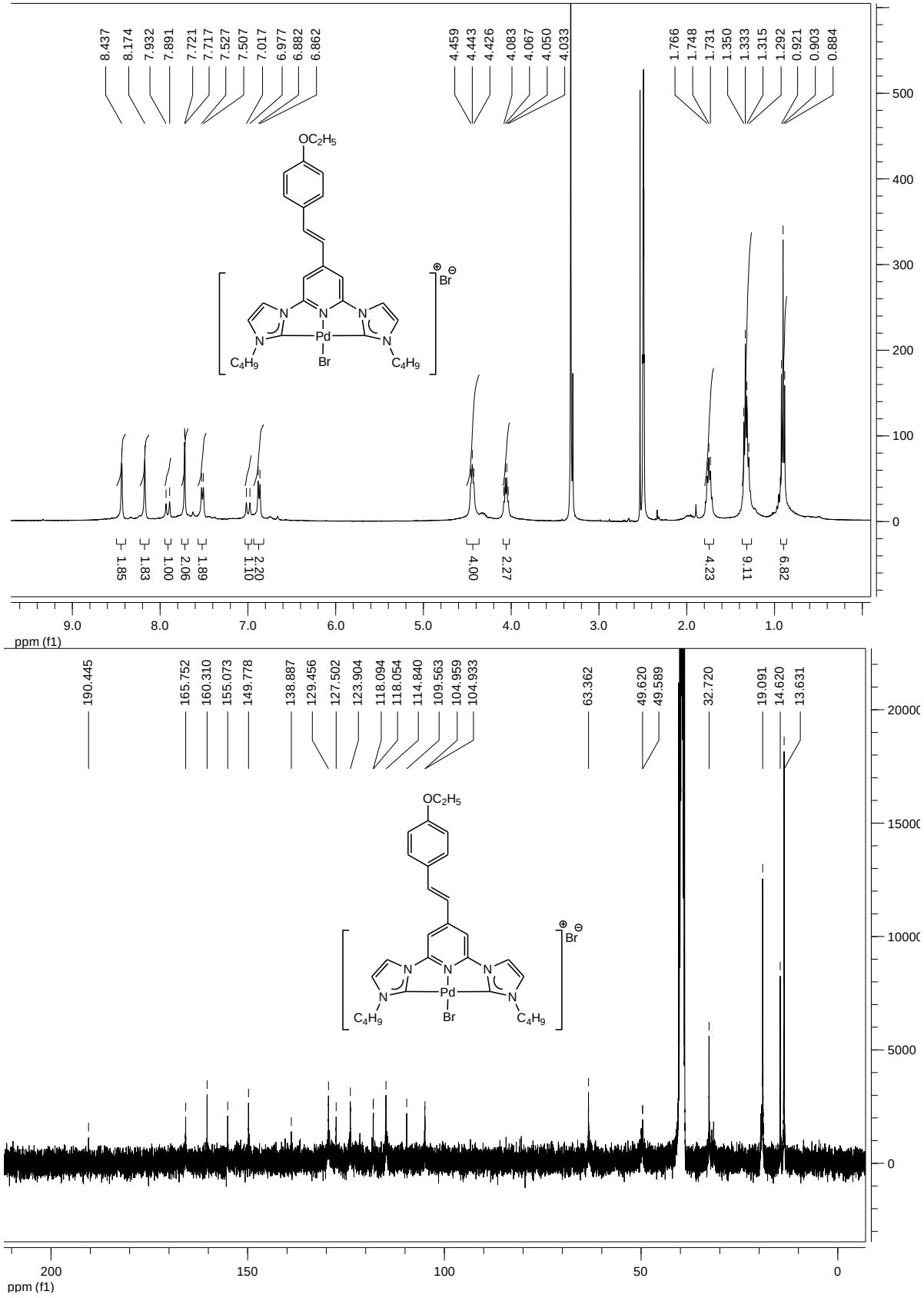
8.437
8.174
7.932
7.891
7.721
7.717
7.527
7.507
7.017
6.977
6.882
6.862
4.459
4.443
4.426
4.083
4.067
4.050
4.033
1.766
1.748
1.731
1.350
1.333
1.315
1.292
0.921
0.903
0.884
OC2H5
Br
N
Pd
Br
C4H9
C4H9
1.85
1.83
1.00
2.06
1.89
2.20
1.10
4.00
2.27
4.23
9.11
9.82
ppm (f1)
190.445
165.752
160.310
155.073
149.778
138.887
129.456
127.502
123.904
118.094
118.054
114.840
109.563
104.959
104.933
63.362
49.620
49.589
32.720
19.091
14.620
13.631
ppm (f1)

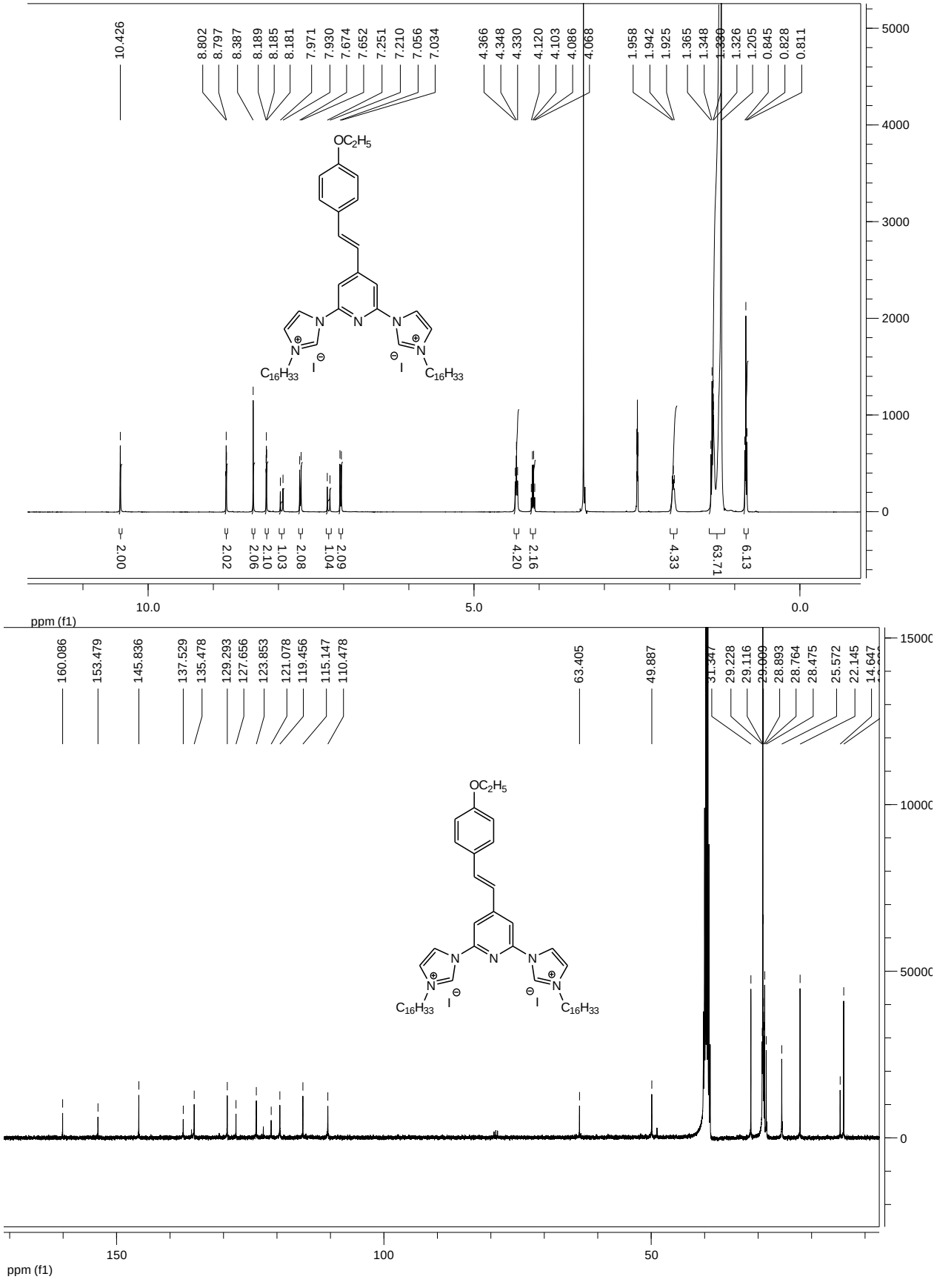
10.426
8.802
8.797
8.387
8.189
8.185
8.181
7.971
7.930
7.674
7.652
7.251
7.210
7.056
7.034
4.366
4.348
4.330
4.120
4.103
4.086
4.068
1.958
1.942
1.925
1.365
1.348
1.330
1.326
1.205
0.845
0.828
0.811
OC2H5
C16H33
2.00
2.02
2.06
2.10
1.03
2.08
1.04
2.09
4.20
2.16
4.33
63.71
6.13
ppm (f1)
160.086
153.479
145.836
137.529
135.478
129.293
127.656
123.853
121.078
119.456
115.147
110.478
63.405
49.887
31.347
29.228
29.116
29.009
28.893
28.764
28.475
25.572
22.145
14.647
ppm (f1)

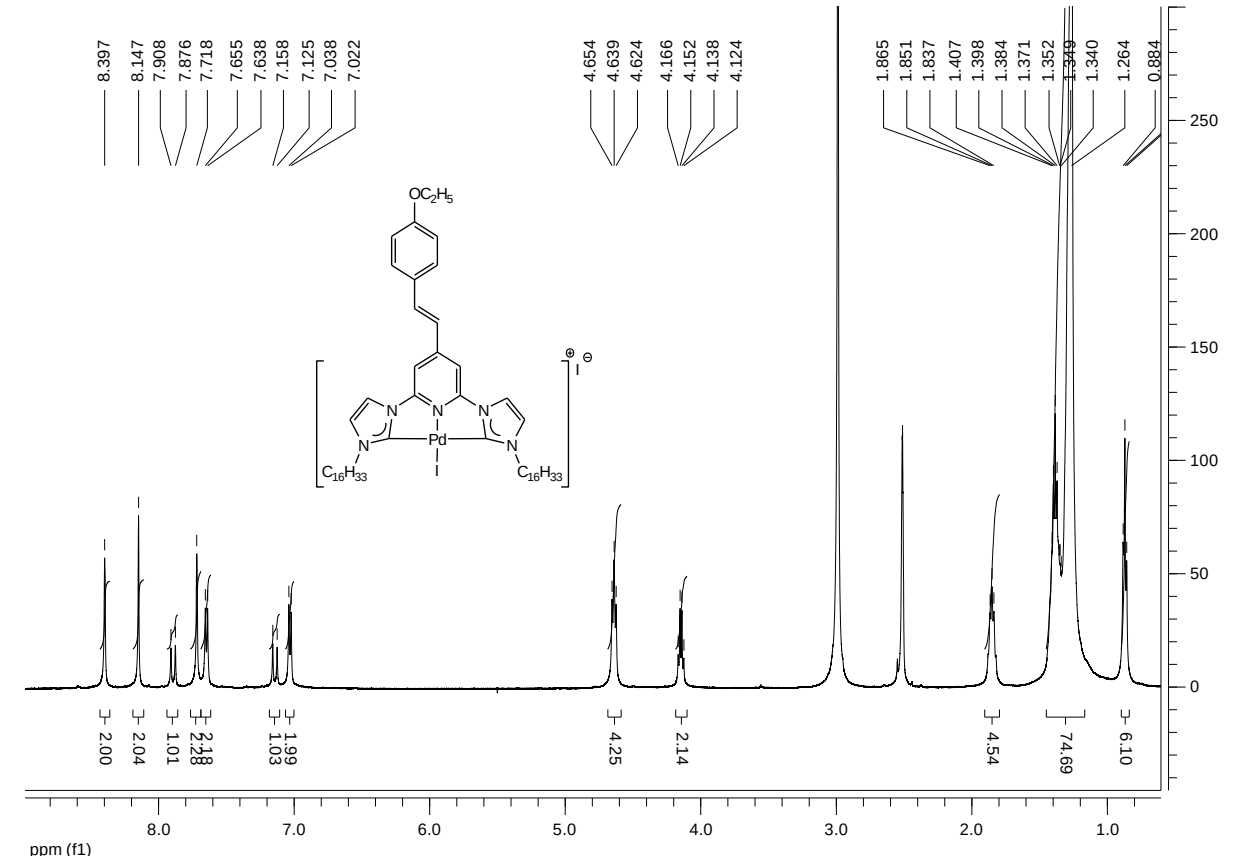
8.397
8.147
7.908
7.876
7.718
7.655
7.638
7.158
7.125
7.038
7.022
4.654
4.639
4.624
4.166
4.152
4.138
4.124
1.865
1.851
1.837
1.407
1.398
1.384
1.371
1.352
1.349
1.340
1.264
0.884
OC2H5
C16H33
C16H33
Pd
I
2.00
2.04
1.01
2.18
2.08
1.03
1.99
4.25
2.14
4.54
7.69
9.10
ppm (f1)

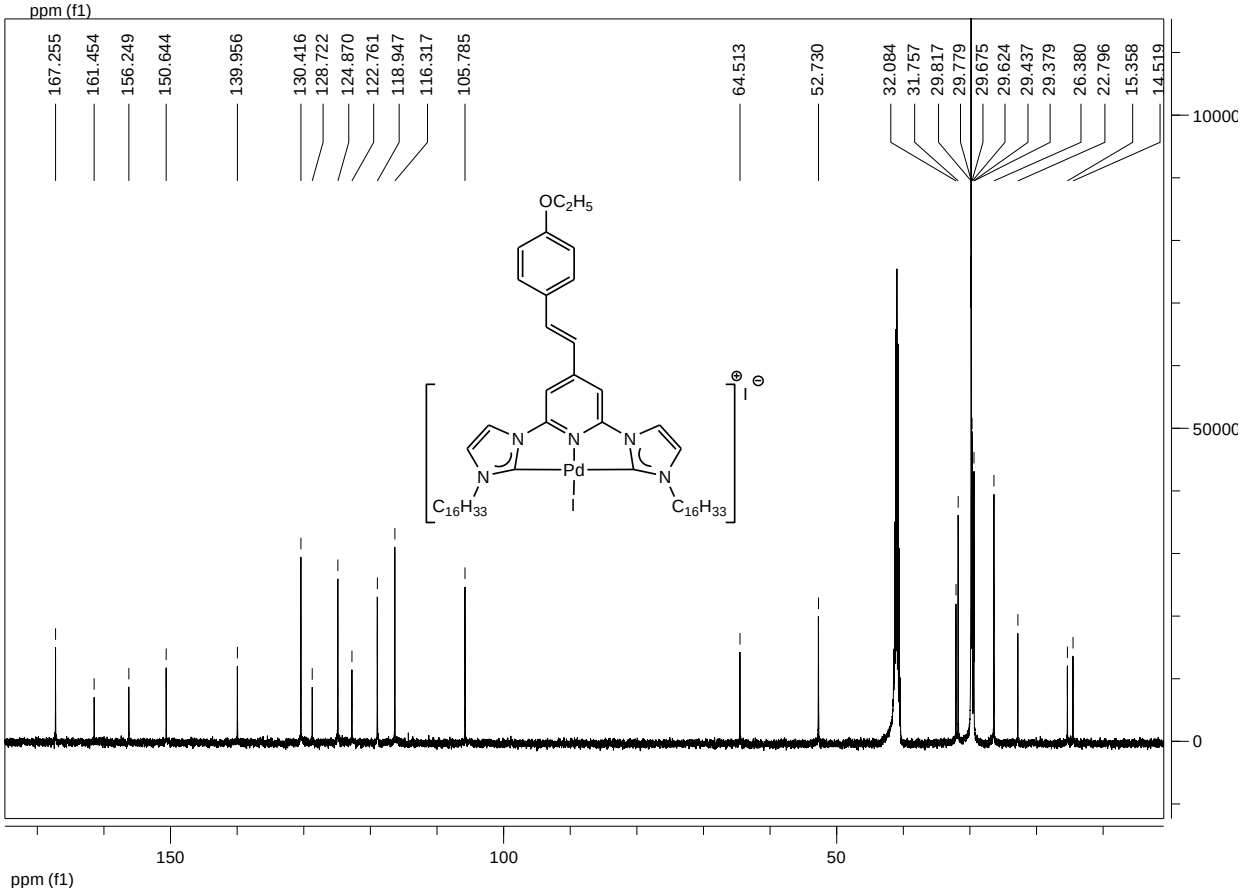
167.255
161.454
156.249
150.644
139.956
130.416
128.722
124.870
122.761
118.947
116.317
105.785
64.513
52.730
32.084
31.757
29.817
29.779
29.675
29.624
29.437
29.379
26.380
22.796
15.358
14.519
OC2H5
C16H33
C16H33
Pd
I
ppm (f1)

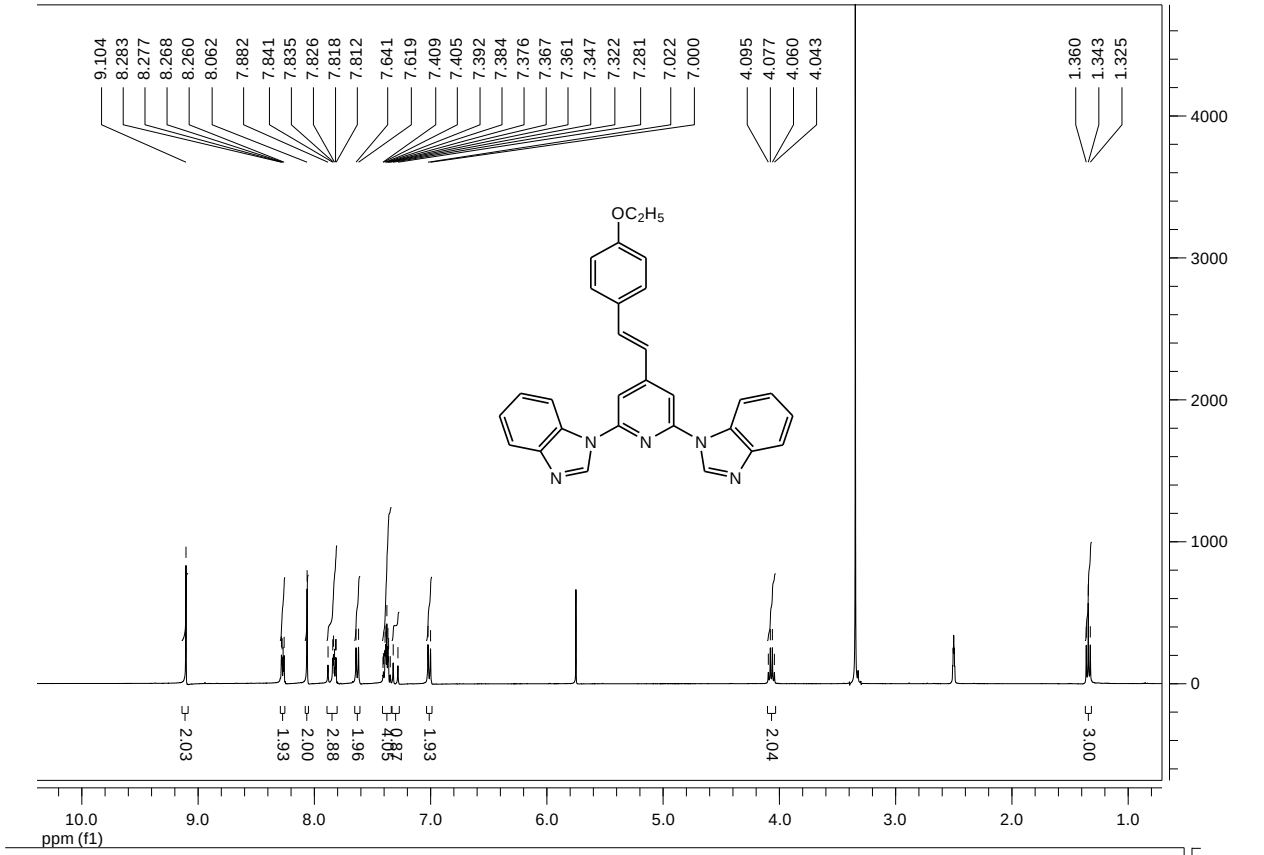
9.104
8.283
8.277
8.268
8.260
8.062
7.882
7.841
7.835
7.826
7.818
7.812
7.641
7.619
7.409
7.405
7.392
7.384
7.376
7.367
7.361
7.347
7.322
7.281
7.022
7.000
4.095
4.077
4.060
4.043
1.360
1.343
1.325
OC2H5
2.03
1.93
2.00
2.88
1.96
4.05
0.87
1.93
2.04
3.00
ppm (f1)

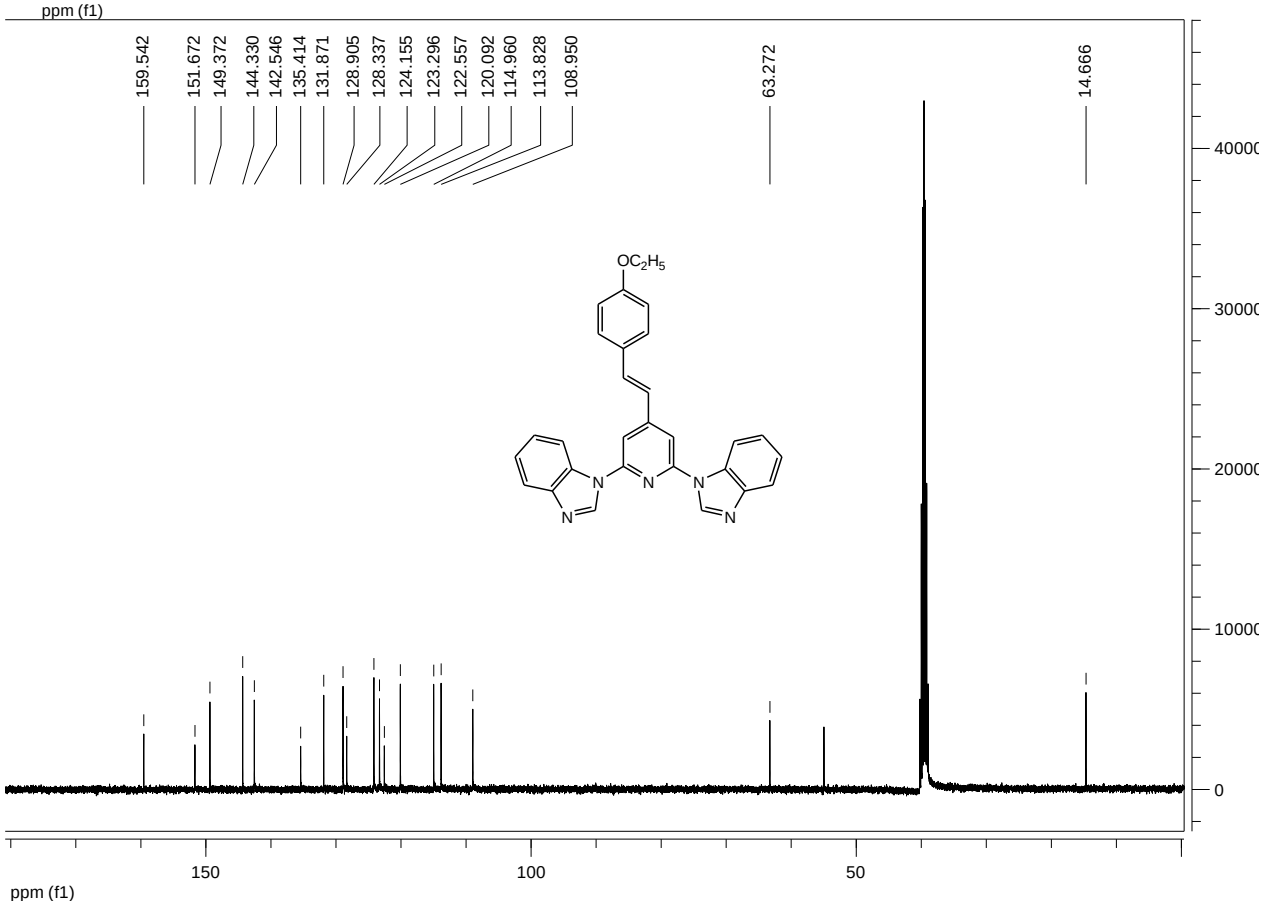
159.542
151.672
149.372
144.330
142.546
135.414
131.871
128.905
128.337
124.155
123.296
122.557
120.092
114.960
113.828
108.950
63.272
14.666
OC2H5
ppm (f1)

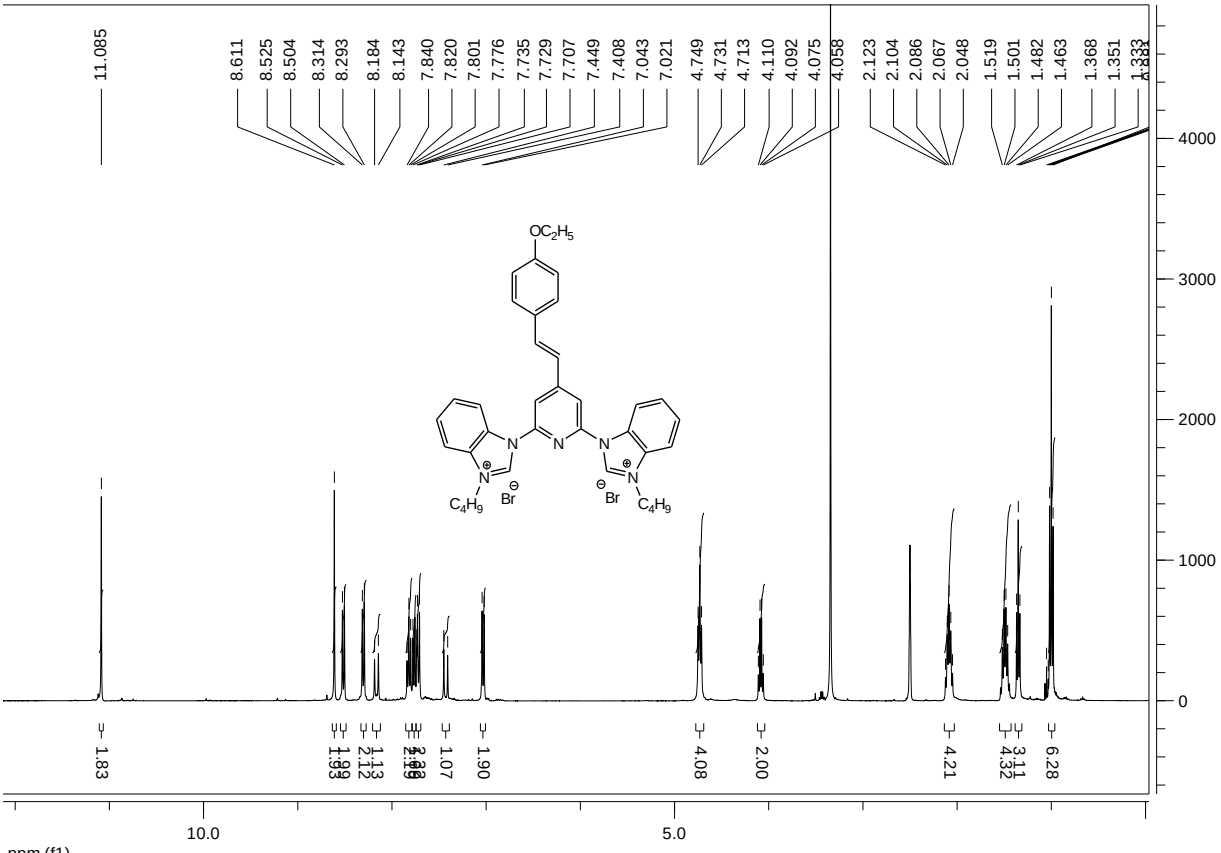
11.085
8.611
8.525
8.504
8.314
8.293
8.184
8.143
7.840
7.820
7.801
7.776
7.735
7.729
7.707
7.449
7.408
7.043
7.021
4.749
4.731
4.713
4.110
4.092
4.075
4.058
2.123
2.104
2.086
2.067
2.048
1.519
1.501
1.482
1.463
1.368
1.351
1.333
1.83
1.90
1.07
4.08
2.00
4.21
3.11
4.32
6.28
10.0
5.0
ppm (f1)

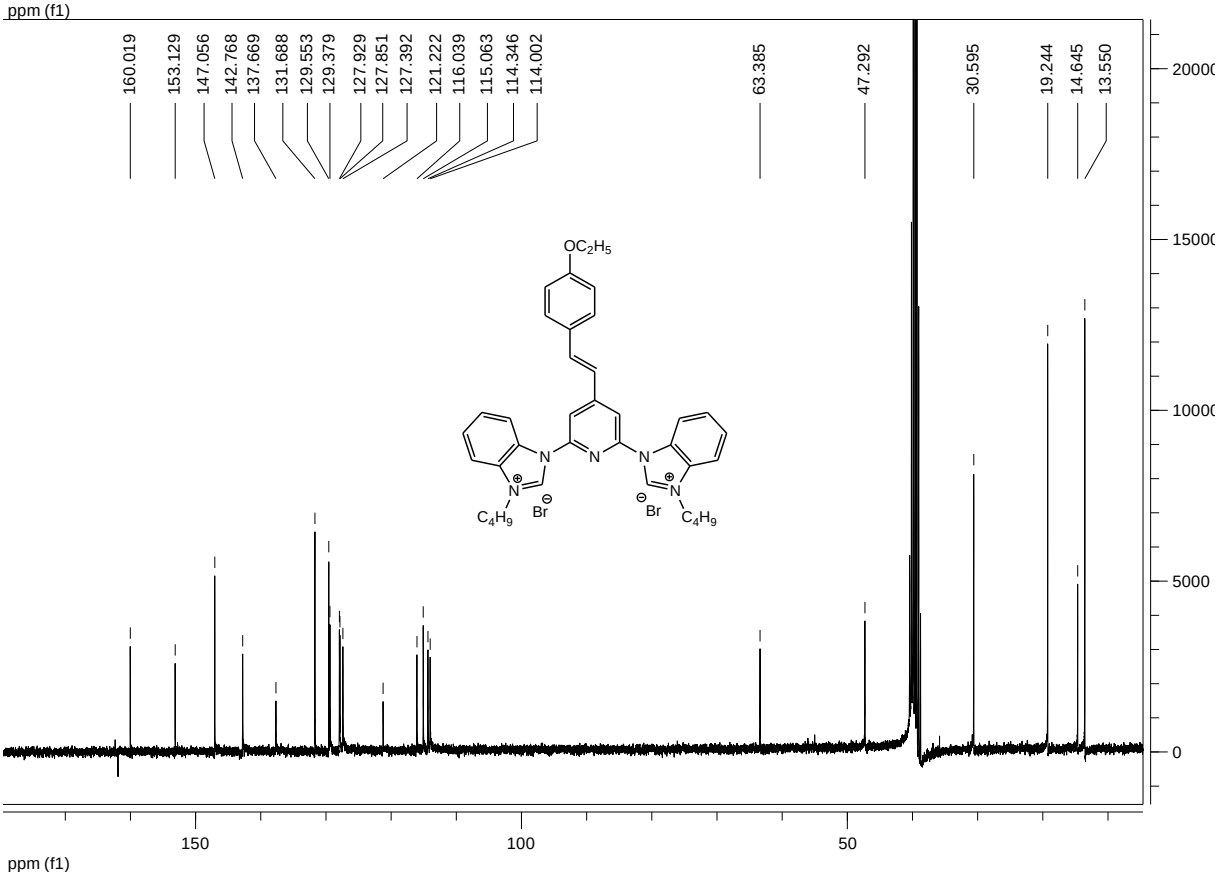
160.019
153.129
147.056
142.768
137.669
131.688
129.553
129.379
127.929
127.851
127.392
121.222
116.039
115.063
114.346
114.002
63.385
47.292
30.595
19.244
14.645
13.550
150
100
50
ppm (f1)

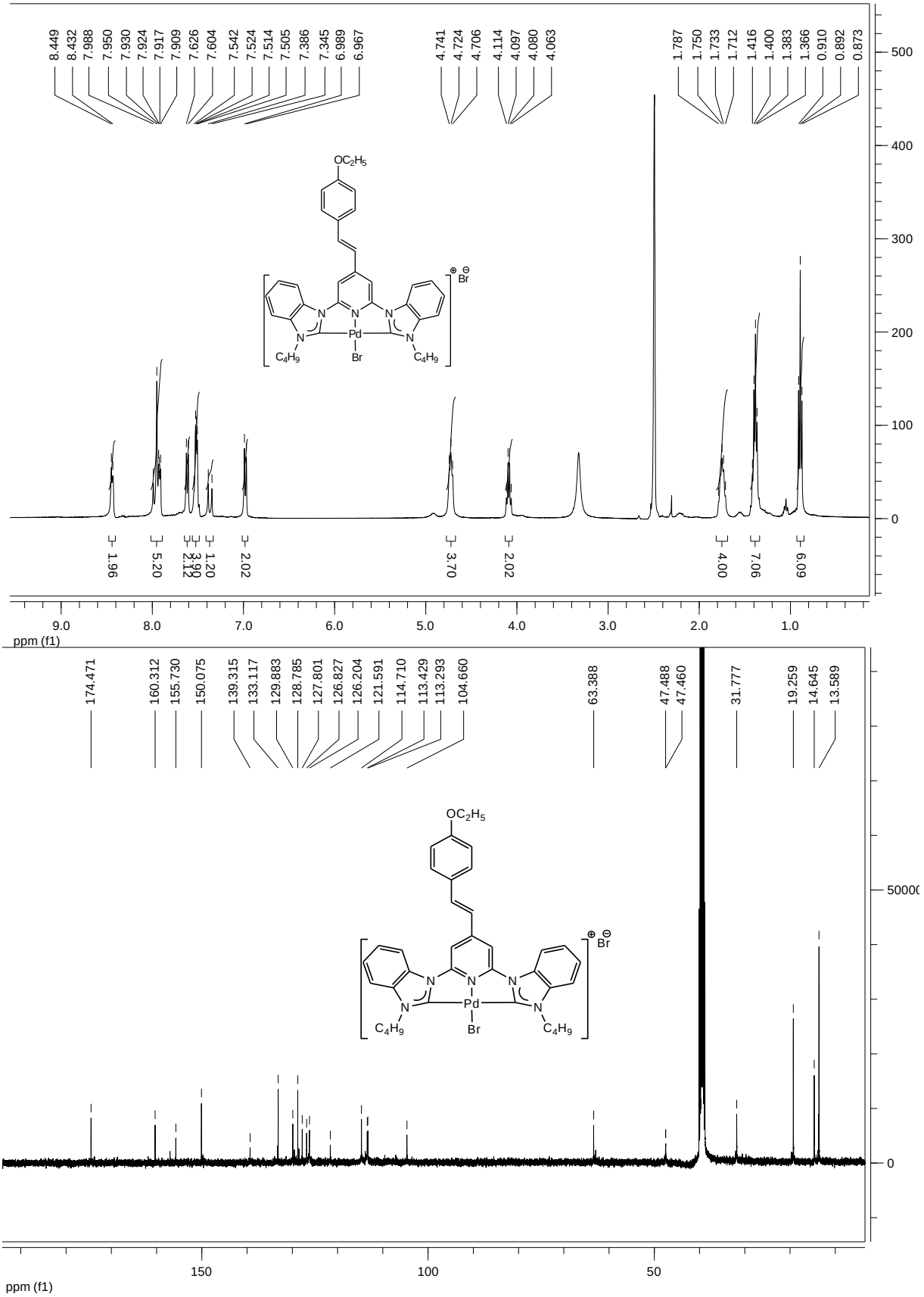
8.449
8.432
7.988
7.950
7.930
7.924
7.917
7.909
7.626
7.604
7.542
7.524
7.514
7.505
7.386
7.345
6.989
6.967
4.741
4.724
4.706
4.114
4.097
4.080
4.063
1.787
1.750
1.733
1.712
1.416
1.400
1.383
1.366
0.910
0.892
0.873
OC2H5
Br
N
Pd
C4H9
1.96
5.20
3.12
1.20
2.02
3.70
2.02
4.00
7.06
6.09
ppm (f1)
174.471
160.312
155.730
150.075
139.315
133.117
129.883
128.785
127.801
126.827
126.204
121.591
114.710
113.429
113.293
104.660
63.388
47.488
47.460
31.777
19.259
14.645
13.589
ppm (f1)

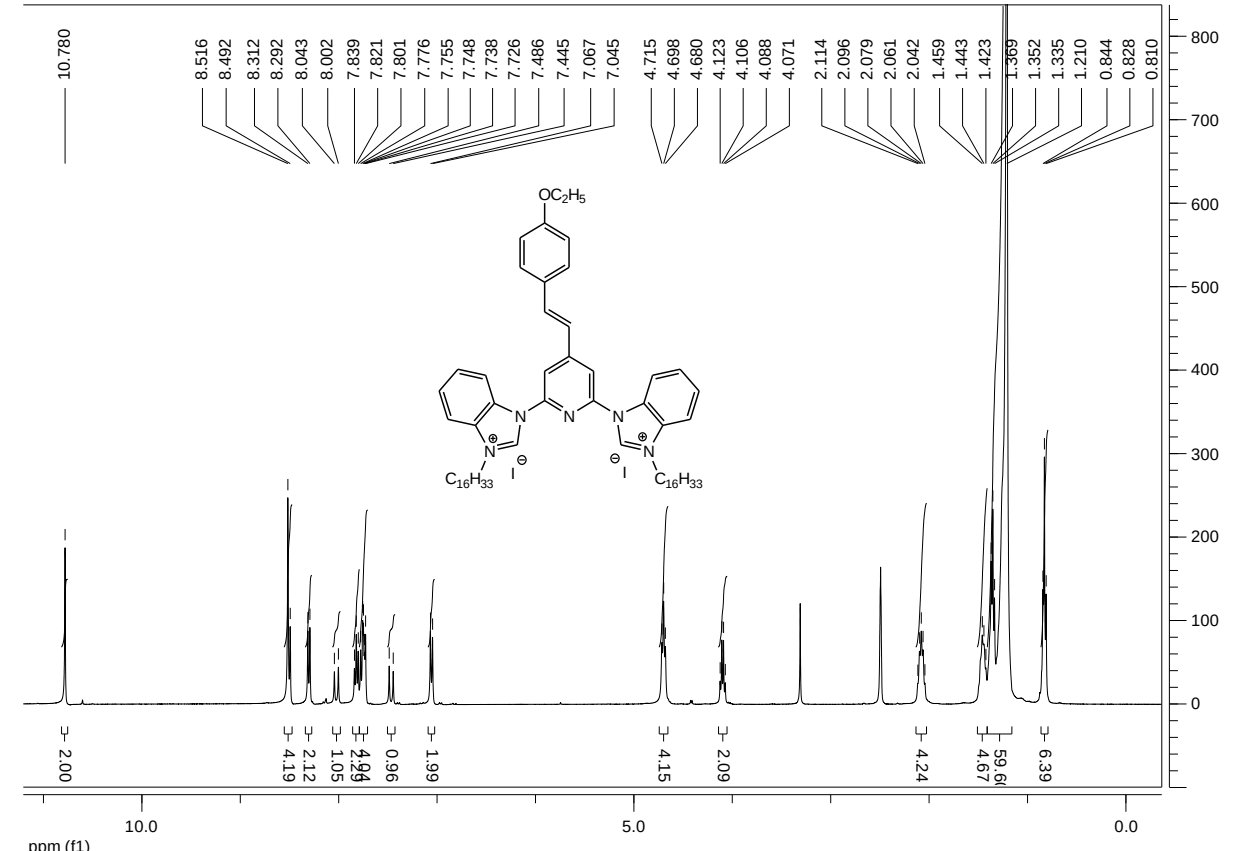
10.780
8.516
8.492
8.312
8.292
8.043
8.002
7.839
7.821
7.801
7.776
7.755
7.748
7.738
7.726
7.486
7.445
7.067
7.045
4.715
4.698
4.680
4.123
4.106
4.088
4.071
2.114
2.096
2.079
2.061
2.042
1.459
1.443
1.423
1.369
1.352
1.335
1.210
0.844
0.828
0.810
OC2H5
C16H33
C16H33
2.00
4.19
2.12
1.05
1.04
0.96
1.99
4.15
2.09
4.24
4.97
6.39
10.0
5.0
0.0
ppm (f1)

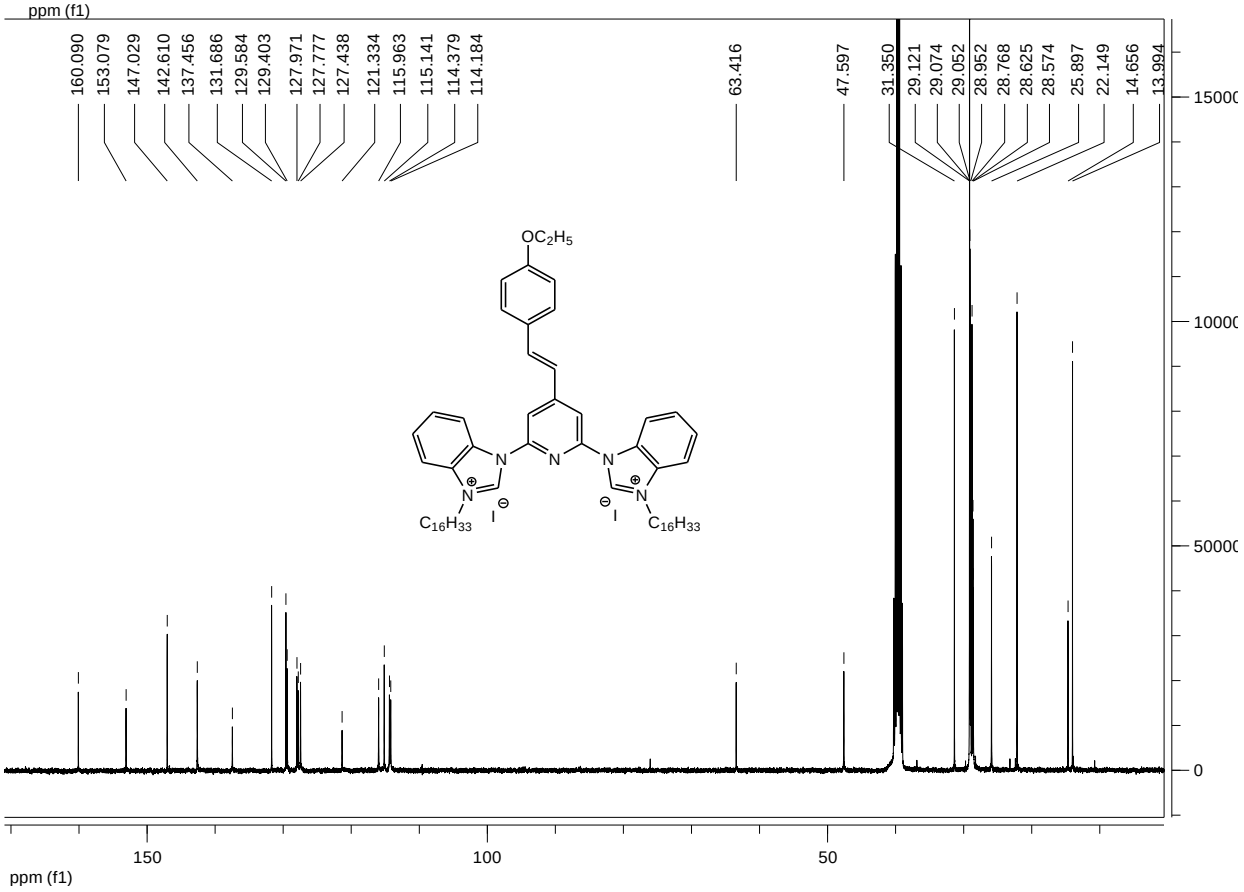
160.090
153.079
147.029
142.610
137.456
131.686
129.584
129.403
127.971
127.777
127.438
121.334
115.963
115.141
114.379
114.184
63.416
47.597
31.350
29.121
29.074
29.052
28.952
28.768
28.625
28.574
25.897
22.149
14.656
13.994
OC2H5
C16H33
C16H33
150
100
50
ppm (f1)

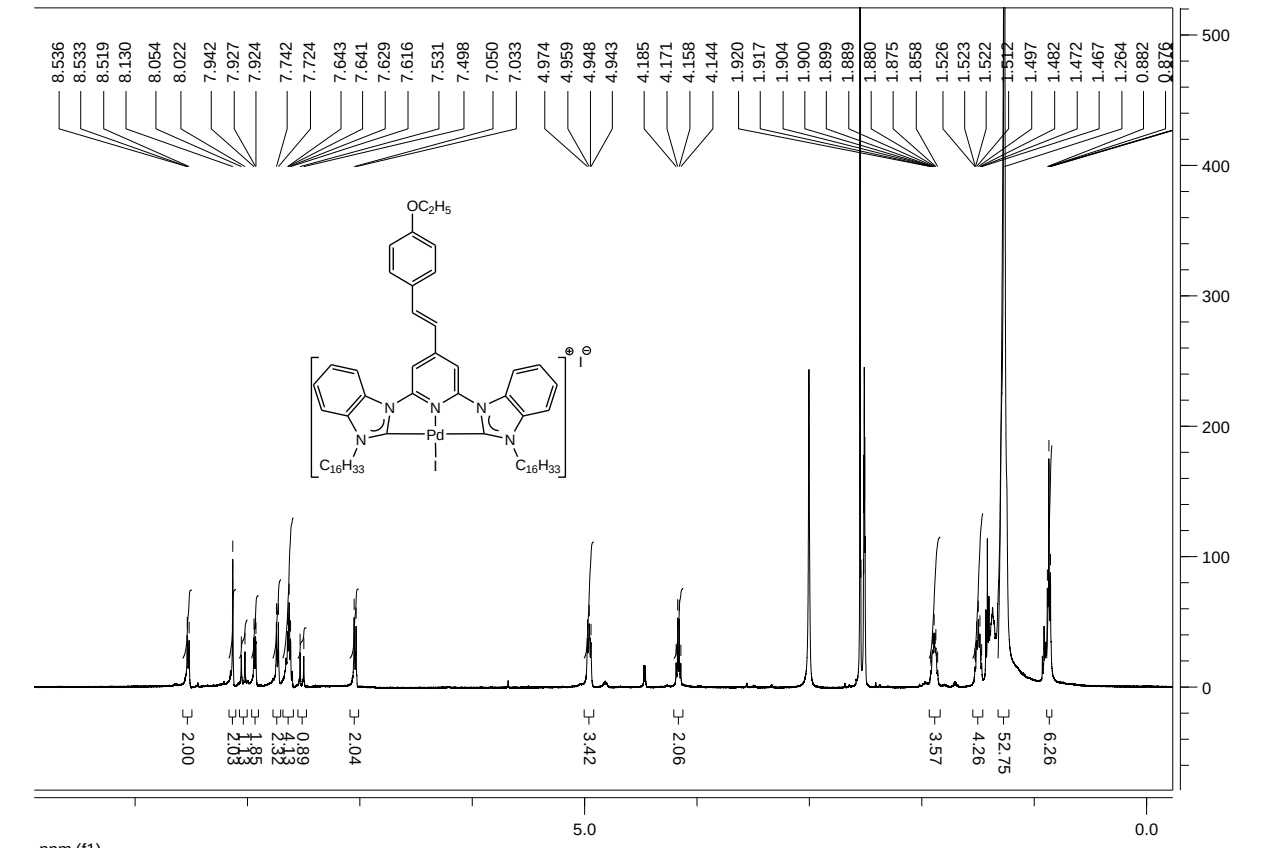
8.536
8.533
8.519
8.130
8.054
8.022
7.942
7.927
7.924
7.742
7.724
7.643
7.641
7.629
7.616
7.531
7.498
7.050
7.033
4.974
4.959
4.948
4.943
4.185
4.171
4.158
4.144
1.920
1.917
1.904
1.900
1.899
1.889
1.880
1.875
1.858
1.526
1.523
1.522
1.512
1.497
1.482
1.472
1.467
1.264
0.882
0.876
OC2H5
I
C16H33
Pd
2.00
2.03
1.85
4.33
0.89
2.04
3.42
2.06
3.57
4.26
52.75
9.26
5.0
0.0
ppm (f1)

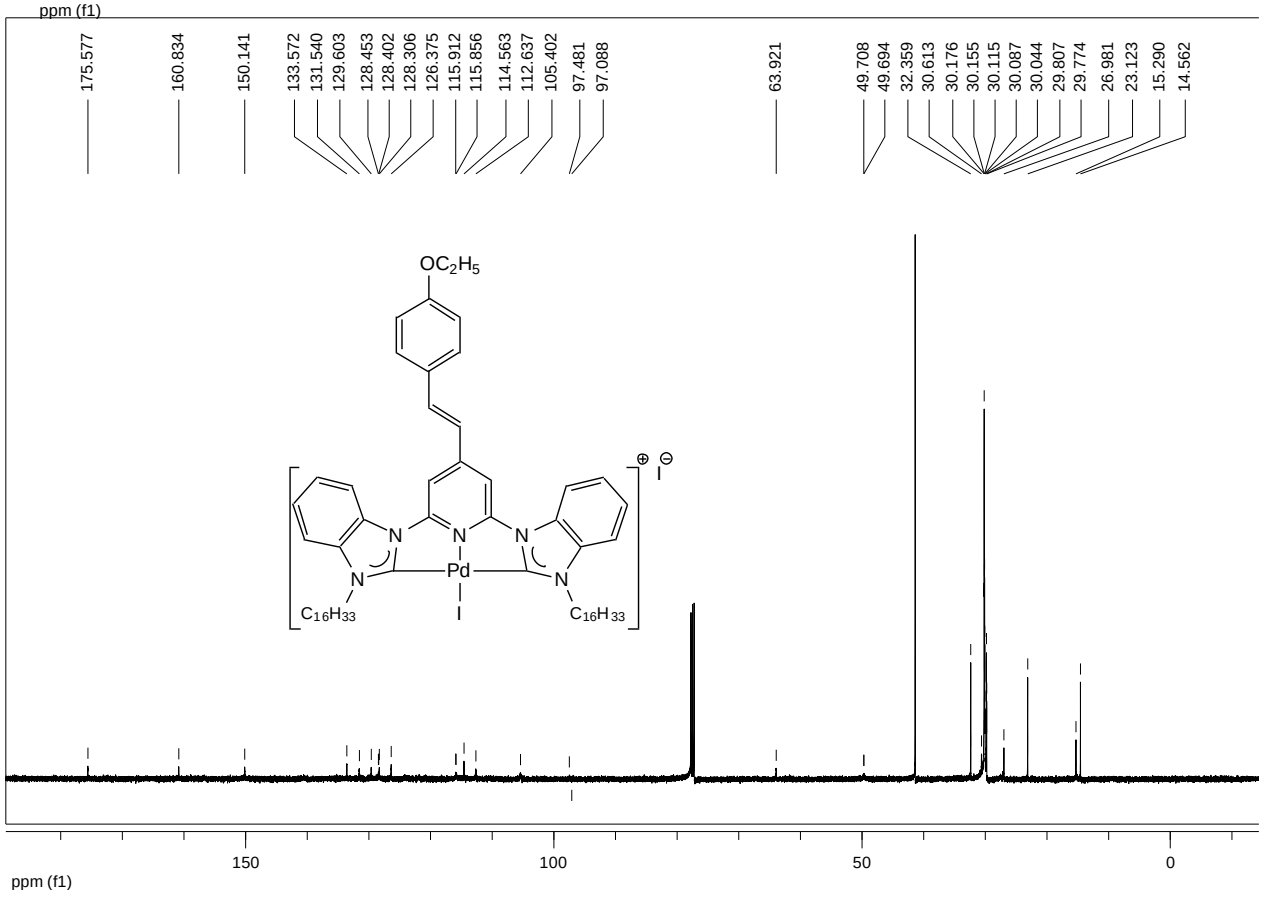
175.577
160.834
150.141
133.572
131.540
129.603
128.453
128.402
128.306
126.375
115.912
115.856
114.563
112.637
105.402
97.481
97.088
63.921
49.708
49.694
32.359
30.613
30.176
30.155
30.115
30.087
30.044
29.807
29.774
26.981
23.123
15.290
14.562
OC2H5
I
C16H33
Pd
150
100
50
0
ppm (f1)

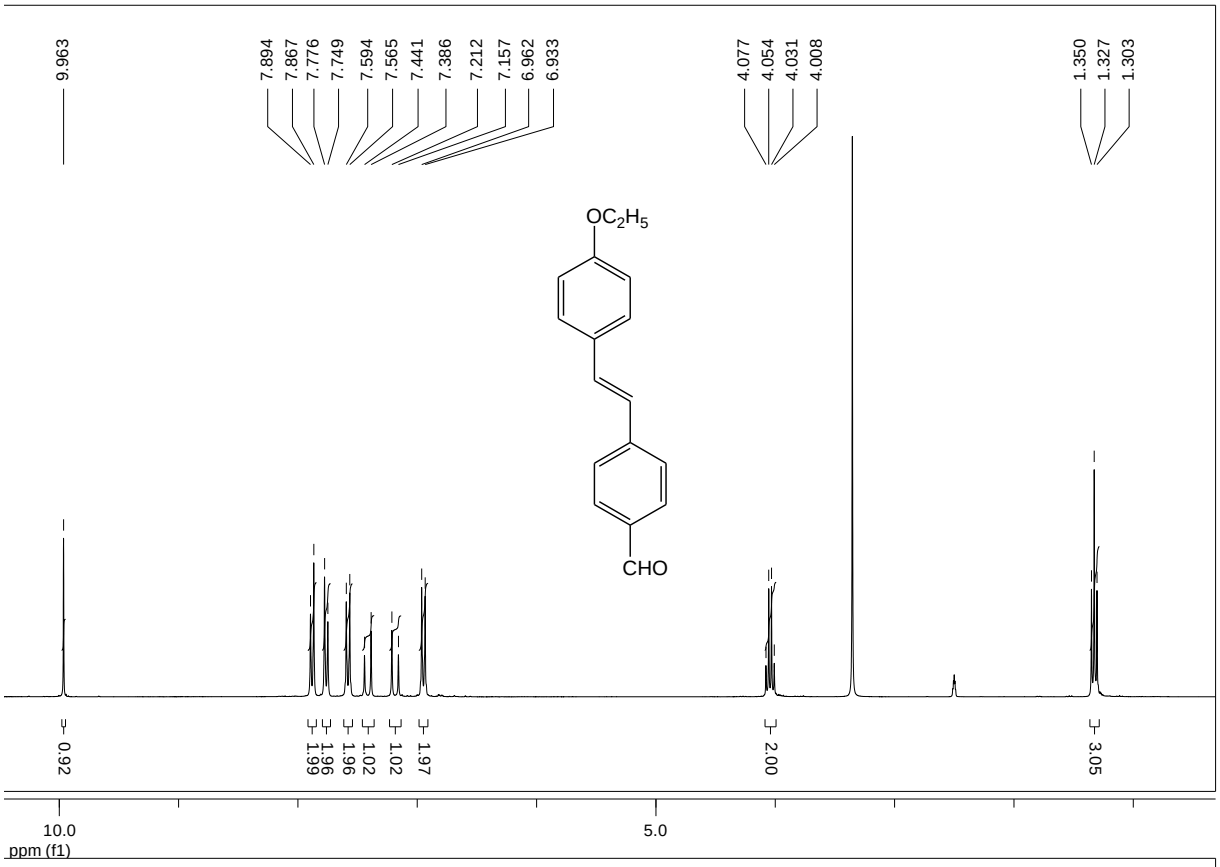
9.963
7.894
7.867
7.776
7.749
7.594
7.565
7.441
7.386
7.212
7.157
6.962
6.933
4.077
4.054
4.031
4.008
1.350
1.327
1.303
OC2H5
CHO
0.92
1.99
1.98
1.96
1.02
1.02
1.97
2.00
3.05
10.0
5.0
ppm (f1)

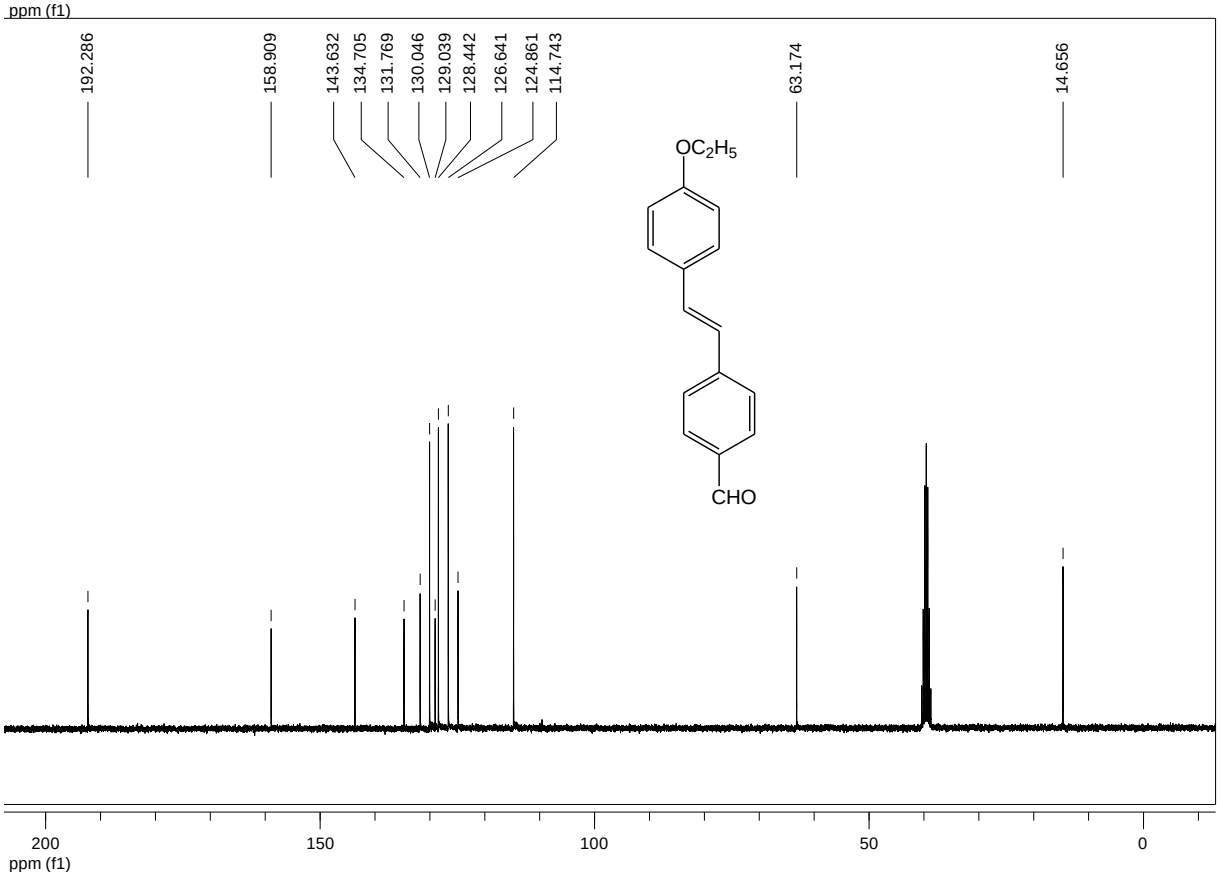
192.286
158.909
143.632
134.705
131.769
130.046
129.039
128.442
126.641
124.861
114.743
63.174
14.656
OC2H5
CHO
200
150
100
50
0
ppm (f1)

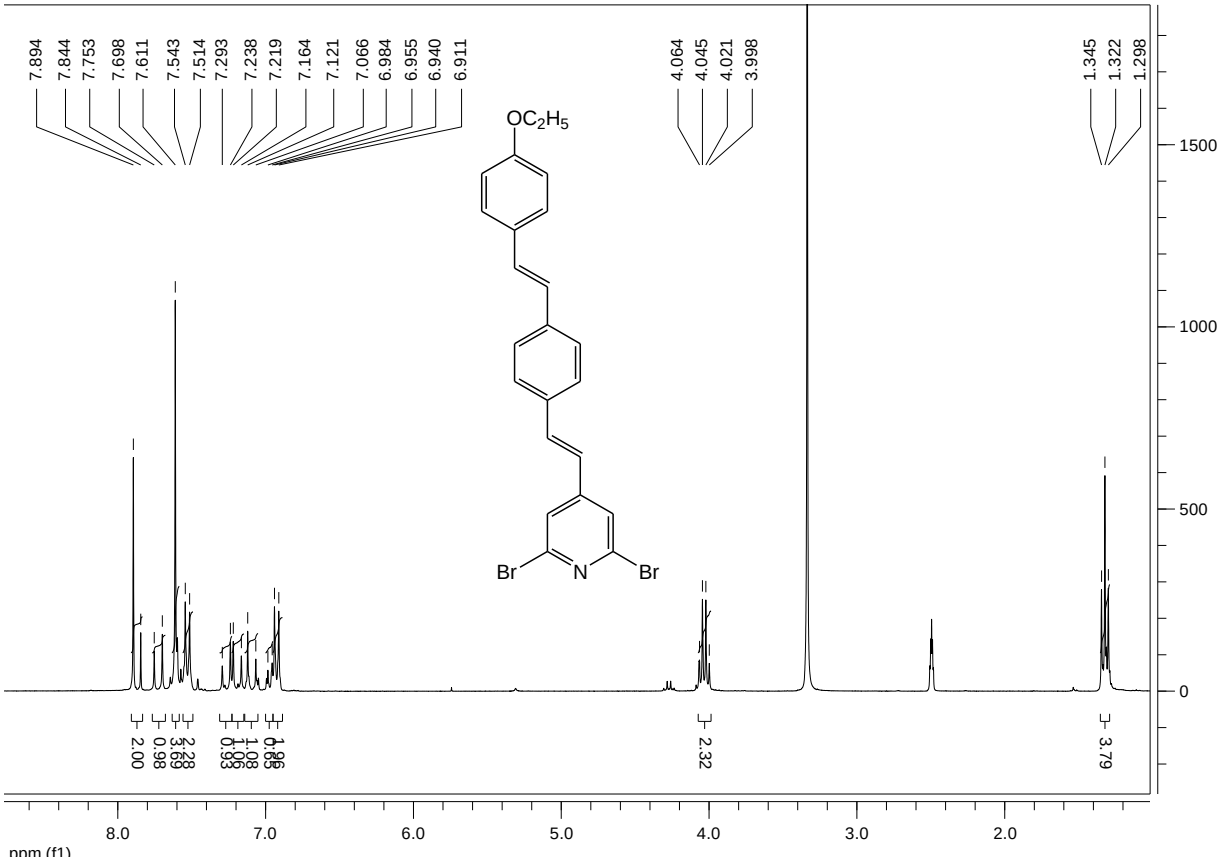
7.894
7.844
7.753
7.698
7.611
7.543
7.514
7.293
7.238
7.219
7.164
7.121
7.066
6.984
6.955
6.940
6.911
4.064
4.045
4.021
3.998
1.345
1.322
1.298
OC2H5
Br
N
Br
2.00
0.98
3.69
2.28
1.00
1.03
1.08
1.06
1.96
2.32
3.79
1500
1000
500
0
8.0
7.0
6.0
5.0
4.0
3.0
2.0
ppm (f1)

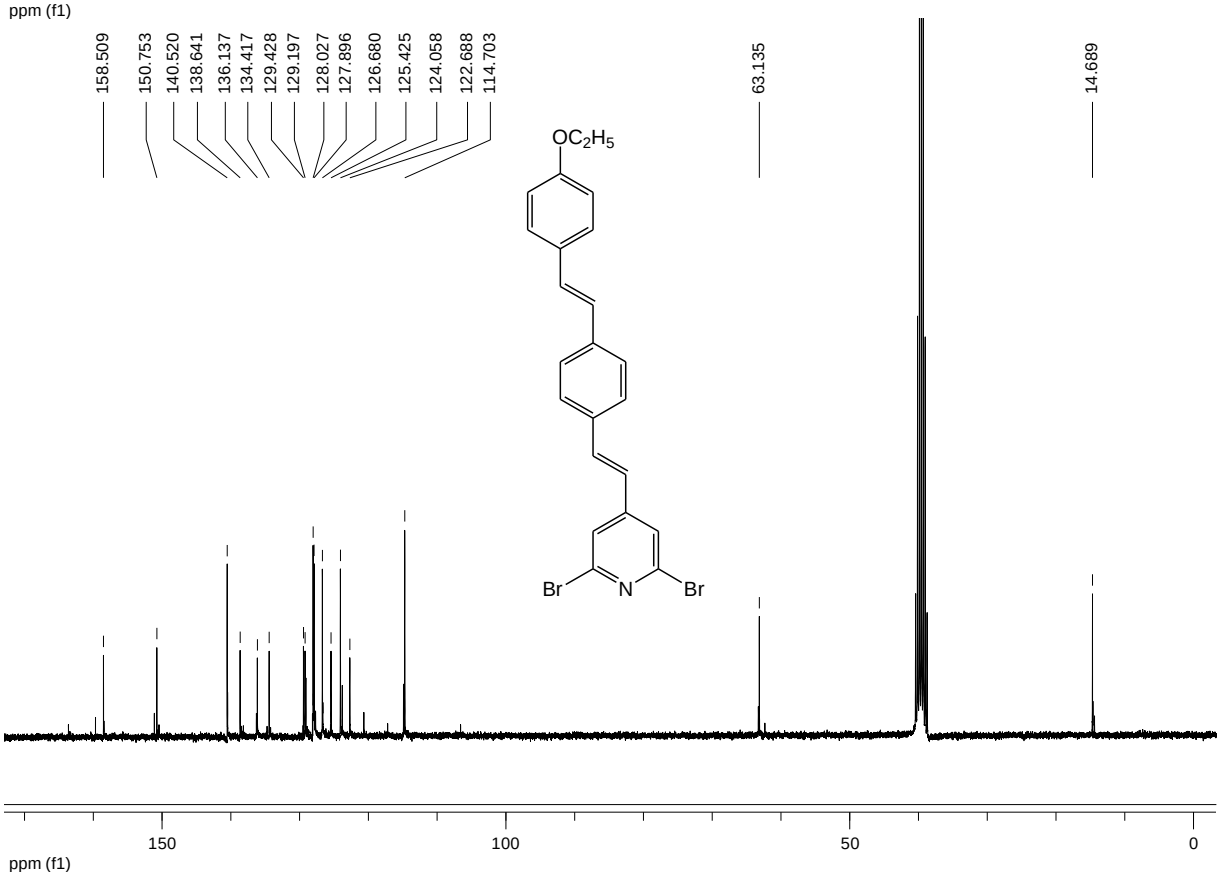
158.509
150.753
140.520
138.641
136.137
134.417
129.428
129.197
128.027
127.896
126.680
125.425
124.058
122.688
114.703
63.135
14.689
OC2H5
Br
N
Br
150
100
50
0
ppm (f1)

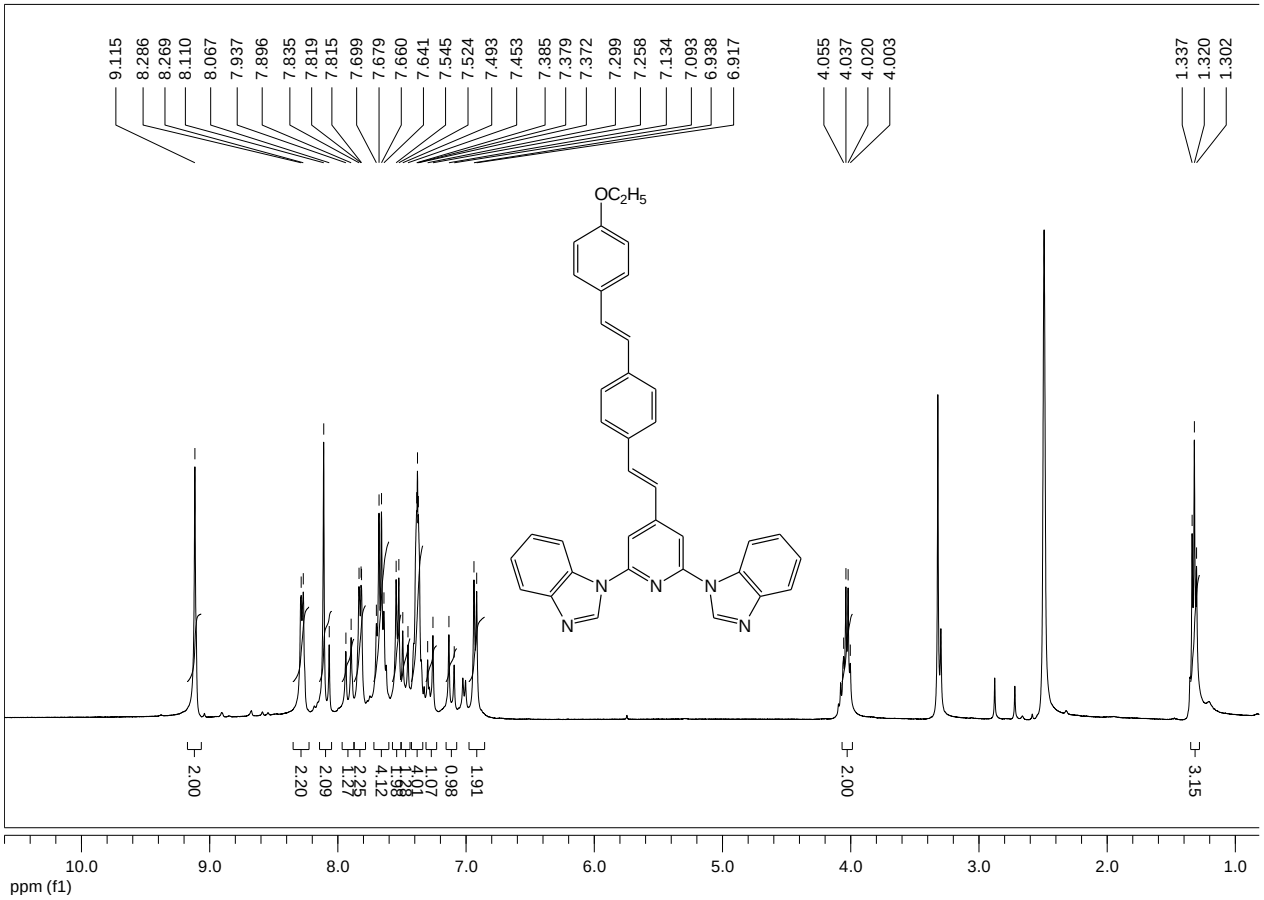
9.115
8.286
8.269
8.110
8.067
7.937
7.896
7.835
7.819
7.815
7.699
7.679
7.660
7.641
7.545
7.524
7.493
7.453
7.385
7.379
7.372
7.299
7.258
7.134
7.093
6.938
6.917
4.055
4.037
4.020
4.003
1.337
1.320
1.302
OC2H5
N
N
N
N
N
2.00
2.20
2.09
1.27
2.25
4.12
1.07
0.98
1.91
2.00
3.15
10.0
9.0
8.0
7.0
6.0
5.0
4.0
3.0
2.0
1.0
ppm (f1)

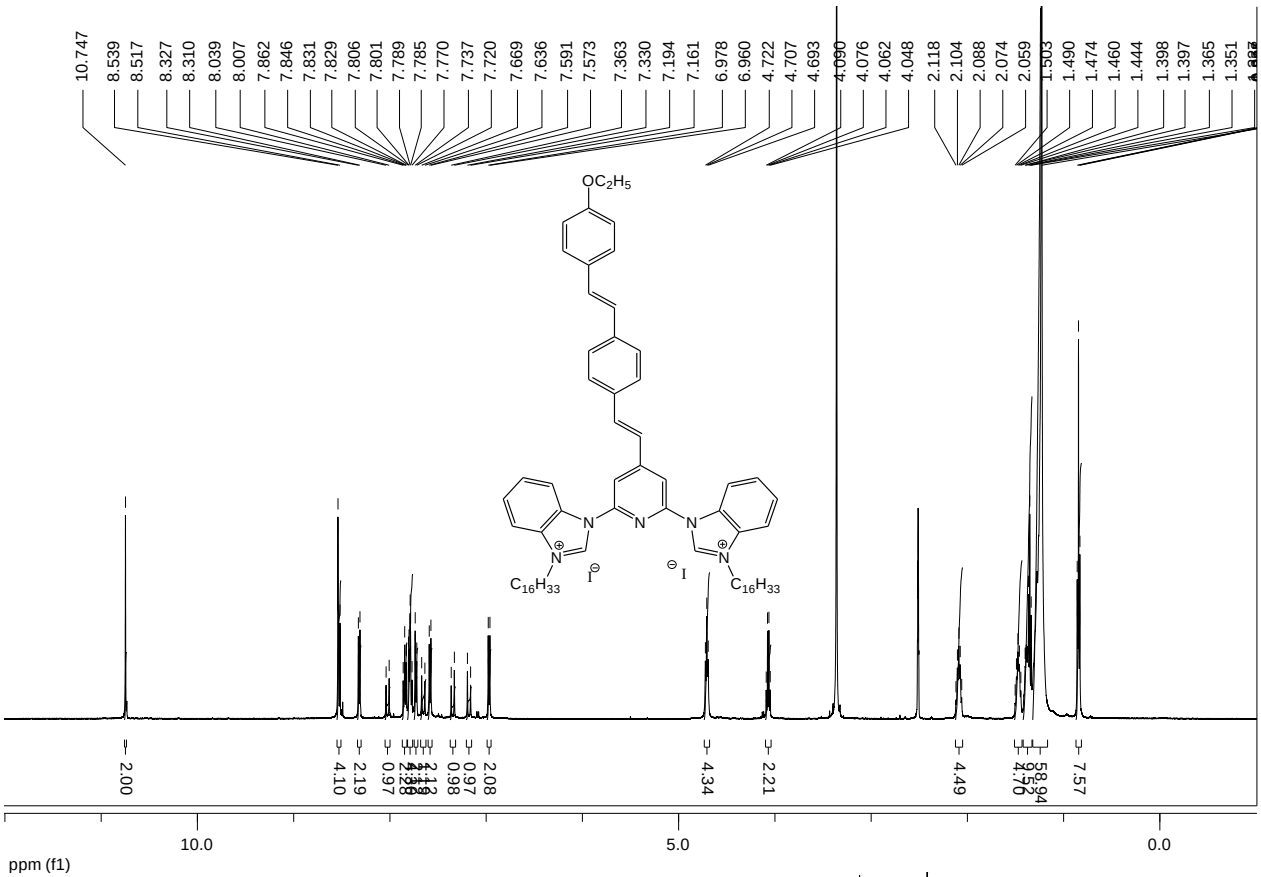
10.747
8.539
8.517
8.327
8.310
8.039
8.007
7.862
7.846
7.831
7.829
7.806
7.801
7.789
7.785
7.770
7.737
7.720
7.669
7.636
7.591
7.573
7.363
7.330
7.194
7.161
6.978
6.960
4.722
4.707
4.693
4.090
4.076
4.062
4.048
2.118
2.104
2.088
2.074
2.059
1.503
1.490
1.474
1.460
1.444
1.398
1.397
1.365
1.351
OC2H5
C16H33
C16H33
2.00
4.10
2.19
0.97
0.98
0.97
2.08
4.34
2.21
4.49
58.94
4.70
7.57
10.0
5.0
0.0
ppm (f1)

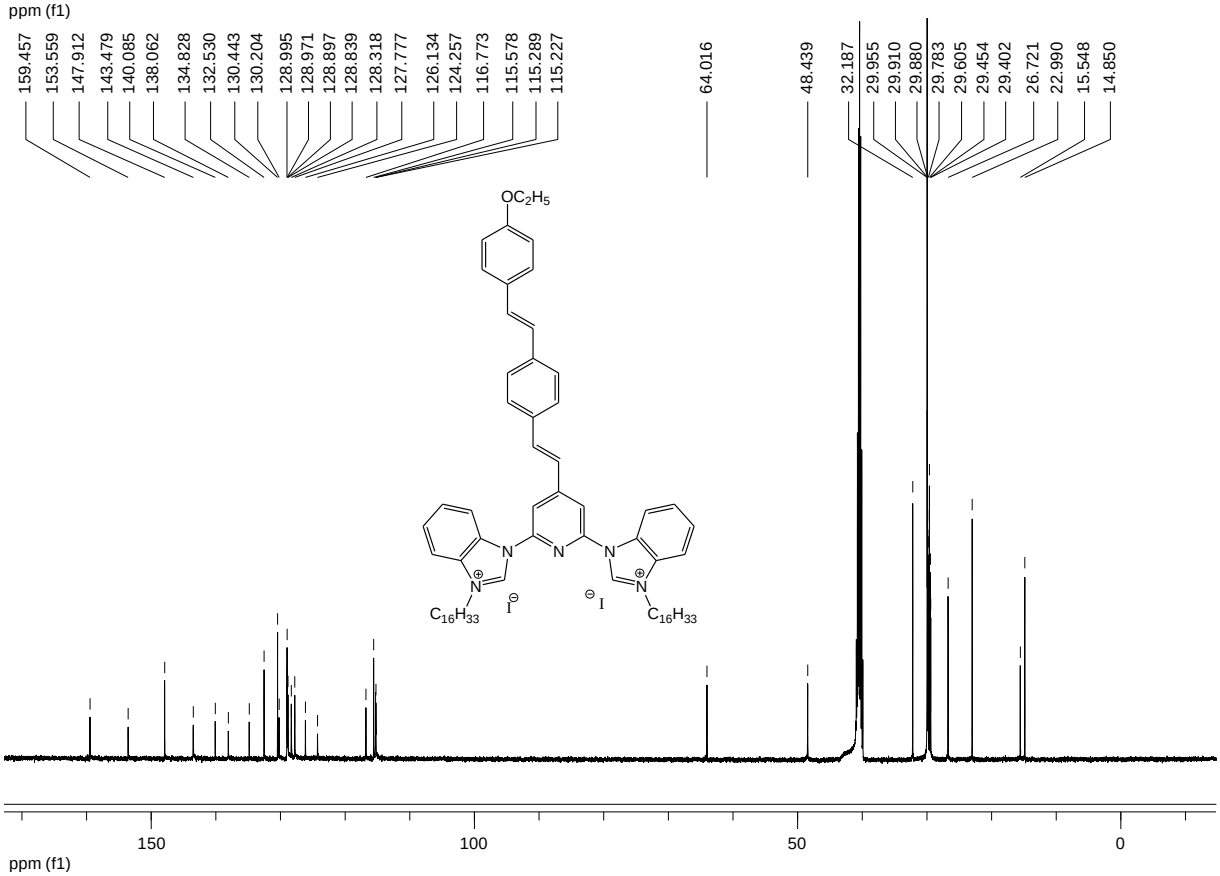
159.457
153.559
147.912
143.479
140.085
138.062
134.828
132.530
130.443
130.204
128.995
128.971
128.897
128.839
128.318
127.777
126.134
124.257
116.773
115.578
115.289
115.227
64.016
48.439
32.187
29.955
29.910
29.880
29.783
29.605
29.454
29.402
26.721
22.990
15.548
14.850
OC2H5
C16H33
C16H33
150
100
50
0
ppm (f1)

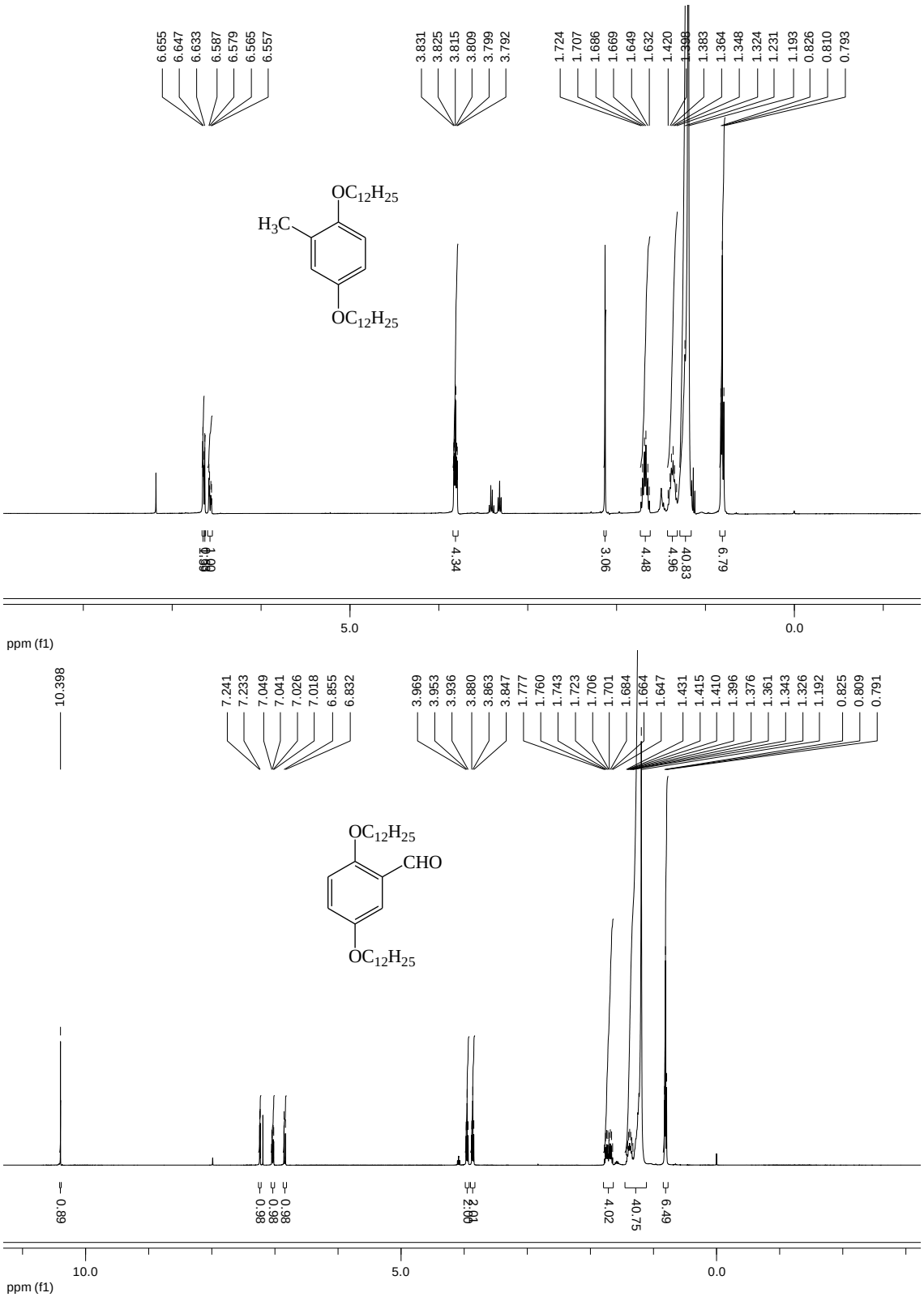
6.655
6.647
6.633
6.587
6.579
6.565
6.557
3.831
3.825
3.815
3.809
3.799
3.792
1.724
1.707
1.686
1.669
1.649
1.632
1.420
1.398
1.383
1.364
1.348
1.324
1.231
1.193
0.826
0.810
0.793
OC12H25
H3C
OC12H25
4.34
3.06
4.48
40.83
4.96
9.79
5.0
0.0
ppm (f1)
10.398
7.241
7.233
7.049
7.041
7.026
7.018
6.855
6.832
3.969
3.953
3.936
3.880
3.863
3.847
1.777
1.760
1.743
1.723
1.706
1.701
1.684
1.664
1.647
1.431
1.415
1.410
1.396
1.376
1.361
1.343
1.326
1.192
0.825
0.809
0.791
OC12H25
CHO
OC12H25
0.89
0.98
0.98
0.98
2.00
4.02
40.75
6.49
10.0
5.0
0.0
ppm (f1)

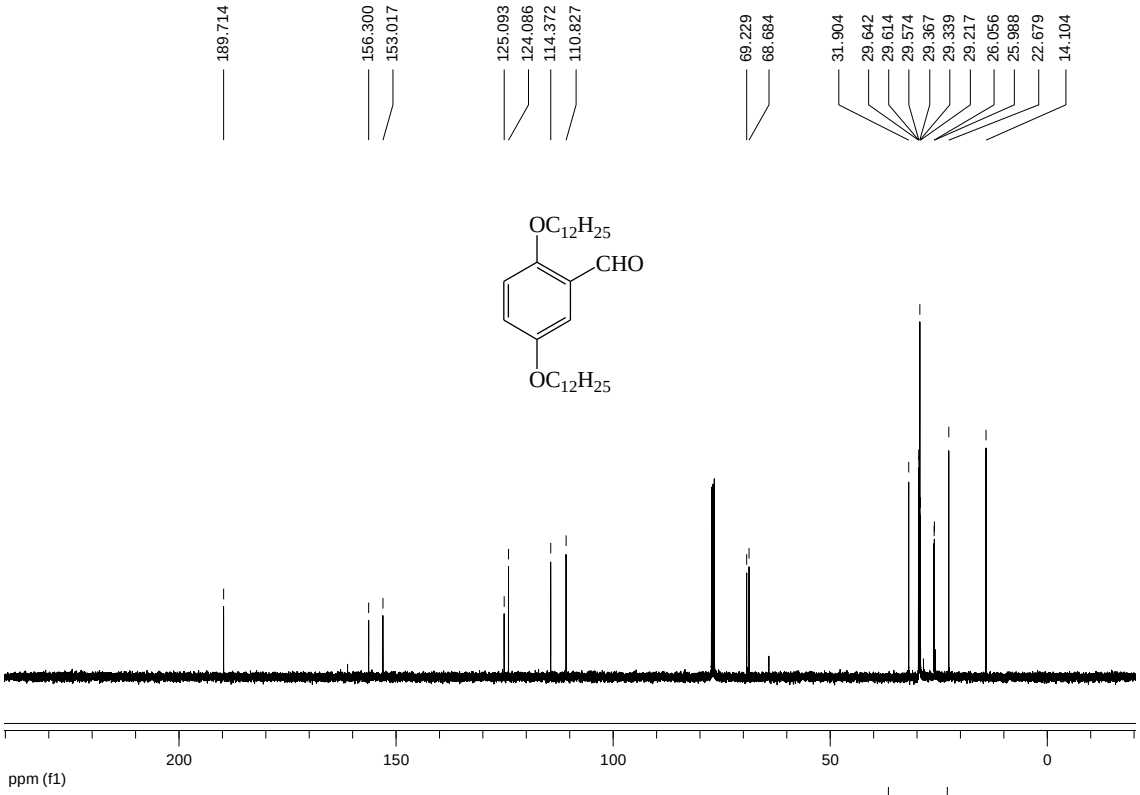
189.714
156.300
153.017
125.093
124.086
114.372
110.827
69.229
68.684
31.904
29.642
29.614
29.574
29.367
29.339
29.217
26.056
25.988
22.679
14.104
OC12H25
CHO
OC12H25
200
150
100
50
0
ppm (f1)

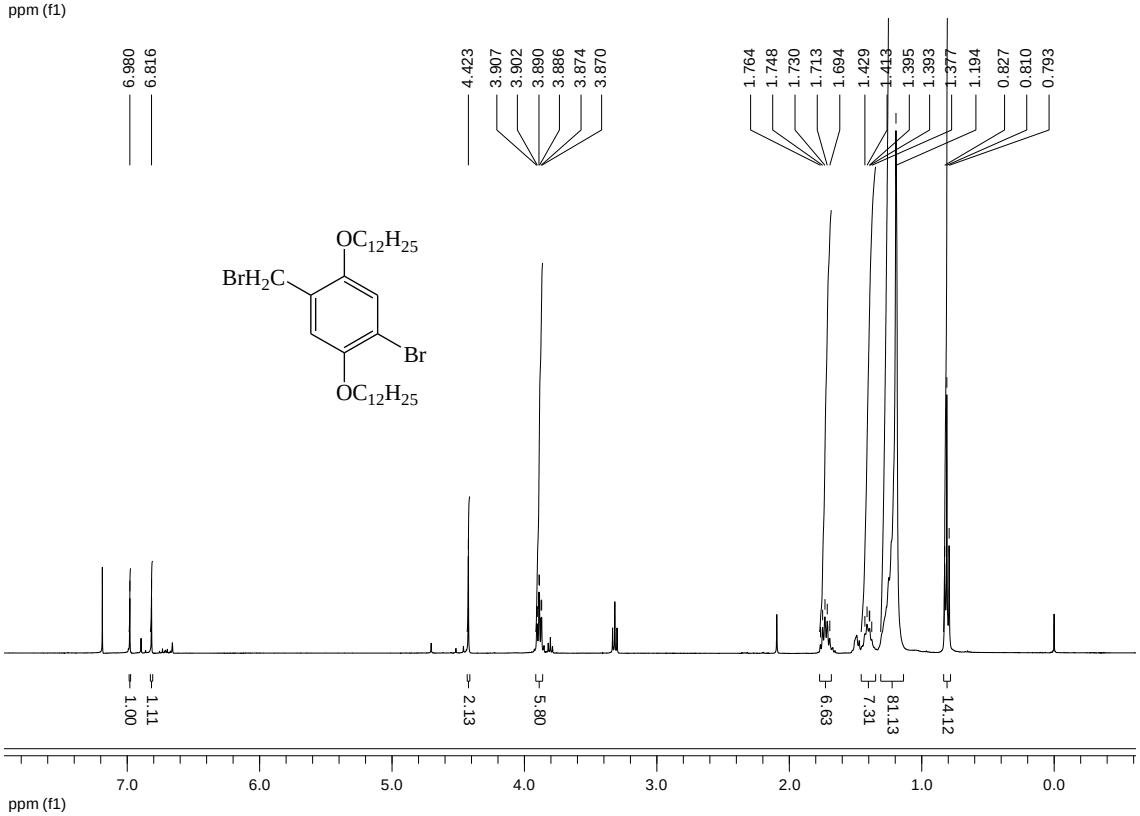
6.980
6.816
4.423
3.907
3.902
3.890
3.886
3.874
3.870
1.764
1.748
1.730
1.713
1.694
1.429
1.413
1.395
1.393
1.377
1.194
0.827
0.810
0.793
OC12H25
BrH2C
Br
OC12H25
1.00
1.11
2.13
5.80
6.63
7.31
81.13
14.12
7.0
6.0
5.0
4.0
3.0
2.0
1.0
0.0
ppm (f1)

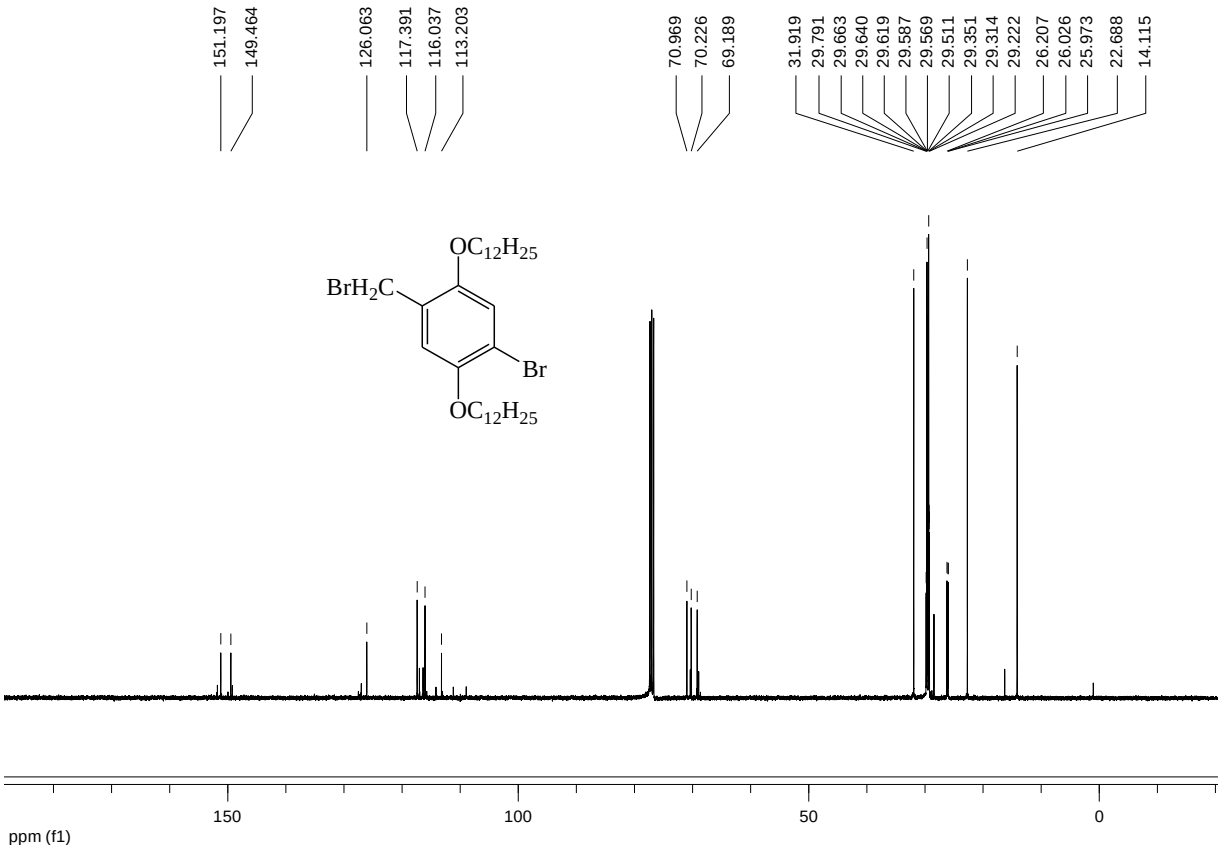
151.197
149.464
126.063
117.391
116.037
113.203
70.969
70.226
69.189
31.919
29.791
29.663
29.640
29.619
29.587
29.569
29.511
29.351
29.314
29.222
26.207
26.026
25.973
22.688
14.115
OC12H25
BrH2C
Br
OC12H25
150
100
50
0
ppm (f1)

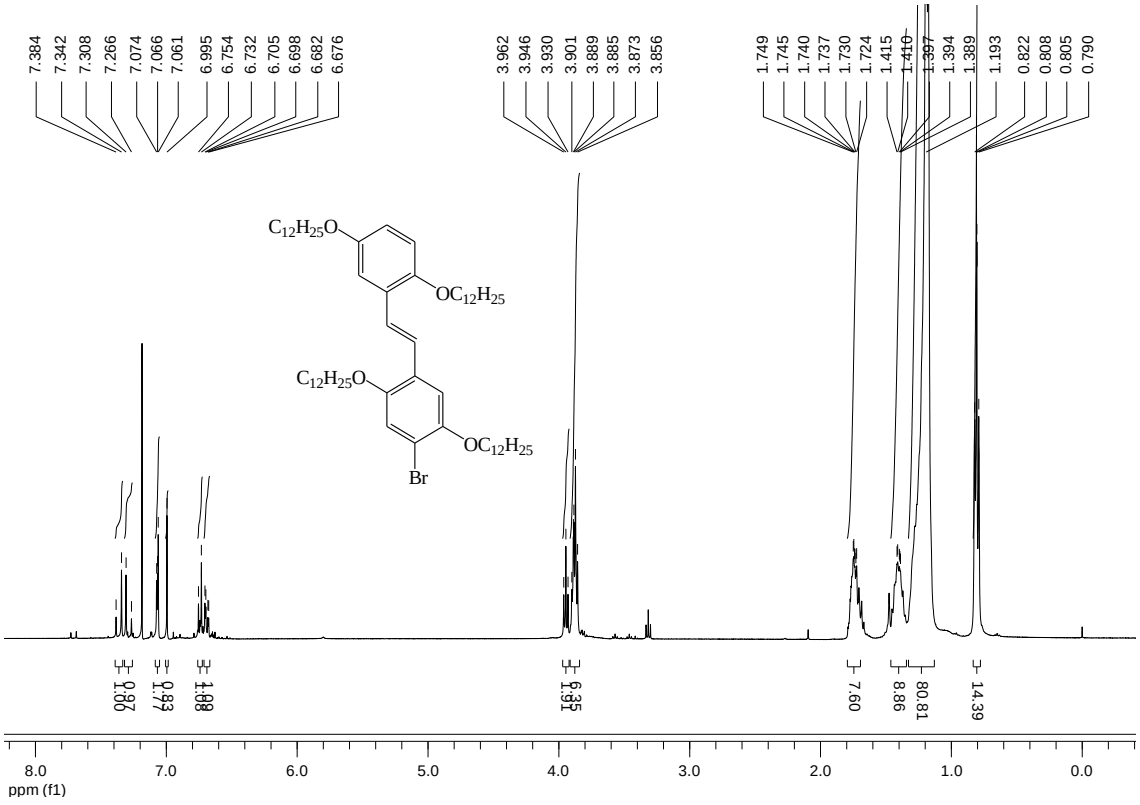
7.384
7.342
7.308
7.266
7.074
7.066
7.061
6.995
6.754
6.732
6.705
6.698
6.682
6.676
3.962
3.946
3.930
3.901
3.889
3.885
3.873
3.856
1.749
1.745
1.740
1.737
1.730
1.724
1.415
1.410
1.397
1.394
1.389
1.193
0.822
0.808
0.805
0.790
C12H25O
OC12H25
C12H25O
OC12H25
Br
1.00
0.87
1.73
1.08
1.08
1.91
6.35
7.60
8.86
8.08
14.39
8.0
7.0
6.0
5.0
4.0
3.0
2.0
1.0
0.0
ppm (f1)

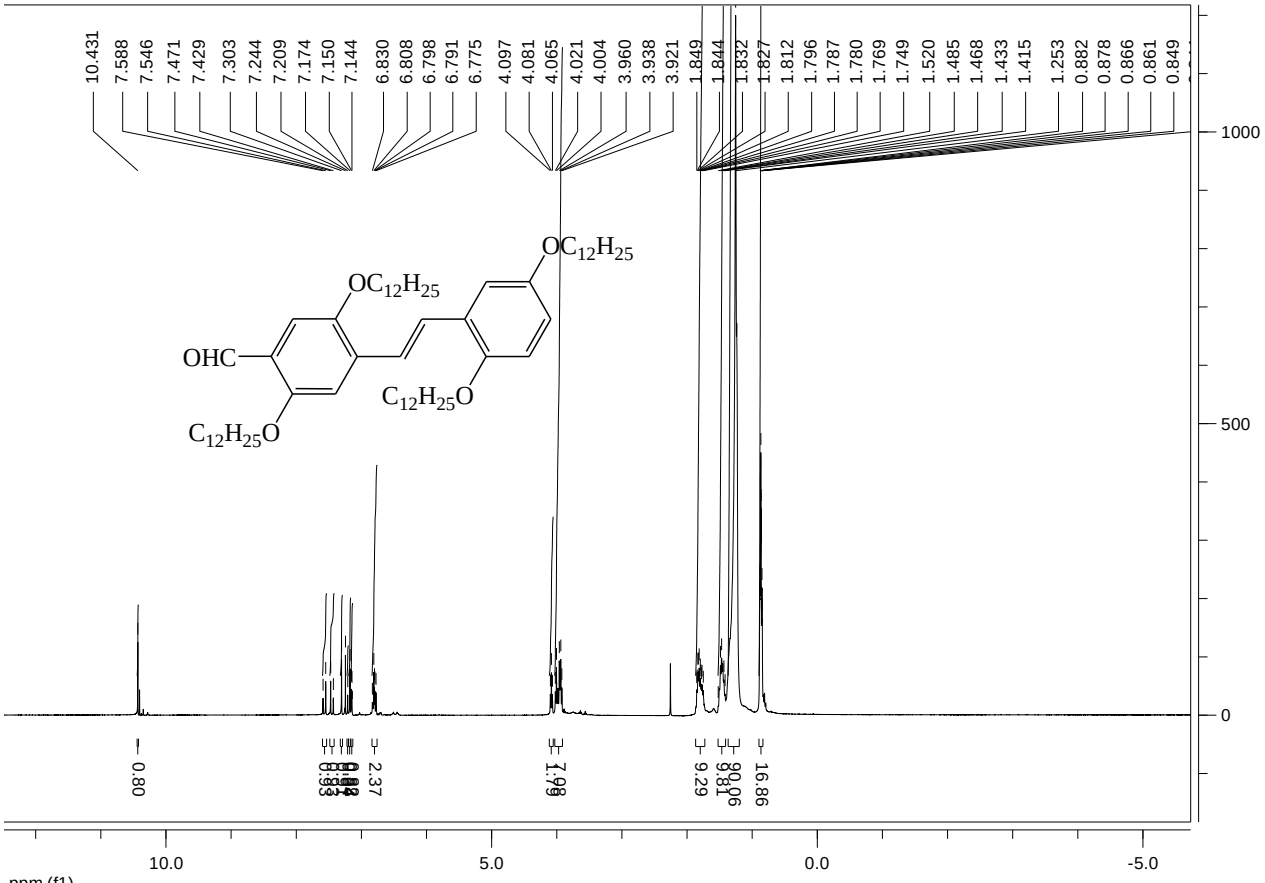
10.431
7.588
7.546
7.471
7.429
7.303
7.244
7.209
7.174
7.150
7.144
6.830
6.808
6.798
6.791
6.775
4.097
4.081
4.065
4.021
4.004
3.960
3.938
3.921
1.849
1.844
1.832
1.827
1.812
1.796
1.787
1.780
1.769
1.749
1.520
1.485
1.468
1.433
1.415
1.253
0.882
0.878
0.866
0.861
0.849
OC12H25
OC12H25
OHC
C12H25O
C12H25O
0.80
2.37
7.98
9.29
16.86
1000
500
0
10.0
5.0
0.0
-5.0
ppm (f1)

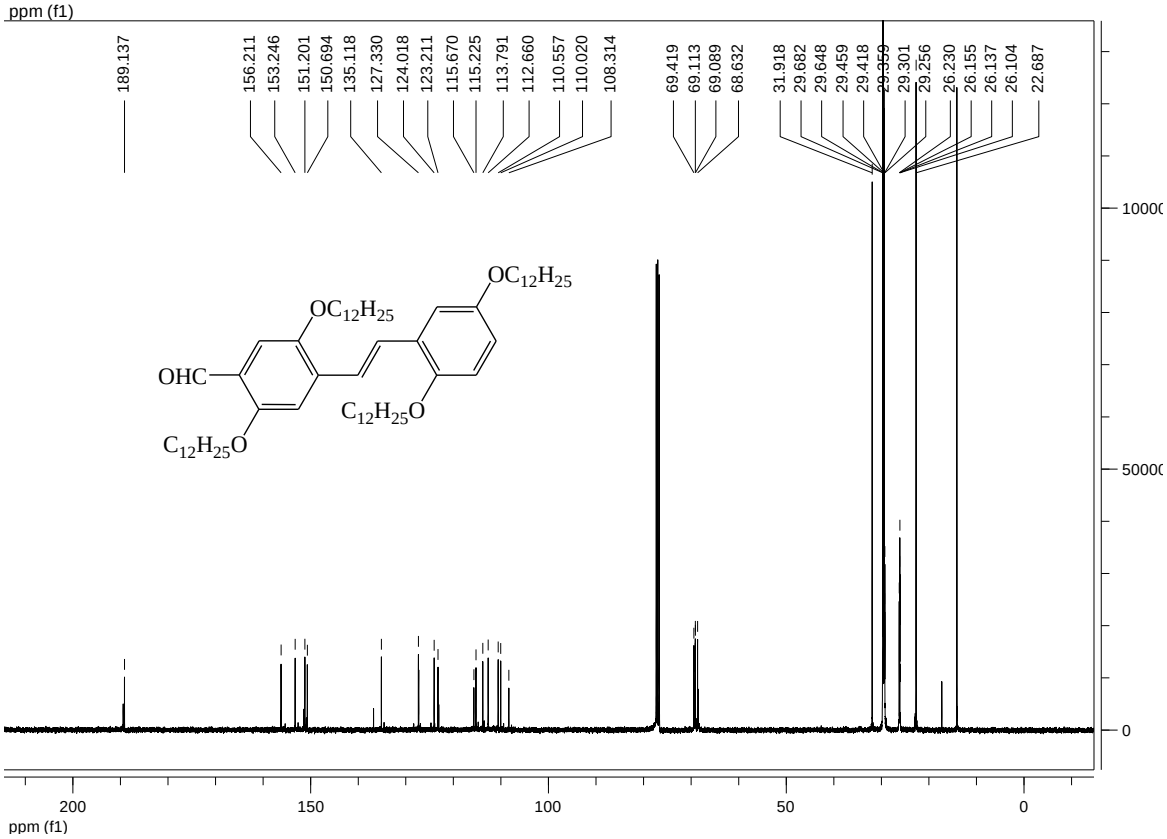
189.137
156.211
153.246
151.201
150.694
135.118
127.330
124.018
123.211
115.670
115.225
113.791
112.660
110.557
110.020
108.314
69.419
69.113
69.089
68.632
31.918
29.682
29.648
29.459
29.418
29.359
29.301
29.256
26.230
26.155
26.137
26.104
22.687
OC12H25
OC12H25
OHC
C12H25O
C12H25O
10000
5000
0
200
150
100
50
0
ppm (f1)

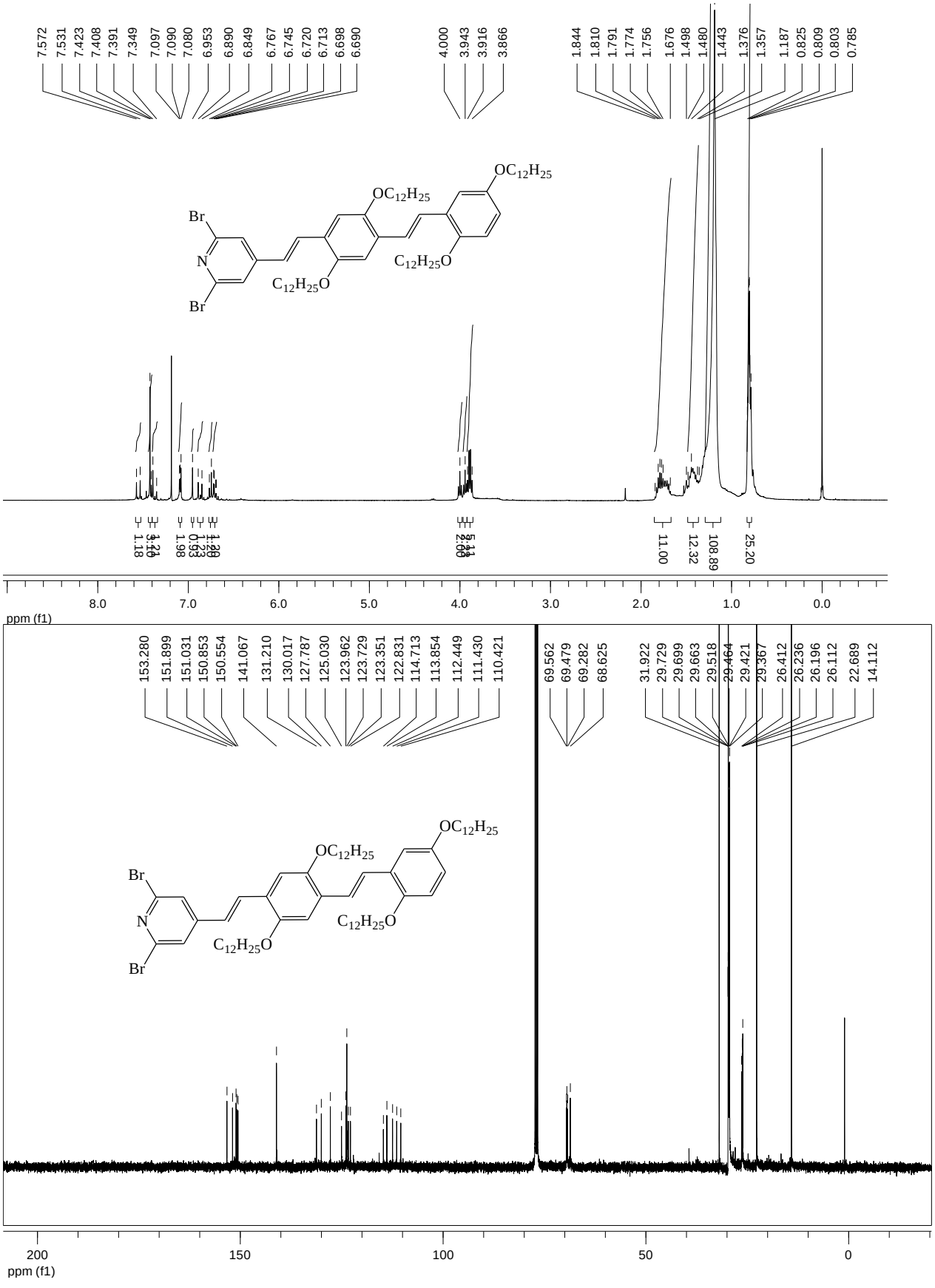
7.572
7.531
7.423
7.408
7.391
7.349
7.097
7.090
7.080
6.953
6.890
6.849
6.767
6.745
6.720
6.713
6.698
6.690
4.000
3.943
3.916
3.866
1.844
1.810
1.791
1.774
1.756
1.676
1.498
1.480
1.443
1.376
1.357
1.187
0.825
0.809
0.803
0.785
OC12H25
OC12H25
Br
N
C12H25O
C12H25O
Br
1.18
3.12
1.98
0.63
0.63
1.20
5.11
2.00
11.00
12.32
108.89
25.20
8.0
7.0
6.0
5.0
4.0
3.0
2.0
1.0
0.0
ppm (f1)
153.280
151.899
151.031
150.853
150.554
141.067
131.210
130.017
127.787
125.030
123.962
123.729
123.351
122.831
114.713
113.854
112.449
111.430
110.421
69.562
69.479
69.282
68.625
31.922
29.729
29.699
29.663
29.518
29.464
29.421
29.367
26.412
26.236
26.196
26.112
22.689
14.112
OC12H25
OC12H25
Br
N
C12H25O
C12H25O
Br
200
150
100
50
0
ppm (f1)

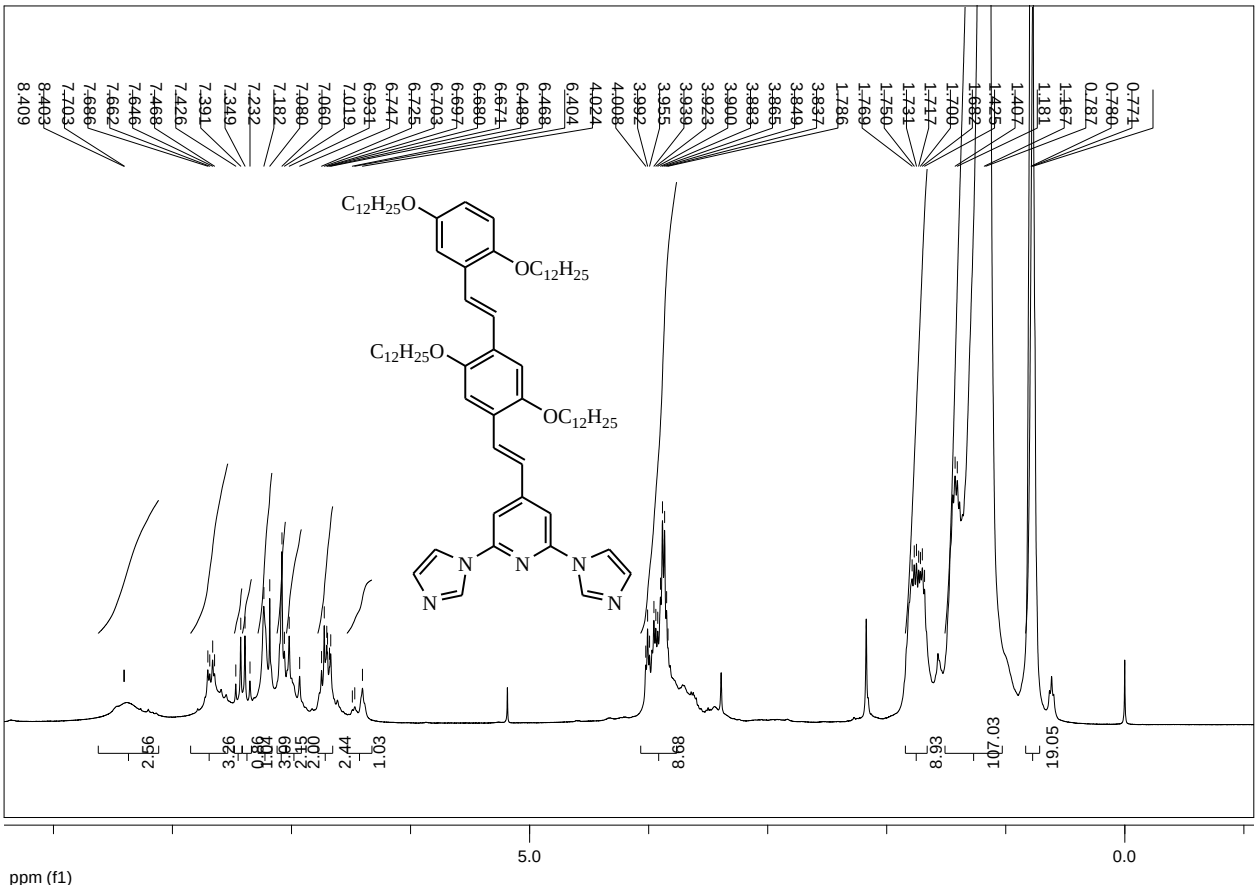
8.409
8.403
7.703
7.686
7.662
7.646
7.468
7.426
7.391
7.349
7.232
7.182
7.080
7.060
7.019
6.931
6.747
6.725
6.703
6.697
6.680
6.671
6.489
6.468
6.404
4.024
4.008
3.992
3.955
3.939
3.923
3.900
3.883
3.865
3.849
3.837
1.786
1.769
1.750
1.731
1.717
1.700
1.682
1.425
1.407
1.181
1.167
0.787
0.780
0.771
C12H25O
OC12H25
C12H25O
OC12H25
N
N
N
N
N
2.56
3.26
0.86
1.04
3.99
2.15
2.00
2.44
1.03
8.68
8.93
17.03
19.05
5.0
0.0
ppm (f1)

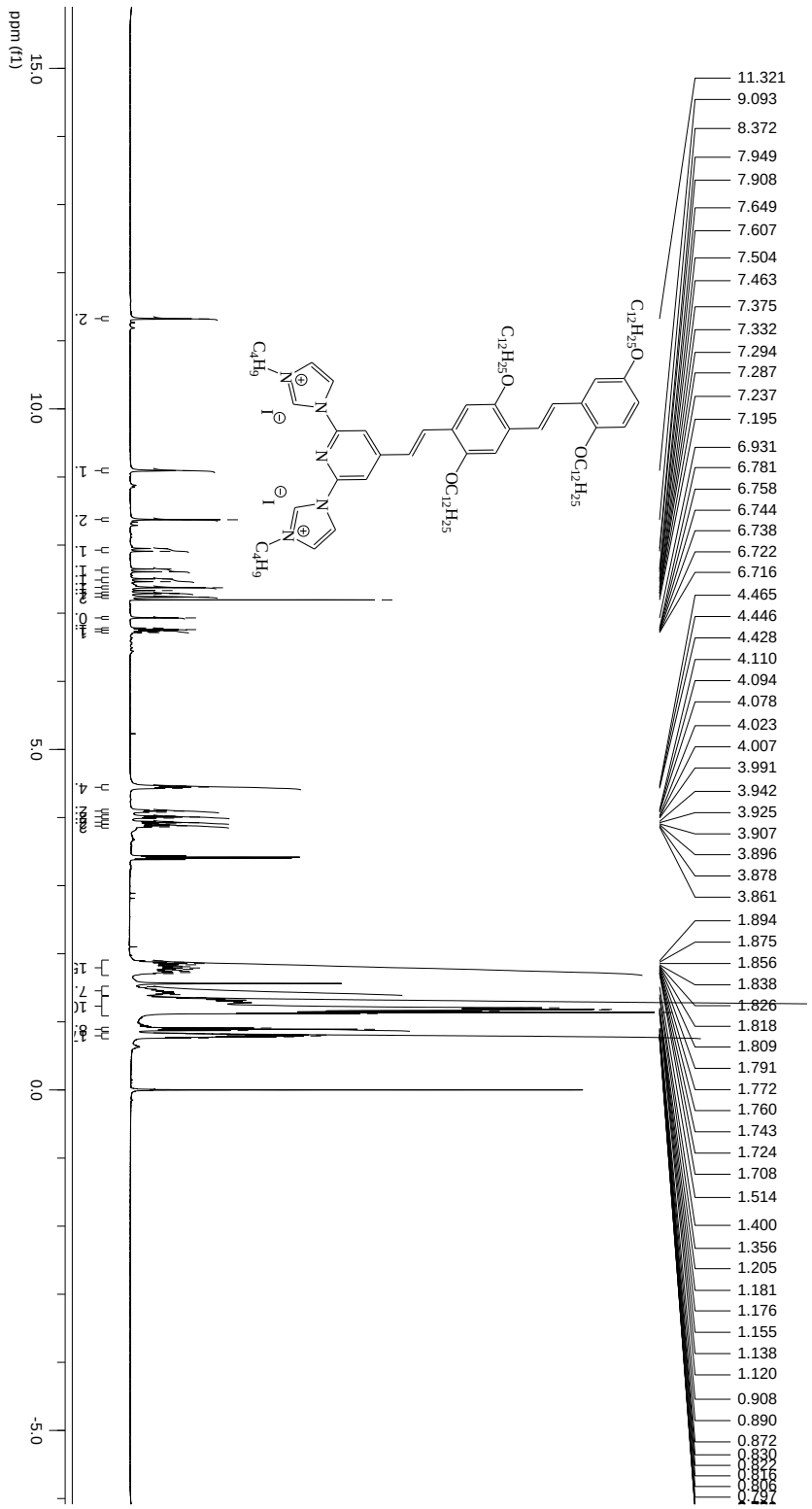
ppm (f1)
15.0
10.0
5.0
0.0
-5.0
11.321
9.093
8.372
7.949
7.908
7.649
7.607
7.504
7.463
7.375
7.332
7.294
7.287
7.237
7.195
6.931
6.781
6.758
6.744
6.738
6.722
6.716
4.465
4.446
4.428
4.110
4.094
4.078
4.023
4.007
3.991
3.942
3.925
3.907
3.896
3.878
3.861
1.894
1.875
1.856
1.838
1.826
1.818
1.809
1.791
1.772
1.760
1.743
1.724
1.708
1.514
1.400
1.356
1.205
1.181
1.176
1.155
1.138
1.120
0.908
0.890
0.872
0.830
0.822
0.816
0.806
0.797
C12H25O
OC12H25
C12H25O
OC12H25
C4H9
C4H9
N
I

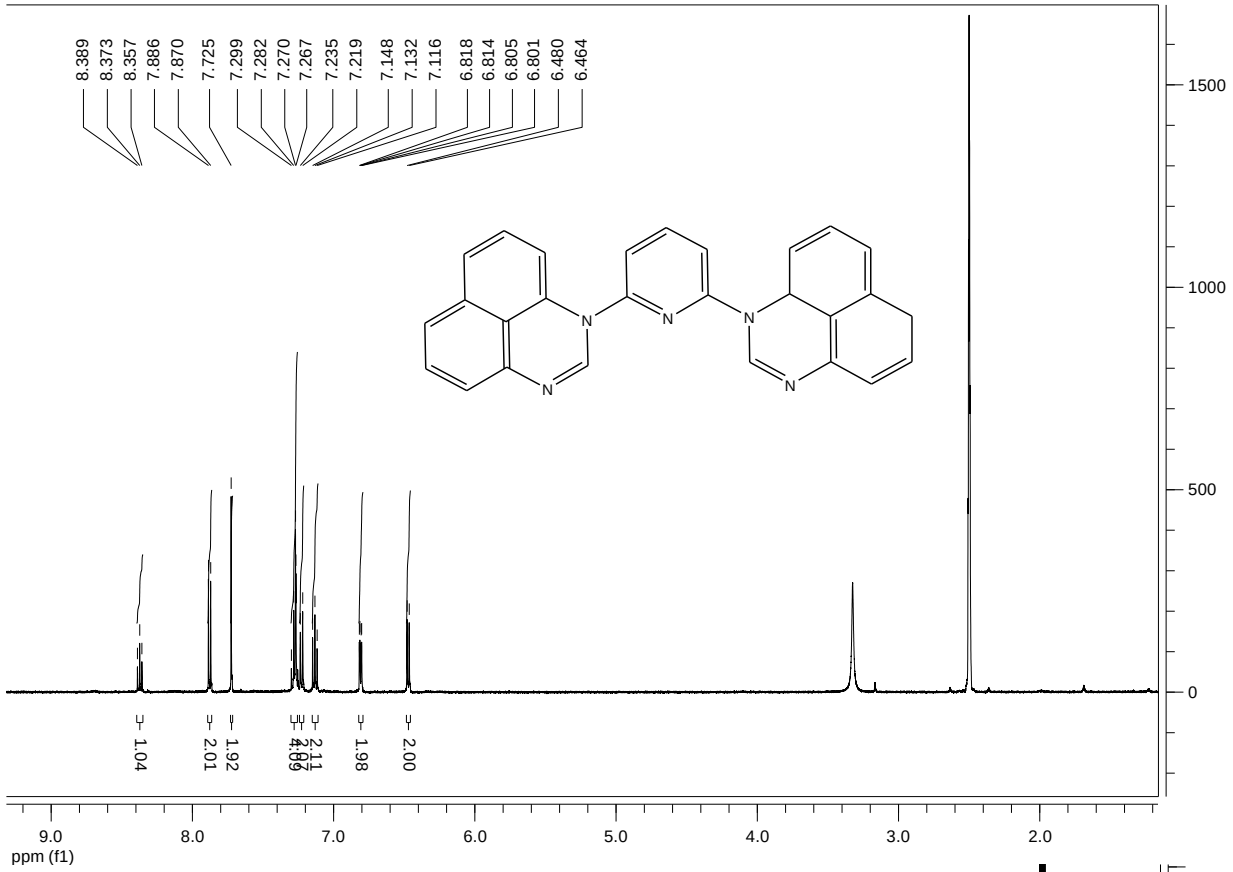
8.389
8.373
8.357
7.886
7.870
7.725
7.299
7.282
7.270
7.267
7.235
7.219
7.148
7.132
7.116
6.818
6.814
6.805
6.801
6.480
6.464
1.04
2.01
1.92
4.00
2.11
1.98
2.00
1500
1000
500
0
9.0
8.0
7.0
6.0
5.0
4.0
3.0
2.0
ppm (f1)

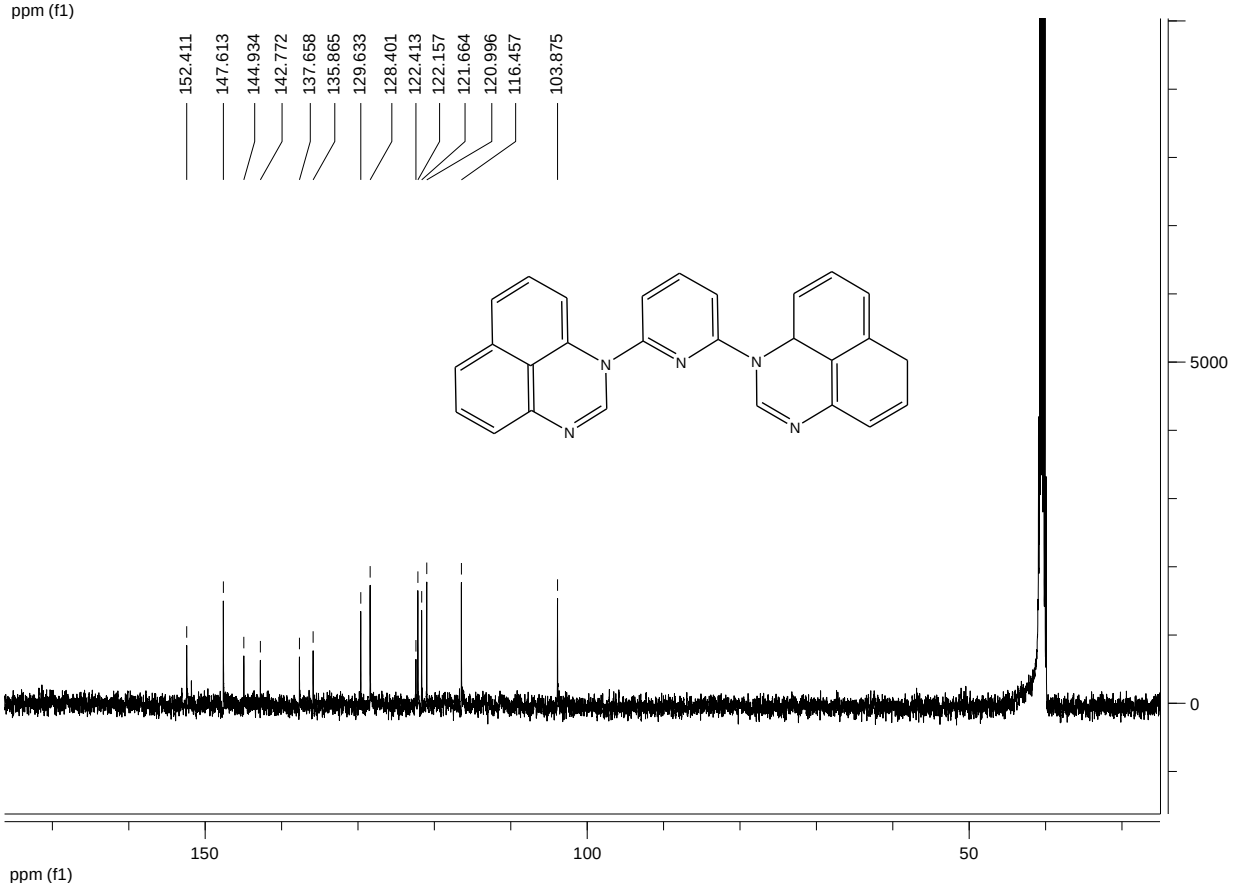
152.411
147.613
144.934
142.772
137.658
135.865
129.633
128.401
122.413
122.157
121.664
120.996
116.457
103.875
5000
0
150
100
50
ppm (f1)

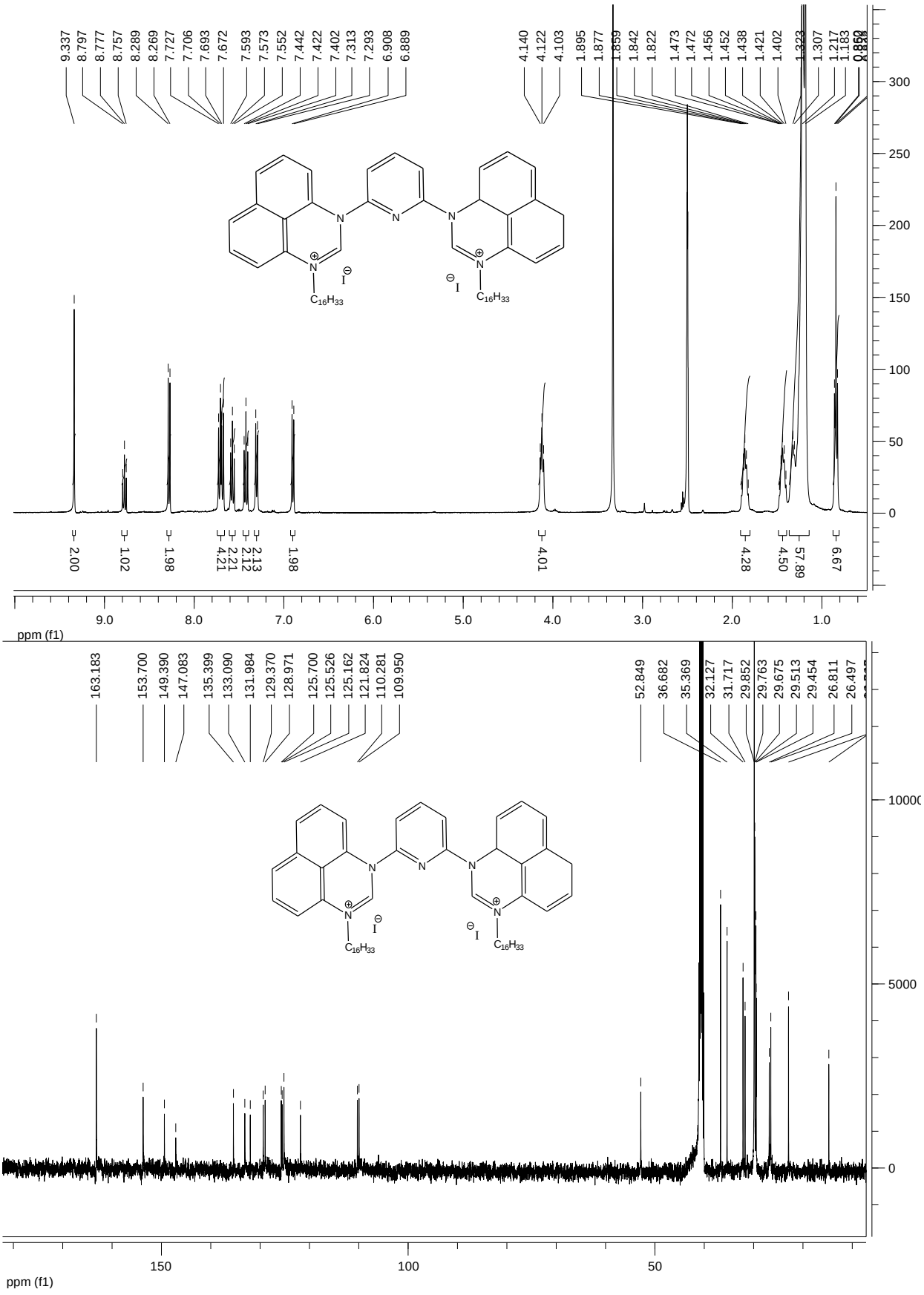
9.337
8.797
8.777
8.757
8.289
8.269
7.727
7.706
7.693
7.672
7.593
7.573
7.552
7.442
7.422
7.402
7.313
7.293
6.908
6.889
4.140
4.122
4.103
1.895
1.877
1.859
1.842
1.822
1.473
1.472
1.456
1.452
1.438
1.421
1.402
1.323
1.307
1.217
1.183
2.00
1.02
1.98
4.21
2.21
2.12
2.13
1.98
4.01
4.28
4.50
57.89
6.67
ppm (f1)
163.183
153.700
149.390
147.083
135.399
133.090
131.984
129.370
128.971
125.700
125.526
125.162
121.824
110.281
109.950
52.849
36.682
35.369
32.127
31.717
29.852
29.763
29.675
29.513
29.454
26.811
26.497
ppm (f1)

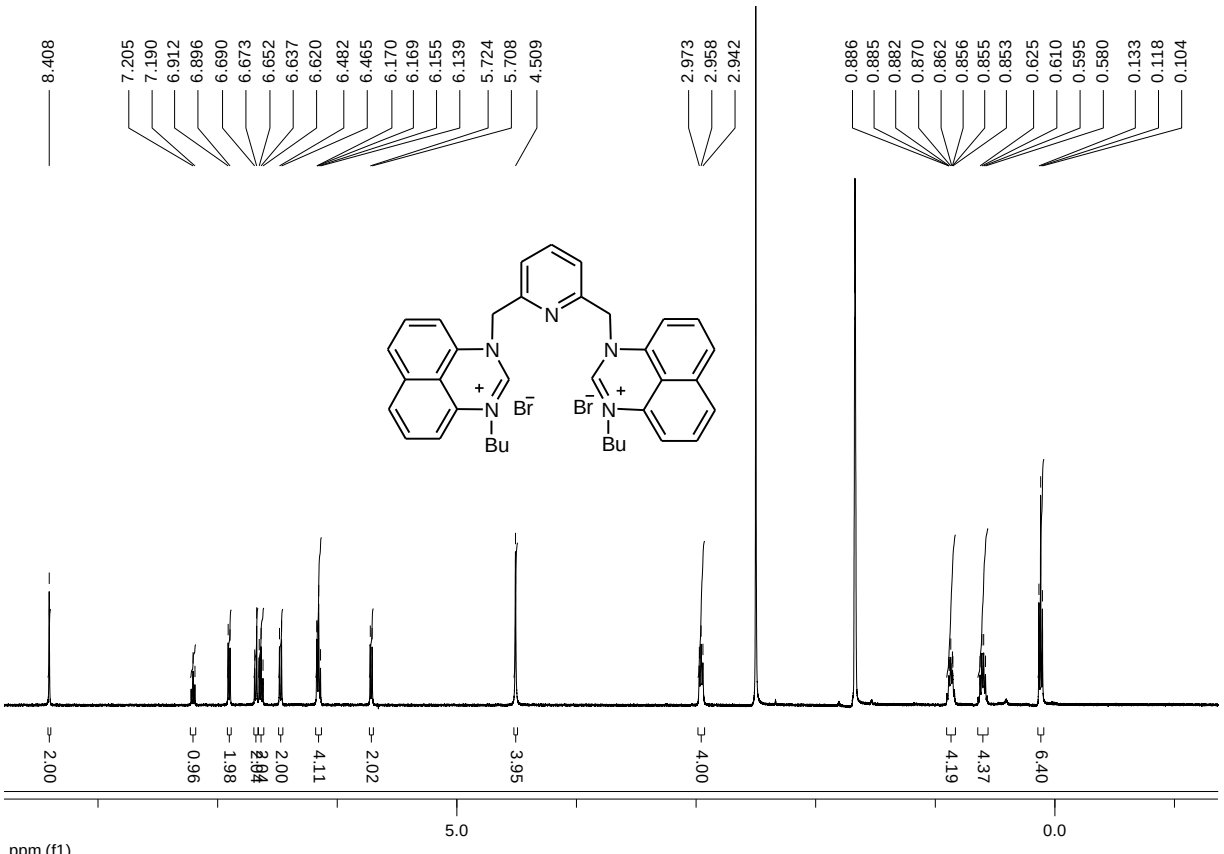
8.408
7.205
7.190
6.912
6.896
6.690
6.673
6.652
6.637
6.620
6.482
6.465
6.170
6.169
6.155
6.139
5.724
5.708
4.509
2.973
2.958
2.942
0.886
0.885
0.882
0.870
0.862
0.856
0.855
0.853
0.625
0.610
0.595
0.580
0.133
0.118
0.104
2.00
0.96
1.98
2.04
2.00
4.11
2.02
3.95
4.00
4.19
4.37
6.40
5.0
0.0
ppm (f1)

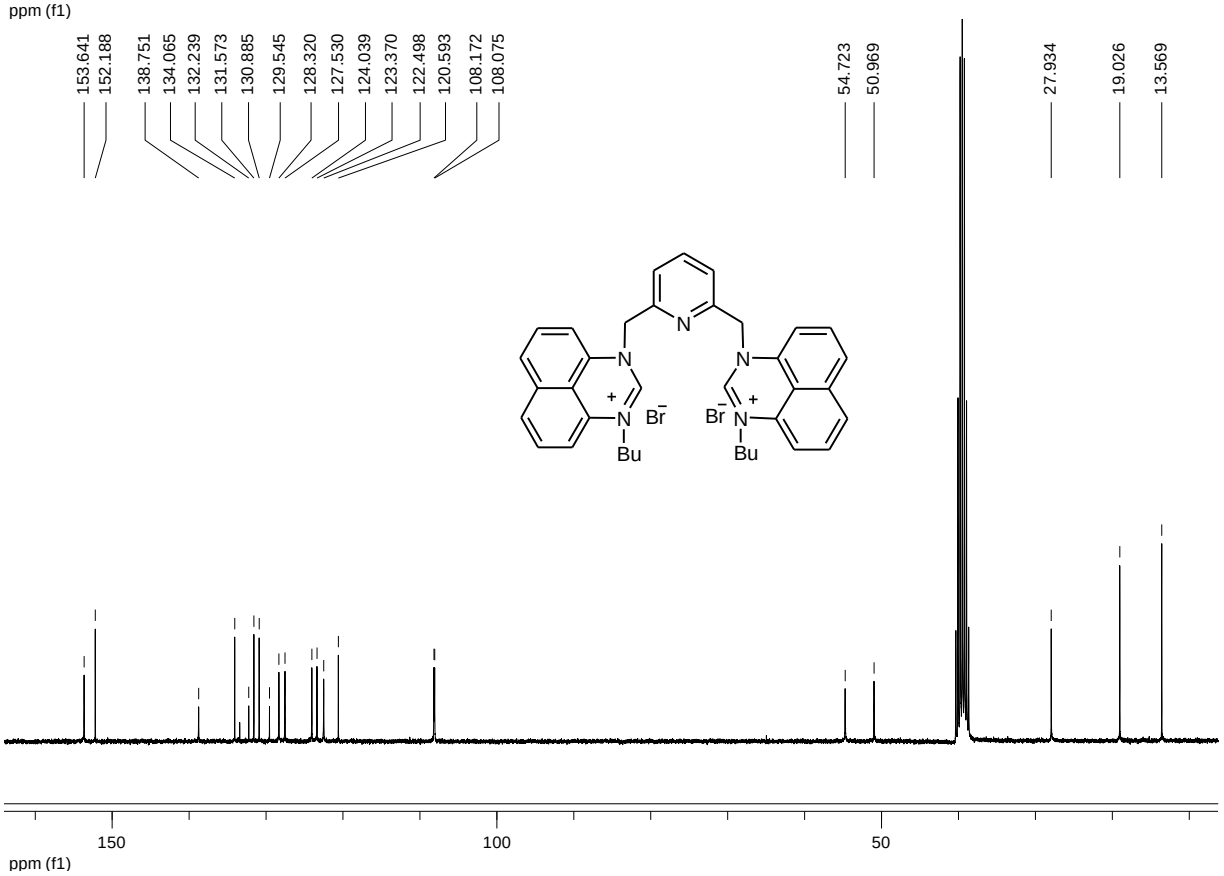
153.641
152.188
138.751
134.065
132.239
131.573
130.885
129.545
128.320
127.530
124.039
123.370
122.498
120.593
108.172
108.075
54.723
50.969
27.934
19.026
13.569
150
100
50
ppm (f1)

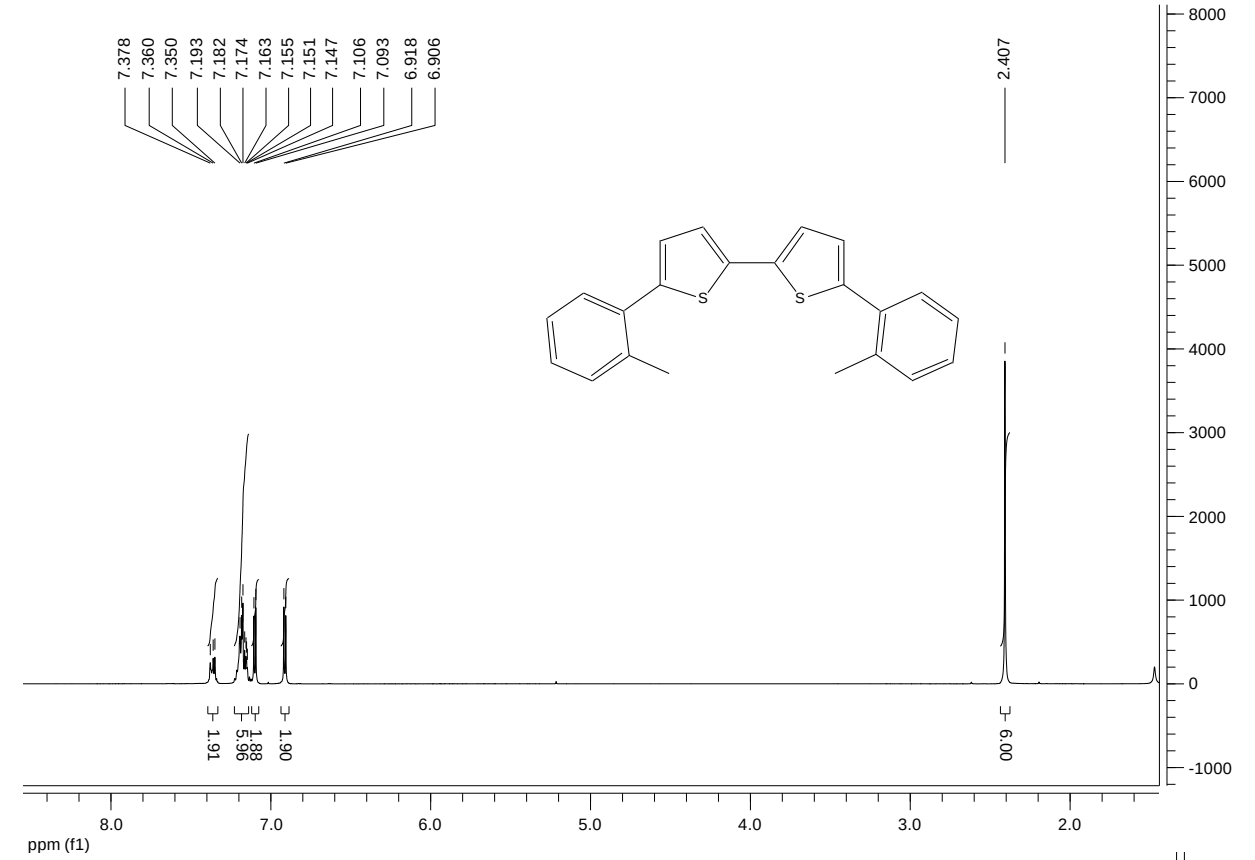
7.378
7.360
7.350
7.193
7.182
7.174
7.163
7.155
7.151
7.147
7.106
7.093
6.918
6.906
2.407
S
S
1.91
5.96
1.88
1.90
6.00
ppm (f1)

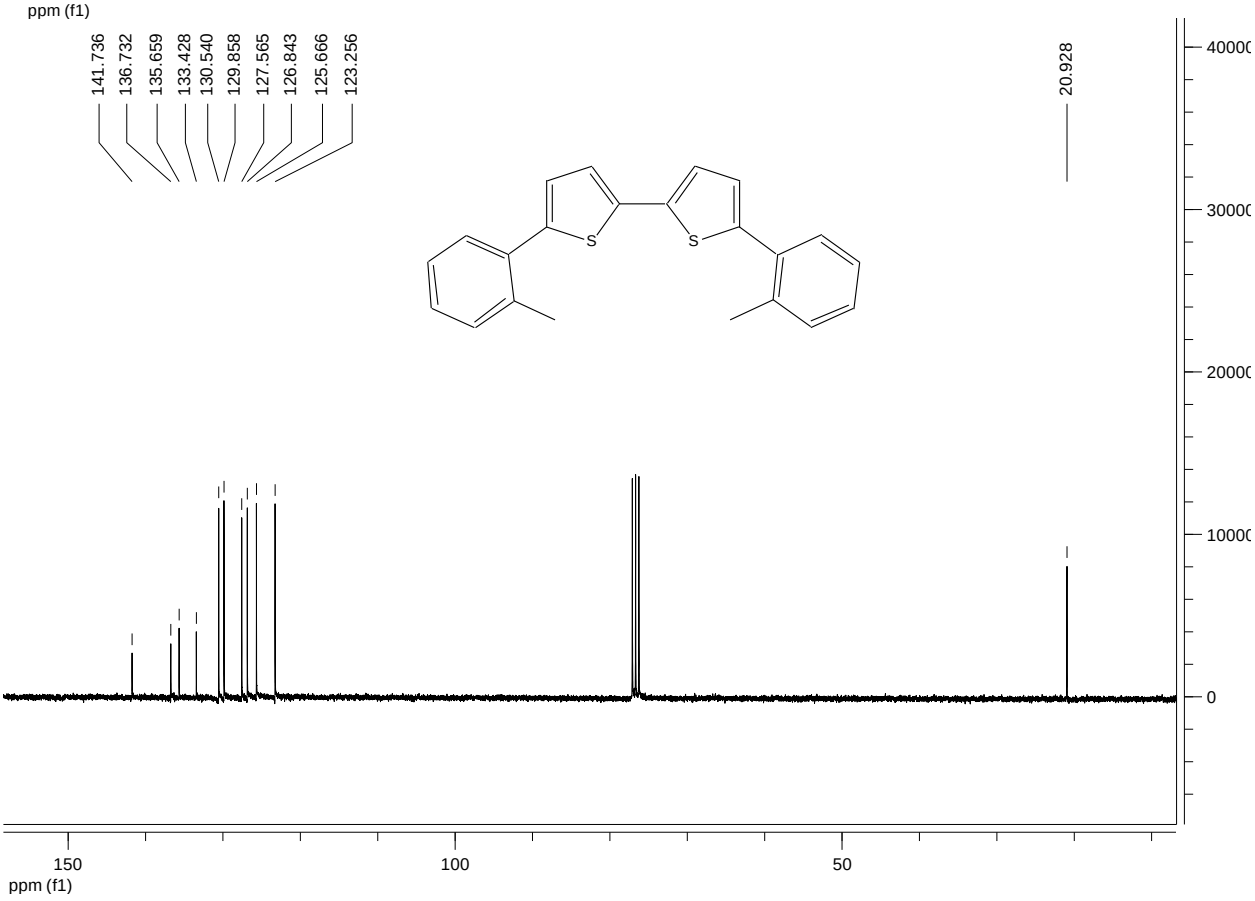
141.736
136.732
135.659
133.428
130.540
129.858
127.565
126.843
125.666
123.256
20.928
S
S
ppm (f1)

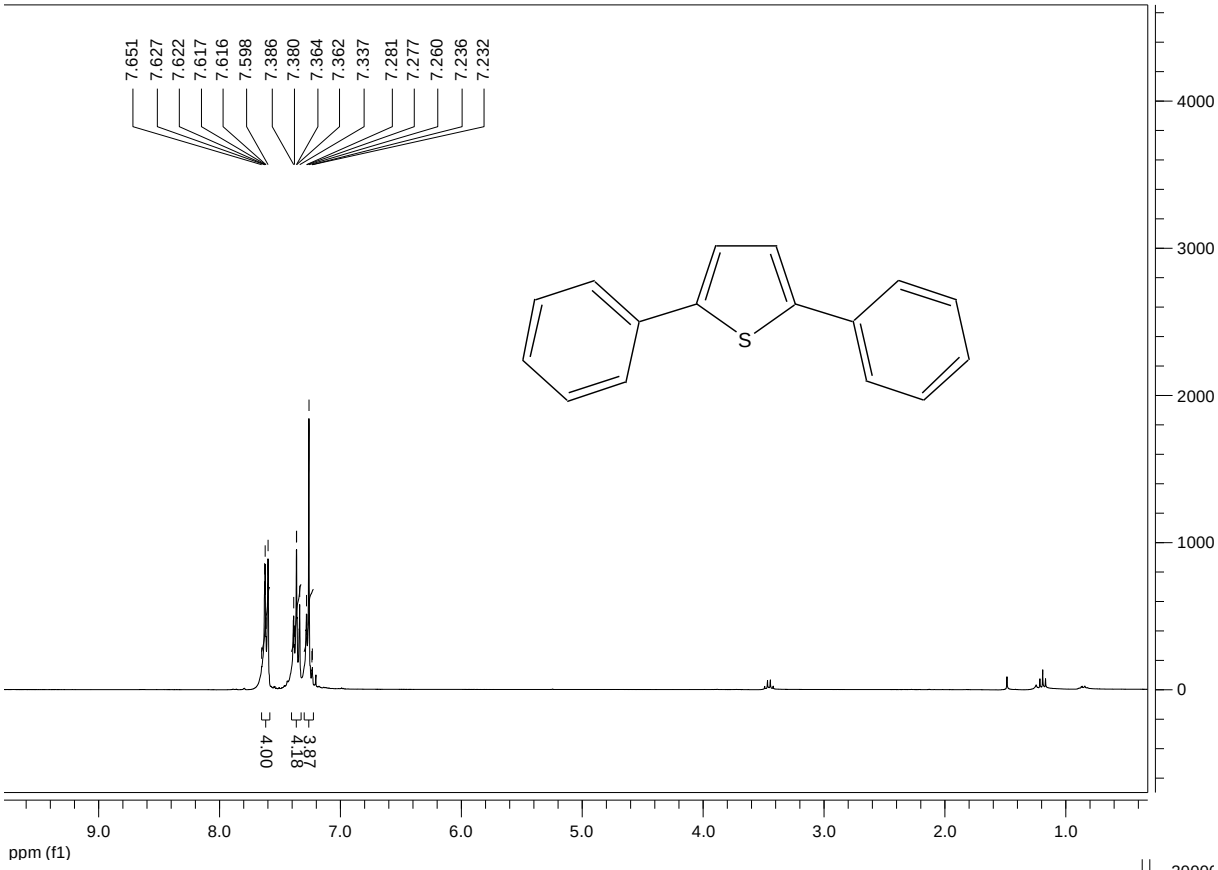
7.651
7.627
7.622
7.617
7.616
7.598
7.386
7.380
7.364
7.362
7.337
7.281
7.277
7.260
7.236
7.232
S
4.00
3.87
4.18
9.0
8.0
7.0
6.0
5.0
4.0
3.0
2.0
1.0
ppm (f1)
4000
3000
2000
1000
0

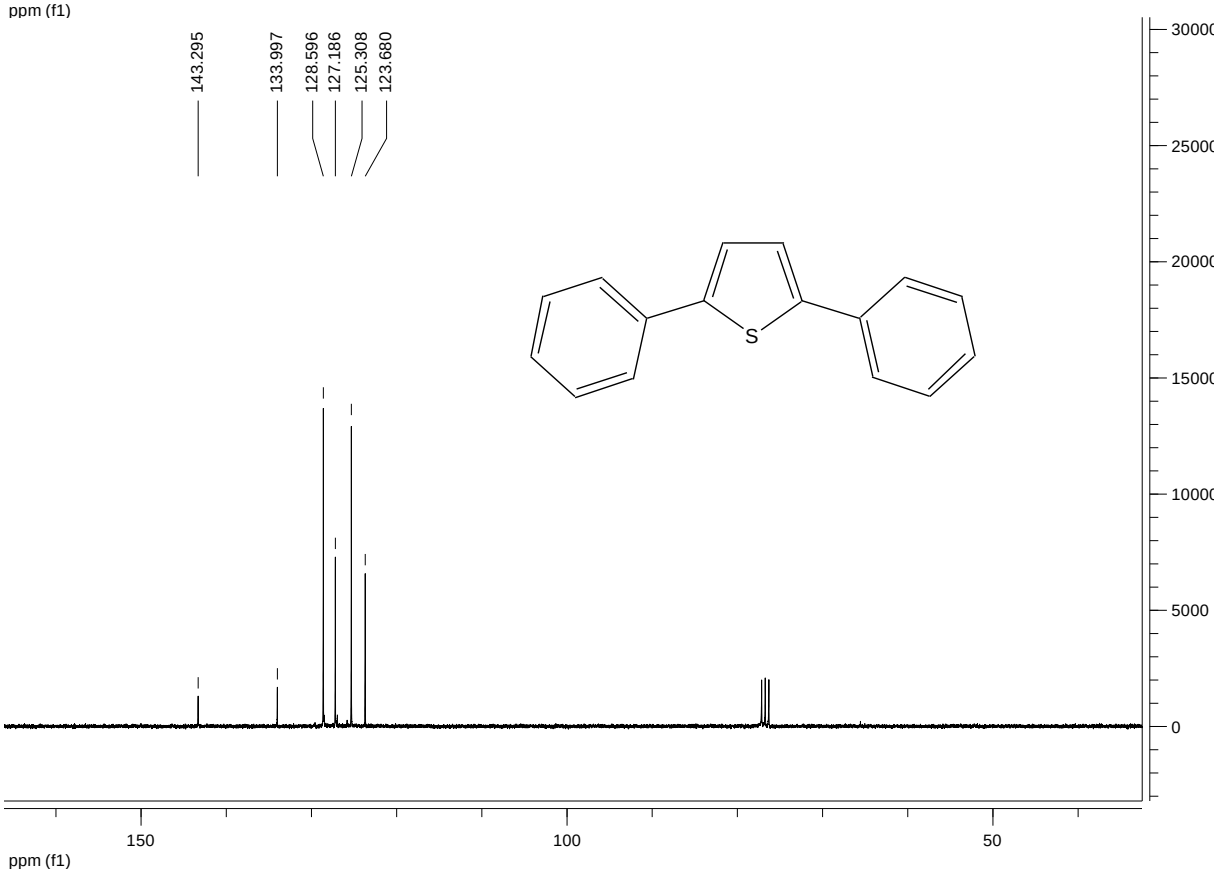
143.295
133.997
128.596
127.186
125.308
123.680
S
150
100
50
ppm (f1)
30000
25000
20000
15000
10000
5000
0

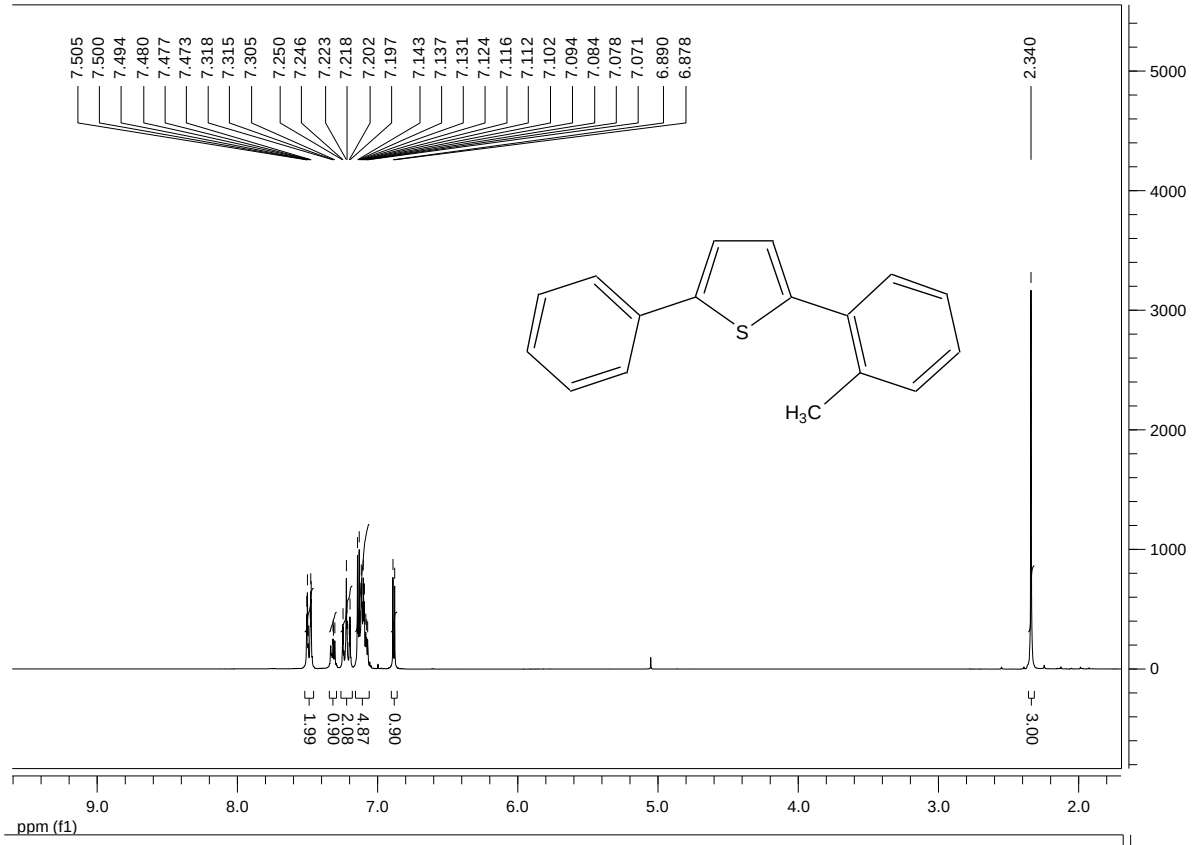
7.505
7.500
7.494
7.480
7.477
7.473
7.318
7.315
7.305
7.250
7.246
7.223
7.218
7.202
7.197
7.143
7.137
7.131
7.124
7.116
7.112
7.102
7.094
7.084
7.078
7.071
6.890
6.878
2.340
S
H3C
1.99
0.90
2.08
0.90
4.87
0.90
3.00
9.0
8.0
7.0
6.0
5.0
4.0
3.0
2.0
ppm (f1)

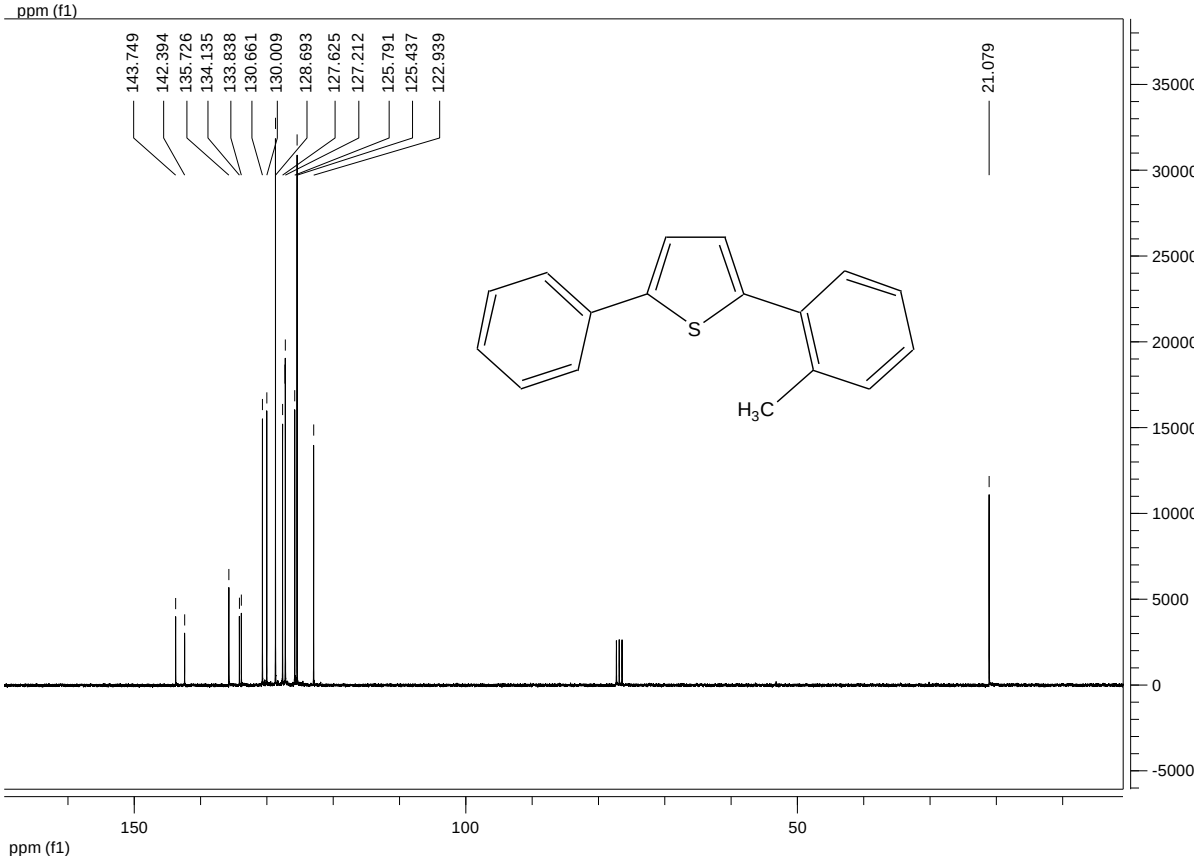
143.749
142.394
135.726
134.135
133.838
130.661
130.009
128.693
127.625
127.212
125.791
125.437
122.939
21.079
S
H3C
150
100
50
ppm (f1)

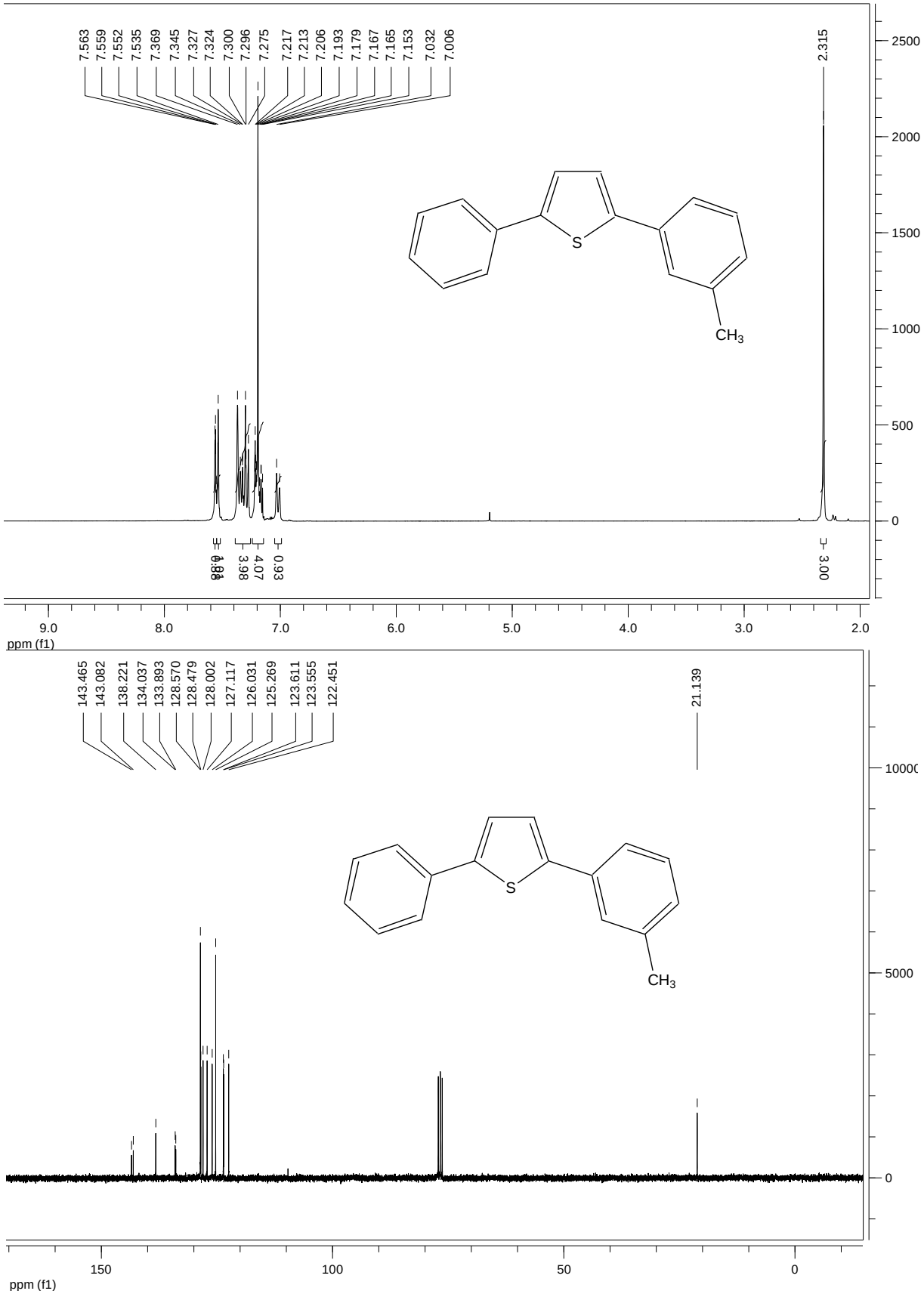
7.563
7.559
7.552
7.535
7.369
7.345
7.327
7.324
7.300
7.296
7.275
7.217
7.213
7.206
7.193
7.179
7.167
7.165
7.153
7.032
7.006
2.315
S
CH3
0.88
3.98
4.07
0.93
3.00
ppm (f1)
143.465
143.082
138.221
134.037
133.893
128.570
128.479
128.002
127.117
126.031
125.269
123.611
123.555
122.451
21.139
S
CH3
ppm (f1)

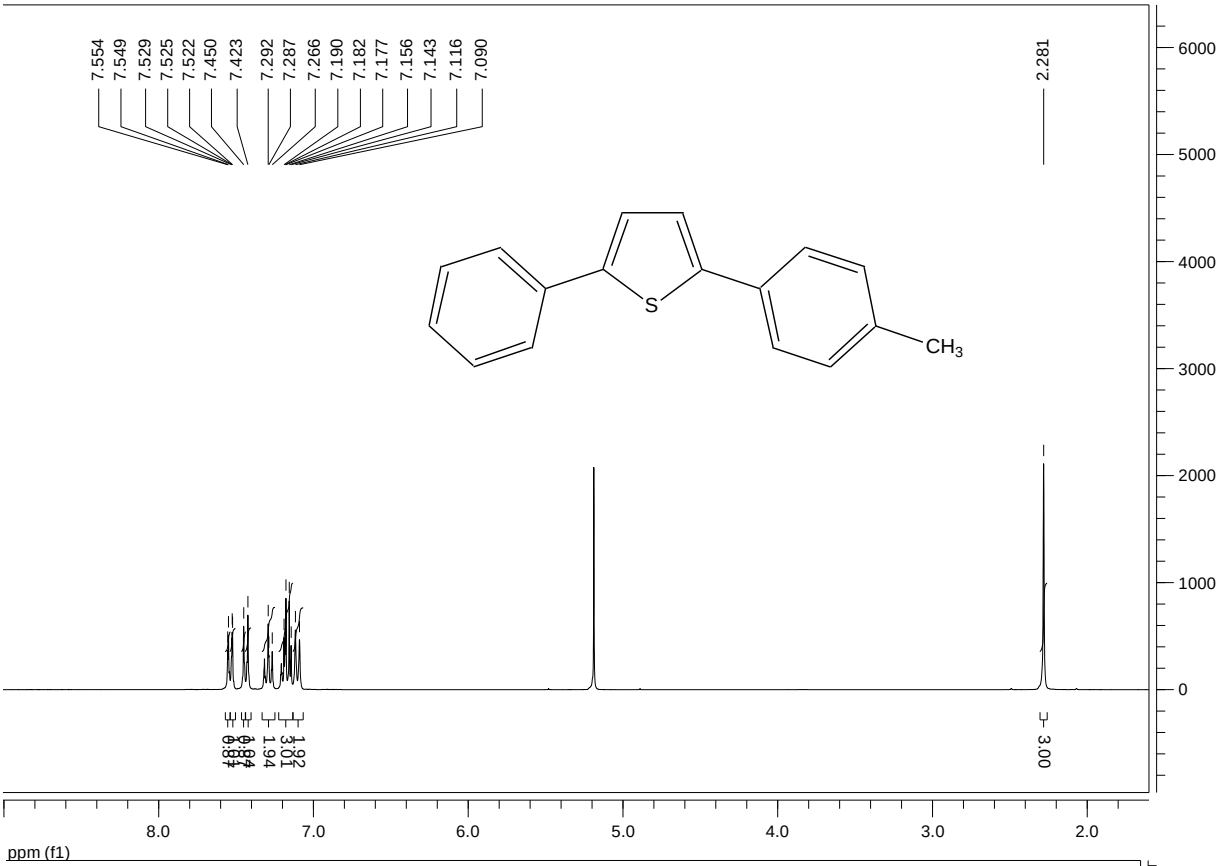
7.554
7.549
7.529
7.525
7.522
7.450
7.423
7.292
7.287
7.266
7.190
7.182
7.177
7.156
7.143
7.116
7.090
2.281
S
CH3
1.94
1.92
3.00
8.0
7.0
6.0
5.0
4.0
3.0
2.0
ppm (f1)

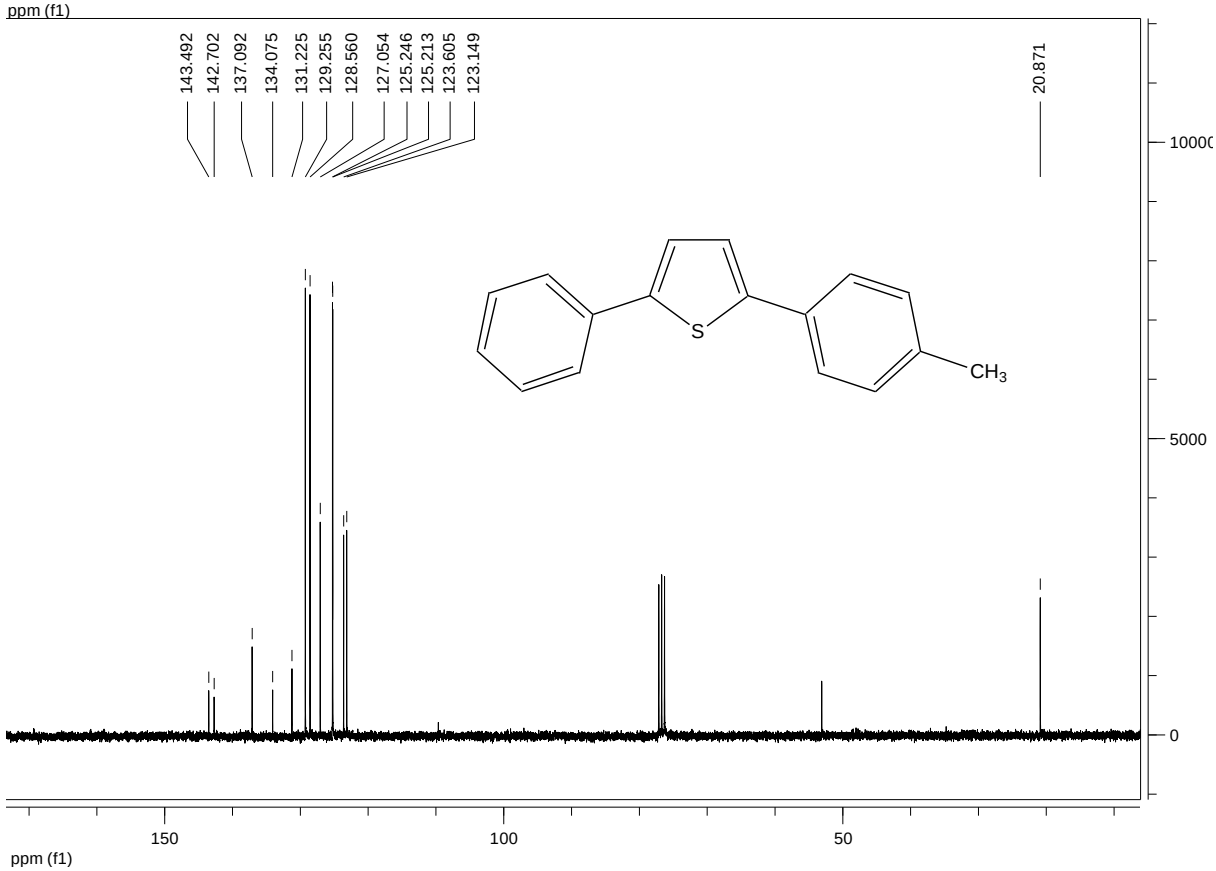
143.492
142.702
137.092
134.075
131.225
129.255
128.560
127.054
125.246
125.213
123.605
123.149
20.871
S
CH3
150
100
50
ppm (f1)

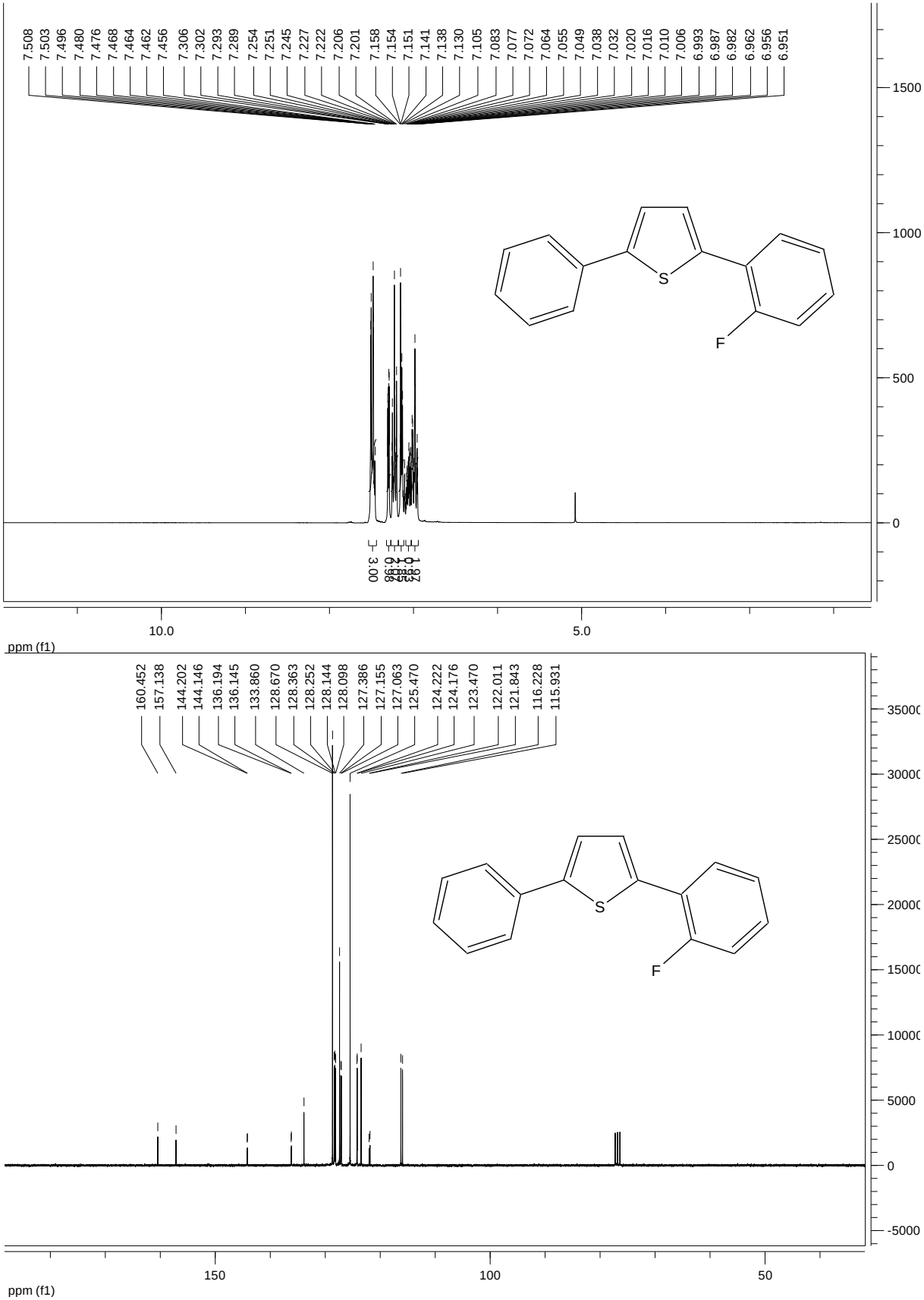
7.508
7.503
7.496
7.480
7.476
7.468
7.464
7.462
7.456
7.306
7.302
7.293
7.289
7.254
7.251
7.245
7.227
7.222
7.206
7.201
7.158
7.154
7.151
7.141
7.138
7.130
7.105
7.083
7.077
7.072
7.064
7.055
7.049
7.038
7.032
7.020
7.016
7.010
7.006
6.993
6.987
6.982
6.962
6.956
6.951
3.00
1.97
S
F
1500
1000
500
0
10.0
5.0
ppm (f1)
160.452
157.138
144.202
144.146
136.194
136.145
133.860
128.670
128.363
128.252
128.144
128.098
127.386
127.155
127.063
125.470
124.222
124.176
123.470
122.011
121.843
116.228
115.931
S
F
35000
30000
25000
20000
15000
10000
5000
0
-5000
150
100
50
ppm (f1)

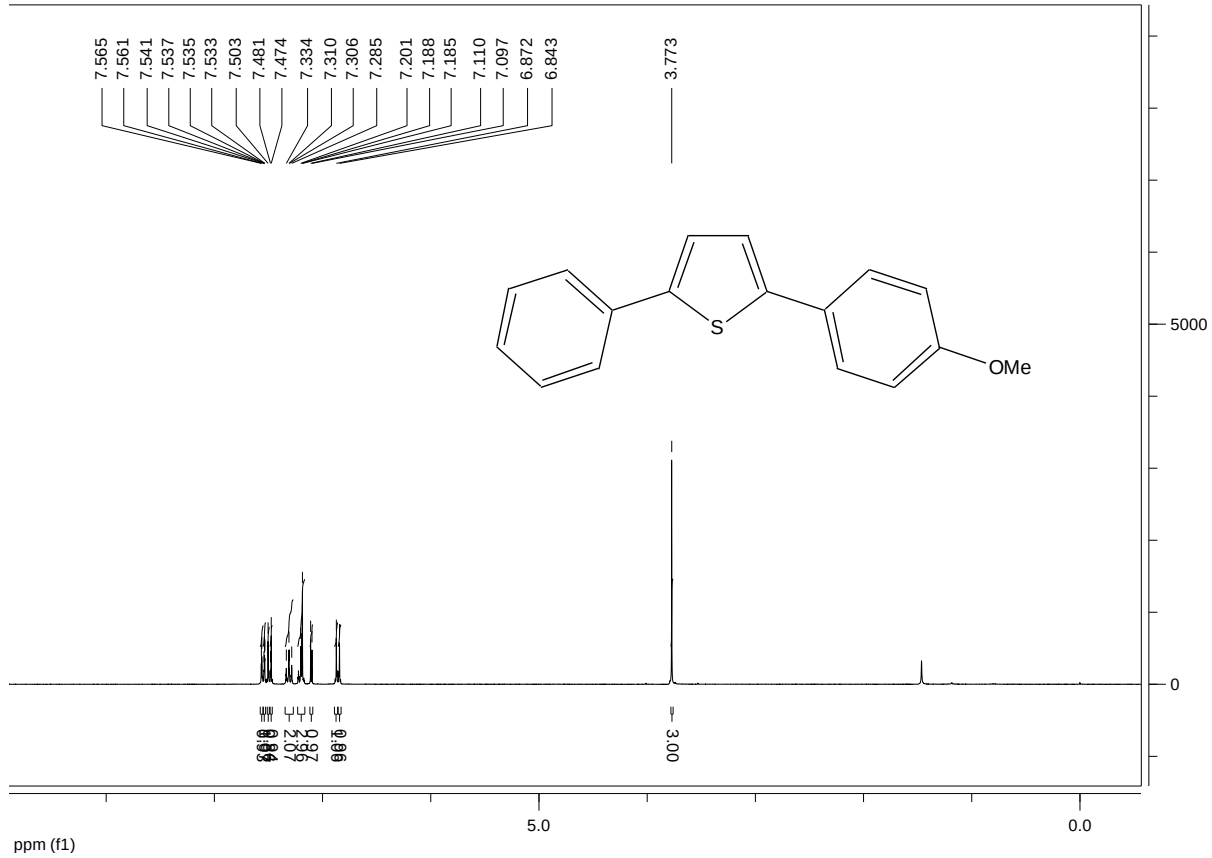
7.565
7.561
7.541
7.537
7.535
7.533
7.503
7.481
7.474
7.334
7.310
7.306
7.285
7.201
7.188
7.185
7.110
7.097
6.872
6.843
3.773
S
OMe
5000
0
3.00
5.0
0.0
ppm (f1)

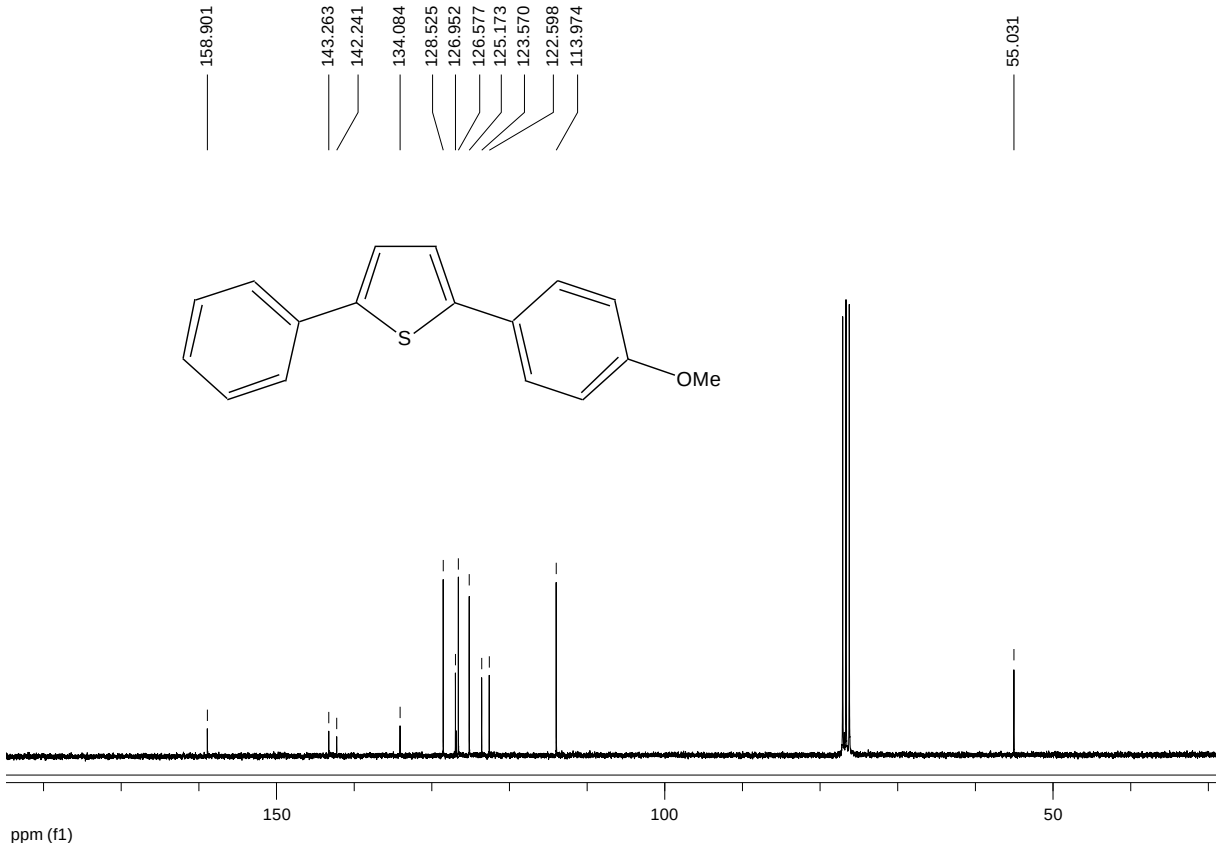
158.901
143.263
142.241
134.084
128.525
126.952
126.577
125.173
123.570
122.598
113.974
55.031
S
OMe
150
100
50
ppm (f1)

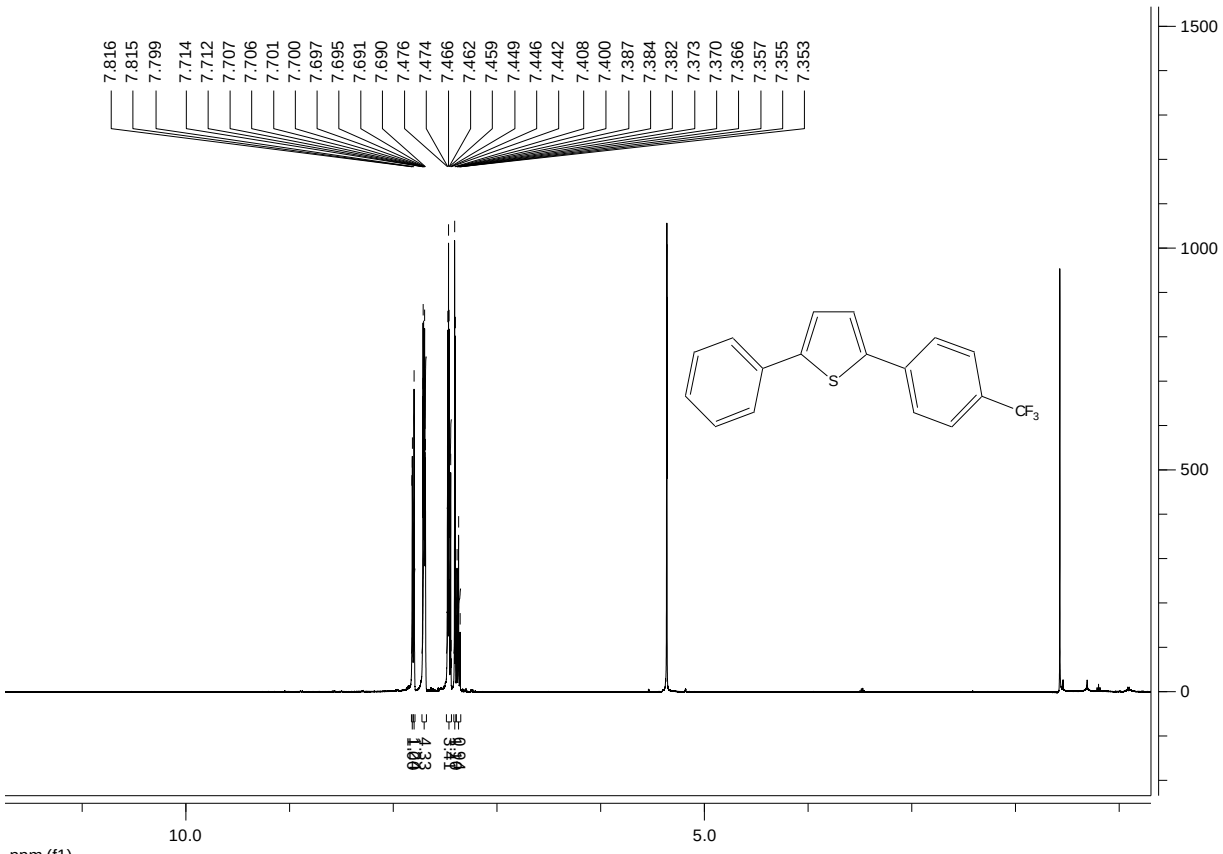
7.816
7.815
7.799
7.714
7.712
7.707
7.706
7.701
7.700
7.697
7.695
7.691
7.690
7.476
7.474
7.466
7.462
7.459
7.449
7.446
7.442
7.408
7.400
7.387
7.384
7.382
7.373
7.370
7.366
7.357
7.355
7.353
S
CF3
1500
1000
500
0
10.0
5.0
ppm (f1)

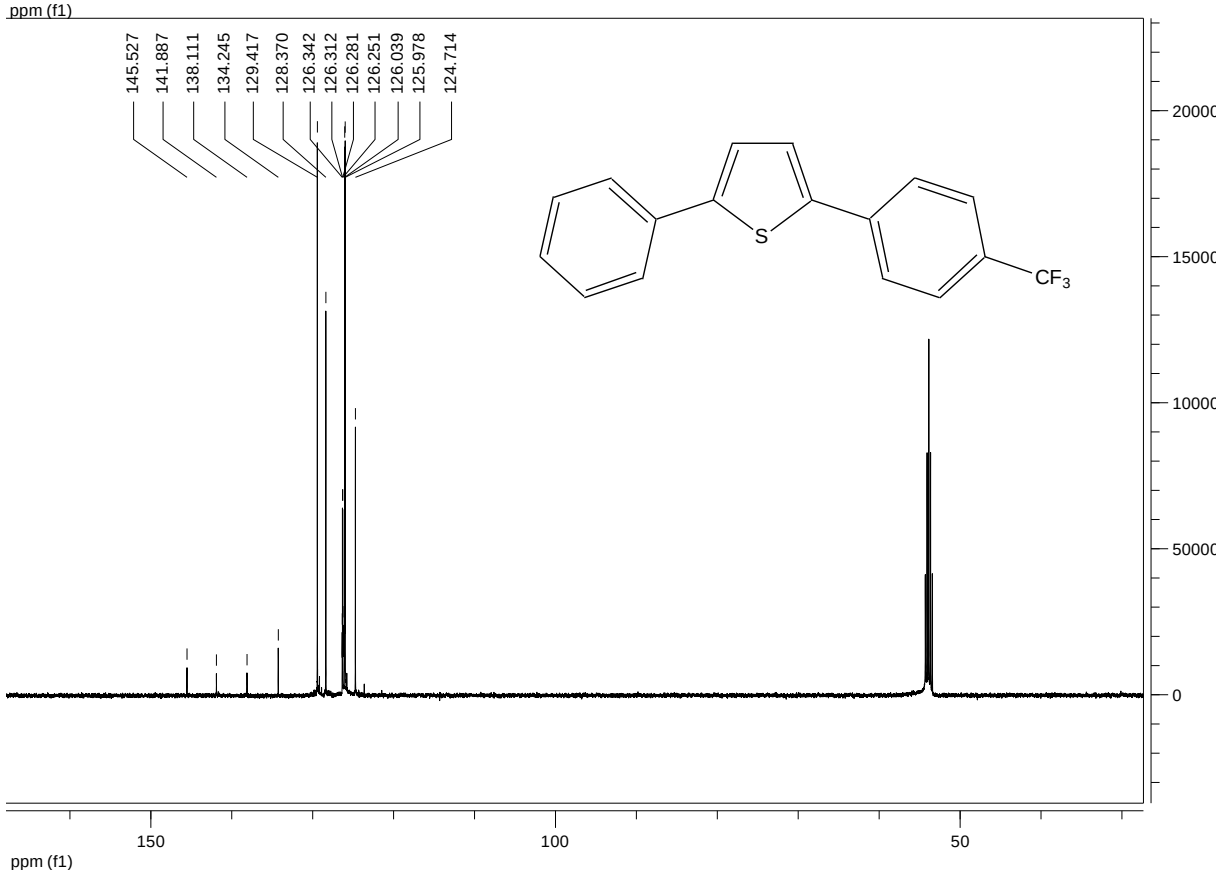
145.527
141.887
138.111
134.245
129.417
128.370
126.342
126.312
126.281
126.251
126.039
125.978
124.714
S
CF3
20000
15000
10000
50000
0
150
100
50
ppm (f1)

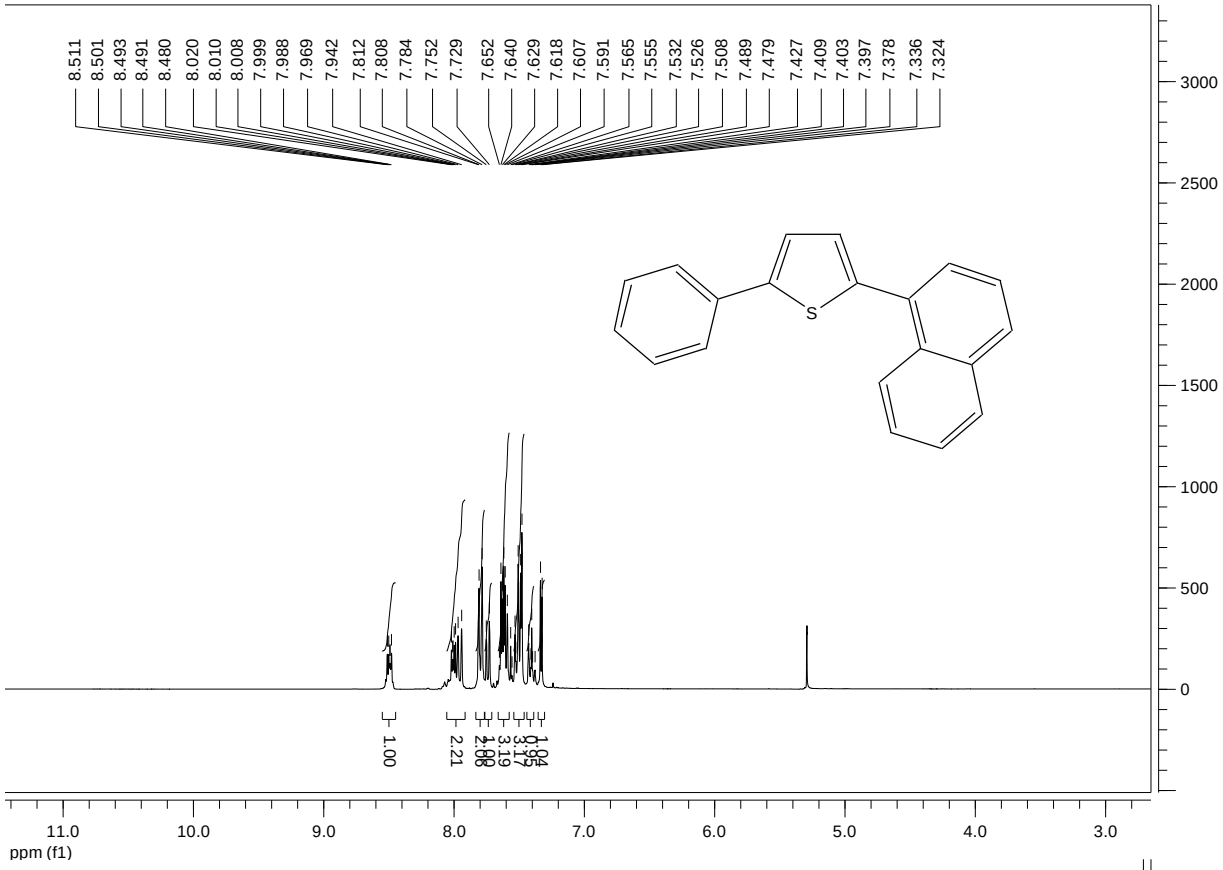
8.511
8.501
8.493
8.491
8.480
8.020
8.010
8.008
7.999
7.988
7.969
7.942
7.812
7.808
7.784
7.752
7.729
7.652
7.640
7.629
7.618
7.607
7.591
7.565
7.555
7.532
7.526
7.508
7.489
7.479
7.427
7.409
7.403
7.397
7.378
7.336
7.324
S
1.00
2.21
ppm (f1)

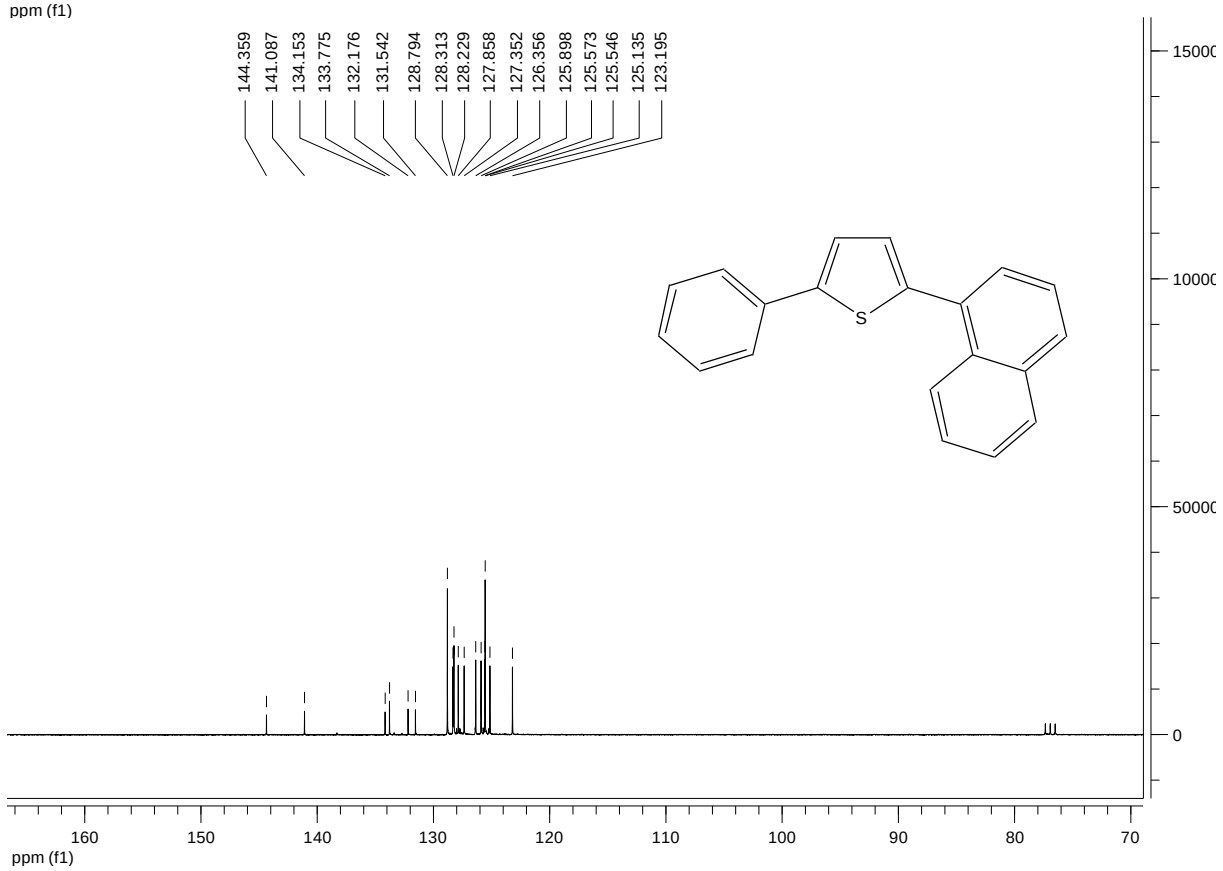
144.359
141.087
134.153
133.775
132.176
131.542
128.794
128.313
128.229
127.858
127.352
126.356
125.898
125.573
125.546
125.135
123.195
S
ppm (f1)

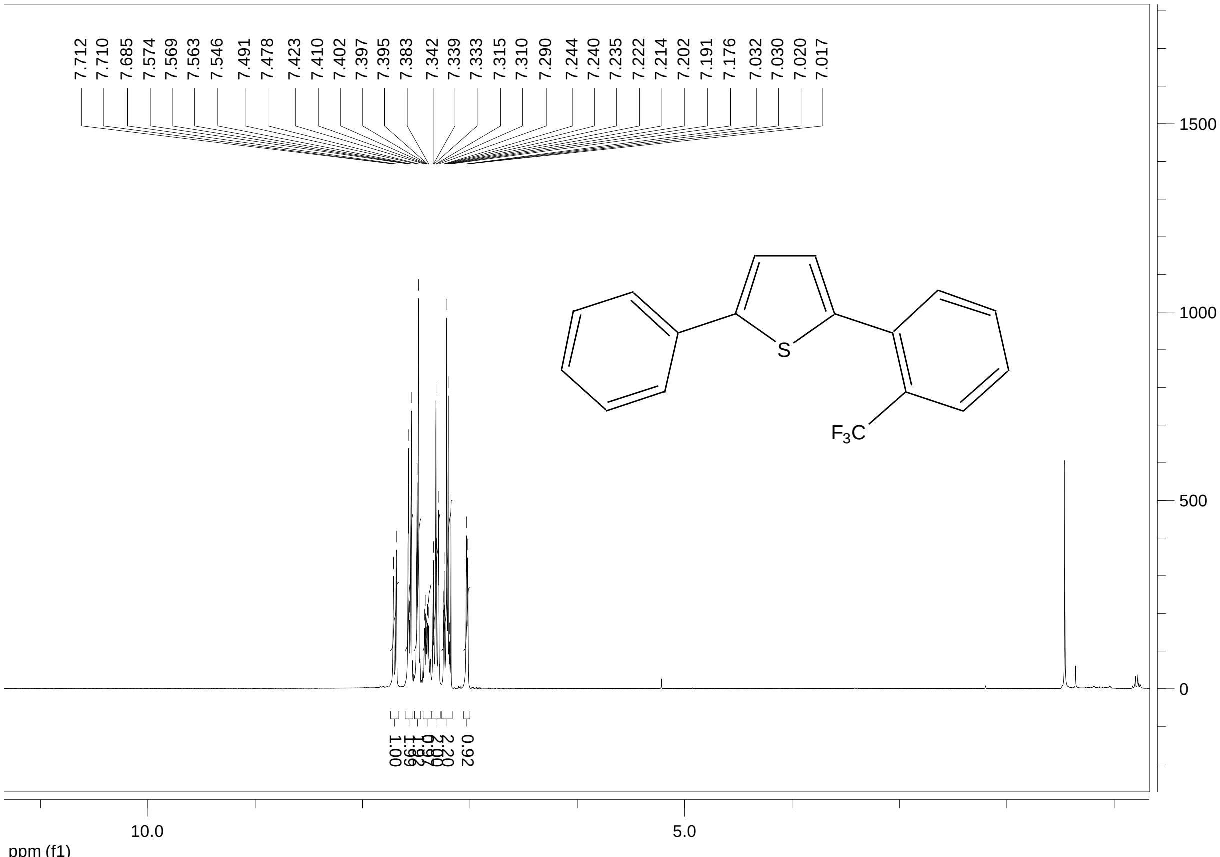
7.712
7.710
7.685
7.574
7.569
7.563
7.546
7.491
7.478
7.423
7.410
7.402
7.397
7.395
7.383
7.342
7.339
7.333
7.315
7.310
7.290
7.244
7.240
7.235
7.222
7.214
7.202
7.191
7.176
7.032
7.030
7.020
7.017
S
F3C
1500
1000
500
0
1.00
0.92
10.0
5.0
ppm (f1)

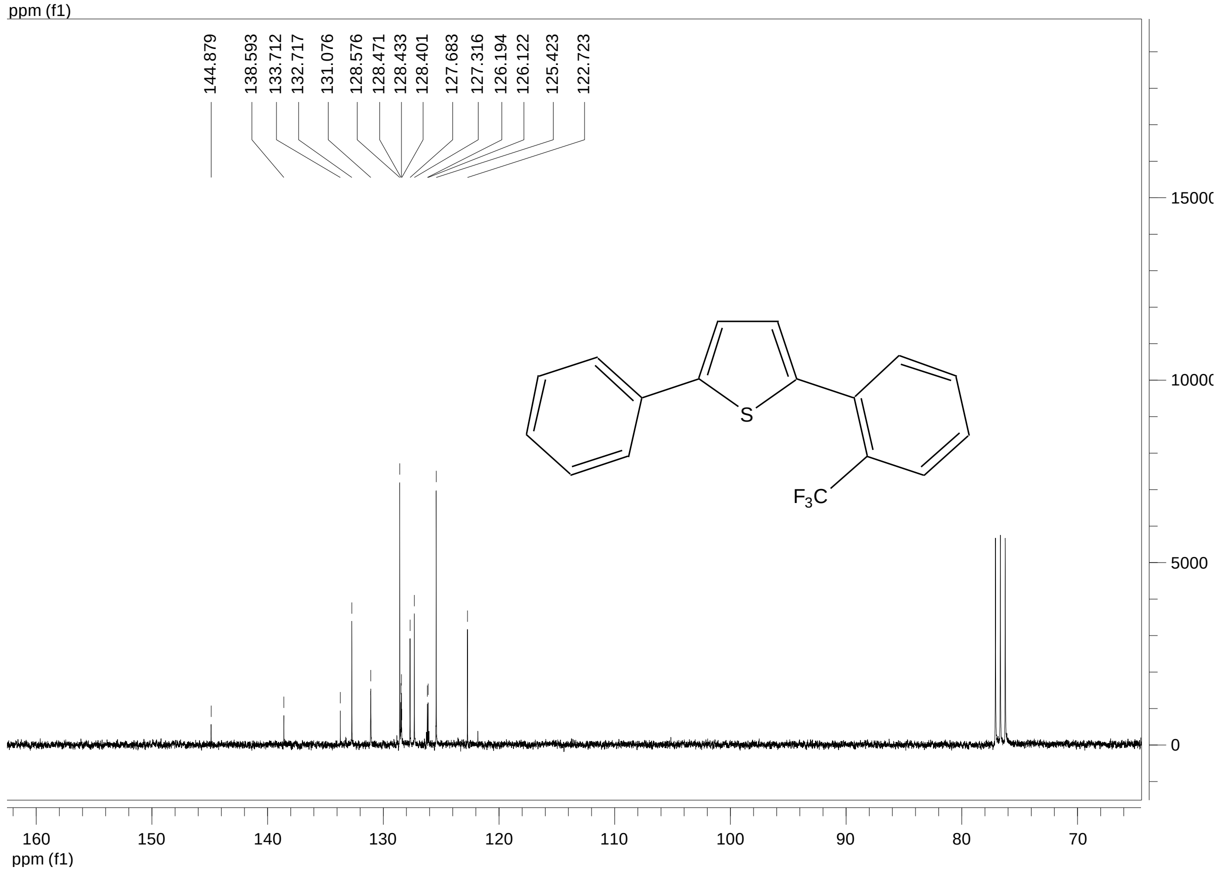
144.879
138.593
133.712
132.717
131.076
128.576
128.471
128.433
128.401
127.683
127.316
126.194
126.122
125.423
122.723
S
F3C
15000
10000
5000
0
160
150
140
130
120
110
100
90
80
70
ppm (f1)

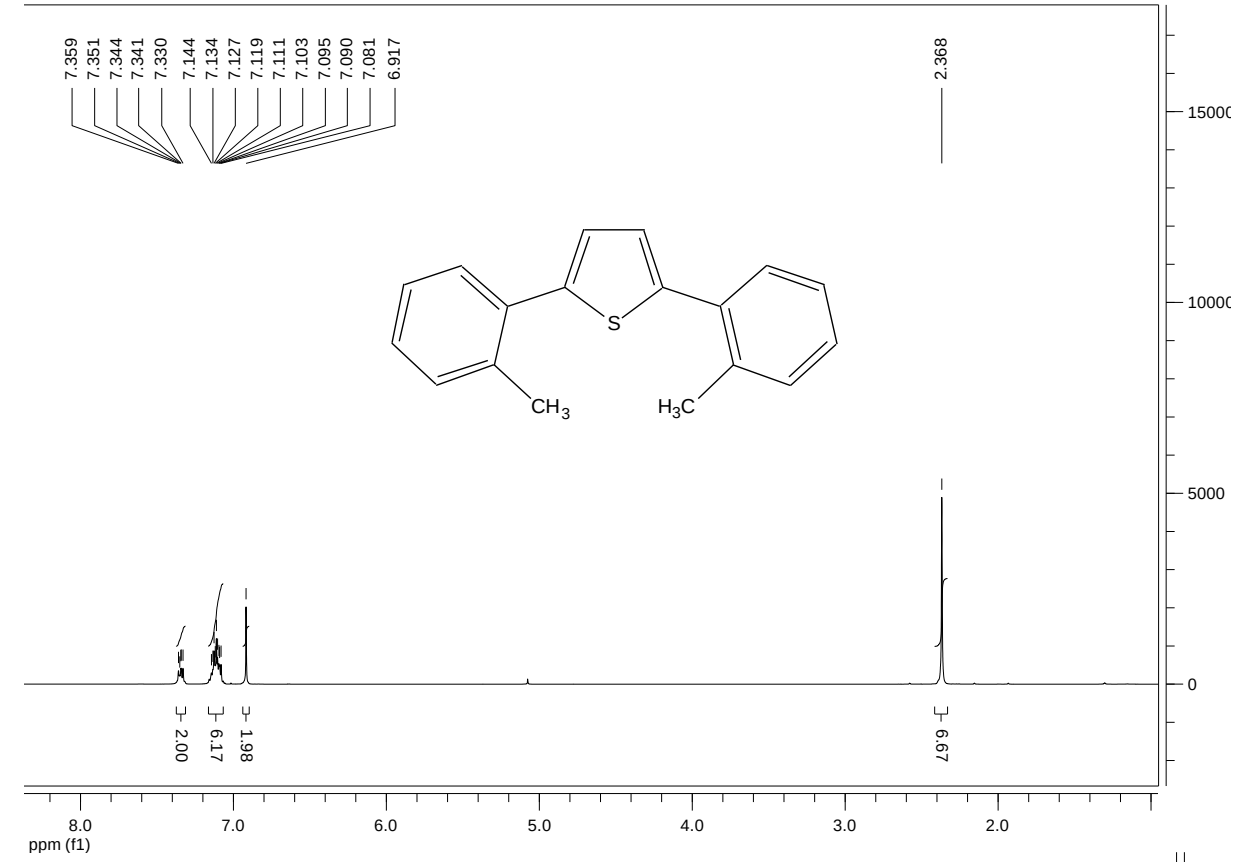
7.359
7.351
7.344
7.341
7.330
7.144
7.134
7.127
7.119
7.111
7.103
7.095
7.090
7.081
6.917
2.368
S
CH3
H3C
2.00
6.17
1.98
6.67
8.0
7.0
6.0
5.0
4.0
3.0
2.0
ppm (f1)

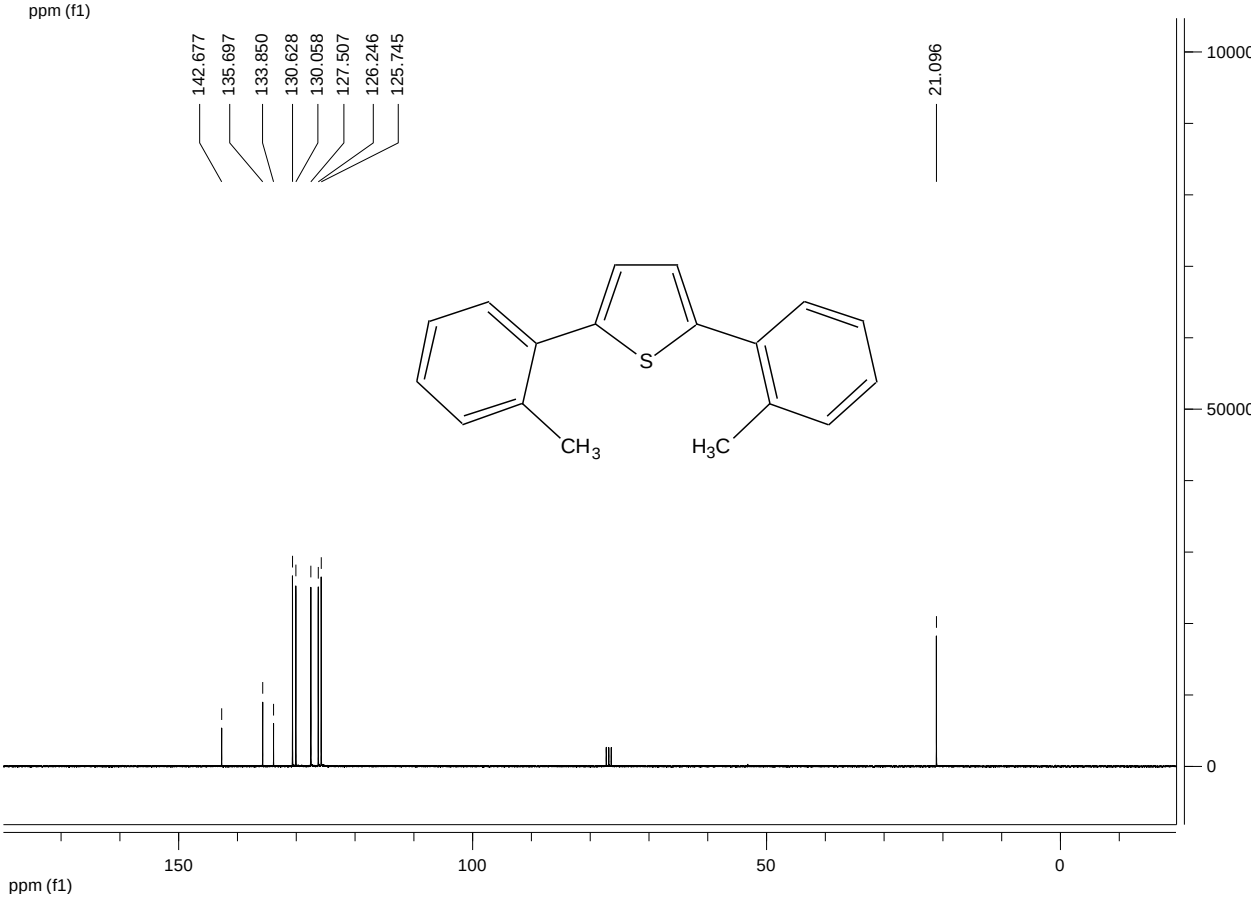
142.677
135.697
133.850
130.628
130.058
127.507
126.246
125.745
21.096
S
CH3
H3C
150
100
50
0
ppm (f1)

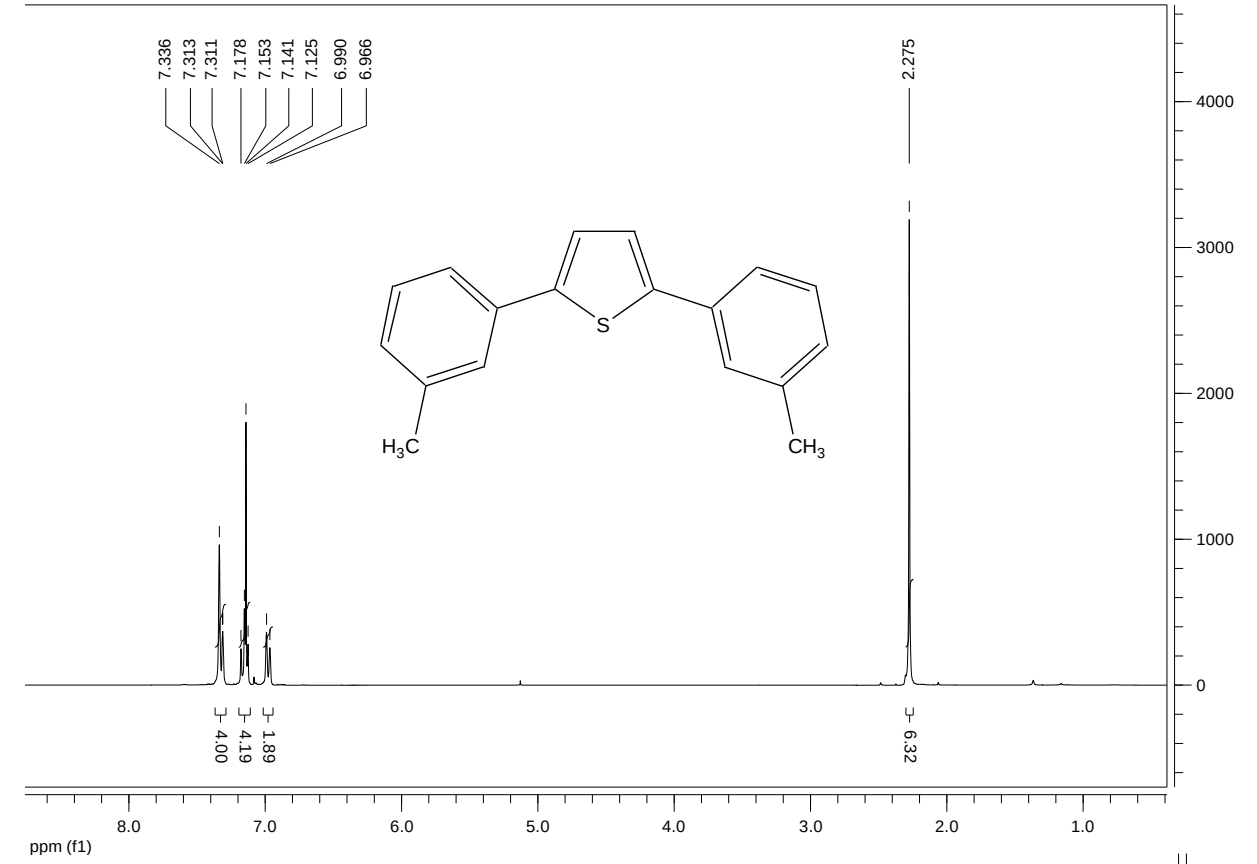
7.336
7.313
7.311
7.178
7.153
7.141
7.125
6.990
6.966
2.275
S
H3C
CH3
4.00
4.19
1.89
9.32
8.0
7.0
6.0
5.0
4.0
3.0
2.0
1.0
ppm (f1)

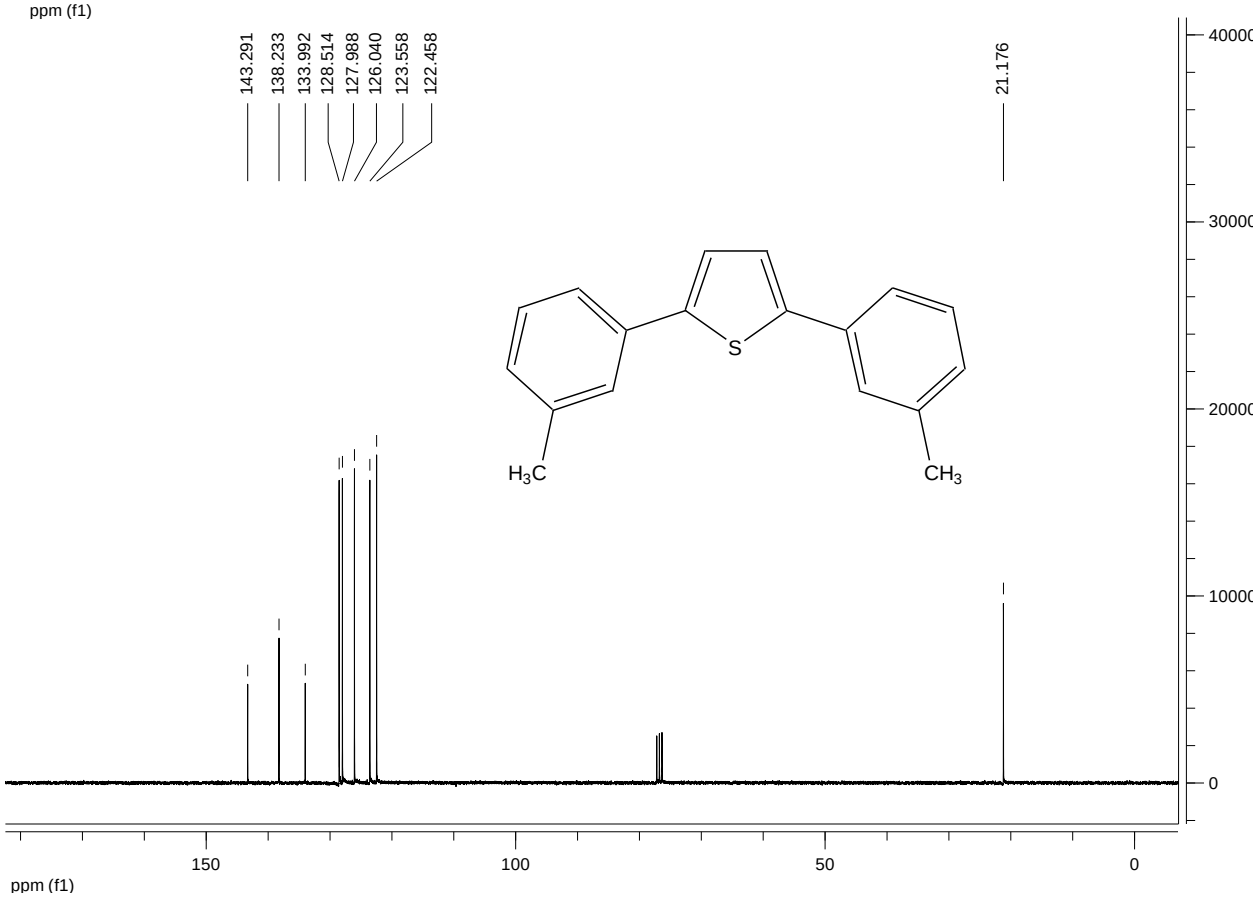
143.291
138.233
133.992
128.514
127.988
126.040
123.558
122.458
21.176
S
H3C
CH3
150
100
50
0
ppm (f1)

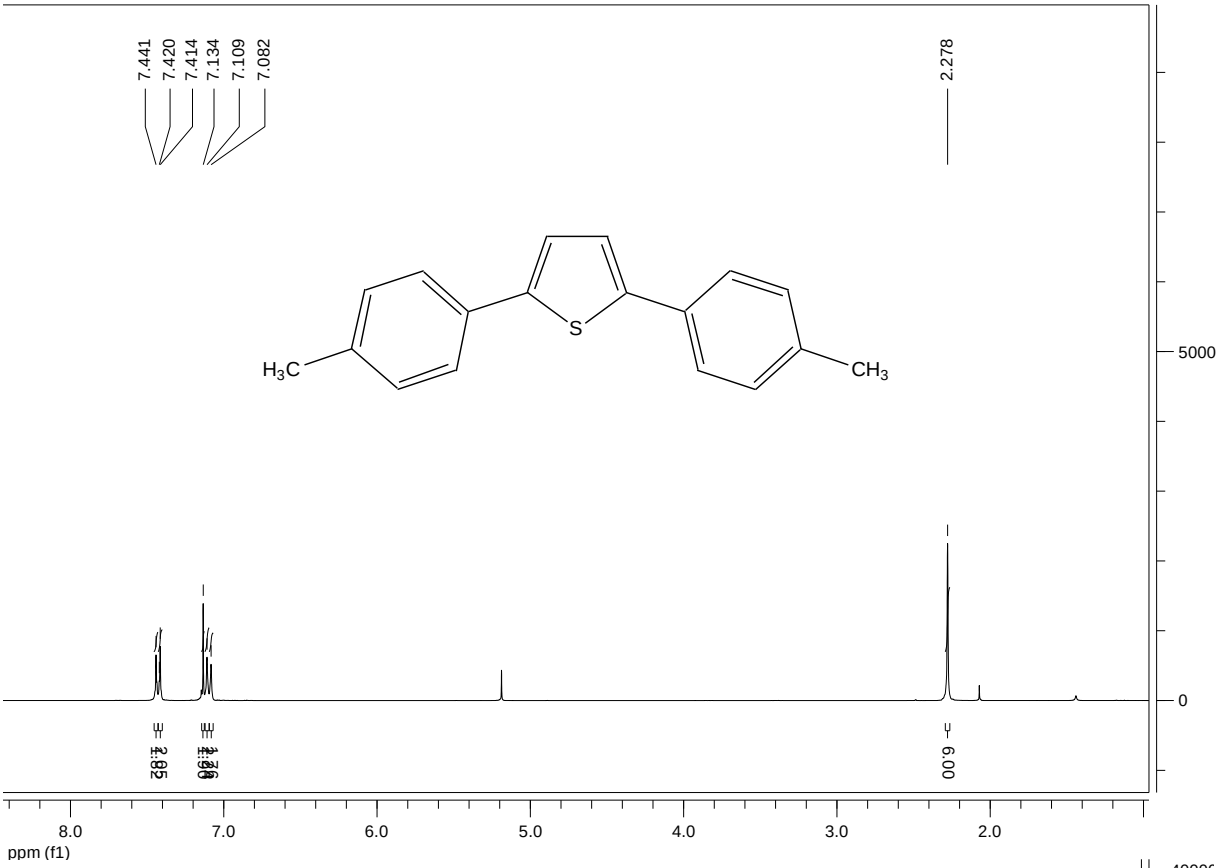
7.441
7.420
7.414
7.134
7.109
7.082
2.278
S
H3C
CH3
5000
0
2.05
2.02
2.00
6.00
8.0
7.0
6.0
5.0
4.0
3.0
2.0
ppm (f1)

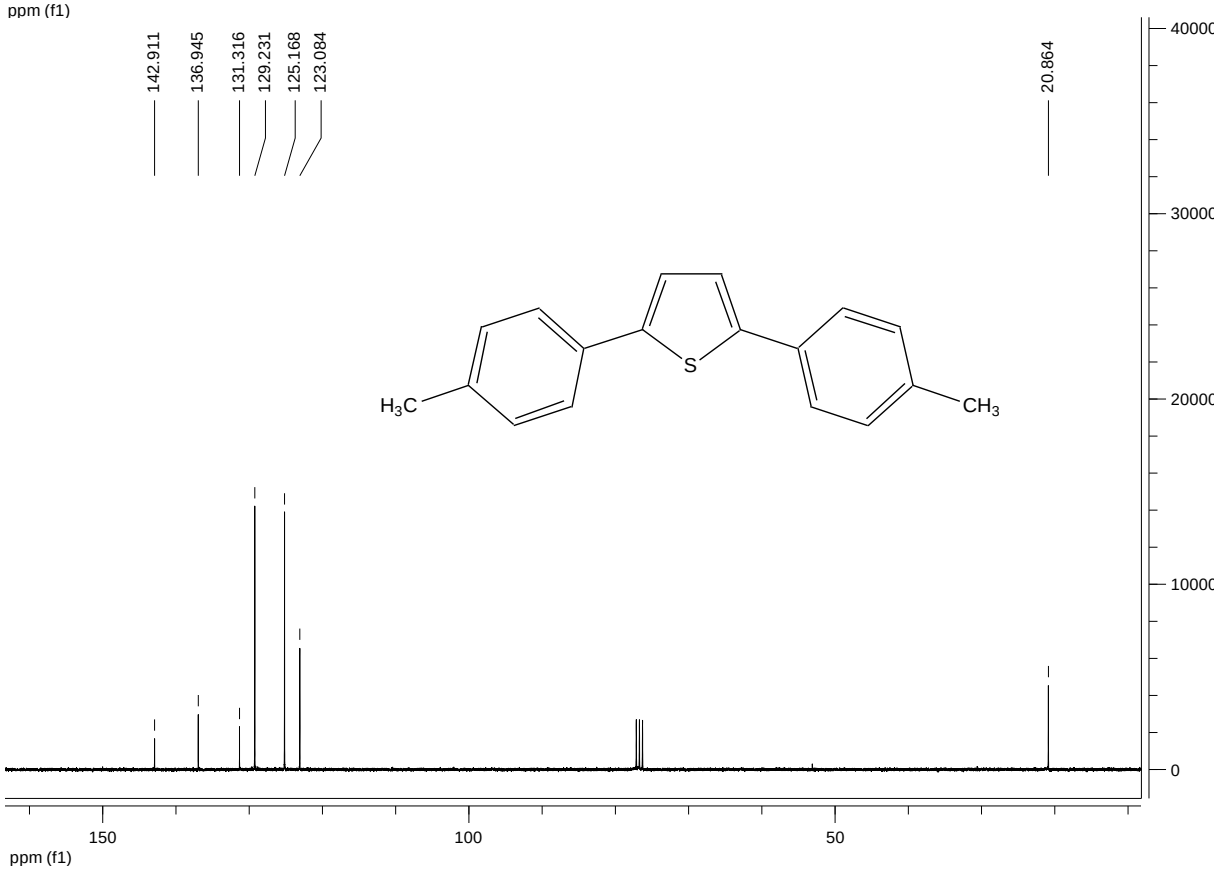
142.911
136.945
131.316
129.231
125.168
123.084
20.864
S
H3C
CH3
40000
30000
20000
10000
0
150
100
50
ppm (f1)

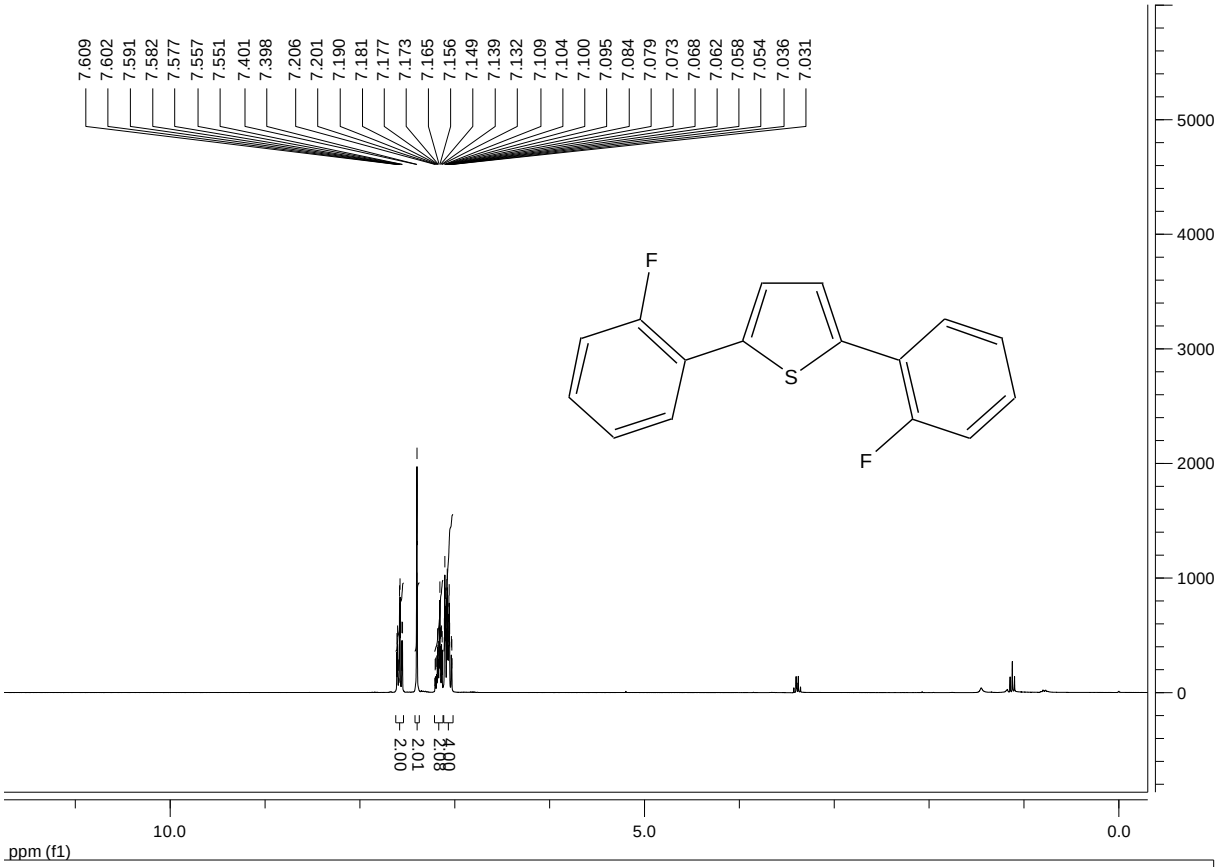
7.609
7.602
7.591
7.582
7.577
7.557
7.551
7.401
7.398
7.206
7.201
7.190
7.181
7.177
7.173
7.165
7.156
7.149
7.139
7.132
7.109
7.104
7.100
7.095
7.084
7.079
7.073
7.068
7.062
7.058
7.054
7.036
7.031
F
S
F
5000
4000
3000
2000
1000
0
2.00
2.01
4.08
10.0
5.0
0.0
ppm (f1)

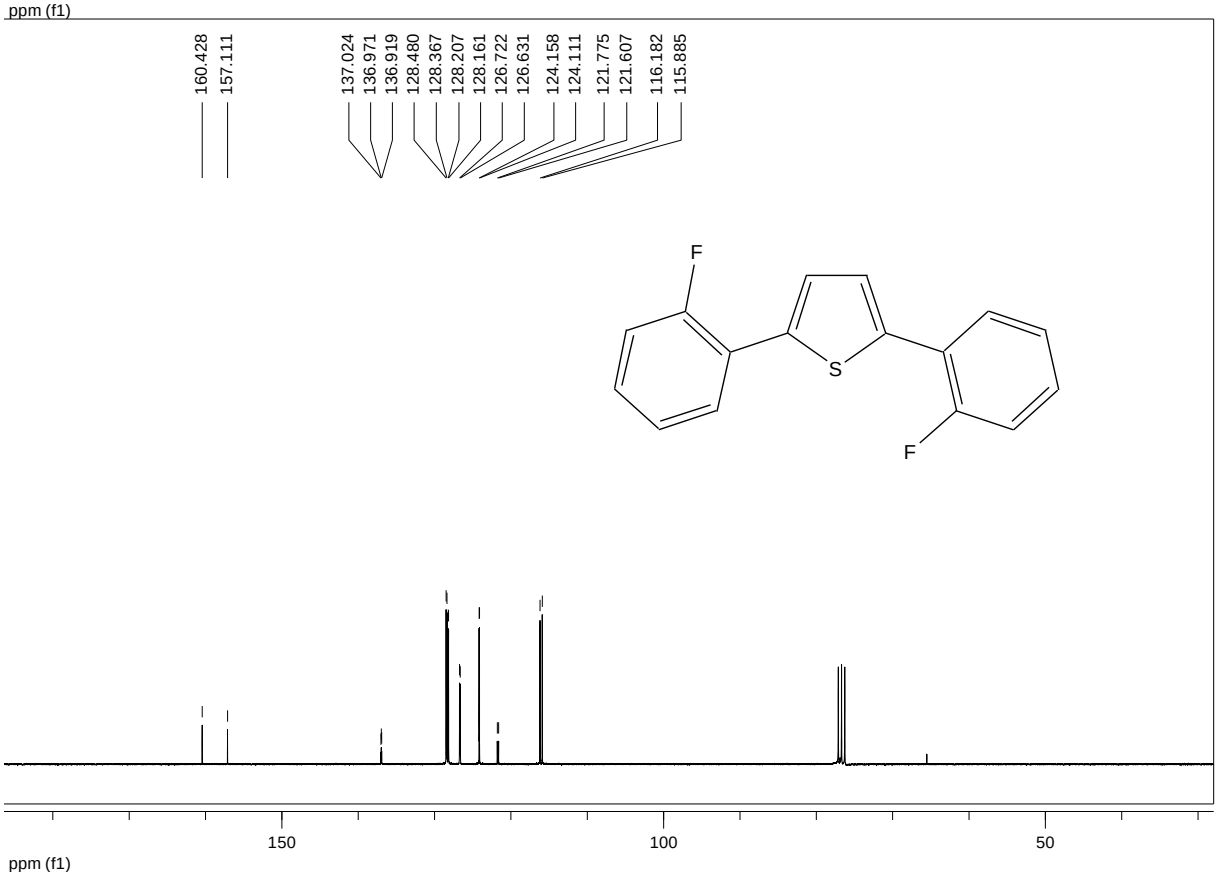
160.428
157.111
137.024
136.971
136.919
128.480
128.367
128.207
128.161
126.722
126.631
124.158
124.111
121.775
121.607
116.182
115.885
F
S
F
150
100
50
ppm (f1)

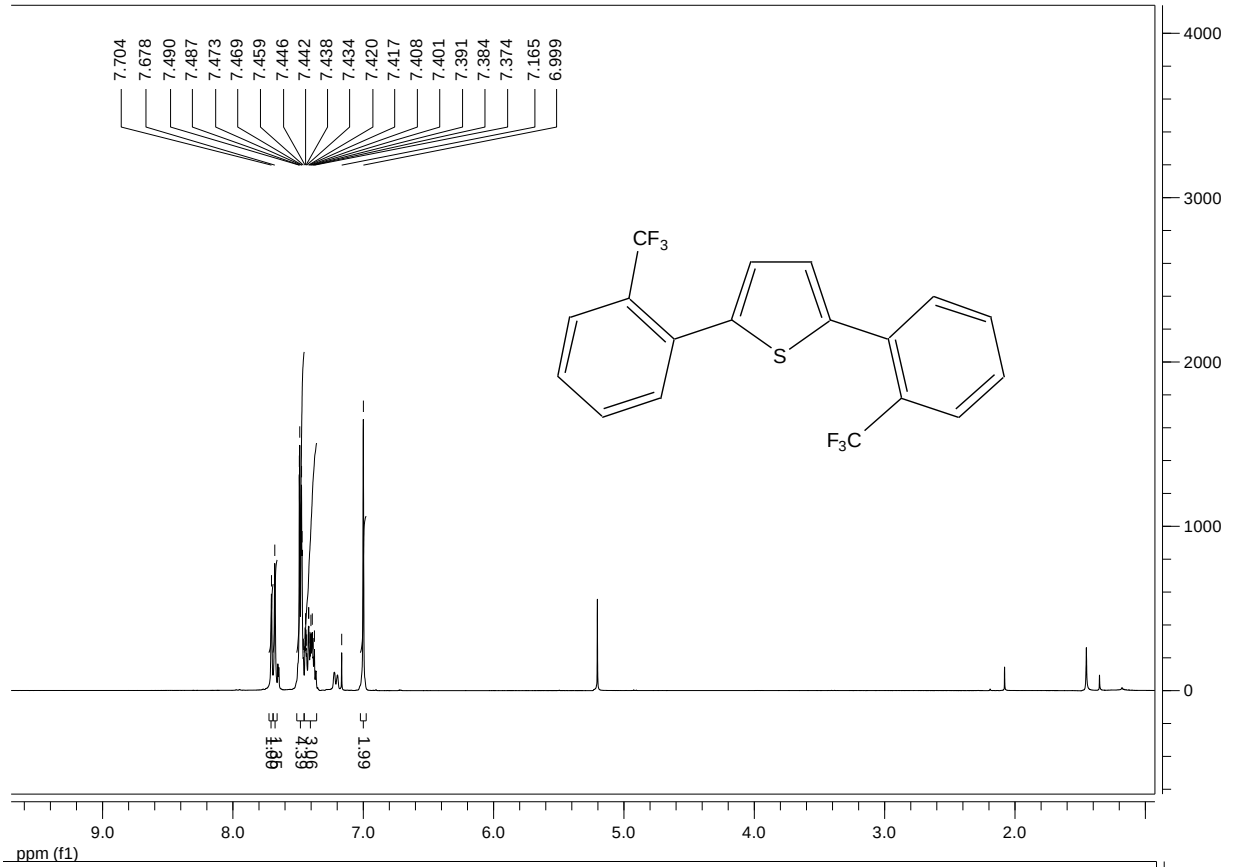
7.704
7.678
7.490
7.487
7.473
7.469
7.459
7.446
7.442
7.438
7.434
7.420
7.417
7.408
7.401
7.391
7.384
7.374
7.165
6.999
CF3
S
F3C
1.00
3.06
1.99
4000
3000
2000
1000
0
9.0
8.0
7.0
6.0
5.0
4.0
3.0
2.0
ppm (f1)

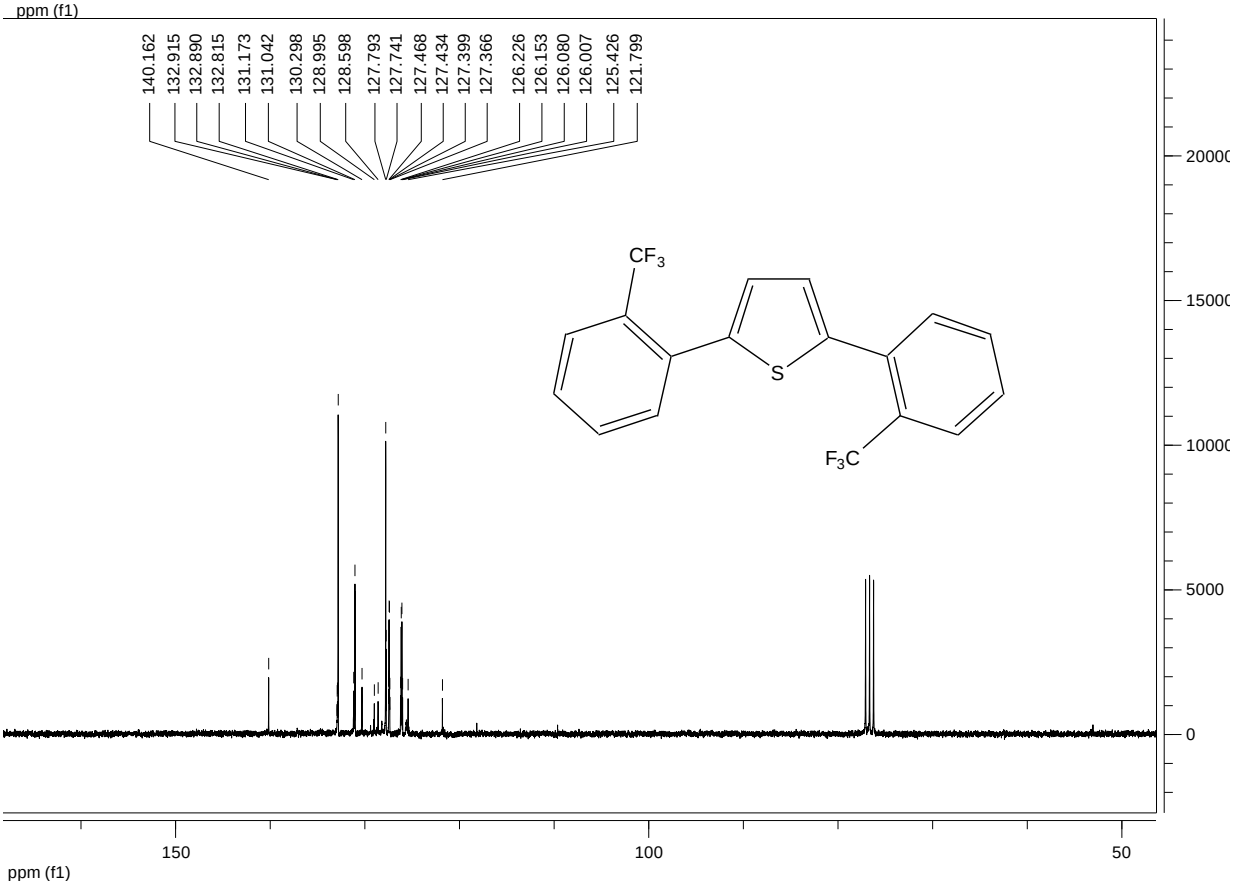
140.162
132.915
132.890
132.815
131.173
131.042
130.298
128.995
128.598
127.793
127.741
127.468
127.434
127.399
127.366
126.226
126.153
126.080
126.007
125.426
121.799
CF3
S
F3C
20000
15000
10000
5000
0
150
100
50
ppm (f1)

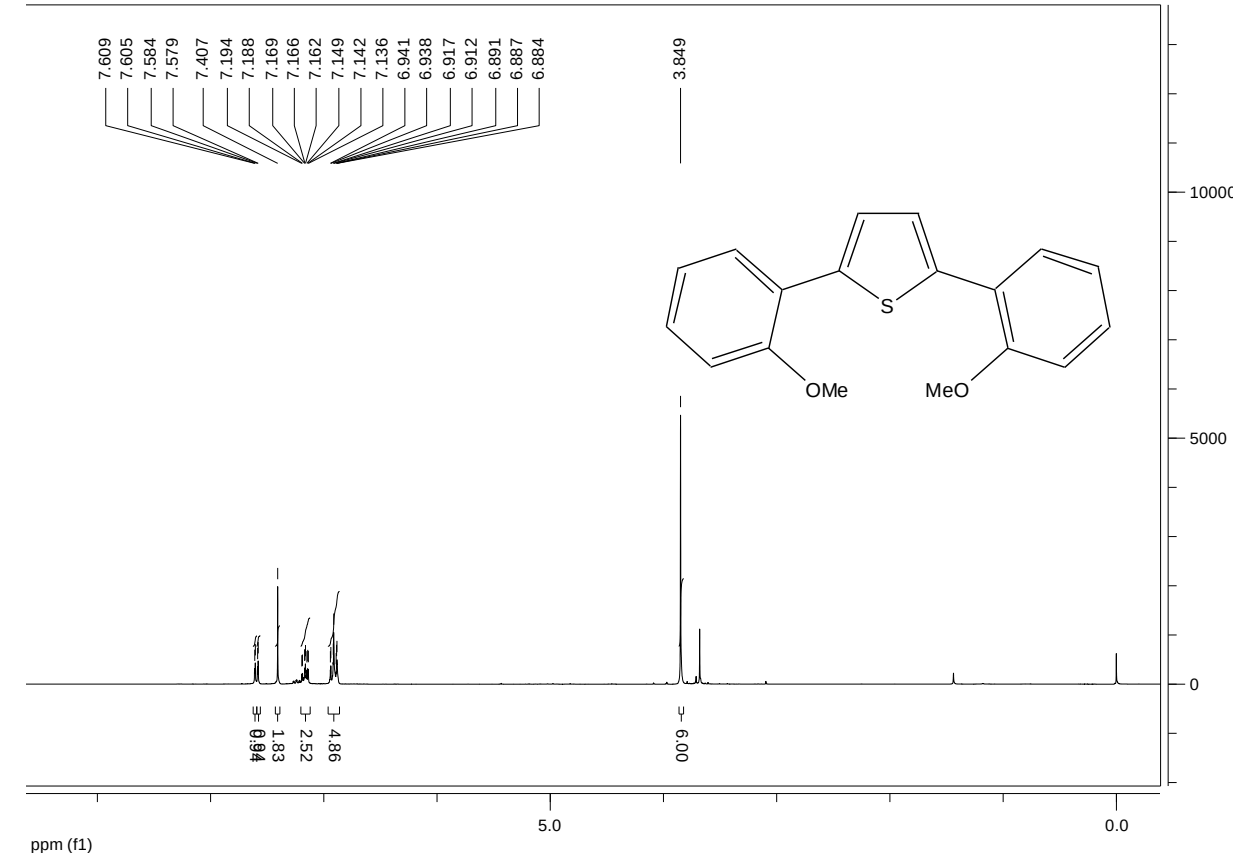
7.609
7.605
7.584
7.579
7.407
7.194
7.188
7.169
7.166
7.162
7.149
7.142
7.136
6.941
6.938
6.917
6.912
6.891
6.887
6.884
3.849
S
OMe
MeO
10000
5000
0
0.94
1.83
2.52
4.86
6.00
5.0
0.0
ppm (f1)

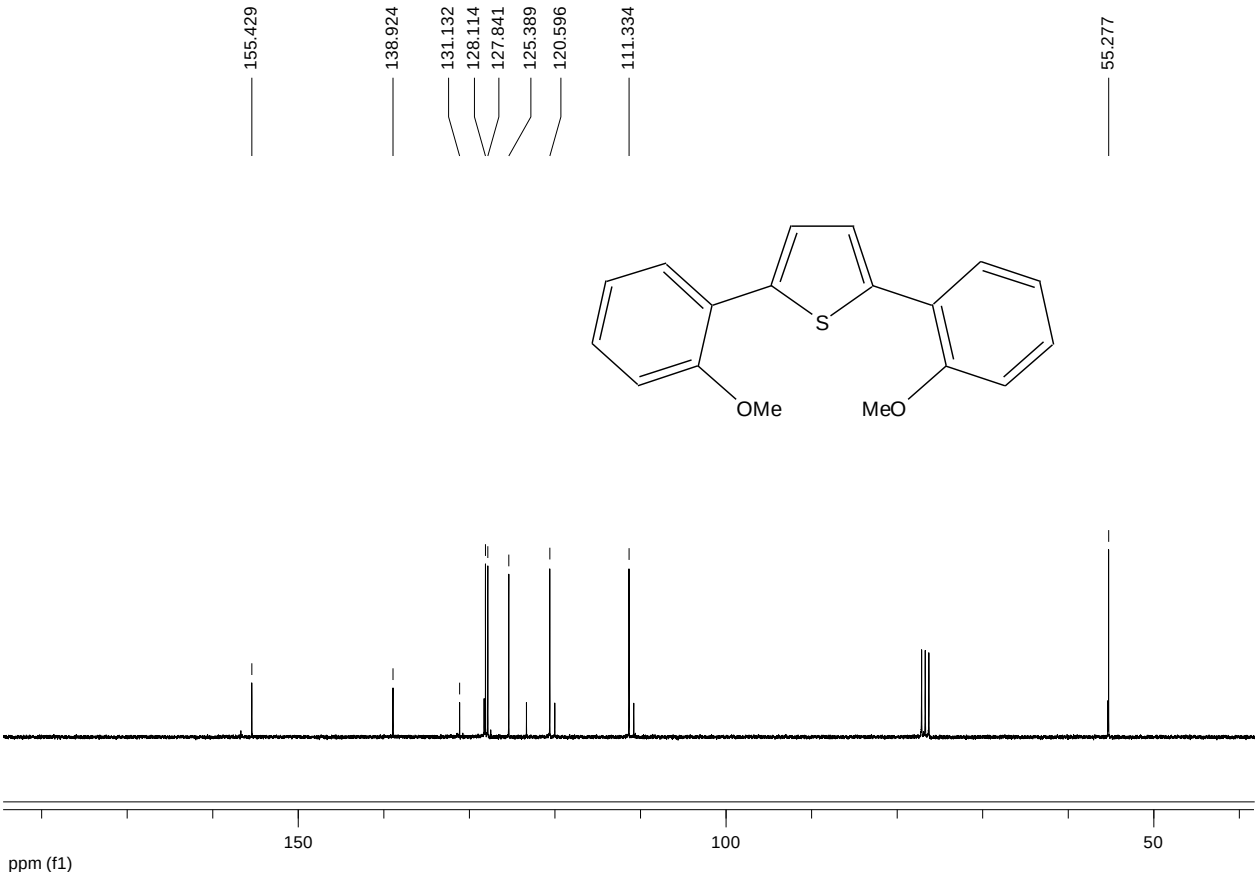
155.429
138.924
131.132
128.114
127.841
125.389
120.596
111.334
55.277
S
OMe
MeO
150
100
50
ppm (f1)

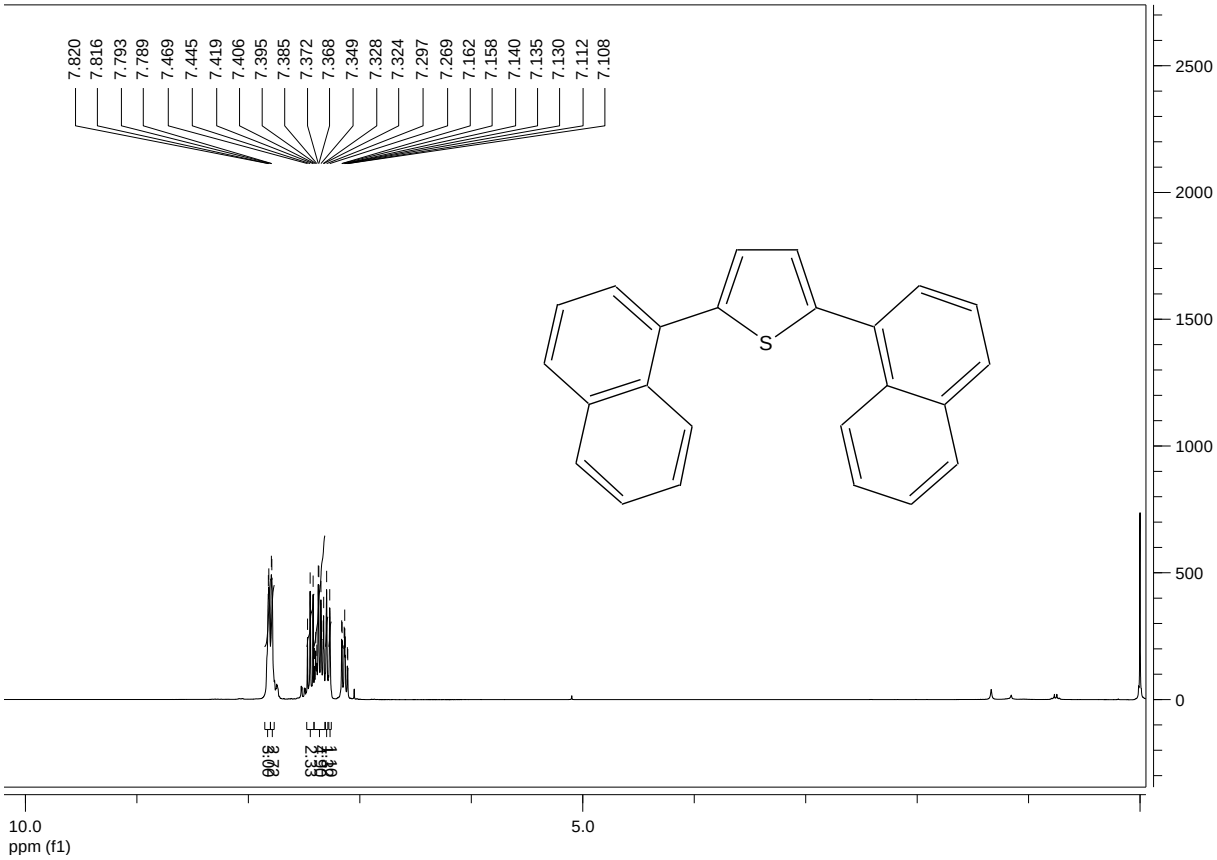
7.820
7.816
7.793
7.789
7.469
7.445
7.419
7.406
7.395
7.385
7.372
7.368
7.349
7.328
7.324
7.297
7.269
7.162
7.158
7.140
7.135
7.130
7.112
7.108
S
2500
2000
1500
1000
500
0
10.0
5.0
ppm (f1)

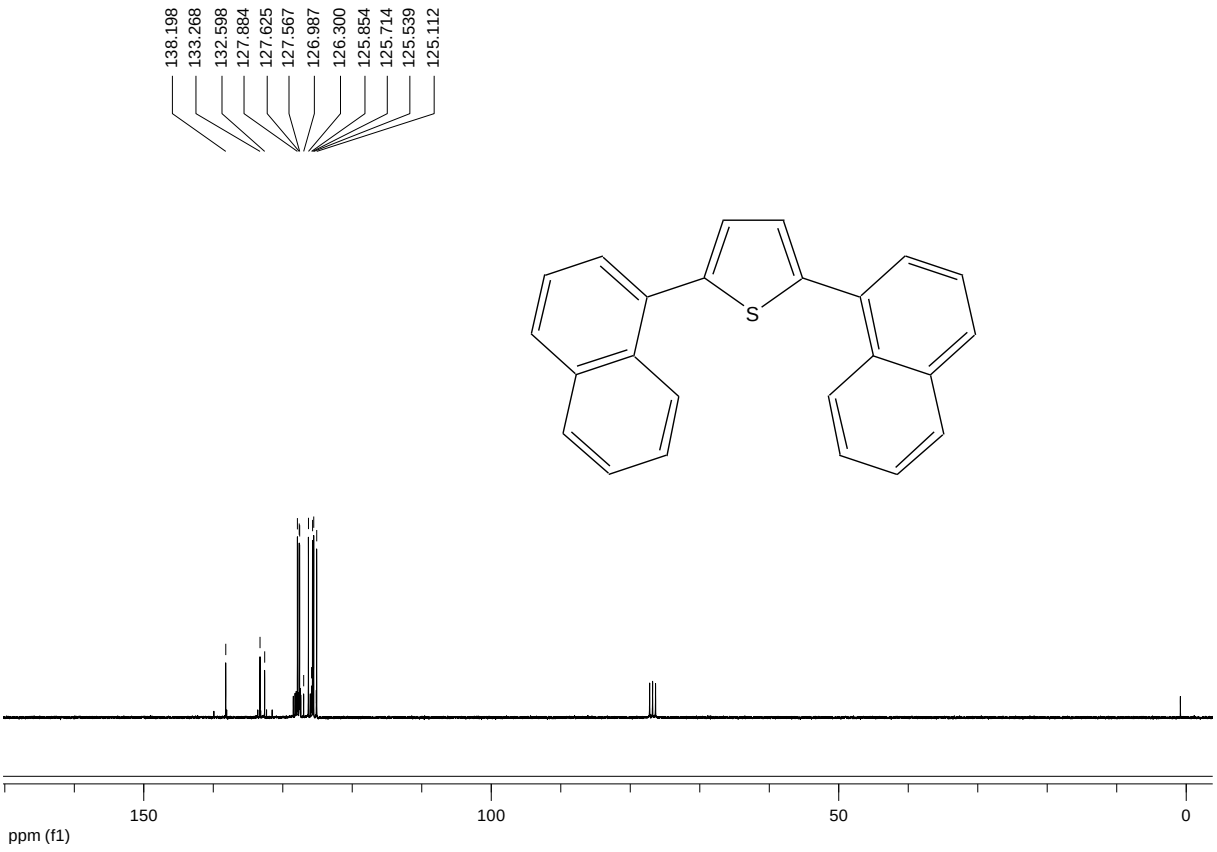
138.198
133.268
132.598
127.884
127.625
127.567
126.987
126.300
125.854
125.714
125.539
125.112
S
150
100
50
0
ppm (f1)

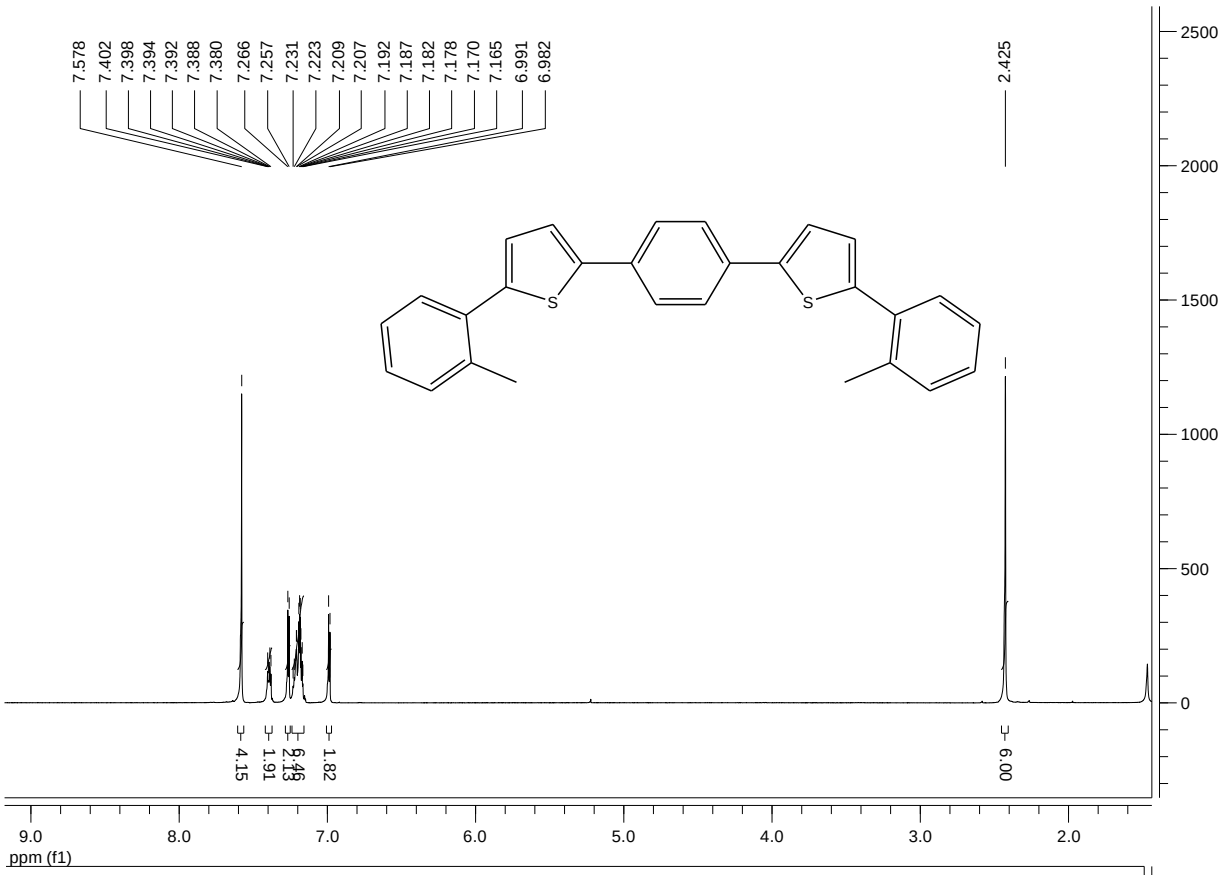
7.578
7.402
7.398
7.394
7.392
7.388
7.380
7.266
7.257
7.231
7.223
7.209
7.207
7.192
7.187
7.182
7.178
7.170
7.165
6.991
6.982
2.425
S
S
4.15
1.91
2.48
2.45
2.43
1.82
6.00
2500
2000
1500
1000
500
0
9.0
8.0
7.0
6.0
5.0
4.0
3.0
2.0
ppm (f1)

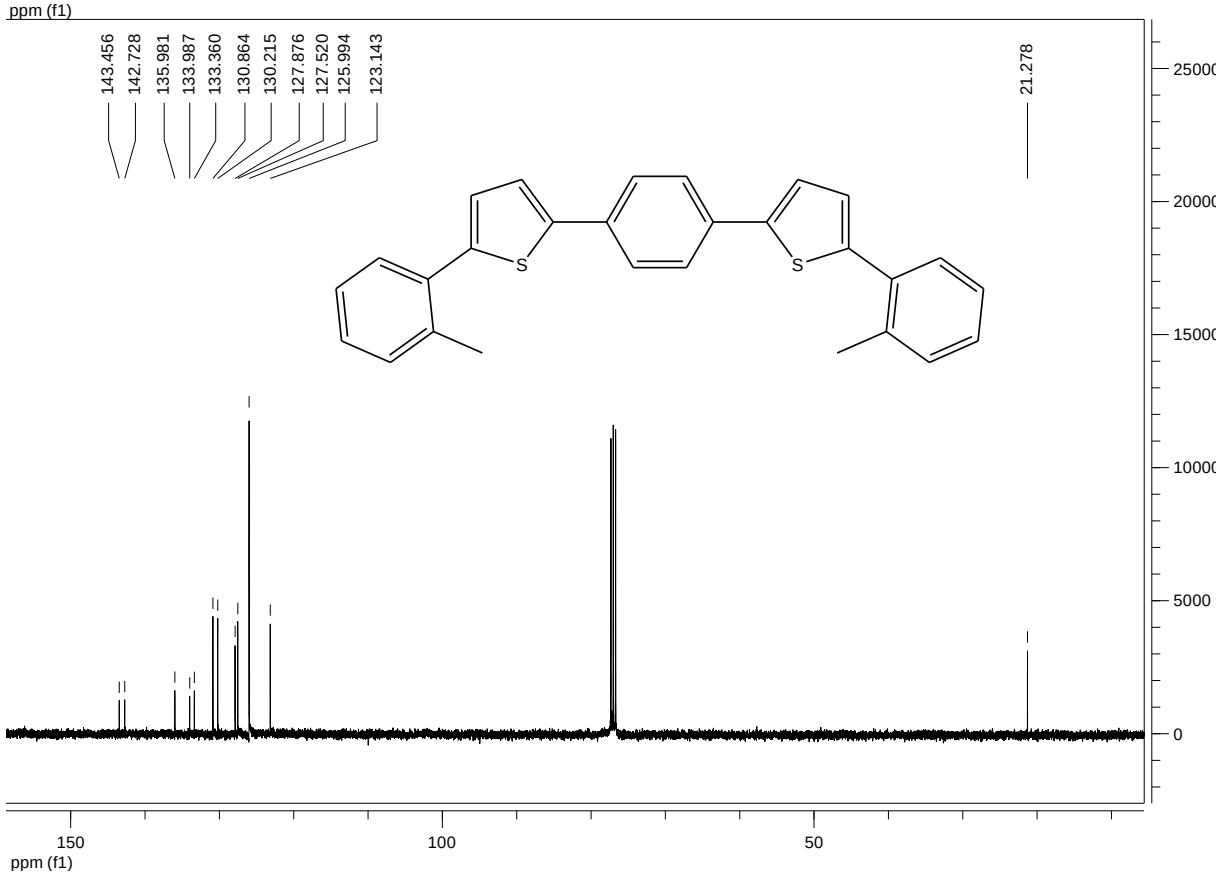
143.456
142.728
135.981
133.987
133.360
130.864
130.215
127.876
127.520
125.994
123.143
21.278
S
S
25000
20000
15000
10000
5000
0
150
100
50
ppm (f1)

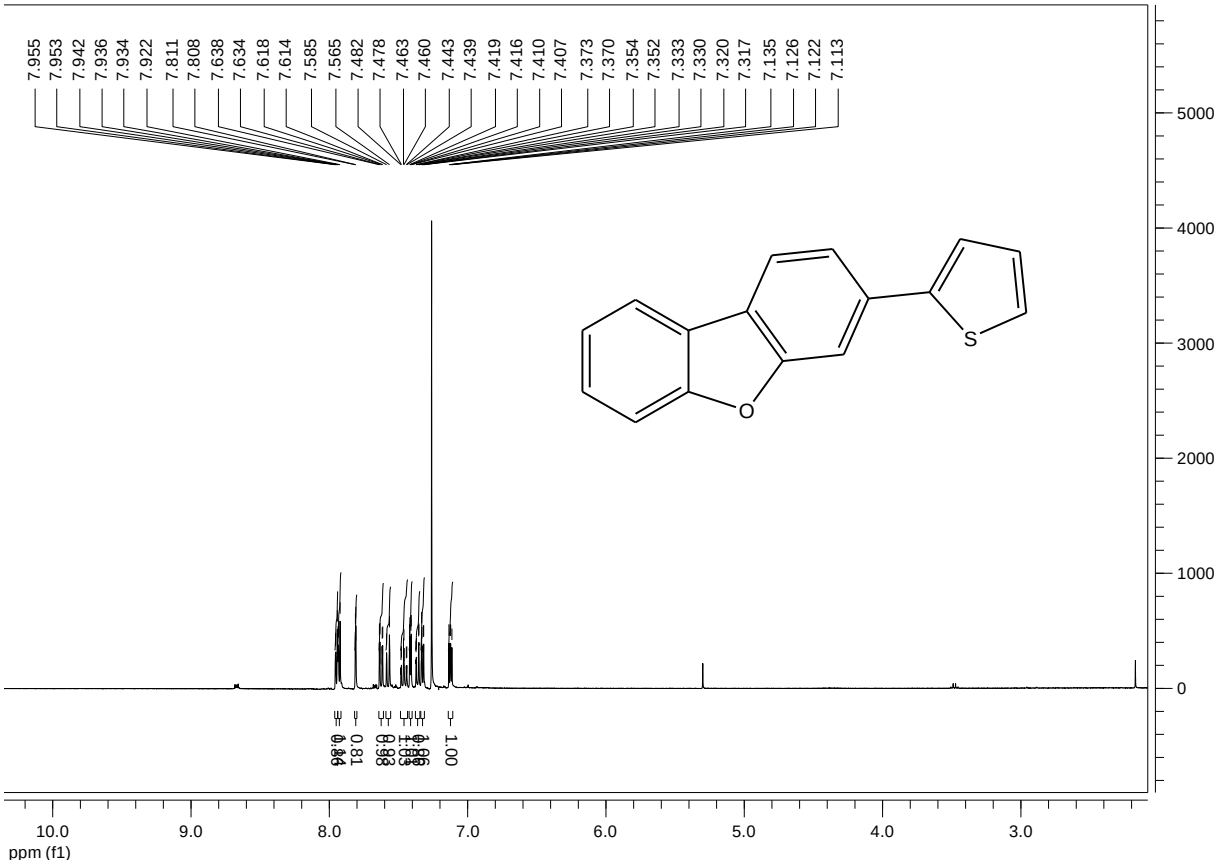
7.955
7.953
7.942
7.936
7.934
7.922
7.811
7.808
7.638
7.634
7.618
7.614
7.585
7.565
7.482
7.478
7.463
7.460
7.443
7.439
7.419
7.416
7.410
7.407
7.373
7.370
7.354
7.352
7.333
7.330
7.320
7.317
7.135
7.126
7.122
7.113
5000
4000
3000
2000
1000
0
S
O
1.00
10.0
9.0
8.0
7.0
6.0
5.0
4.0
3.0
ppm (f1)

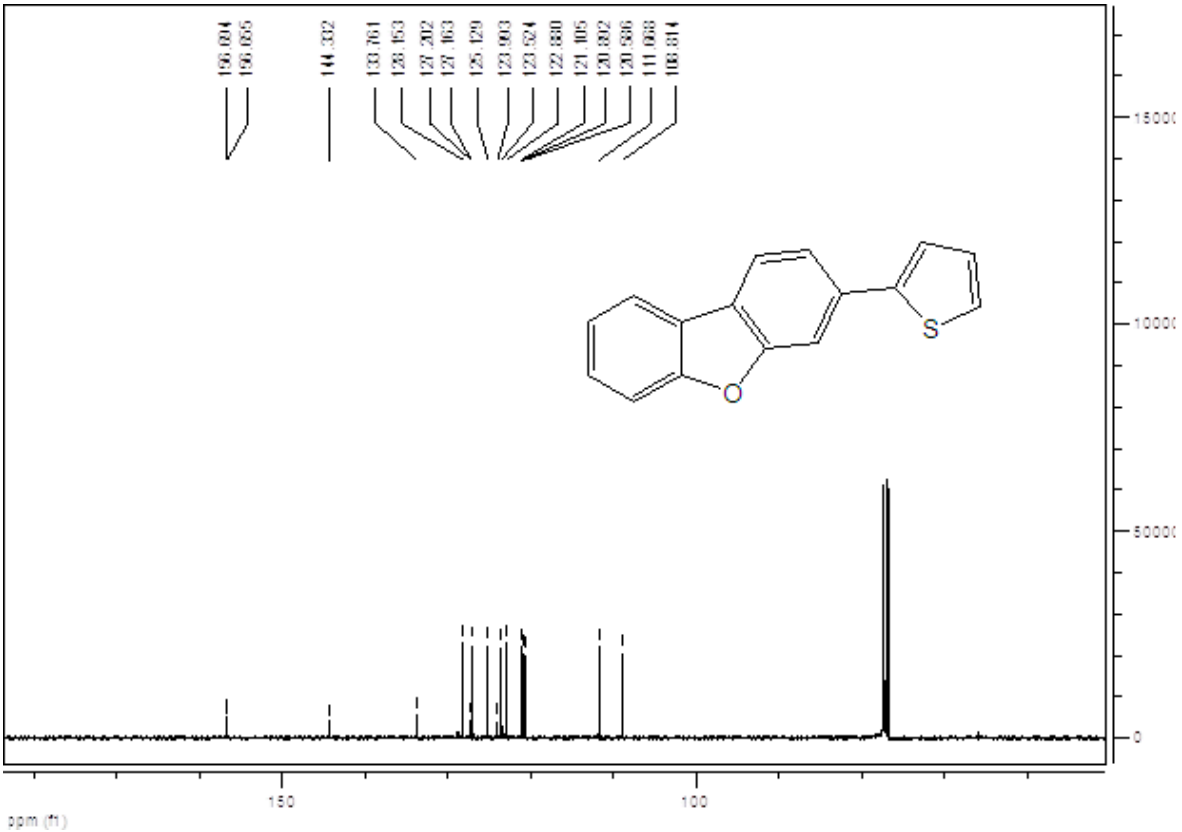
156.6014
156.0035
144.3332
133.7761
128.1453
127.2082
127.1663
125.1299
123.9903
123.5224
122.3880
121.1105
120.8802
120.5586
111.0668
108.8114
S
O
150
100
ppm (f1)

X. Crystal Data

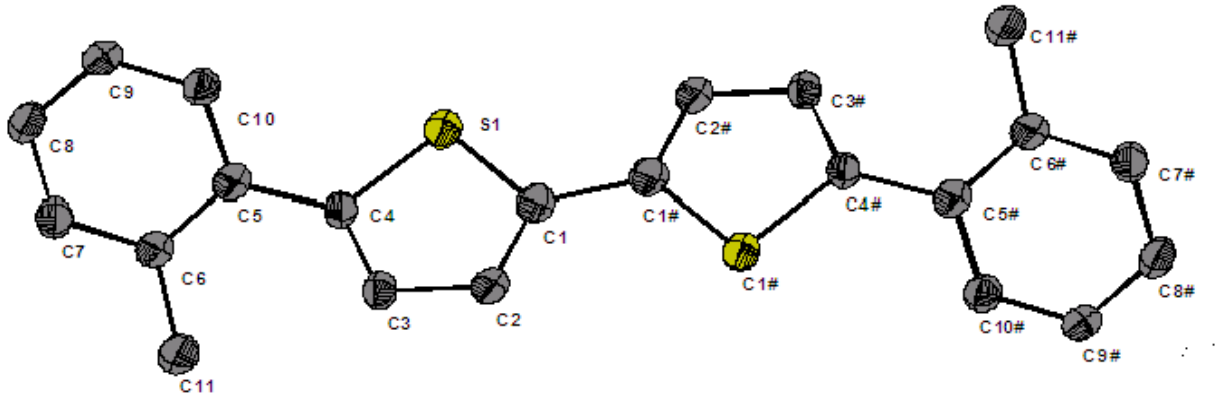

Identification code	GDOE079, Greg733
Device Type	Nonius KappaCCD
Empirical formula	C22 H18 S2
Formula weight	346.48
Temperature	123(2) K
Wavelength	0.71073 A
Crystal system, space group	Triclinic, P -1
Unit cell dimensions	a = 7.397(4) A alpha = 90.06(2) deg.
	b = 8.130(5) A beta = 94.98(4) deg.
	c = 14.655(9) A gamma = 97.25(4) deg.
Volume	870.9(9) A^3
Z, Calculated density	2, 1.321 Mg/m^3
Absorption coefficient	0.305 mm^-1
F(000)	364
Crystal size	0.67 x 0.11 x 0.04 mm

Theta range for data collection	2.79 to 27.69 deg.
Limiting indices	-7<=h<=8, -9<=k<=7, -14<=l<=17
Reflections collected / unique	4483 / 2746 [R(int) = 0.0835]
Completeness to theta = 27.69	67.3 %
Absorption correction	Semi-empirical from equivalents
Max. and min. transmission	0.99000 and 0.81845
Refinement method	Full-matrix least-squares on F^2
Data / restraints / parameters	2746 / 0 / 219
Goodness-of-fit on F^2	0.988
Final R indices [I>2sigma(I)]	R1 = 0.0744, wR2 = 0.1712
R indices (all data)	R1 = 0.1753, wR2 = 0.2130
Largest diff. peak and hole	0.303 and -0.322 e.A^-3

Atomic coordinates

	x	y	z	U(eq)
C(11)	2020(9)	9246(9)	8934(5)	59(2)
C(4)	2463(8)	9669(8)	6893(4)	42(2)
C(2)	69(8)	10935(8)	6197(4)	45(2)
C(9)	6977(9)	8341(8)	7757(5)	48(2)
C(6)	3777(8)	9002(8)	8486(5)	45(2)
C(10)	5573(8)	8829(8)	7202(5)	47(2)
C(8)	6818(9)	8188(8)	8688(5)	54(2)
C(3)	1204(8)	10767(8)	7007(4)	44(2)
C(7)	5217(9)	8519(8)	9039(5)	51(2)
C(21)	-921(10)	5058(8)	2818(5)	51(2)
C(16)	800(8)	5602(8)	2523(5)	44(2)
S(2)	2433(2)	4394(2)	4144(1)	54(1)
C(18)	-616(9)	5993(8)	1017(5)	49(2)
C(20)	-2481(9)	4995(8)	2202(5)	50(2)
C(5)	3936(8)	9165(8)	7532(5)	44(2)
C(12)	4538(8)	5331(8)	4580(4)	42(2)
C(17)	949(9)	6059(8)	1606(5)	48(2)

C(22)	2755(8)	6559(9)	1219(5)	55(2)
C(14)	3986(8)	6874(9)	3259(4)	47(2)
C(15)	2445(9)	5746(8)	3221(4)	46(2)
C(19)	-2345(9)	5458(8)	1313(5)	54(2)
S(1)	2223(2)	8907(2)	5766(1)	52(1)
C(1)	454(8)	10042(8)	5463(4)	45(2)
C(13)	5173(10)	6574(9)	4060(5)	54(2)

Bond lengths [A]

C(11)-C(6)	1.540(9)
C(11)-H(11A)	0.98
C(11)-H(11B)	0.98
C(11)-H(11C)	0.98
C(4)-C(3)	1.389(9)
C(4)-C(5)	1.472(8)
C(4)-S(1)	1.751(6)
C(2)-C(1)	1.367(8)
C(2)-C(3)	1.410(8)
C(2)-H(2A)	0.95
C(9)-C(10)	1.362(9)
C(9)-C(8)	1.384(9)
C(9)-H(9A)	0.95
C(6)-C(7)	1.379(9)
C(6)-C(5)	1.419(9)
C(10)-C(5)	1.400(9)
C(10)-H(10A)	0.95
C(8)-C(7)	1.387(9)
C(8)-H(8A)	0.95
C(3)-H(3A)	0.95
C(7)-H(7A)	0.95
C(21)-C(20)	1.397(9)
C(21)-C(16)	1.399(9)
C(21)-H(21A)	0.95
C(16)-C(17)	1.405(9)
C(16)-C(15)	1.513(9)
S(2)-C(12)	1.715(6)
S(2)-C(15)	1.743(7)
C(18)-C(17)	1.377(9)
C(18)-C(19)	1.403(9)
C(18)-H(18A)	0.95
C(20)-C(19)	1.366(9)
C(20)-H(20A)	0.95
C(12)-C(13)	1.329(9)
C(12)-C(12)#1	1.489(13)
C(17)-C(22)	1.505(9)
C(22)-H(22C)	0.98
C(22)-H(22B)	0.98
C(22)-H(22A)	0.98
C(14)-C(15)	1.368(9)
C(14)-C(13)	1.443(9)
C(14)-H(14A)	0.95
C(19)-H(19A)	0.95
S(1)-C(1)	1.722(7)
C(1)-C(1)#2	1.459(13)
C(13)-H(13A)	0.95

Angles [deg]

C(6)-C(11)-H(11A)	109.5
C(6)-C(11)-H(11B)	109.5
H(11A)-C(11)-H(11B)	109.5
C(6)-C(11)-H(11C)	109.5
H(11A)-C(11)-H(11C)	109.5
H(11B)-C(11)-H(11C)	109.5
C(3)-C(4)-C(5)	130.8(6)
C(3)-C(4)-S(1)	110.4(5)
C(5)-C(4)-S(1)	118.7(5)
C(1)-C(2)-C(3)	114.8(6)
C(1)-C(2)-H(2A)	122.6
C(3)-C(2)-H(2A)	122.6
C(10)-C(9)-C(8)	119.7(6)
C(10)-C(9)-H(9A)	120.2
C(8)-C(9)-H(9A)	120.2

C(7)-C(6)-C(5)	119.1(6)
C(7)-C(6)-C(11)	117.8(6)
C(5)-C(6)-C(11)	123.0(6)
C(9)-C(10)-C(5)	122.6(7)
C(9)-C(10)-H(10A)	118.7
C(5)-C(10)-H(10A)	118.7
C(9)-C(8)-C(7)	119.3(6)
C(9)-C(8)-H(8A)	120.4
C(7)-C(8)-H(8A)	120.4
C(4)-C(3)-C(2)	112.0(6)
C(4)-C(3)-H(3A)	124
C(2)-C(3)-H(3A)	124
C(6)-C(7)-C(8)	121.8(7)
C(6)-C(7)-H(7A)	119.1
C(8)-C(7)-H(7A)	119.1
C(20)-C(21)-C(16)	119.8(7)
C(20)-C(21)-H(21A)	120.1
C(16)-C(21)-H(21A)	120.1
C(21)-C(16)-C(17)	119.7(6)
C(21)-C(16)-C(15)	118.3(6)
C(17)-C(16)-C(15)	122.0(6)
C(12)-S(2)-C(15)	90.9(3)
C(17)-C(18)-C(19)	121.4(7)
C(17)-C(18)-H(18A)	119.3
C(19)-C(18)-H(18A)	119.3
C(19)-C(20)-C(21)	120.7(7)
C(19)-C(20)-H(20A)	119.7
C(21)-C(20)-H(20A)	119.7
C(10)-C(5)-C(6)	117.5(6)
C(10)-C(5)-C(4)	119.9(6)

C(6)-C(5)-C(4)	122.6(6)
C(13)-C(12)-C(12)#1	128.2(7)
C(13)-C(12)-S(2)	111.8(5)
C(12)#1-C(12)-S(2)	120.0(6)
C(18)-C(17)-C(16)	119.1(6)
C(18)-C(17)-C(22)	117.8(6)
C(16)-C(17)-C(22)	123.1(6)
C(17)-C(22)-H(22C)	109.5
C(17)-C(22)-H(22B)	109.5
H(22C)-C(22)-H(22B)	109.5
C(17)-C(22)-H(22A)	109.5
H(22C)-C(22)-H(22A)	109.5
H(22B)-C(22)-H(22A)	109.5
C(15)-C(14)-C(13)	109.4(6)
C(15)-C(14)-H(14A)	125.3
C(13)-C(14)-H(14A)	125.3
C(14)-C(15)-C(16)	128.5(6)
C(14)-C(15)-S(2)	112.6(5)
C(16)-C(15)-S(2)	118.8(5)
C(20)-C(19)-C(18)	119.4(7)
C(20)-C(19)-H(19A)	120.3
C(18)-C(19)-H(19A)	120.3
C(1)-S(1)-C(4)	92.3(3)
C(2)-C(1)-C(1)#2	128.1(8)
C(2)-C(1)-S(1)	110.6(5)
C(1)#2-C(1)-S(1)	121.3(7)
C(12)-C(13)-C(14)	115.3(7)
C(12)-C(13)-H(13A)	122.4
C(14)-C(13)-H(13A)	122.4

Anisotropicdisplacement parameters

	U11	U22	U33	U23	U13	U12
C(11)	47(4)	76(5)	55(5)	8(4)	1(3)	11(4)
C(4)	37(4)	51(4)	36(4)	1(3)	-3(3)	4(3)
C(2)	36(4)	49(4)	48(5)	1(4)	0(3)	6(3)
C(9)	38(4)	54(5)	53(5)	0(4)	3(3)	13(3)
C(6)	39(4)	49(4)	47(5)	-1(3)	2(3)	5(3)
C(10)	43(4)	52(5)	45(4)	6(3)	1(3)	8(3)

C(8)	41(4)	61(5)	58(5)	1(4)	-10(3)	12(4)
C(3)	39(4)	52(4)	38(4)	10(3)	-3(3)	3(3)
C(7)	46(4)	60(5)	44(4)	3(3)	-5(3)	5(4)
C(21)	62(5)	45(4)	48(5)	0(3)	0(4)	12(4)
C(16)	37(4)	43(4)	53(5)	2(3)	0(3)	10(3)
S(2)	44(1)	61(1)	55(1)	5(1)	-1(1)	5(1)
C(18)	51(5)	56(5)	44(4)	2(3)	5(3)	17(3)
C(20)	31(4)	54(5)	64(5)	-2(4)	2(3)	5(3)
C(5)	38(4)	44(4)	49(5)	3(3)	1(3)	4(3)
C(12)	38(4)	47(4)	41(4)	-1(3)	6(3)	2(3)
C(17)	39(4)	54(5)	50(5)	-2(4)	-1(3)	9(3)
C(22)	41(4)	71(5)	51(5)	6(4)	0(3)	5(4)
C(14)	25(4)	70(5)	46(4)	-6(4)	-1(3)	11(3)
C(15)	41(4)	51(4)	50(5)	-1(3)	11(3)	13(3)
C(19)	41(4)	59(5)	61(5)	-8(4)	-8(4)	11(4)
S(1)	46(1)	59(1)	49(1)	-3(1)	-5(1)	14(1)
C(1)	41(4)	43(4)	49(4)	1(4)	0(3)	3(3)
C(13)	53(5)	52(5)	55(5)	-1(4)	4(4)	6(4)

Hydrogen Coordinate

	x	y	z	U(eq)
H(11A)	958	8666	8568	89
H(11B)	1902	10432	8964	89
H(11C)	2082	8797	9554	89
H(2A)	-889	11614	6164	53
H(9A)	8061	8108	7507	57
H(10A)	5710	8945	6566	56
H(8A)	7794	7859	9082	65
H(3A)	1117	11338	7565	52
H(7A)	5111	8410	9678	61
H(21A)	-1029	4733	3435	62
H(18A)	-523	6316	399	59
H(20A)	-3649	4626	2404	60
H(22C)	2619	6357	556	82
H(22B)	3672	5905	1505	82
H(22A)	3149	7740	1344	82
H(14A)	4237	7723	2827	56
H(19A)	-3411	5417	898	65
H(13A)	6325	7219	4205	64

Torsion angles [deg]

C(8)-C(9)-C(10)-C(5)	-1.0(10)
C(10)-C(9)-C(8)-C(7)	0.6(10)
C(5)-C(4)-C(3)-C(2)	177.6(6)
S(1)-C(4)-C(3)-C(2)	1.2(7)
C(1)-C(2)-C(3)-C(4)	-1.9(8)
C(5)-C(6)-C(7)-C(8)	0.0(10)
C(11)-C(6)-C(7)-C(8)	176.7(6)
C(9)-C(8)-C(7)-C(6)	-0.2(10)
C(20)-C(21)-C(16)-C(17)	-0.8(10)
C(20)-C(21)-C(16)-C(15)	176.6(6)
C(16)-C(21)-C(20)-C(19)	0.0(10)
C(9)-C(10)-C(5)-C(6)	0.8(10)
C(9)-C(10)-C(5)-C(4)	179.3(6)
C(7)-C(6)-C(5)-C(10)	-0.3(9)
C(11)-C(6)-C(5)-C(10)	176.8(6)
C(7)-C(6)-C(5)-C(4)	179.8(6)
C(11)-C(6)-C(5)-C(4)	3.3(10)
C(3)-C(4)-C(5)-C(10)	144.9(7)
S(1)-C(4)-C(5)-C(10)	31.2(8)
C(3)-C(4)-C(5)-C(6)	35.0(11)
S(1)-C(4)-C(5)-C(6)	148.9(5)
C(15)-S(2)-C(12)-C(13)	0.3(6)
C(15)-S(2)-C(12)-C(12)#1	176.7(7)
C(19)-C(18)-C(17)-C(16)	-0.9(10)

C(19)-C(18)-C(17)-C(22)	176.7(6)
C(21)-C(16)-C(17)-C(18)	1.2(10)
C(15)-C(16)-C(17)-C(18)	176.1(6)
C(21)-C(16)-C(17)-C(22)	176.2(6)
C(15)-C(16)-C(17)-C(22)	6.5(10)
C(13)-C(14)-C(15)-C(16)	178.3(6)
C(13)-C(14)-C(15)-S(2)	1.1(7)
C(21)-C(16)-C(15)-C(14)	146.1(7)
C(17)-C(16)-C(15)-C(14)	31.3(10)
C(21)-C(16)-C(15)-S(2)	30.9(8)
C(17)-C(16)-C(15)-S(2)	151.7(5)
C(12)-S(2)-C(15)-C(14)	-0.9(5)
C(12)-S(2)-C(15)-C(16)	178.3(5)
C(21)-C(20)-C(19)-C(18)	0.3(10)
C(17)-C(18)-C(19)-C(20)	0.1(10)
C(3)-C(4)-S(1)-C(1)	-0.3(5)
C(5)-C(4)-S(1)-C(1)	177.1(5)
C(3)-C(2)-C(1)-C(1)#2	179.7(8)
C(3)-C(2)-C(1)-S(1)	1.6(7)
C(4)-S(1)-C(1)-C(2)	-0.7(5)
C(4)-S(1)-C(1)-C(1)#2	179.6(7)
C(12)#1-C(12)-C(13)-C(14)	177.0(8)
S(2)-C(12)-C(13)-C(14)	0.2(8)
C(15)-C(14)-C(13)-C(12)	-0.9(8)

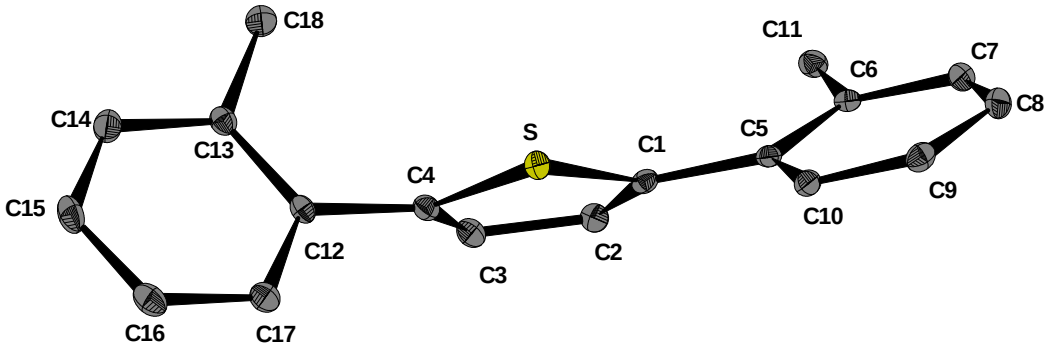

Identification code	Greg1255, GDOE086
Device Type	Nonius KappaCCD
Empirical formula	C18 H16 S
Formula weight	264.37
Temperature	123(2) K
Wavelength	0.71073 A
Crystal system, space group	Monoclinic, P 21/n
Unit cell dimensions	a = 7.6432(5) A alpha = 90 deg. b = 11.8553(14) A beta = 99.758(5) deg. c = 15.5117(13) A gamma = 90 deg.
Volume	1385.2(2) A^3
Z, Calculated density	4, 1.268 Mg/m^3
Absorption coefficient	0.216 mm^-1
F(000)	560
Crystal size	0.60 x 0.20 x 0.12 mm
Theta range for data collection	2.66 to 28.00 deg.
Limiting indices	-10<=h<=8, -15<=k<=14, -18<=l<=20

Reflections collected / unique	9613 / 3277 [R(int) = 0.0729]
Completeness to theta = 28.00	98.10%
Absorption correction	Semi-empirical from equivalents
Max. and min. transmission	0.9745 and 0.8812
Refinement method	Full-matrix least-squares on F^2
Data / restraints / parameters	3277 / 0 / 175
Goodness-of-fit on F^2	0.869
Final R indices [I>2sigma(I)]	R1 = 0.0429, wR2 = 0.0741
R indices (all data)	R1 = 0.1084, wR2 = 0.0871
Extinction coefficient	0.0054(8)
Largest diff. peak and hole	0.304 and -0.306 e.A^-3

Atomic coordinates

	x	y	z	U(eq)
C(1)	7697(2)	5401(2)	1436(1)	20(1)
C(2)	7169(2)	6046(2)	2072(1)	23(1)
C(3)	8174(2)	7046(2)	2254(1)	24(1)
C(4)	9466(2)	7175(2)	1758(1)	22(1)
C(5)	7039(2)	4308(2)	1053(1)	19(1)
C(6)	5224(2)	4022(2)	903(1)	19(1)
C(7)	4735(3)	2985(2)	511(1)	25(1)
C(8)	5945(3)	2249(2)	254(1)	28(1)
C(9)	7724(3)	2535(2)	398(1)	26(1)
C(10)	8254(2)	3547(2)	794(1)	22(1)
C(11)	3802(2)	4792(2)	1129(1)	25(1)
C(12)	10741(2)	8111(2)	1733(1)	21(1)
C(13)	10152(2)	9157(2)	1376(1)	23(1)
C(14)	11400(3)	10014(2)	1370(1)	30(1)
C(15)	13184(3)	9844(2)	1699(1)	33(1)

C(16)	13747(3)	8810(2)	2036(1)	33(1)
C(17)	12544(2)	7947(2)	2054(1)	28(1)
C(18)	8232(2)	9353(2)	991(1)	34(1)
S	9456(1)	6042(1)	1058(1)	22(1)

Bond lengths [A] and angles [deg]

C(1)-C(2)	1.362(3)
C(1)-C(5)	1.478(3)
C(1)-S	1.7313(19)
C(2)-C(3)	1.416(3)
C(2)-H(2)	0.95
C(3)-C(4)	1.360(3)
C(3)-H(3)	0.95
C(4)-C(12)	1.481(3)
C(4)-S	1.726(2)
C(5)-C(10)	1.401(3)
C(5)-C(6)	1.409(2)
C(6)-C(7)	1.394(3)
C(6)-C(11)	1.505(3)
C(7)-C(8)	1.378(3)
C(7)-H(7)	0.95
C(8)-C(9)	1.382(3)
C(8)-H(8)	0.95
C(9)-C(10)	1.378(3)
C(9)-H(9)	0.95
C(10)-H(10)	0.95
C(11)-H(11A)	0.98
C(11)-H(11B)	0.98
C(11)-H(11C)	0.98
C(12)-C(17)	1.397(2)
C(12)-C(13)	1.402(3)
C(13)-C(14)	1.394(3)
C(13)-C(18)	1.506(3)
C(14)-C(15)	1.387(3)
C(14)-H(14)	0.95
C(15)-C(16)	1.374(3)
C(15)-H(15)	0.95
C(16)-C(17)	1.379(3)
C(16)-H(16)	0.95
C(17)-H(17)	0.95
C(18)-H(18A)	0.98
C(18)-H(18B)	0.98
C(18)-H(18C)	0.98
C(2)-C(1)-C(5)	131.37(18)
C(2)-C(1)-S	109.94(15)
C(5)-C(1)-S	118.68(15)
C(1)-C(2)-C(3)	113.42(18)
C(1)-C(2)-H(2)	123.3
C(3)-C(2)-H(2)	123.3
C(4)-C(3)-C(2)	113.74(19)
C(4)-C(3)-H(3)	123.1
C(2)-C(3)-H(3)	123.1
C(3)-C(4)-C(12)	129.96(19)
C(3)-C(4)-S	110.03(15)
C(12)-C(4)-S	119.99(14)
C(10)-C(5)-C(6)	118.69(18)
C(10)-C(5)-C(1)	118.84(16)
C(6)-C(5)-C(1)	122.41(17)
C(7)-C(6)-C(5)	117.90(18)
C(7)-C(6)-C(11)	119.06(16)
C(5)-C(6)-C(11)	123.03(18)
C(8)-C(7)-C(6)	122.71(18)
C(8)-C(7)-H(7)	118.6
C(6)-C(7)-H(7)	118.6
C(7)-C(8)-C(9)	119.24(19)
C(7)-C(8)-H(8)	120.4
C(9)-C(8)-H(8)	120.4
C(10)-C(9)-C(8)	119.49(19)
C(10)-C(9)-H(9)	120.3
C(8)-C(9)-H(9)	120.3
C(9)-C(10)-C(5)	121.95(18)
C(9)-C(10)-H(10)	119
C(5)-C(10)-H(10)	119
C(6)-C(11)-H(11A)	109.5
C(6)-C(11)-H(11B)	109.5
H(11A)-C(11)-H(11B)	109.5
C(6)-C(11)-H(11C)	109.5

H(11A)-C(11)-H(11C)	109.5
H(11B)-C(11)-H(11C)	109.5
C(17)-C(12)-C(13)	119.70(18)
C(17)-C(12)-C(4)	120.01(18)
C(13)-C(12)-C(4)	120.28(16)
C(14)-C(13)-C(12)	118.25(17)
C(14)-C(13)-C(18)	120.42(19)
C(12)-C(13)-C(18)	121.32(17)
C(15)-C(14)-C(13)	121.5(2)
C(15)-C(14)-H(14)	119.2
C(13)-C(14)-H(14)	119.2
C(16)-C(15)-C(14)	119.6(2)
C(16)-C(15)-H(15)	120.2
C(14)-C(15)-H(15)	120.2
C(15)-C(16)-C(17)	120.20(18)

C(15)-C(16)-H(16)	119.9
C(17)-C(16)-H(16)	119.9
C(16)-C(17)-C(12)	120.7(2)
C(16)-C(17)-H(17)	119.7
C(12)-C(17)-H(17)	119.7
C(13)-C(18)-H(18A)	109.5
C(13)-C(18)-H(18B)	109.5
H(18A)-C(18)-H(18B)	109.5
C(13)-C(18)-H(18C)	109.5
H(18A)-C(18)-H(18C)	109.5
H(18B)-C(18)-H(18C)	109.5
C(4)-S-C(1)	92.87(10)

Anisotropic displacement parameters

	U11	U22	U33	U23	U13	U12
C(1)	17(1)	21(1)	22(1)	5(1)	4(1)	2(1)
C(2)	20(1)	27(1)	23(1)	0(1)	7(1)	-1(1)
C(3)	24(1)	27(1)	22(1)	-6(1)	5(1)	1(1)
C(4)	22(1)	22(1)	20(1)	-3(1)	1(1)	1(1)
C(5)	22(1)	19(1)	15(1)	2(1)	1(1)	2(1)
C(6)	19(1)	22(1)	16(1)	3(1)	1(1)	2(1)
C(7)	22(1)	26(1)	28(1)	1(1)	1(1)	-3(1)
C(8)	33(1)	20(1)	31(1)	-3(1)	1(1)	0(1)
C(9)	30(1)	21(1)	28(1)	1(1)	7(1)	7(1)
C(10)	21(1)	23(1)	24(1)	3(1)	4(1)	0(1)
C(11)	20(1)	29(1)	26(1)	2(1)	2(1)	0(1)
C(12)	20(1)	24(1)	20(1)	-5(1)	4(1)	-2(1)
C(13)	24(1)	26(1)	21(1)	-4(1)	5(1)	-2(1)
C(14)	35(1)	26(1)	31(1)	-1(1)	7(1)	-3(1)
C(15)	30(1)	37(2)	34(1)	-7(1)	10(1)	-16(1)
C(16)	21(1)	45(2)	32(1)	-5(1)	3(1)	-4(1)
C(17)	24(1)	31(1)	28(1)	-2(1)	3(1)	0(1)
C(18)	31(1)	30(1)	38(1)	3(1)	-2(1)	1(1)
S	20(1)	23(1)	24(1)	-2(1)	6(1)	-1(1)

Hydrogen coordinates

	x	y	z	U(eq)
H(2)	6218	5844	2364	28
H(3)	7966	7578	2683	29
H(7)	3517	2776	417	30
H(8)	5561	1553	-18	34
H(9)	8574	2037	224	31
H(10)	9480	3735	896	27
H(11A)	2653	4580	785	38
H(11B)	4080	5573	996	38
H(11C)	3748	4723	1753	38
H(14)	11019	10730	1136	36
H(15)	14011	10440	1691	40
H(16)	14969	8688	2258	39
H(17)	12945	7233	2287	33
H(18A)	7806	8736	590	51
H(18B)	8116	10069	671	51
H(18C)	7525	9383	1462	51

Torsion angles [deg]

C(5)-C(1)-C(2)-C(3)	179.55(17)	C(3)-C(4)-C(12)-C(17)	110.1(2)
S-C(1)-C(2)-C(3)	-0.1(2)	S-C(4)-C(12)-C(17)	-71.7(2)
C(1)-C(2)-C(3)-C(4)	0.3(2)	C(3)-C(4)-C(12)-C(13)	-71.0(3)
C(2)-C(3)-C(4)-C(12)	177.94(18)	S-C(4)-C(12)-C(13)	107.20(19)
C(2)-C(3)-C(4)-S	-0.4(2)	C(17)-C(12)-C(13)-C(14)	-1.3(3)
C(2)-C(1)-C(5)-C(10)	-145.5(2)	C(4)-C(12)-C(13)-C(14)	179.77(18)
S-C(1)-C(5)-C(10)	34.1(2)	C(17)-C(12)-C(13)-C(18)	177.54(18)
C(2)-C(1)-C(5)-C(6)	37.3(3)	C(4)-C(12)-C(13)-C(18)	-1.4(3)
S-C(1)-C(5)-C(6)	-143.08(16)	C(12)-C(13)-C(14)-C(15)	0.7(3)
C(10)-C(5)-C(6)-C(7)	0.7(3)	C(18)-C(13)-C(14)-C(15)	-178.21(19)
C(1)-C(5)-C(6)-C(7)	177.89(17)	C(13)-C(14)-C(15)-C(16)	0.3(3)
C(10)-C(5)-C(6)-C(11)	-178.09(17)	C(14)-C(15)-C(16)-C(17)	-0.5(3)
C(1)-C(5)-C(6)-C(11)	-0.9(3)	C(15)-C(16)-C(17)-C(12)	-0.2(3)
C(5)-C(6)-C(7)-C(8)	-1.2(3)	C(13)-C(12)-C(17)-C(16)	1.1(3)
C(11)-C(6)-C(7)-C(8)	177.60(19)	C(4)-C(12)-C(17)-C(16)	-179.98(18)
C(6)-C(7)-C(8)-C(9)	0.8(3)	C(3)-C(4)-S-C(1)	0.25(15)
C(7)-C(8)-C(9)-C(10)	0.1(3)	C(12)-C(4)-S-C(1)	-178.25(15)
C(8)-C(9)-C(10)-C(5)	-0.6(3)	C(2)-C(1)-S-C(4)	-0.07(15)
C(6)-C(5)-C(10)-C(9)	0.2(3)	C(5)-C(1)-S-C(4)	-179.80(14)
C(1)-C(5)-C(10)-C(9)	-177.13(18)		

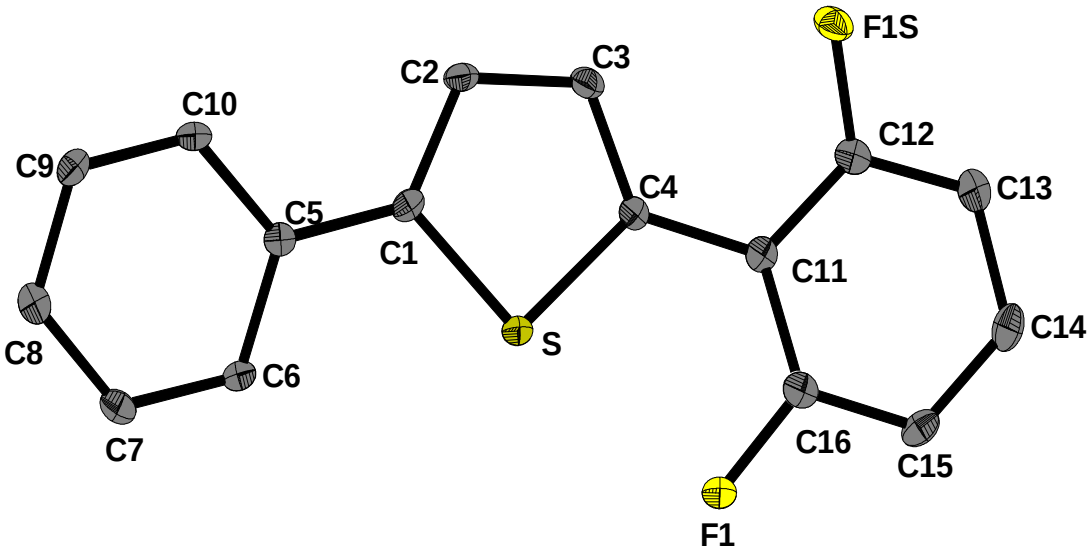

Identification code	GDOE085, Greg1257f
Device Type	Bruker X8-KappaApexII
Empirical formula	C16 H11 F S
Formula weight	254.31
Temperature	100(2) K
Wavelength	0.71073 A
Crystal system, space group	Monoclinic, P 21/n
Unit cell dimensions	a = 5.7499(5) A alpha = 90 deg. b = 7.6024(10) A beta = 94.595(4) deg. c = 27.083(3) A gamma = 90 deg.
Volume	1180.1(2) A^3
Z, Calculated density	4, 1.431 Mg/m^3
Absorption coefficient	0.262 mm^-1

F(000)	528
Crystal size	0.49 x 0.10 x 0.02 mm
Theta range for data collection	2.78 to 28.00 deg.
Limiting indices	-4<=h<=7, -10<=k<=9, -35<=l<=33
Reflections collected / unique	7382 / 2843 [R(int) = 0.0619]
Completeness to theta = 28.00	99.80%
Absorption correction	Semi-empirical from equivalents
Max. and min. transmission	0.9953 and 0.8828
Refinement method	Full-matrix least-squares on F^2
Data / restraints / parameters	2843 / 0 / 173
Goodness-of-fit on F^2	1.027
Final R indices [I>2sigma(I)]	R1 = 0.0500, wR2 = 0.0996
R indices (all data)	R1 = 0.0901, wR2 = 0.1154
Largest diff. peak and hole	0.336 and -0.327 e.A^-3

Atomic coordinates

	x	y	z	U(eq)
C(1)	9145(4)	6482(3)	8105(1)	17(1)
C(2)	7154(4)	5804(3)	8285(1)	21(1)
C(3)	7094(4)	6012(3)	8798(1)	22(1)
C(4)	9007(4)	6845(3)	9025(1)	17(1)
C(5)	9817(4)	6499(3)	7595(1)	17(1)
C(6)	11844(4)	7363(3)	7465(1)	19(1)
C(7)	12490(4)	7318(3)	6984(1)	22(1)
C(8)	11152(4)	6425(3)	6619(1)	22(1)
C(9)	9123(4)	5575(3)	6741(1)	22(1)

C(10)	8466(4)	5623(3)	7220(1)	19(1)
C(11)	9522(4)	7214(3)	9555(1)	19(1)
C(12)	7995(4)	6683(3)	9900(1)	22(1)
C(12S)	7995(4)	6683(3)	9900(1)	22(1)
F(1S)	6105(12)	5748(10)	9787(3)	29(2)
C(13)	8450(4)	6946(3)	10403(1)	25(1)
C(14)	10502(4)	7776(3)	10580(1)	27(1)
C(15)	12057(4)	8334(3)	10251(1)	24(1)
C(16)	11543(4)	8050(3)	9752(1)	21(1)
F(1)	13125(3)	8629(2)	9449(1)	26(1)
C(16S)	11543(4)	8050(3)	9752(1)	21(1)
S	10926(1)	7374(1)	8583(1)	20(1)

Bond lengths [A] and angles [deg]

C(1)-C(2)	1.379(3)
C(1)-C(5)	1.465(3)
C(1)-S	1.724(2)
C(2)-C(3)	1.402(3)
C(2)-H(2)	0.95
C(3)-C(4)	1.371(3)
C(3)-H(3)	0.95
C(4)-C(11)	1.469(3)
C(4)-S	1.738(2)
C(5)-C(10)	1.397(3)
C(5)-C(6)	1.406(3)
C(6)-C(7)	1.384(3)
C(6)-H(6)	0.95
C(7)-C(8)	1.380(3)
C(7)-H(7)	0.95
C(8)-C(9)	1.396(3)
C(8)-H(8)	0.95
C(9)-C(10)	1.380(3)
C(9)-H(9)	0.95
C(10)-H(10)	0.95
C(11)-C(16)	1.393(3)
C(11)-C(12)	1.394(3)
C(12)-C(13)	1.380(3)
C(12)-H(12)	0.95
C(13)-C(14)	1.389(3)
C(13)-H(13)	0.95
C(14)-C(15)	1.378(3)
C(14)-H(14)	0.95

C(15)-C(16)	1.378(3)
C(15)-H(15)	0.95
C(16)-F(1)	1.347(3)
C(2)-C(1)-C(5)	128.7(2)
C(2)-C(1)-S	109.97(18)
C(5)-C(1)-S	121.31(17)
C(1)-C(2)-C(3)	113.2(2)
C(1)-C(2)-H(2)	123.4
C(3)-C(2)-H(2)	123.4
C(4)-C(3)-C(2)	114.4(2)
C(4)-C(3)-H(3)	122.8
C(2)-C(3)-H(3)	122.8
C(3)-C(4)-C(11)	128.1(2)
C(3)-C(4)-S	109.25(18)
C(11)-C(4)-S	122.58(17)
C(10)-C(5)-C(6)	117.7(2)
C(10)-C(5)-C(1)	120.5(2)
C(6)-C(5)-C(1)	121.7(2)
C(7)-C(6)-C(5)	120.9(2)
C(7)-C(6)-H(6)	119.5
C(5)-C(6)-H(6)	119.5
C(8)-C(7)-C(6)	120.6(2)
C(8)-C(7)-H(7)	119.7
C(6)-C(7)-H(7)	119.7
C(7)-C(8)-C(9)	119.2(2)
C(7)-C(8)-H(8)	120.4

C(9)-C(8)-H(8)	120.4
C(10)-C(9)-C(8)	120.4(2)
C(10)-C(9)-H(9)	119.8
C(8)-C(9)-H(9)	119.8
C(9)-C(10)-C(5)	121.2(2)
C(9)-C(10)-H(10)	119.4
C(5)-C(10)-H(10)	119.4
C(16)-C(11)-C(12)	115.2(2)
C(16)-C(11)-C(4)	123.9(2)
C(12)-C(11)-C(4)	120.8(2)
C(13)-C(12)-C(11)	122.7(2)
C(13)-C(12)-H(12)	118.6
C(11)-C(12)-H(12)	118.6

C(12)-C(13)-C(14)	119.6(2)
C(12)-C(13)-H(13)	120.2
C(14)-C(13)-H(13)	120.2
C(15)-C(14)-C(13)	119.6(2)
C(15)-C(14)-H(14)	120.2
C(13)-C(14)-H(14)	120.2
C(16)-C(15)-C(14)	119.1(2)
C(16)-C(15)-H(15)	120.4
C(14)-C(15)-H(15)	120.4
F(1)-C(16)-C(15)	116.4(2)
F(1)-C(16)-C(11)	120.0(2)
C(15)-C(16)-C(11)	123.7(2)
C(1)-S-C(4)	93.11(11)

Anisotropic displacement parameters

	U11	U22	U33	U23	U13	U12
C(1)	15(1)	15(1)	21(1)	1(1)	-4(1)	4(1)
C(2)	15(1)	23(1)	26(1)	2(1)	-2(1)	-4(1)
C(3)	19(1)	22(1)	25(1)	5(1)	3(1)	-4(1)
C(4)	16(1)	17(1)	19(1)	3(1)	1(1)	3(1)
C(5)	17(1)	13(1)	21(1)	1(1)	1(1)	4(1)
C(6)	15(1)	18(1)	24(1)	-2(1)	-1(1)	-1(1)
C(7)	20(1)	19(1)	28(1)	5(1)	6(1)	0(1)
C(8)	26(1)	17(1)	24(1)	2(1)	5(1)	5(1)
C(9)	25(1)	19(1)	22(1)	-1(1)	-4(1)	0(1)
C(10)	14(1)	17(1)	27(1)	1(1)	0(1)	-1(1)
C(11)	18(1)	17(1)	21(1)	4(1)	-1(1)	5(1)
C(12)	21(1)	17(1)	28(2)	2(1)	3(1)	2(1)
C(12S)	21(1)	17(1)	28(2)	2(1)	3(1)	2(1)
F(1S)	31(4)	23(4)	35(5)	-3(4)	11(4)	-11(3)
C(13)	29(1)	22(1)	24(1)	2(1)	6(1)	4(1)
C(14)	33(1)	25(1)	21(1)	-3(1)	-3(1)	9(1)
C(15)	20(1)	23(1)	29(2)	-4(1)	-6(1)	3(1)
C(16)	19(1)	19(1)	26(1)	5(1)	1(1)	3(1)
F(1)	18(1)	34(1)	25(1)	-1(1)	2(1)	-6(1)
C(16S)	19(1)	19(1)	26(1)	5(1)	1(1)	3(1)
S	15(1)	23(1)	20(1)	-1(1)	1(1)	-3(1)

Hydrogen coordinates

	x	y	Z	U(eq)
H(2)	5944	5252	8081	26
H(3)	5834	5608	8974	26
H(6)	12782	7986	7711	23
H(7)	13868	7906	6903	27
H(8)	11607	6389	6290	26
H(9)	8188	4960	6492	26
H(10)	7071	5049	7296	23
H(12)	6581	6117	9785	26
H(13)	7367	6560	10627	30
H(14)	10832	7959	10925	32
H(15)	13465	8906	10367	29
H(16S)	12628	8446	9529	26

Torsion angles [deg]

C(5)-C(1)-C(2)-C(3)	179.7(2)	S-C(4)-C(11)-C(16)	1.6(3)
S-C(1)-C(2)-C(3)	0.0(3)	C(3)-C(4)-C(11)-C(12)	0.9(4)
C(1)-C(2)-C(3)-C(4)	0.1(3)	S-C(4)-C(11)-C(12)	-176.46(18)
C(2)-C(3)-C(4)-C(11)	-177.8(2)	C(16)-C(11)-C(12)-C(13)	-0.6(3)
C(2)-C(3)-C(4)-S	-0.2(3)	C(4)-C(11)-C(12)-C(13)	177.6(2)
C(2)-C(1)-C(5)-C(10)	-5.9(4)	C(11)-C(12)-C(13)-C(14)	0.2(4)
S-C(1)-C(5)-C(10)	173.79(17)	C(12)-C(13)-C(14)-C(15)	0.2(4)
C(2)-C(1)-C(5)-C(6)	175.2(2)	C(13)-C(14)-C(15)-C(16)	-0.2(4)
S-C(1)-C(5)-C(6)	-5.1(3)	C(14)-C(15)-C(16)-F(1)	179.8(2)
C(10)-C(5)-C(6)-C(7)	-1.1(3)	C(14)-C(15)-C(16)-C(11)	-0.3(4)
C(1)-C(5)-C(6)-C(7)	177.9(2)	C(12)-C(11)-C(16)-F(1)	-179.4(2)
C(5)-C(6)-C(7)-C(8)	0.2(4)	C(4)-C(11)-C(16)-F(1)	2.5(3)
C(6)-C(7)-C(8)-C(9)	0.5(3)	C(12)-C(11)-C(16)-C(15)	0.7(3)
C(7)-C(8)-C(9)-C(10)	-0.2(3)	C(4)-C(11)-C(16)-C(15)	-177.5(2)
C(8)-C(9)-C(10)-C(5)	-0.7(4)	C(2)-C(1)-S-C(4)	-0.08(18)
C(6)-C(5)-C(10)-C(9)	1.3(3)	C(5)-C(1)-S-C(4)	-179.80(19)
C(1)-C(5)-C(10)-C(9)	-177.7(2)	C(3)-C(4)-S-C(1)	0.14(18)
C(3)-C(4)-C(11)-C(16)	178.9(2)	C(11)-C(4)-S-C(1)	177.93(19)

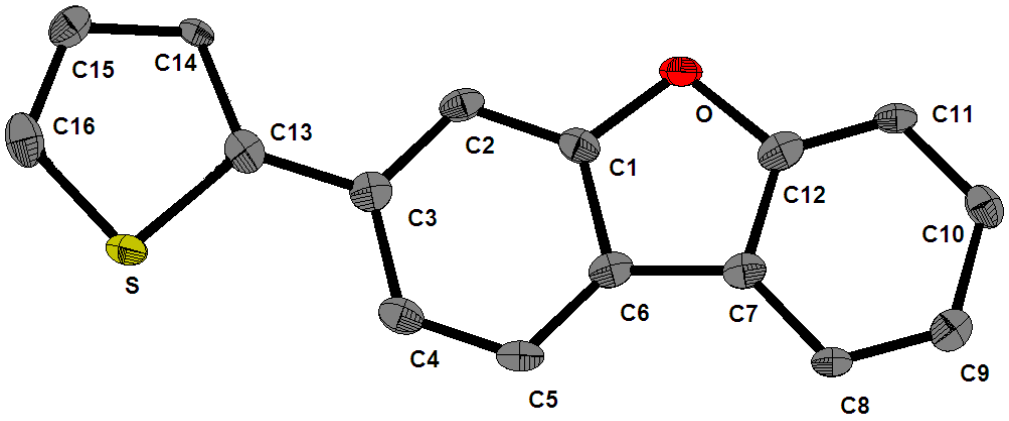

Identification code	GDOE088, Greg1394f
Device Type	Bruker X8-KappaApexII
Empirical formula	C16 H10 O S
Formula weight	250.3
Temperature	100(2) K
Wavelength	0.71073 A
Crystal system, space group	Monoclinic, P 21
Unit cell dimensions	a = 7.9131(16) A alpha = 90 deg. b = 5.7711(11) A beta = 98.085(7) deg. c = 12.724(3) A gamma = 90 deg.
Volume	575.3(2) A^3
Z, Calculated density	2, 1.445 Mg/m^3
Absorption coefficient	0.262 mm^-1
F(000)	260
Crystal size	0.60 x 0.50 x 0.02 mm

Theta range for data collection	2.86 to 26.00 deg.
Limiting indices	-9<=h<=9, -4<=k<=6, -15<=l<=15
Reflections collected / unique	4033 / 1831 [R(int) = 0.0407]
Completeness to theta = 26.00	98.00%
Absorption correction	Empirical
Max. and min. transmission	0.9948 and 0.8584
Refinement method	Full-matrix least-squares on F^2
Data / restraints / parameters	1831 / 36 / 170
Goodness-of-fit on F^2	1.053
Final R indices [I>2sigma(I)]	R1 = 0.0530, wR2 = 0.1255
R indices (all data)	R1 = 0.0766, wR2 = 0.1389
Absolute structure parameter	-0.08(18)
Largest diff. peak and hole	0.420 and -0.402 e.A^-3

Atomic coordinates

	x	y	z	U(eq)
C(1)	7450(5)	5348(9)	10594(4)	28(1)
C(2)	6510(6)	4831(9)	9626(4)	30(1)
C(3)	6511(6)	6439(9)	8809(4)	30(1)
C(4)	7426(6)	8508(9)	9001(4)	32(1)
C(5)	8353(5)	9021(9)	9984(4)	30(1)
C(6)	8372(5)	7420(9)	10795(4)	28(1)
C(7)	9220(5)	7211(9)	11904(4)	28(1)
C(8)	10346(5)	8606(8)	12577(3)	23(1)
C(9)	10896(5)	7864(11)	13586(4)	33(1)
C(10)	10348(6)	5719(10)	13935(4)	32(1)
C(11)	9236(5)	4368(9)	13249(3)	25(1)

C(12)	8724(6)	5115(10)	12275(4)	32(1)
C(13)	5607(5)	5906(8)	7751(3)	30(1)
C(14)	4637(8)	3950(11)	7403(4)	21(1)
C(15)	3958(5)	3998(9)	6319(3)	33(1)
C(16)	4411(6)	5974(10)	5866(4)	41(2)
S	5608(3)	7717(3)	6680(1)	32(1)
C(16S)	3958(5)	3998(9)	6319(3)	33(1)
C(15S)	4411(6)	5974(10)	5866(4)	41(2)
SS	4595(12)	3377(13)	7550(6)	32(1)
C(14S)	5390(40)	7070(40)	6741(10)	21(1)
O	7618(4)	3922(6)	11484(2)	32(1)

Bond lengths [A] and angles [deg]

C(1)-C(2)	1.379(6)
C(1)-O	1.391(6)
C(1)-C(6)	1.405(7)
C(2)-C(3)	1.394(7)
C(2)-H(2A)	0.95
C(3)-C(4)	1.400(7)
C(3)-C(13)	1.465(6)
C(4)-C(5)	1.391(7)
C(4)-H(4A)	0.95
C(5)-C(6)	1.384(7)
C(5)-H(5A)	0.95
C(6)-C(7)	1.479(6)
C(7)-C(12)	1.376(8)
C(7)-C(8)	1.400(6)
C(8)-C(9)	1.365(6)
C(8)-H(8A)	0.95
C(9)-C(10)	1.404(8)
C(9)-H(9A)	0.95
C(10)-C(11)	1.388(7)
C(10)-H(10A)	0.95
C(11)-C(12)	1.321(7)
C(11)-H(11A)	0.95
C(12)-O	1.416(6)
C(13)-C(14)	1.401(7)
C(13)-C(14S)	1.437(9)
C(13)-SS	1.667(8)
C(13)-S	1.717(4)
C(14)-C(15)	1.409(6)

C(15)-C(16)	1.348(7)
C(15)-H(15A)	0.95
C(16)-S	1.645(5)
C(16)-H(16A)	0.95
C(14S)-H(14S)	0.95
C(2)-C(1)-O	125.2(4)
C(2)-C(1)-C(6)	123.2(4)
O-C(1)-C(6)	111.6(4)
C(1)-C(2)-C(3)	117.7(4)
C(1)-C(2)-H(2A)	121.1
C(3)-C(2)-H(2A)	121.1
C(2)-C(3)-C(4)	119.5(4)
C(2)-C(3)-C(13)	119.6(4)
C(4)-C(3)-C(13)	120.8(4)
C(5)-C(4)-C(3)	122.2(5)
C(5)-C(4)-H(4A)	118.9
C(3)-C(4)-H(4A)	118.9
C(6)-C(5)-C(4)	118.6(5)
C(6)-C(5)-H(5A)	120.7
C(4)-C(5)-H(5A)	120.7
C(5)-C(6)-C(1)	118.8(4)
C(5)-C(6)-C(7)	136.2(5)
C(1)-C(6)-C(7)	105.0(4)
C(12)-C(7)-C(8)	118.9(5)
C(12)-C(7)-C(6)	106.6(4)
C(8)-C(7)-C(6)	134.5(5)

C(9)-C(8)-C(7)	119.1(5)
C(9)-C(8)-H(8A)	120.4
C(7)-C(8)-H(8A)	120.4
C(8)-C(9)-C(10)	120.1(5)
C(8)-C(9)-H(9A)	119.9
C(10)-C(9)-H(9A)	119.9
C(11)-C(10)-C(9)	119.5(4)
C(11)-C(10)-H(10A)	120.2
C(9)-C(10)-H(10A)	120.2
C(12)-C(11)-C(10)	119.4(5)
C(12)-C(11)-H(11A)	120.3
C(10)-C(11)-H(11A)	120.3
C(11)-C(12)-C(7)	123.0(5)
C(11)-C(12)-O	125.8(5)
C(7)-C(12)-O	111.2(4)
C(14)-C(13)-C(14S)	95.8(6)
C(14)-C(13)-C(3)	129.3(4)
C(14S)-C(13)-C(3)	134.9(6)

C(14)-C(13)-SS	10.4(4)
C(14S)-C(13)-SS	106.0(6)
C(3)-C(13)-SS	119.1(4)
C(14)-C(13)-S	107.5(4)
C(14S)-C(13)-S	11.7(5)
C(3)-C(13)-S	123.1(4)
SS-C(13)-S	117.7(4)
C(13)-C(14)-C(15)	114.2(5)
C(13)-C(14)-H(14)	122.9
C(15)-C(14)-H(14)	122.9
C(16)-C(15)-C(14)	110.3(5)
C(16)-C(15)-H(15A)	124.8
C(14)-C(15)-H(15A)	124.8
C(15)-C(16)-S	114.3(4)
C(15)-C(16)-H(16A)	122.8
S-C(16)-H(16A)	122.8
C(16)-S-C(13)	93.6(3)
C(13)-C(14S)-H(14S)	120.6
C(1)-O-C(12)	105.6(4)

Anisotropic displacement parameters

	U11	U22	U33	U23	U13	U12
C(1)	30(2)	23(3)	33(3)	2(2)	12(2)	4(2)
C(2)	26(2)	20(3)	43(3)	-9(2)	8(2)	2(2)
C(3)	27(2)	30(3)	36(3)	-4(2)	10(2)	6(2)
C(4)	31(2)	25(3)	42(3)	4(2)	14(2)	5(2)
C(5)	28(2)	19(3)	46(3)	-2(2)	16(2)	-2(2)
C(6)	22(2)	24(3)	39(3)	-8(2)	12(2)	3(2)
C(7)	26(2)	24(3)	36(3)	-6(2)	12(2)	3(2)
C(8)	19(2)	17(3)	35(2)	-2(2)	10(2)	1(2)
C(9)	25(2)	35(3)	40(3)	-6(3)	4(2)	3(2)
C(10)	31(2)	31(3)	34(3)	6(2)	4(2)	13(2)
C(11)	21(2)	17(3)	39(3)	-3(2)	11(2)	1(2)
C(12)	26(2)	30(3)	43(3)	-11(2)	11(2)	2(2)
C(13)	24(2)	34(3)	33(3)	2(2)	11(2)	9(2)
C(14)	22(2)	17(2)	25(2)	5(1)	9(1)	-1(1)
C(15)	21(2)	36(3)	41(3)	-9(3)	2(2)	0(2)
C(16)	33(3)	55(4)	34(3)	7(3)	4(2)	14(3)
S	38(1)	21(1)	38(1)	5(1)	5(1)	-5(1)

C(16S)	21(2)	36(3)	41(3)	-9(3)	2(2)	0(2)
C(15S)	33(3)	55(4)	34(3)	7(3)	4(2)	14(3)
SS	38(1)	21(1)	38(1)	5(1)	5(1)	-5(1)
C(14S)	22(2)	17(2)	25(2)	5(1)	9(1)	-1(1)
O	38(2)	19(2)	40(2)	1(2)	5(2)	-5(2)

Hydrogen coordinates

	x	y	z	U(eq)
H(2A)	5883	3426	9520	35
H(4A)	7412	9599	8440	38
H(5A)	8960	10440	10097	36
H(8A)	10723	10048	12335	28
H(9A)	11650	8802	14054	40
H(10A)	10737	5195	14635	38
H(11A)	8846	2922	13478	30
H(14)	4453	2700	7859	25
H(15A)	3279	2808	5958	40
H(16A)	4067	6330	5138	49
H(16B)	3239	2932	5899	40
H(15B)	4145	6490	5152	49
H(14S)	5888	8542	6665	25

Torsion angles [deg]

O-C(1)-C(2)-C(3)	-178.6(4)
C(6)-C(1)-C(2)-C(3)	1.2(6)
C(1)-C(2)-C(3)-C(4)	-1.1(6)
C(1)-C(2)-C(3)-C(13)	176.6(4)
C(2)-C(3)-C(4)-C(5)	0.4(6)
C(13)-C(3)-C(4)-C(5)	-177.3(4)
C(3)-C(4)-C(5)-C(6)	0.3(6)
C(4)-C(5)-C(6)-C(1)	-0.3(6)
C(4)-C(5)-C(6)-C(7)	176.5(4)
C(2)-C(1)-C(6)-C(5)	-0.5(6)
O-C(1)-C(6)-C(5)	179.3(4)
C(2)-C(1)-C(6)-C(7)	-178.2(4)
O-C(1)-C(6)-C(7)	1.6(4)
C(5)-C(6)-C(7)-C(12)	-178.3(5)

C(1)-C(6)-C(7)-C(12)	-1.2(4)
C(5)-C(6)-C(7)-C(8)	0.8(8)
C(1)-C(6)-C(7)-C(8)	177.8(4)
C(12)-C(7)-C(8)-C(9)	-1.1(6)
C(6)-C(7)-C(8)-C(9)	180.0(4)
C(7)-C(8)-C(9)-C(10)	0.7(6)
C(8)-C(9)-C(10)-C(11)	-0.5(7)
C(9)-C(10)-C(11)-C(12)	0.7(6)
C(10)-C(11)-C(12)-C(7)	-1.2(7)
C(10)-C(11)-C(12)-O	179.0(4)
C(8)-C(7)-C(12)-C(11)	1.3(7)
C(6)-C(7)-C(12)-C(11)	-179.4(4)
C(8)-C(7)-C(12)-O	-178.8(4)

C(6)-C(7)-C(12)-O	0.4(5)
C(2)-C(3)-C(13)-C(14)	2.1(7)
C(4)-C(3)-C(13)-C(14)	179.8(5)
C(2)-C(3)-C(13)-C(14S)	-178(2)
C(4)-C(3)-C(13)-C(14S)	0(2)
C(2)-C(3)-C(13)-SS	0.0(7)
C(4)-C(3)-C(13)-SS	177.8(5)
C(2)-C(3)-C(13)-S	-177.2(3)
C(4)-C(3)-C(13)-S	0.5(6)
C(14S)-C(13)-C(14)-C(15)	0.4(16)
C(3)-C(13)-C(14)-C(15)	-179.3(4)
SS-C(13)-C(14)-C(15)	-169(4)

S-C(13)-C(14)-C(15)	0.1(6)
C(13)-C(14)-C(15)-C(16)	-0.4(7)
C(14)-C(15)-C(16)-S	0.5(6)
C(15)-C(16)-S-C(13)	-0.4(4)
C(14)-C(13)-S-C(16)	0.2(4)
C(14S)-C(13)-S-C(16)	-2(8)
C(3)-C(13)-S-C(16)	179.6(4)
SS-C(13)-S-C(16)	2.4(5)
C(2)-C(1)-O-C(12)	178.4(4)
C(6)-C(1)-O-C(12)	-1.4(5)
C(11)-C(12)-O-C(1)	-179.6(4)
C(7)-C(12)-O-C(1)	0.5(5)

XI. Chemical structure of selected compounds

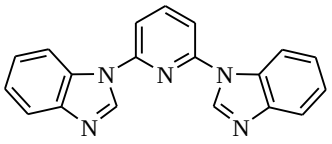

4

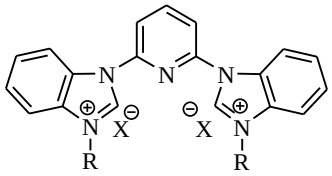

5e: R = C_4H_9, X = Br

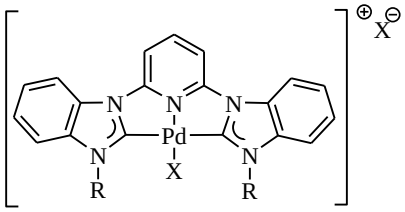

6: R = C_4H_9, X = Br

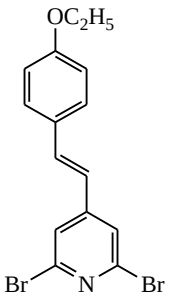

9

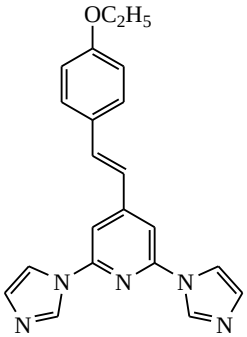

10

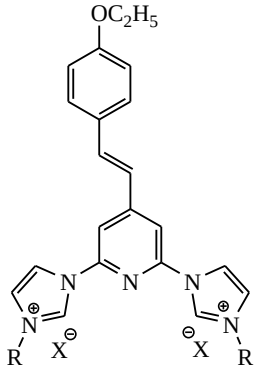

11a: R = C_4H_9, X = Br
11b: R = $C_{16}H_{33}$, X = I

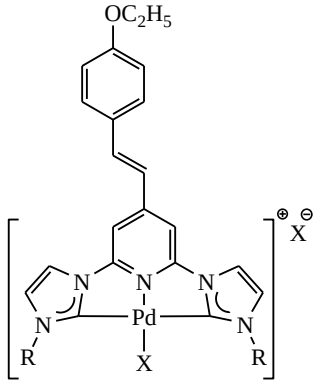

12a: R = C_4H_9, X = Br
12b: R = $C_{16}H_{33}$, X = I

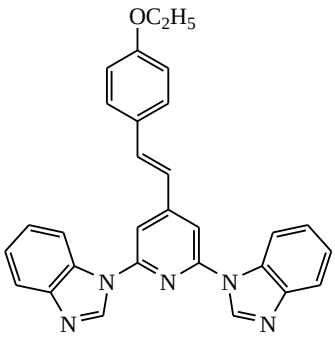

13

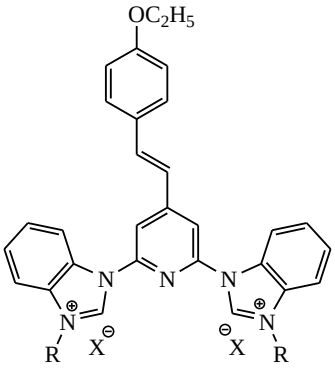

14a, R = C_4H_9, X = Br
14b, R = $C_{16}H_{33}$, X = I

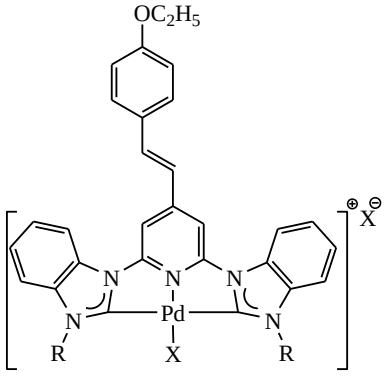

15a, R = C_4H_9, X = Br
15b, R = $C_{16}H_{33}$, X = I

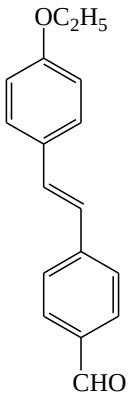

16

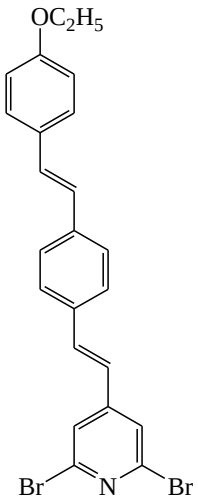

17

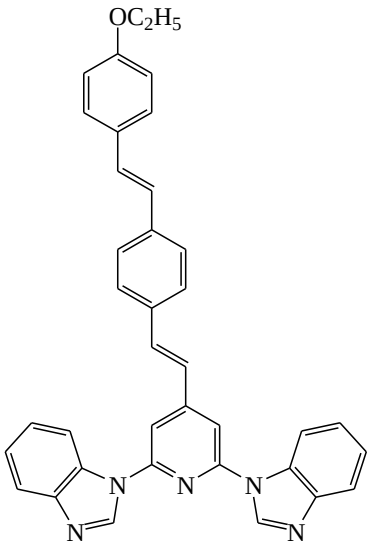

18

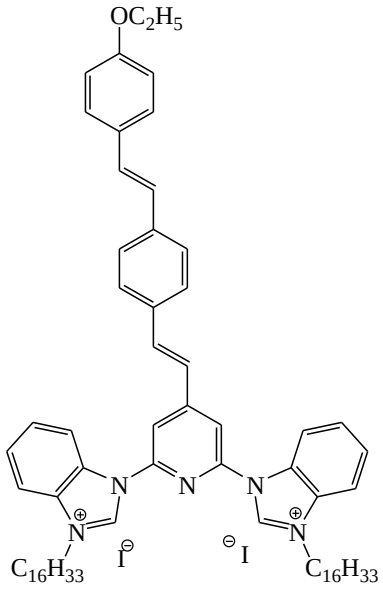

19

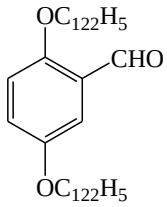

20

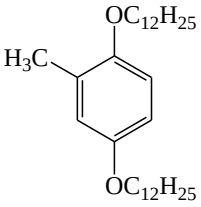

21

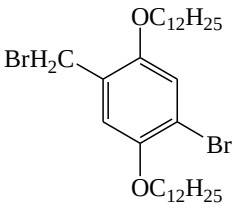

22

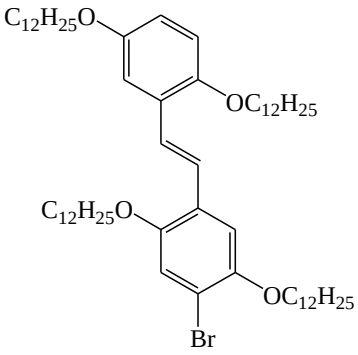

24

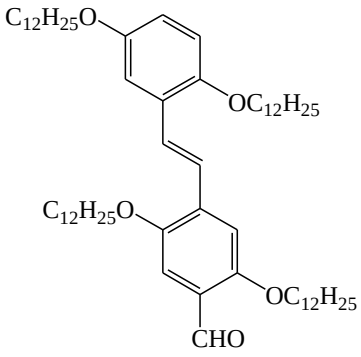

25

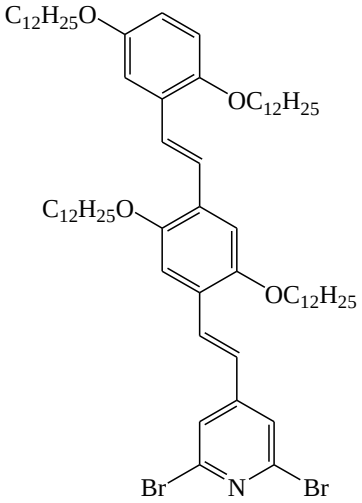

26

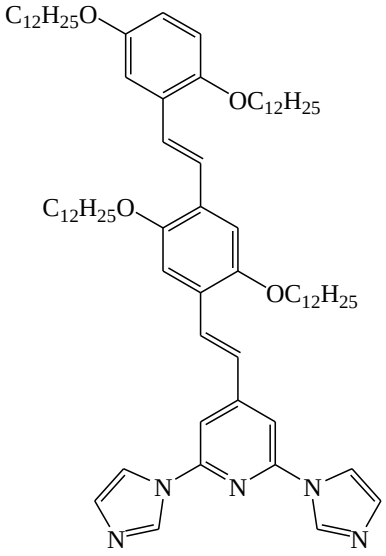

27

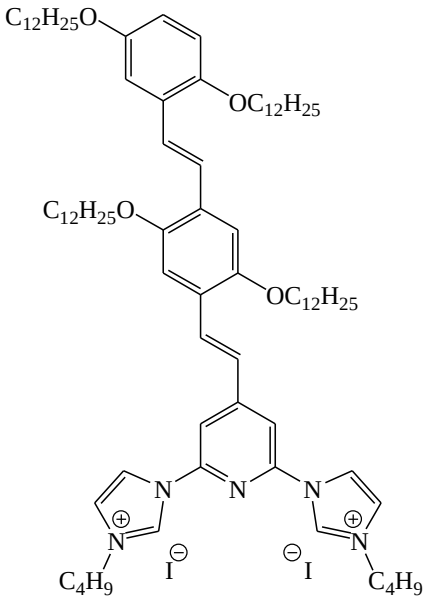

28

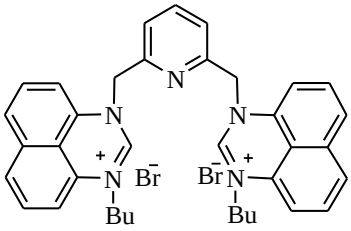

38

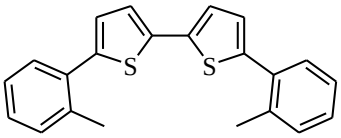

41

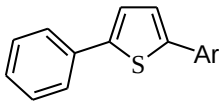

42 a-i

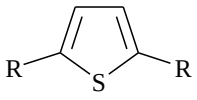

43 a-h

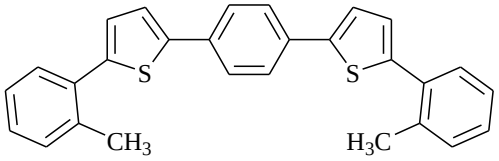

45

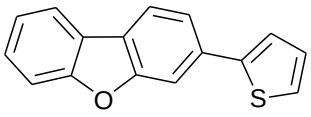

47

Work Experience:

1) "*Synthesis of valuable intermediates -for acetylenic macro cycles*" summer Project in 2005 at IIT Madras under guidance of **Prof. S. Sakararaman**.

2) "*Synthesis of five and six membered Hetero cyclic compounds*" advanced project 2005-2006 at Pondicherry University under supervision of **Prof. H. Surya Prakash Rao**.

3) "*Synthesis of polytethynyl pyrenes and studies on their physical Properties*" from 2006-2007 at IIT Madras under guidance of **Prof. S. Sakararaman**.

4) "*Synthesis of heterocyclic natural products*" from 2007-2008 at IICT Hyderabad under guidance of **Dr. B. China Raju**.

Ich versichere, die vorliegende Arbeit selbstständig verfasst zu haben. Es wurden keine anderen als die angegebenen Hilfsmittel verwendet, sowie alle Zitate kenntlich gemacht.

Bonn, den _____

Jagadeesh Malineni